

NSF/CEE-85001

PB 88-10784 2

**IN SITU TESTING PROCEDURE  
FOR OBTAINING DYNAMIC AND  
CYCLIC SOIL PROPERTIES**

Dynamic In Situ Geotechnical Testing, Inc.

Houston, Texas

Prepared for the

National Science Foundation

Washington, D.C.

July, 1985

**Any opinions, findings, conclusions  
or recommendations expressed in this  
publication are those of the author(s)  
and do not necessarily reflect the views  
of the National Science Foundation.**

REPRODUCED BY  
U.S. DEPARTMENT OF COMMERCE  
NATIONAL TECHNICAL  
INFORMATION SERVICE  
SPRINGFIELD, VA. 22161



ATTENTION

AS NOTED IN THE NTIS ANNOUNCEMENT, PORTIONS OF THIS REPORT ARE NOT LEGIBLE. HOWEVER, IT IS THE BEST REPRODUCTION AVAILABLE FROM THE COPY SENT TO NTIS.

#### ACKNOWLEDGMENT

This material is based upon work supported by the National Science Foundation under award number CEE-8460719. Any opinions, findings, and conclusions or recommendations expressed in this publication are those of the authors and do not necessarily reflect the views of the National Science Foundation.

## TECHNICAL SUMMARY

### Introduction

This document reports on feasibility studies, conducted for the National Science Foundation, which indicate the feasibility of a proposed in situ geotechnical testing procedure for obtaining in situ cyclic and dynamic engineering soil properties. The studies represent Phase I of a planned three phase project. The project falls under the domain of the Earthquake Hazard Mitigation program.

### Purpose of Project

The purpose of the project is to develop an in situ geotechnical testing procedure for obtaining accurate and detailed descriptions of the in situ liquefaction and cyclic degradation characteristics of a soil, the low amplitude dynamic shear modulus, and the variation in the dynamic shear modulus with shear strain. This information is required for analyses which predict the behavior of soil-structure-equipment systems during earthquakes. The level of accuracy and detail to be provided is intended to be appropriate for the intermediate and final stages of the analysis and design of important structures located in seismically active areas.

### Existing Methods

While a number of important advances have been made in the area of determining in situ cyclic and dynamic soil properties, further worthwhile advancement is possible. We feel that there are no existing procedures for determining in situ cyclic degradation and liquefaction characteristics in the detail and to the accuracy that is needed for the effective use of the costly and potentially powerful analysis procedures appropriate for the intermediate and final stages of analysis and design. Additionally, there are significant limitations or drawbacks in existing procedures for determining dynamic shear moduli.

Currently, in situ cyclic and dynamic soil properties are obtained by laboratory and in situ testing. Laboratory testing of samples is plagued by the serious problem of disturbance to in situ conditions. Generally, with in situ testing, in situ conditions are preserved to a greater degree; however, it is difficult in situ to apply earthquake-type cyclic shear loads to a well-defined element of soil, to induce important phenomena observed during earthquakes, and to obtain information in appropriate detail. The problems with laboratory and in situ testing procedures may cause considerable uncertainty and potential for error in defining in situ soil properties.

Uncertainty and error in defining in situ soil properties will create uncertainty and error in the results of analyses relying on these properties. In fact, the limitations in our ability to accurately and descriptively define in situ soil properties can severely limit the effectiveness of the costly and potentially powerful analysis procedures which have been developed during recent years. This can lead to either costly, excessively conservative designs or unconservative designs.

### Proposed Method

The proposed testing procedure is intended to provide more accurate and detailed descriptions of in situ cyclic and dynamic soil properties than can currently be provided. It is to do so by effectively combining attractive features of in situ testing and laboratory testing while minimizing shortcomings.

The method will be direct. Cyclic earthquake-type shear loads will be applied to a well-defined element of soil in a simple but effective manner. The behavior of the test soil is expected to correspond closely to behavior expected during earthquakes. Thus, uncertainties associated with the loading of the soil and its mode of failure will be reduced. Tests will be conducted in situ and a number of steps will be taken to minimize disturbances to in situ conditions. Thus, the very important effects of in situ factors are expected to be captured in measurements. Several features are to be provided to help induce the phenomena of interest and also to simplify the interpretation of test results. The detailed information needed by earthquake analyses will be directly provided, minimizing intermediate interpretation. Also, the procedure is expected to apply to most soils of interest. Finally, the method will require only a single borehole so that it may be used in confined and harsh environments.

The probe of the testing system will consist of two concentric thin-walled cylinders. In practice, the cylinders will be carefully penetrated below the base of a borehole. The test soil will be the well-defined annular zone of soil between the two cylinders. A cyclic or impulsive torsional loading will be applied to the inner cylinder. In response, the inner cylinder is expected to rotate in a manner dependent on the shear properties of the test soil. Both torques and rotations will be measured by transducers in an instrumented head. Soil properties will be inferred by modeling tests analytically using descriptive procedures.

### Potential Benefits

The proposed in situ testing procedure is intended to provide descriptions of in situ cyclic and dynamic soil properties to the level of accuracy and detail appropriate for the intermediate and final stages of the analysis and design of important structures located in seismically active areas. This would allow more effective use of the costly and potentially powerful analysis procedures used for this application. Defining in situ cyclic and dynamic soil properties more accurately and in greater detail will reduce error and uncertainty in predicted site-specific earthquake excitations and predicted behaviors of soil-structure-equipment systems (dams, buildings, offshore structures, embankments, etc.) during earthquakes. In turn, this would advance our ability to economically insure the integrity and reliability of soil-structure-equipment systems during earthquakes.

### Potential Commercial Applications and Users

There are several potential commercial applications of the proposed testing procedure. The main application is intended to be the design,

construction, and maintenance of soil-structure-equipment systems to insure resistance to earthquakes. Additionally, the procedure is expected to apply to the design, construction, and maintenance of 1) soil-structure-equipment systems to insure resistance to water wave and blast loadings, 2) machine foundations, and 3) delicate soil-structure-equipment systems to insure isolation from vibrations. Potential users of the testing system or the information provided by the testing system include agencies of governments, universities, geotechnical engineering firms, oil companies, and power companies.

#### Phase I Objectives, Procedures, and Accomplishments

Phase I work included several studies: a theoretical feasibility study, a supplementary theoretical feasibility study, and an operational feasibility study.

We conducted a theoretical feasibility study to determine the theoretical feasibility of the proposed testing system. Tests were simulated analytically considering expected ranges of selected soil properties. Studies were carried out to determine the theoretical feasibility of the testing system for determining 1) the low amplitude dynamic shear modulus and the variation in the dynamic shear modulus with shear strain, 2) the degradation characteristics of clays, and 3) the degradation and liquefaction characteristics of sands and silts.

Results from our study indicate that the proposed testing system is theoretically feasible. The behavior of the testing system was predicted to be sensitive to each soil property considered in a clear, physically reasonable manner.

During our study, we identified one area requiring further study. The configuration of the inner cylinder, specified for the preliminary design of a laboratory research prototype testing system, was thought to be torsionally more flexible, relative to the test soil, than we had originally considered. As a result, we carried out a cursory supplementary study in addition to our proposed theoretical feasibility study. The purpose of the supplementary study was to estimate roughly the rotational flexibility of the inner cylinder, as configured in the preliminary design of the testing system, relative to the rotational flexibility of the test soil. The estimate was made to help determine whether special attention would be required as a result of such relative flexibility. The results of the study indicate that the inner cylinder may be torsionally flexible relative to the test soil under certain conditions. This may increase somewhat uncertainty in inferring soil properties from test results. However, we concluded that because of the many effective steps which could be taken, if necessary, to mitigate this concern, the proposed testing system should serve its stated purpose well and advance our ability to determine in situ cyclic and dynamic soil properties.

An operational feasibility study was conducted to determine the operational feasibility of a laboratory research prototype testing system. This system will be functionally similar to the field system scheduled for development during Phase III. The mechanical engineering design firm of Sweet & Aiken, Inc., (Sweet & Aiken) conducted the study. Studies were carried out to determine the operational feasibility of a laboratory testing system for determining 1) the low amplitude dynamic shear modulus and the

variation in the dynamic shear modulus with shear strain, 2) the cyclic degradation characteristics of clays, and 3) the cyclic degradation and liquefaction characteristics of sands and silts.

Results from the operational feasibility study indicate that the laboratory research prototype testing system is operationally feasible. The main components of the system, which satisfy reasonably well design criteria specified by our firm, were found to be either available or readily producible and it was determined that these components could be assembled into a convenient, workable arrangement. The operational feasibility study resulted in a preliminary design for a laboratory research prototype testing system.

Not all specified criteria were satisfied; however, the resulting consequences are not expected to be severe. For example, Sweet & Aiken was unable to find a transducer capable of accurately measuring the smallest specified angles of rotation of the inner cylinder. However, it appears that reasonably small angles will be able to be measured. Thus, the potential increase in uncertainty in inferring soil properties from test results was judged to be only modest. Also, advances in appropriate technologies are expected to advance our ability to infer soil properties using the proposed testing system.

Sweet & Aiken estimated a cost of \$78,260 for the detailed design and construction of a complete laboratory research prototype testing system. This is a conservative estimate and such a cost is consistent with that of the design and construction of comparable testing systems. The benefits of a working system are expected to greatly exceed the overall cost. The cost saving alone, resulting from basing the design of a single major structure on appropriately accurate and detailed information on in situ dynamic and cyclic soil properties, is expected to greatly exceed the cost of the development of the testing system.

#### Estimate of Feasibility

Based on the results of the feasibility studies discussed in this report, we concluded that the proposed in situ testing system is feasible. Ultimately, the testing system is expected to effectively provide information on in situ cyclic and dynamic soil properties to the level of accuracy and detail appropriate for the intermediate and final stages of the analysis and design of important structures located in seismically active areas. The Phase I studies indicate that a laboratory research prototype testing system is theoretically, operationally, and economically feasible. Since the additional equipment required for a field system is reasonably conventional, and since the additional problems that could be encountered in the field appear to be either small or surmountable, we believe that an in situ field testing system is feasible.

Much research and development will be required before the full potential of the testing system can be realized. This is consistent with comparable testing systems. Much effort will be needed because the problem of determining in situ cyclic and dynamic soil properties is not a simple problem, the testing system is somewhat complex, and the testing system has considerable safety and economic implications.

TABLE OF CONTENTS

<u>Sections and Subsections</u>	<u>Page</u>
SUMMARY OF COMPLETED PROJECT.....	i
ACKNOWLEDGMENT.....	ii
TECHNICAL SUMMARY.....	iii
Introduction.....	iii
Purpose of Project.....	iii
Existing Methods.....	iii
Proposed Method.....	iv
Potential Benefits.....	iv
Potential Commercial Applications and Users.....	iv
Phase I Objectives, Procedures, and Accomplishments.....	v
Estimate of Feasibility.....	vi
TABLE OF CONTENTS.....	vii
NOMENCLATURE.....	ix
INTRODUCTION.....	1
PURPOSE OF PROJECT.....	2
TECHNICAL DEFINITIONS AND TERMINOLOGY.....	4
Low Amplitude Dynamic Shear Modulus, $G_0$ .....	4
Variation in Dynamic Shear Modulus with Shear Strain.....	4
Relative Density, $D_r$ , of a Sand or Silt.....	4
Degradation and Liquefaction Characteristics of Sands and Silts.....	4
Degradation Characteristics of Clays.....	4
EXISTING METHODS.....	7
PROPOSED METHOD.....	15
POTENTIAL BENEFITS.....	23
POTENTIAL COMMERCIAL APPLICATIONS AND USERS.....	26
RECIPIENTS OF REPORT.....	27
PHASE I OBJECTIVES, PROCEDURES, AND ACCOMPLISHMENTS.....	28
Theoretical Feasibility Study.....	28
Introduction and Summary.....	28
Objectives.....	28
General Procedures.....	29
Analysis Procedures.....	29
Analytical Modeling.....	29
Solution Procedures.....	33
Solution Check Procedure.....	36
Assumptions.....	38
Validations.....	38
Presentation and Discussion of Results.....	38
Model Parameters Common to Most Simulations.....	38

Low Amplitude Dynamic Shear Modulus.....	39
Variation in the Dynamic Shear Modulus with Shear Strain.....	43
Degradation Characteristics of Clays.....	49
Degradation and Liquefaction Characteristics of Sands and Silts.....	53
Conclusions.....	62
Supplementary Theoretical Feasibility Study.....	63
Introduction and Summary.....	63
Objective.....	63
Procedures.....	64
Presentation and Discussion of Results.....	65
Mitigating Steps.....	66
Conclusions.....	68
Operational Feasibility Study.....	69
Introduction and Summary.....	69
Objectives.....	70
Procedures.....	70
Main Components.....	71
Design Criteria.....	71
Mechanical Requirements.....	71
Excitation and Measurement Requirements.....	75
Presentation and Discussion of Results.....	76
Preliminary Design of Laboratory Research	
Prototype Testing System.....	76
Operation of Laboratory Testing System.....	77
Mechanical Components, Systems, and Features.....	77
Excitation and Measurement Systems.....	78
Cost Estimate.....	81
Conclusions.....	82
ESTIMATE OF FEASIBILITY.....	83
REFERENCES.....	86
APPENDICES	
A. Validation of Computer Procedures.....	A-1
B. Derivations for Key Relationships.....	B-1
C. Report on Operational Feasibility Study from Sweet & Aiken, Inc.....	C-1

### NOMENCLATURE

In this section, we define the nomenclature used in the main body of this report and in Appendices A and B.

- A = Surface area of active (unshielded) portion of inner cylinder
- $C_T$  = Coefficient of viscous damping
- $C_1$  = Parameter of Ramberg-Osgood equations; Parameter of liquefaction and degradation submodel
- $C_2, C_3, C_4$  = Parameters of liquefaction and degradation submodel
- DE = Energy lost in test soil due to viscous damping
- $D_i$  = Inner diameter of inner cylinder
- $D_o$  = Outer diameter of inner cylinder
- $D_r$  = Relative density
- $\bar{D}_i$  = Inner diameter of circular shaft
- $\bar{D}_o$  = Outer diameter of circular shaft
- $E_R$  = Energy ratio
- e = Void ratio
- $F_i$  = Rotational flexibility of inner cylinder relative to rotational flexibility of test soil during initial cycle of loading
- f = Frequency in cycles per second
- G = Tangent shear modulus of test soil
- $G_i$  = Shear modulus of inner cylinder
- $G_{m0}$  = Undegraded low amplitude shear modulus
- $G_o$  = Low amplitude dynamic shear modulus
- $\bar{G}$  = Shear modulus of circular shaft
- g = Acceleration due to gravity
- $h_c$  = Thickness of wall of inner cylinder (mass moment of inertia calculations)
- $h_s$  = Thickness of segment of test soil (mass moment of inertia calculations)

$I$  = Total mass moment of inertia of effectively rotating mass  
 $\bar{J}$  = Polar moment of inertia of cross section  
 $KE$  = Instantaneous kinetic energy of rotating mass  
 $K_0$  = Coefficient of earth pressure at rest  
 $K_T$  = Tangent torsional spring constant  
 $K_{T0}$  = Low amplitude torsional spring constant  
 $k_2$  = Parameter of liquefaction and degradation submodel  
 $\bar{L}$  = Length of circular shaft  
 $l$  = Length of active (unshielded) portion of inner cylinder  
 $l_{IH}$  = Height of instrumented head (mass moment of inertia calculations)  
 $l_C$  = Length of inner cylinder (mass moment of inertia calculations)  
 $l_S$  = Length of segment of test soil (mass moment of inertia calculations)  
 $m$  = Parameter of liquefaction and degradation submodel  
 $N_C$  = Number of cycles  
 $N_q$  = Bearing capacity factor  
 $N_\gamma$  = Bearing capacity factor  
 $n$  = Parameter of liquefaction and degradation submodel  
 $R$  = Parameter of Ramberg-Osgood equations  
 $R_{IH}$  = Radius of instrumented head (mass moment of inertia calculations)  
 $R_C$  = Radius of inner cylinder (mass moment of inertia calculations)  
 $R_S$  = Radius of segment of test soil (mass moment of inertia calculations)  
 $r$  = Radius  
 $r_i$  = Outer radius of inner cylinder  
 $r_o$  = Inner radius of outer cylinder

$SE$  = Sum of energy lost in test soil due to hysteresis and instantaneous elastic strain energy stored within test soil  
 $S_u$  = Rotational stiffness of inner cylinder relative to rotational stiffness of test soil during ultimate cycle of loading  
 $T$  = Torque applied to inner cylinder  
 $T_A$  = Amplitude of cyclic torque applied to inner cylinder  
 $T_D$  = Damping torque  
 $T_s$  = Spring torque  
 $T_{sA}$  = Amplitude of cyclic spring torque  
 $\bar{T}$  = Static torque acting throughout circular shaft  
 $t$  = Time; Degradation parameter  
 $u$  = Horizontal displacement  
 $\bar{u}$  = excess porewater pressure  
 $W$  = Work done by applied load  
 $z$  = Depth below surface of ground  
 $\alpha$  = Parameter of Ramberg-Osgood equations  
 $\gamma$  = Shear strain; Amplitude of cyclic shear strain  
 $\gamma_A$  = Amplitude of cyclic shear strain  
 $\gamma_{IH}$  = Weight per unit volume of instrumented head  
 $\gamma_c$  = Weight per unit volume of inner cylinder  
 $\gamma_r$  = Shear strain developed in test soil in horizontal planes  
 $\gamma_{rA}$  = Amplitude of cyclic shear strain developed in test soil in horizontal planes  
 $\gamma_{ruA}$  = Peak shear strain developed in test soil in horizontal planes during ultimate cycle of loading  
 $\gamma_s$  = Total weight per unit volume of test soil  
 $\bar{\gamma}$  = Effective weight per unit volume of soil  
 $\zeta$  = ratio of damping to critical damping

- $\theta, \dot{\theta}$  = Rotation and rotational velocity of rigid inner cylinder  
 $\theta_A$  = Amplitude of cyclic rotation of rigid inner cylinder  
 $\theta_{AL}$  = Limiting amplitude of cyclic rotation of rigid inner cylinder  
 $\theta_i$  = Static twist of active portion of flexible inner cylinder  
 $\theta_{si}$  = Static rotation of rigid inner cylinder embedded in undegraded test soil due to static torque, T  
 $\theta_{suA}$  = Amplitude of low frequency (inertia and viscous damping forces negligible), cyclic rotation of rigid inner cylinder embedded in fully degraded test soil caused by low frequency, cyclic torque having amplitude, T  
 $\bar{\theta}$  = Static twist between ends of circular shaft  
 $\rho$  = Mass density of soil  
 $\bar{\sigma}_o$  = Average effective confining pressure  
 $\sigma'_o$  = Initial effective vertical stress  
 $\bar{\sigma}_v$  = Effective vertical stress  
 $\bar{\sigma}_{vi}, \sigma'_{vi}$  = Initial effective vertical stress  
 $\tau$  = Shear stress; Amplitude of cyclic shear stress  
 $\tau_A$  = Amplitude of cyclic shear stress  
 $\tau_h$  = Amplitude of cyclic shear stress applied to horizontal planes  
 $\tau_m$  = Average of shear strengths in horizontal and vertical planes  
 $\tau_{mo}$  = Undegraded shear strength  
 $\tau_r$  = Shear stress developed in test soil in horizontal planes  
 $\tau_{rA}$  = Amplitude of cyclic shear stress developed in test soil in horizontal planes  
 $\tau_{rs}$  = Shear stress developed in test soil, in horizontal planes, as a result of shear strain  
 $\bar{\phi}$  = Effective angle of internal friction  
 $\omega$  = Circular frequency in radians per second  
 $\omega_n$  = Damped natural circular frequency in radians per second

## INTRODUCTION

This report, to the National Science Foundation, covers work performed during Phase I of a planned three phase project. The purpose of the project is to develop an in situ testing procedure for determining in situ cyclic and dynamic soil properties. Phase I was a feasibility study, Phase II will be a research phase, and Phase III will be a commercialization phase. Phase I work was supported by a Small Business Innovation Research (SBIR) grant awarded to our firm, Dynamic In Situ Geotechnical Testing, Inc. The project falls under the domain of the Earthquake Hazard Mitigation program.

In the remainder of this report, we present and discuss, in detail, the purpose of the project, existing methods, the proposed method and its potential benefits, Phase I objectives, procedures, and accomplishments, and our estimate of feasibility. We also present technical definitions and terminology, discuss potential commercial applications and users, identify recipients of this report, provide references, and provide supplementary information in the appendices.

## PURPOSE OF PROJECT

In this section, we state the purpose of our project. We also summarize potential benefits, relevant definitions, and background information.

The purpose of our project is to develop an in situ geotechnical testing procedure for obtaining accurate and detailed descriptions of in situ cyclic and dynamic engineering soil properties. This information is required for earthquake analyses involving foundation soils. The level of accuracy and detail to be provided is intended to be appropriate for the intermediate and final stages of the analysis and design of important structures located in seismically active areas. Based on our experiences, we feel that there are no existing procedures for determining most of the soil properties of interest in the detail and to the accuracy that is needed for the effective use of the costly and potentially powerful analysis procedures used at the later stages of analysis and design.

If successfully completed, the project should advance earthquake hazard mitigation technology by advancing our ability to economically insure the integrity and reliability of soil-structure-equipment systems during earthquakes. These systems include earth structures (dams, embankments, etc.) as well as concrete and steel structures (buildings, offshore platforms, etc.). The testing procedure is intended to reduce potential for error and uncertainty in predicting site-specific earthquake ground motions and system response and stability. This should result in greater safety, reliability, and economy.

Specifically, we are developing an in situ testing procedure for defining accurately and in detail the in situ liquefaction and cyclic degradation characteristics of a soil, the low amplitude dynamic shear modulus, and the variation in the dynamic shear modulus with shear strain.

Herein, liquefaction is defined as the almost total loss of the stiffness and strength of a sand or silt. Liquefaction is caused by the buildup of excess porewater pressure in the soil. Degradation, a related phenomenon, which may occur in sands, silts, and clays, is the reduction in the stiffness of a soil. Both phenomena may be caused by cyclic loads resulting from earthquakes. The dynamic shear modulus is the shear stiffness of a material under dynamic loading. In soils, this property varies considerably with shear strain (24).

These soil properties are important because they significantly affect the excitation, response, and stability of soil-structure-equipment systems during earthquakes. Liquefaction primarily affects stability. It does so, for example, by reducing the bearing capacity of foundation soils, the integrity of earth structures, and the resistance of pile-founded structures to lateral loads. Liquefaction has caused considerable damage to soil-structure-equipment systems during recent earthquakes, notably in Alaska, 1964, and in Niigata, 1964 (28) (38). The low amplitude dynamic shear modulus of a soil deposit and the variation in the dynamic shear modulus with shear strain affect the nature of both the excitation to and the response of systems. The response of an earth structure is additionally affected by the dynamic shear modulus of the structure itself. Cyclic degradation of a soil during earthquakes affects excitation, response, and stability. Degradation

changes the stiffness of a soil deposit during an earthquake, and thus, changes the nature of the excitation to and the response of a system. Degradation changes the stiffness of an earth structure itself, and thus, additionally affects the nature of its response. Degradation, in a manner similar to liquefaction, but to a lesser degree, also affects the stability of soil-structure-equipment systems.

Because of the importance of these soil properties, they are required for earthquake analyses which predict the excitation to, response of, and stability of soil-structure-equipment systems. Such analyses serve as a basis for earthquake resistant design and include: 1) earthquake site response analyses used to estimate liquefaction potential and to obtain site-specific ground motion histories and design response spectra, 2) earthquake soil-structure interaction analyses used to obtain the response of soil-structure systems or the excitation to supported equipment, and 3) earthquake stability analyses used to predict the stability of natural slopes or the slopes of earth structures. Examples of earthquake analysis procedures are DESRA (12) and CHARSOIL (35).

Uncertainty and error in defining in situ soil properties will create uncertainty and error in the results of analyses relying on these properties. In fact, the limitations in our ability to accurately and descriptively define in situ soil properties can severely limit the effectiveness of the costly and potentially powerful analysis procedures which have been developed during recent years. To be effective, such analysis procedures, which are most appropriate for the intermediate and final stages of the analysis and design of important structures located in seismically active areas, require detailed and accurate descriptions of the in situ properties of interest.

By improving our ability to define the in situ soil properties of interest, in both accuracy and detail, we will reduce uncertainty and potential for error in the results of earthquake analyses. This will allow, in particular, the potential benefits of costly and potentially powerful analysis procedures to be realized to a far greater degree. This will result in greater safety, reliability, and economy of soil-structure-equipment systems constructed in seismically active areas and may eliminate earthquake resistance as a barrier to the feasibility of construction at a site.

## TECHNICAL DEFINITIONS AND TERMINOLOGY

In this section, we define and explain important technical terms used in this report. These terms include the low amplitude dynamic shear modulus, the variation in the dynamic shear modulus with shear strain, relative density, the degradation and liquefaction characteristics of sands and silts, and the degradation characteristics of clays.

Low Amplitude Dynamic Shear Modulus,  $G_0$ --Referring to Fig. 1, the low amplitude dynamic shear modulus is the slope, at low levels of shear strain (<0.001%), of the nonlinear shear stress-strain curve for a soil loaded dynamically. Generally, stress-strain behavior of soils at these levels of shear strain is linear. Reference 25 provides more detail.

Variation in Dynamic Shear Modulus with Shear Strain--As shown in Fig. 1, high levels of shear strain induce highly nonlinear shear stress-strain behavior in soils. As a result, the tangent shear modulus,  $G$ , may vary considerably with shear strain. Reference 24 provides more detail.

Relative Density,  $D_r$ , of a Sand or Silt--The relative density of a sand or cohesionless silt is a measure of the compactness of the arrangement of its grains. Relative density is indicated with a scale of 0 to 100%. A sand with a relative density of 0% is a structurally "loose" sand in its least compact state. A sand with a relative density of 100% is a structurally "dense" sand in its most compact state. The relative density of a sand or silt has a strong influence on its cyclic degradation and liquefaction characteristics. Generally, sands or silts with lower relative densities (<50%) have little resistance to degradation and liquefaction while sands or silts with higher relative densities (>70%) have high resistance. Reference 28 provides more detail.

Degradation and Liquefaction Characteristics of Sands and Silts--Under large, earthquake-type, cyclic shear loads, because of buildups in excess porewater pressure, the shear stiffness (slope of straight line through peaks of shear stress-strain curve) of a sand or silt may decrease with an increase in the number of cycles of loading. This cyclic decrease in shear stiffness is referred to as cyclic degradation. As shown in Fig. 2, the degradation of an element of soil, under a cyclic shear load having a uniform amplitude, may be observed as an increase in the amplitude of the resulting cyclic shear strain of the element with an increase in the number of cycles of loading. Under loadings corresponding to large earthquakes, loose sands will generally show severe degradation while dense sands will show only mild degradation. After a sufficient number of cycles of loading, the loose sands may undergo unrestrained deformation, which is termed liquefaction. Dense sands will not liquefy because of the restraining effects of dilation, the expansion of the volume of the structure of a soil due to shear load. Rather, a dense sand will show only limited deformations regardless of the number of cycles of loading. The frequently used term, initial liquefaction (28), identifies the instant, during cyclic loading, when the excess porewater pressure of an element of soil first rises to the level of the initial effective confining pressure. Initial liquefaction may occur in loose and in dense sands. References 28 and 29 provide more detail.

Degradation Characteristics of Clays--Under large, earthquake-type,

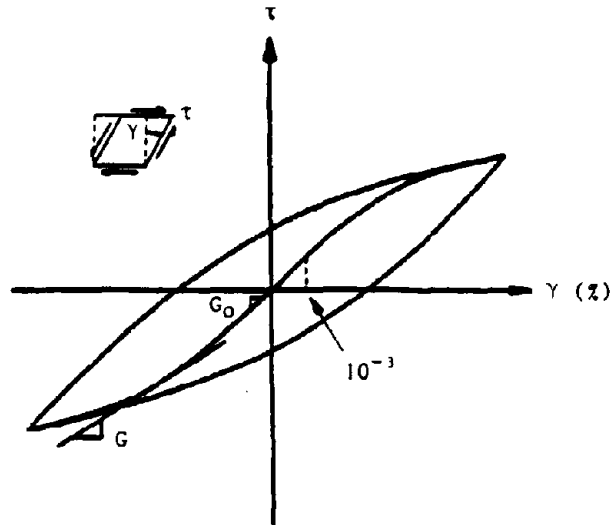


Figure 1: Nonlinear Shear Stress-Strain Curve for Soils

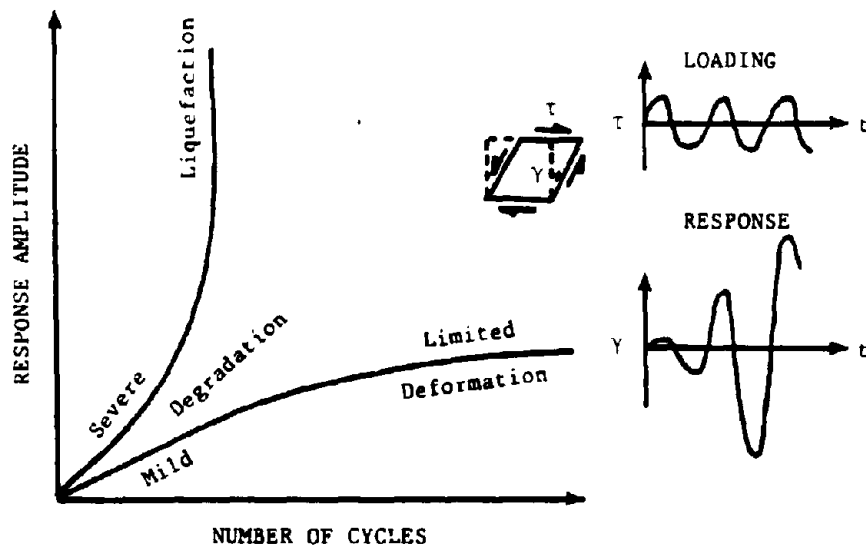


Figure 2: Degradation and Liquefaction

cyclic shear loads, because of buildups in excess porewater pressure and structural breakdown (21), the shear stiffnesses of clays may degrade similarly to those of sands and silts. Clays, however, generally do not liquefy (29). Instead, like dense sands, clays usually develop limited deformations after a large number of cycles of loading (see Fig. 2). References 20, 21, and 29 provide more detail.

## EXISTING METHODS

In this section, we critically review the existing methods for performing the functions of the proposed testing system. These functions include determining the cyclic degradation and liquefaction characteristics of a soil, the low amplitude dynamic shear modulus, and the variation in the dynamic shear modulus with shear strain.

We mainly discuss methods for determining degradation and liquefaction characteristics of soils. Providing in situ cyclic degradation and liquefaction characteristics, to a level of accuracy and detail appropriate for the intermediate and final stages of the analysis and design of important structures located in seismically active areas, is expected to be the main capability of the proposed testing system. Methods for determining in situ liquefaction and degradation characteristics are at an early stage of development and thus, involve considerable uncertainty and potential for error. Also, the consequences of uncertainty and error in estimates of in situ degradation and liquefaction characteristics are generally expected to be greater than those in estimates of dynamic shear moduli.

A number of significant advances have been made in the very active field of dynamic and cyclic soil testing (37); however, because of the need for safety, reliability, and economy in the massive or delicate soil-structure-equipment systems of the future, there is still considerable motivation for further advancement. The proposed testing procedure is intended to advance our ability to determine in situ cyclic and dynamic soil properties by overcoming some of the shortcomings of existing methods. These shortcomings can create error and uncertainty which can severely limit the effectiveness of costly and potentially powerful analysis procedures. Currently, the properties of interest are obtained either by laboratory testing of soil samples recovered from a site, in situ testing at the site, or a combination of these methods.

Laboratory testing is attractive because the soil properties of interest can be determined directly. That is, cyclic shear loads, representative of earthquakes, can be applied to samples to induce appropriate responses. Detailed information (for example, cyclic strain history), required at the intermediate and final stages of analysis and design, can be readily obtained, and laboratory testing is applicable to all soils. Additionally, laboratory testing offers the means to create conditions different from those existing in situ. However, laboratory testing suffers from the problem of disturbance to in situ conditions. This problem can lead to considerable uncertainty and potential for error in interpreted soil properties. We feel that this uncertainty and potential for error can be excessive for the intermediate and final stages of analysis and design and inconsistent with that introduced by analysis procedures appropriate for these stages.

Our experiences indicate that in situ conditions can be greatly disturbed and difficult to recreate. For example, during the recovery, transport, and test preparation of samples, loose sand samples may be densified significantly (28) leading to considerable uncertainty and potential for error in estimates of liquefaction resistance. In contrast, dense sand samples may be significantly loosened. Additionally, it is often difficult to recreate the in situ state of stress. This is because it is

often difficult and costly to determine this state of stress. Even when the state of stress has been determined, commonly used laboratory tests frequently cannot adequately recreate the defined state of stress. This difficulty leads to even further uncertainty and potential for error in estimates of liquefaction resistance. While freezing of samples has been offered as a means to minimize disturbances, based on our experiences, this process is complicated and can itself introduce considerable uncertainty and potential for error. Also, the in situ state of stress and degree of saturation may not be preserved. Arulmoli et al. (2) suggest the use of electrical measurements to reconstruct a sample to its original in situ state. This procedure may be difficult for two reasons: 1) we would expect considerable uncertainty in relating electrical measurements taken in laboratory samples to those taken in situ when in situ conditions are complex (i.e., many factors such as age and cementation act on soil, Ref. 28), and 2) it would be very difficult to recreate complex in situ conditions in laboratory samples. In addition to uncertainty and potential for error in estimates of liquefaction resistance, disturbance to in situ conditions may also cause considerable uncertainty and potential for error in interpreted degradation characteristics and shear moduli.

In situ testing overcomes, to a degree, some of the problems with laboratory testing since in situ conditions may be better preserved. However, our experiences with in situ testing have given rise to concerns which are unique to each property of interest.

Several concerns arise in determining liquefaction and cyclic degradation characteristics of sands and silts by in situ testing, and as pointed out by Woods (37), "...in situ evaluation of liquefaction potential remains elusive." We feel that there are no in situ methods which can provide the information on in situ cyclic degradation and liquefaction characteristics to the level of accuracy and detail appropriate for the intermediate and final stages of the analysis and design of important structures located in seismically active areas. The basic problem of most methods is that they are indirect methods. That is, loads corresponding to earthquakes are not applied to elements of soil and appropriate responses are not induced. Cyclic degradation and liquefaction are very complex phenomena which are functions of many parameters. Thus, measuring these phenomena indirectly may result in considerable uncertainty in deriving single parameters to describe liquefaction and degradation characteristics (for example, amplitude of cyclic shear stress needed for initial liquefaction in 10 cycles of loading, Ref. 29). As a result of additional assumptions, even greater uncertainty may result in deriving detailed information regarding cyclic degradation and liquefaction characteristics (for example, increase in cyclic shear strain amplitude with an increase in the number of cycles of loading). In situ methods for determining liquefaction and degradation characteristics are discussed in the following paragraphs.

Currently, tests for determining in situ liquefaction resistance involve penetrating devices into the ground. Liquefaction resistance is estimated from penetration resistance (29). Penetration tests are useful for the preliminary stage of analysis or design. Additionally, penetration tests may be used to extrapolate detailed and accurate information over a site and to

identify locations where further detailed and accurate information should be obtained.

However, penetration tests would not be expected to provide information on cyclic degradation and liquefaction characteristics to a high level of certainty. With penetration testing, one concern, believed to cause considerable scatter in data relating penetration and liquefaction resistances, is that the loading of the soil and its mode of failure are considerably different from those induced by earthquakes. In the cone penetrometer test (CPT), a cone is slowly pushed into the soil, and in the standard penetration test (SPT), an open cylinder is violently driven into the soil. In each case, the failure of the soil is immediate and severe. In contrast, earthquake-induced loads are cyclic and generally of lower intensity. The soil fails by gradually losing its resistance to load over a number of cycles of loading. A second concern, resulting from the fact that penetration resistance is an indirect measure of liquefaction resistance and also believed to cause considerable scatter in data relating liquefaction and penetration resistances, is the effect of the numerous factors such as age, past seismic history, and cementation which can affect the properties of a soil (28). Although it is argued that these factors affect the two resistances in directionally the same manner (28), because of the differences in loading and failure discussed above, the factors are unlikely to affect both resistances to the same degree. Thus, it is easily conceived that two soils having a given penetration resistance may have two different liquefaction resistances. As a result of scatter and the need for safety, design curves relating liquefaction and penetration resistances are very conservative. Use of such curves may lead to excessively, and possibly prohibitively, costly designs. Furthermore, correlations are not available for all soils which could liquefy (for example, calcareous soils).

New in situ approaches for inferring in situ degradation and liquefaction characteristics are being advanced. Sasaki and Koga (27) propose the use of a vibrating cone penetrometer to estimate liquefaction resistance. The force required to advance a vibrated cone penetrometer at a controlled rate or the difference between the forces required to advance the cone penetrometer with and without vibrations is taken as an indicator of liquefaction resistance. The static component of this test (penetration without vibrations) is expected to share the advantages and disadvantages of the CPT discussed in the previous paragraph. However, the vibratory component is not expected to offer a strong advantage over the conventional CPT in evaluating liquefaction resistance. While vibratory loads are more appropriate for estimating the potential for earthquake-induced liquefaction, the results from the vibratory component of the vibratory cone penetrometer test would be expected to be dominated by the cyclic properties of the zone of soil immediately adjacent to the tip and sides of the cone. This zone would be highly disturbed as a result of displacement by the cone. This displacement would be expected to alter greatly the most important factors affecting liquefaction resistance: relative density, structure, the in situ state of stress, cementation, effects of stress history, etc. (28).

Dobry et al. (10) and Stokoe and Nazarian (34) propose the use of in situ shear wave velocity as an indicator of in situ liquefaction susceptibility. Dobry et al. (10) combine shear wave velocity measurements

with the concept of the strain approach. This results in a convenient, simplified procedure for predicting the threshold ground acceleration below which excess porewater pressures will not develop. Shear wave velocity, used with or without the strain approach, is potentially a useful indicator of liquefaction susceptibility appropriate for the preliminary stage of analysis or design. Additionally, shear wave velocity measurements, which may be conveniently made (at least for onshore sites) (34), are potentially useful for extrapolating detailed and accurate information over a site and identifying locations where further detailed and accurate information should be obtained.

However, approaches based on shear wave velocity would not be expected to provide detailed information on cyclic degradation and liquefaction characteristics to a high level of accuracy. Shear wave velocity, like penetration resistance, is an indirect measure of liquefaction resistance during earthquakes. The low levels of loading generally induced in a soil by shear waves and the responses developed do not generally correspond to the loads and responses developed during large earthquakes. Thus, like the use of penetration resistance, the use of shear wave velocity as a measure of liquefaction resistance during earthquakes would be expected to involve excessive uncertainty for higher stages of analysis and design. This is supported by the work of DeAlba et al. (8). They observed, from laboratory tests, that samples may show similar shear wave velocities but very different resistances to liquefaction. Additionally, it is difficult to determine shear wave velocity offshore; however, considerable effort is being directed toward this problem (33) (26).

Castro et al. (5) propose the use of an in situ vane shear test to provide an indication of in situ liquefaction resistance. The difference between the in situ shear resistance of a soil at high strain, and the shear resistance of the soil at high strain under a constant confining pressure corresponding to the initial in situ pressure, is taken as an indicator of liquefaction resistance. This difference provides a measure of the in situ potential for the contraction or dilation of a cohesionless deposit under shear loads. This procedure, although slightly more complicated than other in situ index tests because of the need for additional information, is potentially a useful indicator of liquefaction resistance appropriate for the preliminary stage of analysis or design. The procedure is also potentially useful for extrapolating detailed and accurate information over a site and identifying locations where further detailed and accurate information should be obtained.

However, this approach would not be expected to provide detailed information on cyclic degradation and liquefaction characteristics to a high level of accuracy. Like the other index tests discussed, this method is indirect. The high levels of noncyclic shear loads applied to the soil and the noncyclic responses developed do not correspond to the loads and responses developed during earthquakes. Thus, this method would be expected to involve excessive uncertainty for advanced stages of analysis and design. While Castro et al. did apply cyclic, earthquake-type loads with the vane, they apparently did this only to compare static behavior before and after the application of the cyclic loads. Since this method has much in common with our proposed method, we mention further aspects of this method in the sections entitled PROPOSED METHOD, pg. 21, and ESTIMATE OF FEASIBILITY, pg. 83.

Arulmoli et al. (2) propose the use of electrical measurements to determine liquefaction and degradation characteristics. Detailed information concerning the in situ liquefaction and degradation characteristics of sandy soils may be derived from correlations between liquefaction and degradation characteristics and combinations of various electrical parameters. The electrical parameters are obtained from the in situ measurement of electrical quantities. The electrical parameters are potentially useful indicators of liquefaction resistance appropriate for the preliminary stage of analysis or design. Additionally, as with other index tests, the electrical method is potentially useful for extrapolating detailed and accurate information over a site and identifying locations where further detailed and accurate information should be obtained.

However, electrical measurements would not be expected to provide detailed information on cyclic degradation and liquefaction characteristics to a high level of accuracy. The electrical method is clearly an indirect method. Additionally, it is not apparent how in situ factors such as the in situ state of stress and cementation would be taken into account. For example, Arulmoli et al. (2) appear to indicate that electrical measurements are fairly insensitive to the state of stress. Thus, like other indirect methods, the electrical method would be expected to involve considerable uncertainty in estimating liquefaction and degradation characteristics. The level of uncertainty would be expected to be excessive for the intermediate and final stages of analysis and design.

Esashi et al. (11) and Briaud and Meyer (4) propose the use of cyclic pressuremeters for determining the cyclic degradation characteristics of soils. Using this procedure, cyclic lateral pressures are applied through a cylindrical rubber membrane to the cylindrical wall of the soil in which the pressuremeter is embedded. The cyclic lateral movement of the membrane is estimated. The procedure has two important features: 1) the procedure is direct, and 2) the procedure is conducted in situ and when using the self boring capability (1), would not be expected to introduce excessive disturbance to the test soil. Thus, assuming adequate analytical procedures exist for interpreting test results, the procedure would be expected to provide information appropriate for advanced stages of analysis and design. Because of the nature of the loading induced by the cyclic pressuremeter, it would be expected to be effective for predicting the behavior of foundations subjected to cyclic lateral loads generated from above the foundation (for example, behavior of offshore piles subjected to wave loading).

However, the cyclic pressuremeter is expected to have several significant drawbacks with respect to determining the behavior of soils during earthquakes. These drawbacks would be expected to create excessive uncertainty in deriving in situ cyclic degradation and liquefaction characteristics to the level of accuracy and detail appropriate for the intermediate and final stages of the analysis and design of important structures located in seismically active areas. The drawbacks include 1) apparent limitations on the intensity of the applied cyclic loads, 2) potentially excessive drainage from the test soil during testing, and 3) poorly defined boundaries for the test soil.

The intensity of the cyclic load which can be applied appears to be limited because the pressuremeter seems to be able to load the soil

effectively only after exceeding the original in situ lateral stress. Unloading below this level appears to result in unrepresentative stress-strain behavior (3). Thus, it would appear that the peak to peak cyclic shear stress which may be induced in the test soil by the pressuremeter may be somewhat less than 1/2 of that which could be induced by large earthquakes. This would be expected to limit considerably the ability of the pressuremeter to induce cyclic degradation and liquefaction and may be one reason why material degradation (see Degradation and Liquefaction Characteristics of Sands and Silts, pg. 4) does not seem to be particularly significant during a cyclic pressuremeter test in a highly plastic clay (Fig. 2, Ref. 3). This may also be one reason why results from cyclic pressuremeter tests presented by Esashi et al. (11) do not appear to show the level of cyclic degradation expected in soils subjected to earthquake loadings. Their data indicates a decrease in the modulus of deformation of only about 30% during the first 20 cycles of loading when testing a "soft silt". After this the modulus stabilized. Their data also shows that the modulus of a "comparatively hard" soil remained unchanged over about 200 cycles of loading.

Excessive drainage would be expected during the cyclic testing of permeable sandy soils because the pressuremeter does not provide barriers to drainage. When using a vane shear device, Castro et al. (5) observed substantial drainage during somewhat comparable cyclic tests in sandy soils. The vane shear device also does not provide barriers to drainage. Generally, earthquakes can induce high levels of degradation and liquefaction because significant drainage does not occur leading to increased excess porewater pressures and decreased effective stresses. Thus, when cyclically testing sandy soils with the pressuremeter, the levels of cyclic degradation expected during earthquakes may not be observed. Additionally, the effects of volumetric changes of the soil structure permitted by drainage are expected to be complex and difficult to estimate. It could be easily visualized that under cyclic loading a freely draining soil could densify, and in the absence of high porewater pressure, actually increase in rigidity with an increase in the number of cycles of loading. Excessive drainage may partially explain the low levels of degradation which seem to have taken place during the tests conducted by Esashi et al. (11).

Finally, the poorly defined boundaries of the test soil may present some difficulty. Drainage, stresses, and strains may be distributed over a relatively large region in a complex manner. This may create uncertainties in analytical modeling. As a result, interpretation of test results in terms of the cyclic degradation and liquefaction characteristics of the test soil would be expected to be relatively difficult.

To our knowledge, there are no commonly used in situ testing procedures for determining the in situ cyclic degradation characteristics of clays to the level of accuracy and detail appropriate for the intermediate and final stages of the analysis and design of important structures located in seismically active areas. The level of effort that has been and still is being directed at determining the in situ behavior of sands and silts during earthquakes does not appear to have been directed at determining the in situ behavior of clays.

An example of recent work in determining the cyclic degradation characteristics of clays is the work of Briaud et al. (3). They discuss the

testing of clays using a cyclic pressuremeter. As indicated previously, the cyclic pressuremeter offers considerable potential for certain important problems, but is expected to have drawbacks with regards to determining the behavior of soils during earthquakes. We feel the most serious drawback with regard to testing clayey soils would be the apparent limitation on the intensity of the applied cyclic stress and thus, on the potential to induce cyclic degradation. Drainage would not be expected to be a problem when testing clays using the pressuremeter. As a result, the difficulties presented by a poorly defined sample would not be expected to be as large when testing clays as when testing sands.

To our knowledge, there are no commonly used in situ testing procedures for determining the in situ variation in the dynamic shear modulus with shear strain. However, considerable effort has been directed toward developing this capability. References 1 and 37 discuss in detail past efforts, pointing out strengths and drawbacks of various proposed procedures.

Examples of recent work toward providing in situ testing procedures for determining the in situ variation in the shear modulus with shear strain include pressuremeter studies conducted by Esashi et al. (11) and Briaud et al. (3) and developmental work undertaken by Sidey et al. (31).

The pressuremeter appears to be a potential means for determining the variation in the shear modulus with shear strain. The greatest source of uncertainty in interpreting shear moduli from test results would be expected to be poorly defined sample boundaries. Since, in general, volume change, porewater pressure buildup, and drainage would not be expected to be dominant factors in tests for determining shear moduli, this uncertainty may not be excessive.

Sidey et al. (31) presented feasibility and preliminary studies for a borehole shear device. This device also appears to be a potential means for determining the variation in the shear modulus with shear strain. With this system, which is conceptually similar in some respects to our proposed system, a single cylinder will be embedded into the test soil below the base of a borehole. The cylinder will be excited cyclically in torsion and the in situ variation in the shear modulus with shear strain will be inferred from the response of the system. Uncertainty would be expected in interpreting soil properties since the boundaries of the test soil will not be particularly well defined. However, as with the pressuremeter, this uncertainty may not be excessive. The system does not appear to be compact and portable; thus, the system would be expected to be difficult to use in harsh (for example, offshore) or confined (for example, indoors) environments.

There are a number of in situ methods in use for determining the in situ low amplitude dynamic shear modulus; however, each has drawbacks or limitations as discussed in detail in Ref. 37. For example, the widely accepted seismic crosshole test, in which the wave propagation velocity in a soil is measured, requires at least two boreholes; thus, this test may be relatively expensive and difficult to use in confined or harsh environments.

Recently, testing procedures have been advanced for determining the low amplitude dynamic shear modulus within a single borehole. These procedures

include wave propagation procedures such as one developed by the Oyo Corporation in Japan (no known reference) and one developed by K. H. Stokoe et al. (33). With the Oyo system, the wavespeed of waves propagated along the wall of a borehole is measured. Since these walls are generally quite disturbed from the drilling process, measured wavespeeds are not expected to correspond to wavespeeds in undisturbed soils. To our knowledge, the system developed by K. H. Stokoe et al. has not yet been applied in practice. An alternative procedure developed by Hardin (14) involves a harmonically rotating, cone-ended, torsional sleeve which may be either penetrated below the base of a borehole or lodged against the walls of the borehole. In either mode, the test soil is expected to be disturbed. The borehole wall would have been disturbed by the drilling process, and, in penetrating the cone-ended device below the base of a borehole, much of the soil in the test zone would have been displaced by the device.

## PROPOSED METHOD

In this section, we describe the proposed testing procedure in some detail and discuss the major features of the procedure and various potential modes of operation.

The proposed testing procedure is intended to provide accurate and detailed descriptions of in situ cyclic and dynamic soil properties. This information is needed for earthquake analyses involving foundation soils. The level of accuracy and detail to be provided is intended to be appropriate for the intermediate and final stages of the analysis and design of important structures located in seismically active areas. Alternatively, the procedure could be used as an index test.

The testing procedure is intended to effectively combine attractive features of laboratory and in situ testing while minimizing shortcomings. The method will be direct. Cyclic earthquake-type shear loads will be applied to a well-defined element of soil in a simple but effective manner. The response of the test soil is expected to correspond closely to behavior during earthquakes. Thus, uncertainties associated with the loading of the soil and its mode of failure will be reduced. Tests will be conducted in situ and a number of steps will be taken to minimize disturbances to in situ conditions. Thus, the very important effects of in situ factors are expected to be captured in measurements. Several features are to be provided to help induce the phenomena of interest and to simplify the interpretation of test results. The information needed by earthquake analyses will be directly provided, minimizing intermediate interpretation. Also, the procedure is expected to apply to most soils of interest. Finally, the method will require only a single borehole so that it may be used in confined and harsh environments.

Figures 3 and 4 show, schematically, the main components of the probe of the testing system. Equipment above the probe is not shown. Using conventional equipment and procedures, two concentric, thin-walled cylinders will be carefully penetrated below the base of the borehole. The test soil will be the well-defined annular zone of soil between the two cylinders. A cyclic or impulsive torque or cyclic rotation of selected amplitude will be applied to the inner cylinder about its vertical axis to induce simple, earthquake-type shear stresses and strains in the test soil. In response, the cylinder is expected to rotate or develop torque in a manner dependent on the shear properties of the test soil. Both the torque and rotation will be measured by transducers in the instrumented head<sup>1</sup>. Secondary responses such as the buildup in excess porewater pressure could also be measured. The torsional shear stress-strain distributions that are expected to develop within the test soil, while not complex, will be nonuniform; thus, soil properties will be inferred by modeling tests analytically (soil-probe

<sup>1</sup>De Domenico (9) was awarded a patent in 1982 for a two cylinder testing system for determining the static strength of soils. This system is configured similarly to ours but functions differently than ours. After penetration, the inner cylinder is removed leaving a pressurized membrane in its place. Thus, lateral pressure is imposed on the test soil. An annular piston located between the two cylinders applies a vertical load to the test soil causing the soil to fail statically.

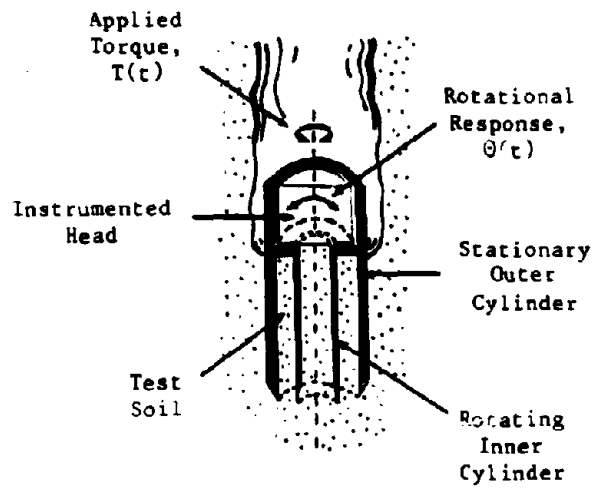


Figure 3: Probe in Borehole Setting (Main Elements Only)

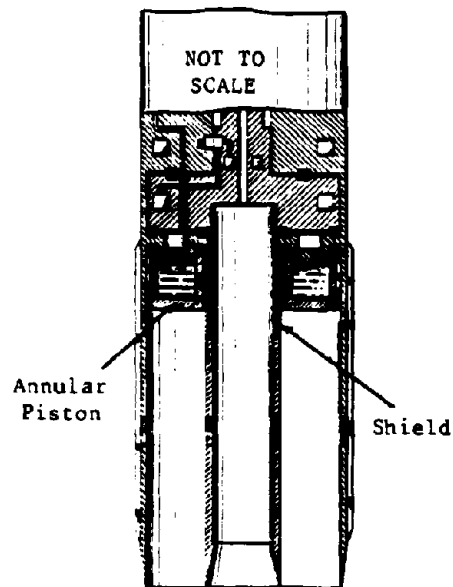


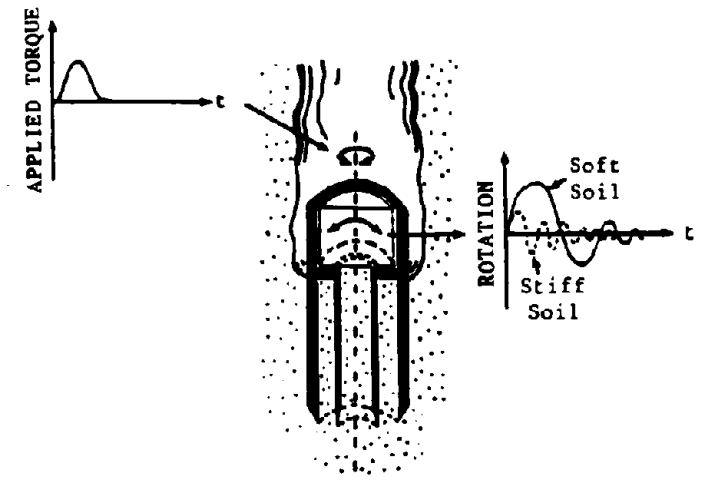
Figure 4: Detailed Schematic Diagram of Probe (Patent Pending)

interaction analysis) using available, well-tested, and easily adaptable analysis procedures. Soil properties will be iteratively assumed until computed and measured results agree acceptably. The final assumed properties are expected to closely represent the in situ properties.

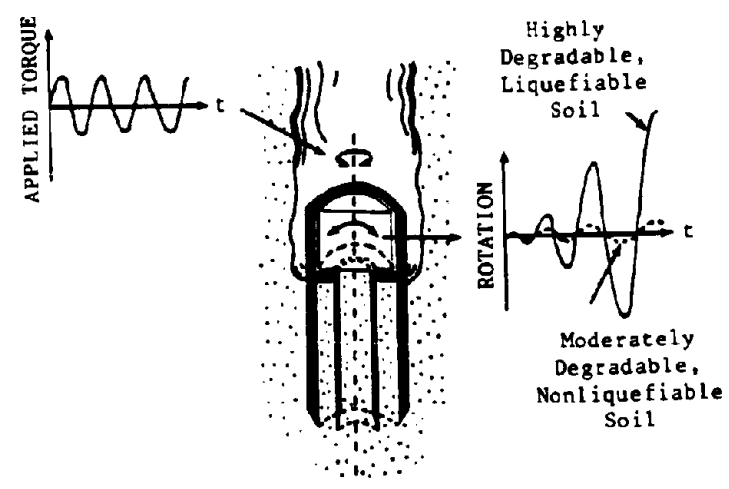
For demonstrative purposes, Fig. 5 presents, schematically, what we would expect to be the most commonly used testing sequence. First, an impulse test would be conducted to determine dynamic shear moduli. An impulsive torque would be applied to the inner cylinder. As shown in Fig. 5(a), the amplitude, frequency, and rate of decay of the oscillating rotational response of the inner cylinder would be expected to be strongly related to the shear stiffness of the test soil. For example, when testing stiffer soils with higher shear moduli, we would expect the inner cylinder to oscillate at lower amplitudes and higher frequencies.

After the impulse test, a low frequency, cyclic test would be conducted to determine degradation and liquefaction characteristics. A cyclic torque having a uniform amplitude would be applied to the inner cylinder. As shown in Fig. 5(b), the rate of increase in the amplitude of the cyclic rotation of the inner cylinder and the ultimate value of this amplitude would be expected to be strongly related to soil characteristics. When testing highly degradable, liquefiable soils (loose sands), under appropriate levels of loading, we would expect rapid increases in the amplitude of rotation of the inner cylinder with an increase in the number of cycles of loading. When testing such soils, if the excess porewater pressure were to rise to the level of the confining pressure, liquefaction, resulting in virtually unrestrained rotation of the inner cylinder, would be expected. When testing more easily liquefiable soils, we would expect liquefaction in fewer cycles. As shown in Fig. 5(b), when testing moderately degradable, nonliquefiable soils (dense sands, clays), we would expect only gradual increases in the amplitude of the rotation of the inner cylinder with an increase in the number of cycles of loading. When testing dense sands, because of the restraining effect of dilation, the inner cylinder would not be expected to undergo unrestrained rotation regardless of the level of excess porewater pressure. Generally, unrestrained rotations would not be expected when testing clays either.

Currently, the testing procedure is to consist of a number of important features and to involve important steps to preserve in situ conditions. Both inner and outer cylinders are to have thin walls. As shown in Figs. 3 and 4, the penetrating edges of the cylinders will be shaped to minimize disturbance to the test soil during penetration. The inside of the outer cylinder and the outside of the inner cylinder will be coated with a low friction material to minimize disturbance to the test soil caused by shear during penetration and to minimize the development of residual shear stresses in the test soil prior to testing. These surfaces are to be grooved vertically to minimize slip during testing without excessively disturbing the test soil during penetration. Additionally, we will relieve the penetration force prior to testing to minimize static stresses developed in the test soil as a result of penetration. We will also incorporate features to minimize the influence of the soil within the inner cylinder on the motion of this cylinder. The smooth inner wall of this cylinder will be coated with a low friction material, soil will be diverted away from the inner wall by juted penetrating edges, shown in Fig. 4, and confining pressures acting on the



(a) Impulse Test



(b) Cyclic Test

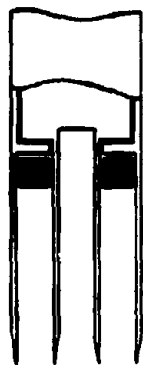
Figure 5: Possible Testing Sequence

soil within the inner cylinder will be minimized by providing excess volume. The upper portion of the rotating inner cylinder will be shielded as shown in Fig. 4. Thus, only the soil some distance below the base of the borehole will be excited and effects of the disturbances near the base of the borehole will be reduced. An annular piston, shown in Fig. 4 and located between the two cylinders, will apply an appropriate vertical pressure to the top of the test soil to recreate, as closely as possible, the vertical state of stress existing prior to removal of soil from the borehole.

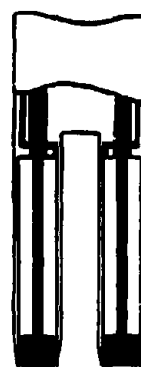
Two vertical pressure systems have been under consideration. The simplest system would use a short stroke piston as shown in Fig. 6(a). Using this system, a selected vertical pressure would be applied after penetration. Because of the low friction of the walls of the inner and outer cylinders, prior to the application of the vertical stress the test soil would be expected to be almost unloaded. After the application of the selected vertical pressure, because of the low friction and the rigidity of the walls of the cylinders, the lateral stress developed in the test soil would be expected to correspond closely to that developed in a normally consolidated level deposit. This is a very common practical condition and simple shear tests have been configured to simulate this condition. In many practical cases, the in situ lateral stress would be expected to either equal or exceed the lateral stress corresponding to this condition. Thus, information on liquefaction and degradation characteristics related to stability, obtained under this condition, would generally be conservative. Test results could be corrected, if necessary, for different lateral pressures as is commonly done in laboratory testing (28). Clearly, this would introduce uncertainty.

The second somewhat more complex system, shown in Fig. 6(b), will consist of a long stroke piston which will move along the entire length of the two cylinders. Similar piston systems have been used in samplers to prevent excessive deformations during sampling (36). With this system, the unloading of the test soil during penetration should be minimized and the original in situ stresses acting on the test soil should be preserved reasonably well. A selected vertical pressure would be applied at an early stage during penetration. Because of the low friction of the cylinder walls, elements of soil immediately ahead of the penetrating cylinders would be expected to be subjected to approximately the vertical stress existing prior to removal of soil from the borehole. The lateral stresses acting on these elements and the lateral deformations of these elements in response to the applied vertical stress would be expected to be reasonably close to those existing prior to the removal of soil from the borehole. The passage of the cylinders over an element would not be expected to alter the state of stress and deformation of the element greatly because of the geometry, low friction, and rigidity of the cylinders and the presence of the vertical pressure. Thus, with this system we would expect to preserve the in situ state of stress reasonably well. Additionally, pressurizing the test soil early during penetration is expected to reduce penetration-induced changes in void ratio.

We plan to use the simpler system shown in Fig. 6(a) during the initial stages of research. During these stages, identifying the torque-rotation characteristics of the testing system is of primary concern. This can be done more effectively using the simpler vertical pressure system. Should the testing system prove to be effective with the simpler system, we would then



(a) Short Stroke Piston System



(b) Long Stroke Piston System

Figure 6: Vertical Pressure Systems

develop the second, more refined system.

Several features of the proposed testing system are expected to help induce the main phenomena of interest, cyclic degradation and liquefaction. We expect to be able to apply shear loads to the test soil equally effectively in either direction. Thus, there should not be test-imposed limitations on the peak to peak amplitudes of the cyclic excitations which can be applied. Therefore, we should be able to induce reasonably well the cyclic degradation expected during earthquakes. The outer cylinder and the piston are intended to impede the flow of water from the test soil during cyclic tests carried out on permeable sands and silts. This should promote the buildup in excess porewater pressure and thus, the development of cyclic degradation and liquefaction. Alternatively, the outer and inner cylinders, and the piston may function to impose approximately constant volume conditions on the test soil. In this mode, instead of relying on excess porewater pressure, we would be relying on constant volume conditions (13) to bring about the cyclic changes in effective confining pressure which give rise to the cyclic degradation and liquefaction of sands and silts. Finally, the outer cylinder would serve to confine the excitation energy in a relatively small zone of soil. Thus, relatively high stresses should be obtainable with a minimum of power.

Also, several features of the proposed testing procedure are intended to simplify the interpretation of test results bringing the test within the descriptive capabilities of state-of-the-art analyses. The configuration of the probe is intended to promote the development of a relatively simple state of axisymmetric torsional shear stress and strain in the test soil. This state is expected to be relatively easy to model with respect to stresses, strains, and porewater flow. Additionally, the inner and outer cylinders, and the piston will provide relatively well-defined boundaries which are expected to be relatively easy to describe analytically. These boundaries will also help isolate the test soil from its surroundings. Thus, complex interactions between the test soil and its surroundings should be reduced. Such interactions were identified by Castro et al. (5) as possible explanations for certain trends in the results from vane shear tests in sands. Finally, the testing system will be designed to test relatively long samples so that effects of end conditions will be reduced.

We plan to use a descriptive soil-probe interaction analysis to accurately infer in situ soil properties from test results. References 17, 18, and 19, describe an applicable analysis procedure which was conceived and developed by the technical advisor of our firm. This multidimensional, dynamic, nonlinear, continuum analysis procedure has been proved capable of accurately simulating the torsional, dynamic behavior of an axisymmetric, soil-rigid body system. The analysis treats the soil as a nonlinear, inelastic continuum and permits slip between the continuum and the rigid body. This analysis will allow us to determine the low amplitude dynamic shear modulus and the variation in the dynamic shear modulus with shear strain. To be able to determine cyclic degradation and liquefaction characteristics, we will extend the soil modeling to describe the degradation of soil stiffness, liquefaction, and the flow of porewater within and out of the test soil during testing. Appropriate modeling for these extensions is discussed in Refs. 12, 20, and 22.

Until appropriate models are well-developed, we will be unable to model precisely the behavior of dense sands and silts at high levels of excess porewater pressure. Current, commonly used, state-of-the-art models, such as the ones we plan to use, do not model dilation. At this time, we do not consider this limitation severely restrictive. The sands and silts that pose the greatest problems in providing earthquake resistant structures are looser sands and silts.

The proposed procedure should provide, with a minimum of intermediate interpretation, the information required by commonly applied earthquake analysis procedures such as DESRA (12) and CHARSOIL (35). This is because the soil modeling to be used in the soil-probe interaction analysis will be almost identical to that used in such analysis procedures.

Variations on tests are expected to be possible. Rather than an impulsive torque, a high frequency, cyclic torque could be applied to the inner cylinder. This would be intended to give resonant response from which shear moduli could be inferred. Similarly, low frequency, cyclic, controlled-rotation tests could be used to determine degradation and liquefaction characteristics of sands and silts, rather than low frequency, cyclic, controlled-torque tests.

Additionally, low frequency, cyclic tests involving sands and silts could be conducted in two different modes, a constant pressure mode and a constant volume mode. In the constant pressure mode, we would rely on excess porewater pressure to cause the changes in effective confining pressure which lead to the cyclic degradation and liquefaction of the test soil. In this mode, the pressure initially applied by the vertical pressure system would be maintained throughout a test. Tests would be carried out at frequencies high enough to permit the development of significant excess porewater pressure, yet low enough to allow the effective simulation of earthquakes. In the constant volume mode, we would rely on approximately constant volume conditions (13) imposed on the test soil to bring about the changes in effective confining pressure which lead to cyclic degradation and liquefaction. In this mode, after the application of the selected vertical pressure, the position of the piston would be maintained throughout a test. Some boundary flexibility would, however, exist at the upper and lower ends of the test soil. Tests would be carried out at frequencies low enough to avoid the development of significant excess porewater pressure.

## POTENTIAL BENEFITS

In this section, we discuss the main potential benefits of the proposed testing system. These benefits, which include technical, safety, and economic benefits, are first discussed in general and then in detail.

The proposed in situ testing procedure is intended to advance our ability to economically insure the integrity and reliability of soil-structure-equipment systems during earthquakes. It is to do so by providing more accurate and detailed descriptions of in situ cyclic and dynamic soil properties than can currently be provided. This would allow more effective use of the costly and potentially powerful analysis procedures used at the intermediate and final stages of the analysis and design of important structures located in seismically active areas.

Currently, the effectiveness of such analysis procedures is limited by our inability to define cyclic and dynamic soil properties accurately and in detail. Thus, defining these properties more accurately and in greater detail will reduce uncertainty and the potential for error in predicted site-specific earthquake excitations and predicted responses and stabilities of soil-structure-equipment systems during earthquakes. In turn, this will lead to greater safety, reliability, and economy of soil-structure-equipment systems.

Technically, the proposed testing procedure should provide more accurate and detailed descriptions of cyclic and dynamic soil properties by effectively combining attractive features of in situ testing and laboratory testing while minimizing shortcomings. The procedure will be direct. Cyclic earthquake-type shear loads will be applied to a well-defined element of soil in a simple but effective manner. The response of the test soil is expected to correspond closely to behavior during earthquakes. Thus, uncertainties associated with the loading of the soil and its mode of failure will be reduced. Tests will be conducted in situ and a number of steps will be taken to preserve in situ conditions. Thus, the very important effects of in situ factors are expected to be captured in measurements. Several features are to be provided to help induce the phenomena of interest and to simplify the interpretation of test results. The method should apply to most soils of interest. Also, by simulating tests analytically using models very similar to those used in earthquake analysis procedures, the method will provide, with a minimum of intermediate interpretation, the soil properties required for earthquake analyses. Finally, the method will require only a single borehole, so that it may be used in confined and harsh environments.

The technical benefits of the proposed testing procedure are expected to produce significant safety benefits. For example, a loose sand sample may densify an unknown amount because of disturbances during recovery, transport, and test preparation. As a result, the sample may show greater resistance to liquefaction in a laboratory test than the sample had in the field. The same sample may also lead to overestimates in dynamic shear moduli or degradation resistance. This may lead to unconservative estimates of site-specific earthquake ground motions for soil-structure-equipment systems with low natural frequencies (offshore structures, for example). Thus, laboratory testing may lead to unconservative estimates of soil behavior. In contrast, the proposed testing procedure, which is expected to minimize disturbances,

would be expected to reduce the possibility of unconservative estimates of soil behavior.

The technical benefits of the proposed testing procedure are also expected to produce significant economic benefits without a reduction in the targeted level of safety. For example, a dense sand sample may be loosened during recovery, transport, and test preparation. As a result, in a laboratory test, the sample may show less resistance to liquefaction than the sample had in the field. The same sample may also lead to underestimates in dynamic shear moduli and degradation resistance. This may lead to excessively conservative and costly predictions of site-specific earthquake ground motions for soil-structure-equipment systems with low natural frequencies (offshore structures, for example). Thus, laboratory testing may lead to excessively conservative and costly estimates of soil behavior. In contrast, the proposed testing procedure, which is expected to minimize disturbances, would be expected to reduce the possibility of excessively conservative estimates of soil behavior.

Additionally, the proposed testing procedure may affect feasibility decisions and design considerations. For example, using this procedure to more fully and accurately account for in situ factors may prove a liquefaction resistant structure to be economically feasible at a marginal site. Similarly, for a superior site, use of the procedure may eliminate the costly need to design and construct a structure to resist liquefaction. (The additional cost for designing and constructing a large offshore platform to resist a modest amount of liquefaction is conservatively estimated to be several million dollars.) These possibilities arise as a result of the very significant effects of in situ factors (age, stress history, etc.) on liquefaction resistance (28). For example, from Fig. 7 it may be inferred that in situ factors can increase the resistance of a soil to initial liquefaction by a factor of 2 to 3.5. Based on our experiences, we believe that such and even lesser factors can have dramatic effects on estimates of the potential for liquefaction and its extent. Thus, using a procedure such as the proposed procedure to preserve in situ conditions can be important to feasibility decisions and design considerations.

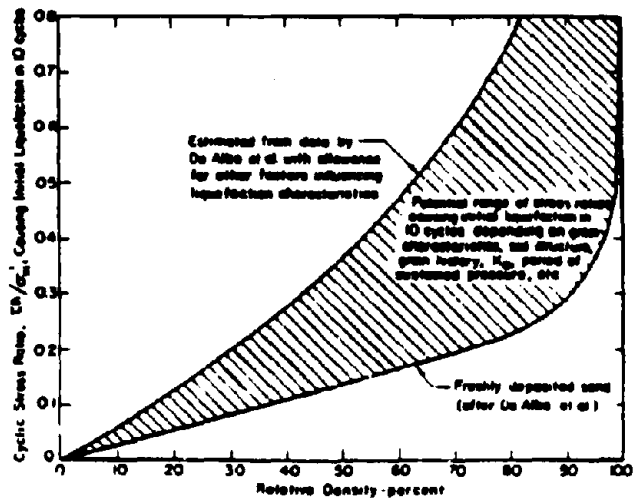


Fig 2D ESTIMATED RANGE OF LIQUEFACTION CHARACTERISTICS FOR IN-SITU DEPOSITS

Figure 7: Effects of In Situ Factors on Resistance of Soil to Initial Liquefaction (after Seed, 1976)

### POTENTIAL COMMERCIAL APPLICATIONS AND USERS

In this section, we discuss the potential commercial applications of the proposed testing procedure. We also identify potential users of the procedure or of the information provided by the procedure.

There are several important potential worldwide commercial applications of the proposed testing procedure. Generally, the procedure is expected to be useful for determining in situ cyclic and dynamic engineering soil properties before, during, and after the construction of soil-structure-equipment systems. The main application of the testing procedure is intended to be the design, construction, and maintenance of soil-structure-equipment systems to insure resistance to earthquakes. Additionally, the procedure is expected to apply to the design, construction, and maintenance of 1) soil-structure-equipment systems to insure resistance to water wave and blast loads, 2) machine foundations, and 3) delicate soil-structure-equipment systems to insure isolation from vibrations.

Also, there are a number of potential users of the proposed testing procedure or of the information provided by the procedure. Potential users include organizations involved in construction related activities, for example, agencies of governments, universities, geotechnical engineering firms, oil companies, and power companies.

#### RECIPIENTS OF REPORT

The Office of Energy-Related Inventions (OERI) of the National Bureau of Standards (NBS) is the only other organization, outside the NSF, which will receive copies of this report. Currently, the OERI is evaluating the proposed testing procedure for possible support from the Department of Energy (DOE). The proposed testing procedure has been advanced to the second stage of evaluation by the OERI.

## PHASE I OBJECTIVES, PROCEDURES, AND ACCOMPLISHMENTS

In this section, we discuss, in detail, the Phase I research objectives, procedures, and accomplishments. The accomplishments cover the performances of the proposed theoretical feasibility study, a supplementary theoretical feasibility study, and the proposed operational feasibility study. First, the theoretical feasibility study is presented, then, the supplementary theoretical feasibility study is presented, and finally, the operational feasibility study is presented.

### Theoretical Feasibility Study

#### Introduction and Summary

We conducted a theoretical feasibility study to determine the theoretical feasibility of the proposed testing system. Tests were simulated analytically considering expected ranges of selected soil properties. Studies were carried out to determine the theoretical feasibility of the testing system for obtaining 1) the low amplitude dynamic shear modulus, 2) the variation in the dynamic shear modulus with shear strain, 3) the degradation characteristics of clays, and 4) the degradation and liquefaction characteristics of sands and silts.

Results from our study indicate that the proposed testing system is theoretically feasible. The behavior of the testing system was predicted to be sensitive to each soil property considered in a clear, physically reasonable manner.

There were also secondary objectives of the theoretical feasibility study. These objectives were generally satisfied.

During our study, we identified one area requiring further study. The configuration of the inner cylinder, specified for the preliminary design of a laboratory research prototype testing system, was thought to be torsionally more flexible, relative to the test soil, than we had originally considered. As a result, we carried out a supplementary cursory study presented in the subsection entitled Supplementary Theoretical Feasibility Study, pg. 63. The study indicates that the inner cylinder may be torsionally flexible under certain conditions. This may increase somewhat uncertainty in inferring soil properties from test results. However, we concluded that because of the number of effective steps which could be taken, if necessary, to mitigate this concern, the proposed testing system should serve its stated purpose well.

Details are provided in the remaining subsections. We state the objectives and general procedures of the theoretical feasibility study, present and discuss analysis procedures used in the study, present and discuss results from the study, and present conclusions.

#### Objectives

The main objective of the theoretical feasibility study was to determine the theoretical feasibility of the proposed testing system for determining 1) the low amplitude dynamic shear modulus, 2) the variation in the dynamic shear modulus with shear strain, 3) the degradation characteristics of clays,

and 4) the degradation and liquefaction characteristics of sands and silts.

There were also several secondary objectives of the theoretical feasibility study. These objectives were 1) to provide the design criteria needed for the detailed design of the laboratory research prototype testing system scheduled for Phase II, 2) to develop an initial testing methodology for Phase II laboratory research testing, and 3) to develop a simple but effective analysis procedure for qualitatively checking, during Phase II, the results from laboratory research tests and developmental results from descriptive soil-probe interaction analyses, to be constructed as part of Phase II research.

#### General Procedures

The theoretical feasibility of the proposed testing system was determined by simulating tests analytically considering expected ranges of selected soil properties. If we predicted the behavior of the testing system to be sensitive to a soil property in a clear, physically reasonable manner, then we concluded that we could reasonably infer this property from the behavior of the testing system and therefore, that the proposed testing procedure is a theoretically feasible means for determining this property.

The secondary objectives of the theoretical feasibility study were pursued in the following manners. We developed preliminary design criteria needed for the preliminary design of the laboratory research prototype testing system. We provided these criteria to the mechanical engineering firm designing the system. Using these criteria, the firm developed a preliminary design of the system. Using the preliminary design as a basis, we had planned to revise our criteria to final design criteria, but we did not carry out this last task. Therefore, this task will be proposed for Phase II research. To satisfy the objective of developing an initial testing methodology for Phase II testing, we reviewed the results of our analytical simulations. Based on this review, we identified the most promising modes of testing. Finally, the performance of the theoretical feasibility study automatically satisfied the objective of developing a simple, but effective, analysis procedure for use in Phase II research.

#### Analysis Procedures

In the following subsections, we present and discuss the analysis procedures used for the theoretical feasibility study. Specifically, we present and discuss our analytical modeling, solution procedures, a solution check procedure, assumptions, and validations of solution procedures.

Analytical Modeling--As shown in Fig. 8, the analytical model developed for the theoretical feasibility study was a simple single-degree-of-freedom, torsional spring-dashpot-mass moment of inertia system. The spring represented the nonlinear, inelastic, degrading, torsional reaction of the test soil to rotation of the inner cylinder. The dashpot represented viscous damping of the test soil. The mass moment of inertia represented the rotational inertia of the inner cylinder, its instrumented head, and an appropriate portion of the test soil.

The modeling involved the following elements: 1) a relationship between

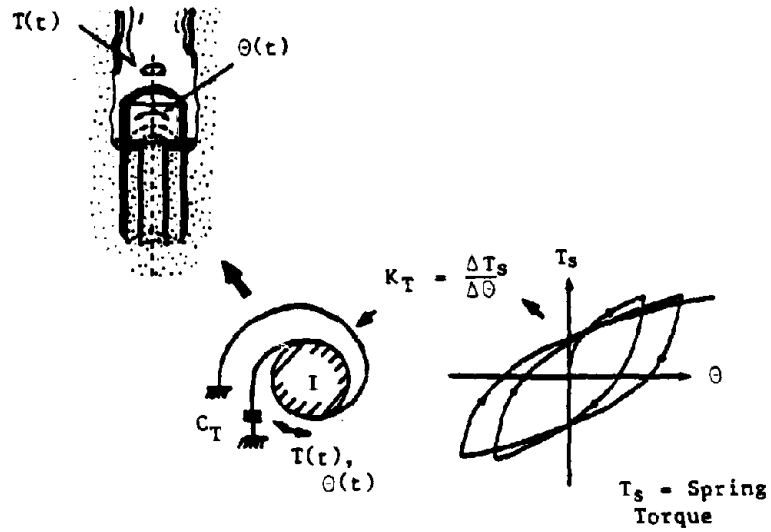


Figure 8: Simple Nonlinear, Inelastic, Degrading Model of Soil-Probe System

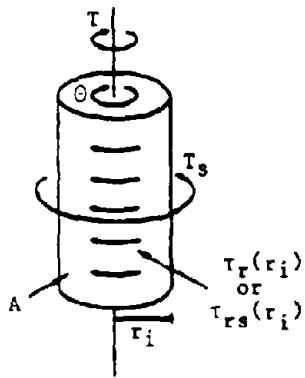


Figure 9: Schematic Diagram of Active (Unshielded) Portion of Inner Cylinder Showing Assumed Uniform Distribution of Shear Stress and Related Terms in Positive Sense

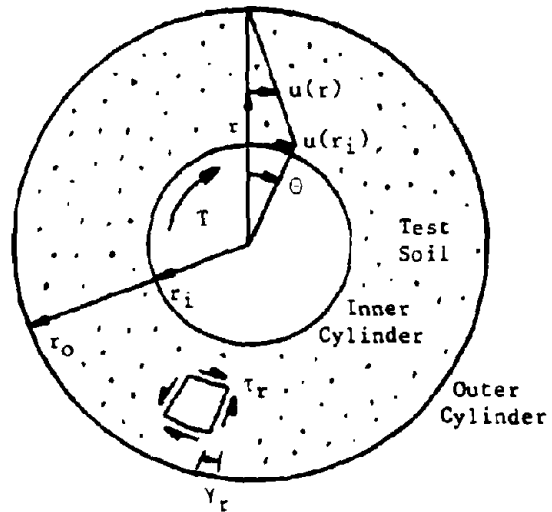


Figure 10: Horizontal Cut Through Probe Showing Assumed Linear, Horizontal Displacement Distribution and General Nomenclature

the spring torque and the corresponding shear stress developed within the test soil along the wall of the active (unshielded) portion of the inner cylinder, 2) a relationship between the rotation of the rigid inner cylinder and the shear strain developed within the test soil along the wall of the active portion of the inner cylinder, 3) a relationship giving the tangent spring stiffness of the single-degree-of-freedom system, 4) relationships describing the nonlinear, inelastic, shear stress-strain behavior of the test soil, 5) relationships describing the cyclic degradation of shear stress-strain behavior observed in clays, 6) relationships describing the cyclic degradation of shear stress-strain behavior observed in sands and silts and the liquefaction of such soils, and 7) a relationship for the mass moment of inertia of the effectively rotating mass. These elements are summarized below. Detailed derivations for elements 1), 2), and 3) are provided in Appendix B.

Assuming a uniform distribution of shear stress in the vertical direction within the test soil along the wall of the inner cylinder (see Fig. 9), the following relationship was derived relating the change in the spring torque,  $\Delta T_s$ , to the corresponding change in the shear stress in the test soil along the wall of the active portion of the inner cylinder,  $\Delta \tau_{rs}(r_i)$ :

$$\Delta \tau_{rs}(r_i) = - \frac{\Delta T_s}{2\pi r_i^2 l} \quad (1)$$

where  $r_i$  = outer radius of inner cylinder  
 $l$  = active length of inner cylinder

A form of Eq. 1, valid when damping and inertia forces are negligible, gives the amplitude of the cyclic torque applied to the inner cylinder,  $T_A$ , as a function of the corresponding cyclic shear stress ratio,  $\tau_{rA}(r_i)/\bar{\sigma}_{vi}$ :

$$T_A = -2\pi r_i^2 l \bar{\sigma}_{vi} \left( \frac{\tau_{rA}(r_i)}{\bar{\sigma}_{vi}} \right) \quad (2)$$

where  $\bar{\sigma}_{vi}$  = initial effective vertical stress  
 $\tau_{rA}(r_i)$  = amplitude of cyclic shear stress

We derived a relationship between the change in the rotation of the rigid inner cylinder,  $\Delta \theta$ , and the change in the shear strain developed in the test soil along the wall of the inner cylinder,  $\Delta \gamma_r(r_i)$ . For this, we assumed an axisymmetric, linear, horizontal displacement distribution in the test soil, as indicated in Fig. 10, and no slip between the cylinders and the test soil. The derived relationship is given as:

$$\Delta \gamma_r(r_i) = - \left( \frac{r_o}{r_o - r_i} \right) \Delta \theta \quad (3)$$

where  $r_o$  = inner radius of outer cylinder

An expression for the tangent spring stiffness,  $K_T$ , was derived and is given as:

$$K_T = \frac{2\pi r_i^2 r_o l}{r_o - r_i} G(r_i) \quad (4)$$

where  $G(r_i)$  = tangent shear modulus of test soil along wall of inner cylinder

The tangent shear modulus,  $G(r_i)$ , needed to define the spring constant,  $K_T$ , using Eq. 4, was derived from the shear stress-strain model describing the behavior of the test soil. We used two models to represent the undegraded, nonlinear, inelastic shear stress-strain behavior of the test soil: a Ramberg-Osgood model (24) and a hyperbolic model (12). The hyperbolic model was used in simulating tests for determining the degradation characteristics of clays and the degradation and liquefaction characteristics of sands and silts, while the Ramberg-Osgood model was used in simulating all other tests. The Ramberg-Osgood model requires the definition of the low amplitude dynamic shear modulus of the test soil, the shear strength, and parameters describing the shape of the shear stress-strain curve. The hyperbolic model requires only the definition of the low amplitude dynamic shear modulus and the shear strength.

To represent the cyclically degrading shear stress-strain behavior expected when conducting low frequency, cyclic tests in degradable clays, we constructed a clay degradation submodel. This submodel corresponds to the model presented in Ref. 20. Using this model, the cyclic degradation of shear stiffness and strength was computed as a function of cyclic strain amplitude and a degradation parameter describing the degradation characteristics of the test soil.

We used two models to represent the cyclically degrading shear stress-strain behavior expected when conducting low frequency, cyclic tests in degradable sands and silts which could possibly liquefy. One model was analytically-based and one was based on published test data.

The analytically-based method involved a sand and silt degradation and liquefaction submodel corresponding to the model presented in Ref. 22. This model is expected to predict, reasonably accurately, the behavior of loose, liquefiable sands and the behavior of dense, nonliquefiable sands at lower levels of excess porewater pressure. Using this model, excess porewater pressure was computed primarily as a function of cyclic strain amplitude and parameters describing the densification and rebound characteristics of the test soil. Shear moduli and strength were cyclically degraded in accordance with the computed excess porewater pressure. Liquefaction, the almost complete loss of the stiffness and strength of a soil, was predicted if the excess porewater pressure rose to the level of the initial effective overburden pressure. Alternatively, a shear failure could be predicted if the applied cyclic shear stress exceeded the cyclically degraded shear strength.

We constructed the second model based upon published test data to more realistically predict the behavior of dense sands at higher levels of excess porewater pressure. One limitation with currently available sand and silt degradation and liquefaction models, with which we are familiar, is that these models do not fully take into account the restraining effects of dilation. These effects are significant for dense sands and prevent the unrestrained deformation which may develop in loose, liquefiable sands (see Fig. 2). The published test data, which includes effects of dilation, relates the cyclic simple shear stress applied to a commonly used test sand, the resulting cyclic shear strain, and the relative density of the sand. Figure 11 taken from Ref. 28, shows the test data. The figure gives the amplitudes of the cyclic shear strains developed in large, freshly prepared samples of Monterey No. 0 sand subjected to cyclic simple shear stresses having uniform amplitudes. Specifically, Fig. 11(a) presents the limiting shear strain amplitude developed as a function of relative density. In this special case of freshly deposited and identically prepared samples tested in the same pressure environment, relative density essentially determines degradation and liquefaction characteristics. Figure 11(b) presents the shear strain amplitude, developed after 10 cycles of loading, as a function of relative density and shear stress ratio,  $\tau_h/\sigma'_0$ . The quantities  $\sigma'_0$  and  $\tau_h$  are the initial effective vertical stress and the amplitude of the applied cyclic horizontal shear stress, respectively.

The total mass moment of inertia was calculated assuming parameters for the inner cylinder, the instrumented head, and the portion of the test soil which we assumed would effectively rotate with the inner cylinder. Figure 12 presents assumed geometries and includes nomenclature. For our study, we assumed a solid disk for the instrumented head and thin-walled cylinders for the inner cylinder and the zone of soil assumed to be effectively rotating. Thus, using basic principles of mechanics, the total mass moment of inertia,  $I$ , was estimated using the following expression:

$$I = \frac{\pi Y_{IH} R_{IH}^4 l_{IH}}{2g} + \frac{2\pi Y_c R_c^3 h_c l_c}{g} + \frac{2\pi Y_s R_s^3 h_s l_s}{g} \quad (5)$$

where  $g$  = acceleration due to gravity  
 $Y_{IH}$  = equivalent unit weight of instrumented head  
 $Y_c$  = unit weight of inner cylinder  
 $Y_s$  = total unit weight of test soil

The remaining symbols are defined in Fig. 12.

Solution Procedures--We used two procedures for obtaining solutions: a dynamic procedure and a static procedure. The dynamic procedure was used to simulate tests for determining dynamic shear moduli and initially to simulate tests for determining cyclic degradation and liquefaction characteristics of sands and silts using the analytical model. The static procedure was used later to simulate tests for determining cyclic degradation characteristics of clays and cyclic degradation and liquefaction characteristics of sands and silts after it was established that dynamic effects were small (see Appendix A, pg. A-14). The dynamic effects were small

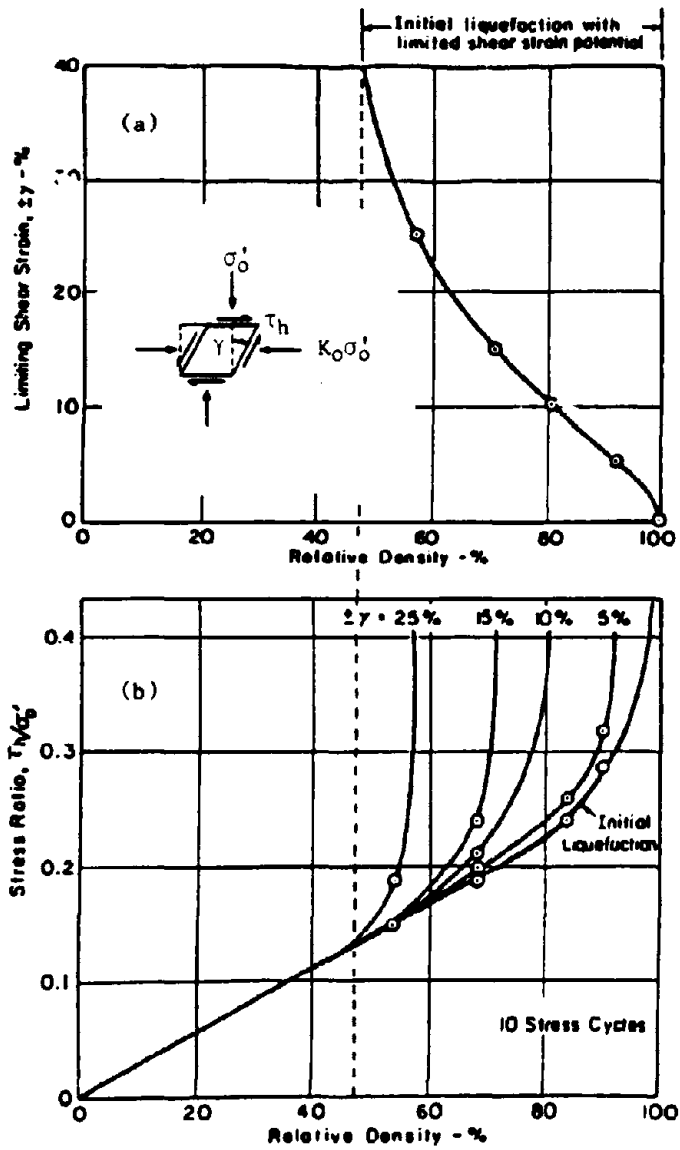


Figure 11: Results from Large Scale, Cyclic, Simple Shear Tests Conducted on Freshly Prepared Samples of Monterey No. 0 Sand (after Seed, 1976)



because of the low excitation and response frequencies considered (1cps).

With the dynamic procedure, we simulated tests by solving the equation of motion for the single-degree-of-freedom system. Because of the nonlinearity of the spring, we used a numerical integration procedure for solving the equation of motion. Specifically, we used the widely accepted step-by-step procedure described in Ref. 6. This procedure is based on the assumptions of a linear variation in acceleration and constant properties during computational time steps.

The basic steps used in the dynamic solution procedure are summarized with reference to Fig. 13. At the beginning of a computational time step, values are known for  $T$ ,  $\Theta$ ,  $d\Theta/dt$ ,  $d^2\Theta/dt^2$ , and  $K_T$ . These values are either specified as initial conditions, or are known from calculations for the previous time step. The values for  $\gamma_r(r_i)$  and  $\tau_{rs}(r_i)$  are obtained from  $\Theta$  and  $K_T$ . Past and current values for  $\gamma_r(r_i)$  and  $\tau_{rs}(r_i)$  are used to obtain a value for the strain-dependent, possibly degraded, tangent shear modulus of the test soil along the wall of the inner cylinder,  $G(r_i)$ . The corresponding tangent spring stiffness,  $K_T$ , is obtained from this tangent shear modulus using Eq. 4. Values for  $\Delta\Theta$  and  $\Delta(d\Theta/dt)$  are obtained for the time step using the above-mentioned numerical solution procedure. These values are used to obtain new values for  $\Theta$ ,  $d\Theta/dt$ , and  $d^2\Theta/dt^2$ . The process is repeated until a solution has been obtained for the duration of interest.

With the static procedure, dynamic effects were neglected, and static equilibrium was satisfied for selected times during the cyclic loading. With this simplification, the torque applied to the instrumented head was equated to the torque applied to the test soil. When using the analytical models to describe cyclic degradation and liquefaction characteristics, we obtained solutions by satisfying equilibrium after each half-cycle of loading. The shear modulus and strength were degraded after each half-cycle. When using the test data published by Seed (28) to define the degrading shear-stress strain behavior of the test soil, we considered only a single time during any test. As stated previously, this data relates the amplitude of the cyclic simple shear stress applied to a test sand, the amplitude of the resulting cyclic shear strain, and the relative density of the sand. To simulate tests using the proposed testing system, we converted the stress amplitudes to equivalent applied torque amplitudes using Eq. 2 and the corresponding strain amplitudes to equivalent rotation amplitudes using Eq. 3. In the conversions, we assumed the behavior of the soil to be independent of the planes on which shear stresses develop. The converted data provided, for a range of cyclic torque loadings and a given time during a test, the predicted amplitude of the cyclic rotation of the inner cylinder as a function of relative density (degradation and liquefaction characteristics).

Solution Check Procedure--We constructed an energy balance procedure to help validate nonlinear dynamic solutions. The basic concept of the energy balance is presented in Refs. 16 and 39 and is summarized in this subsection.

The key parameter of the energy balance is the energy ratio,  $E_R(t)$ , defined as:

$$E_R(t) = \frac{SE(t) + KE(t) + DE(t)}{W(t)} \quad (6)$$

where  $W(t)$  = work done on system by applied load  
 $SE(t)$  = sum of energy lost in test soil due to hysteresis and instantaneous elastic strain energy stored within test soil  
 $DE(t)$  = energy lost in test soil due to viscous damping  
 $KE(t)$  = instantaneous kinetic energy of rotating mass

The individual terms are given as:

$$W(t) = \int_0^{\Theta(t)} T(t) d\Theta \quad (7)$$

$$SE(t) = \int_0^{\Theta(t)} T_S(t) d\Theta \quad (8)$$

$$DE(t) = \int_0^{\Theta(t)} T_D(t) d\Theta \quad (9)$$

$$KE(t) = \frac{1}{2} I \left(\frac{d\Theta}{dt}\right)^2 \quad (10)$$

where  $T(t)$  = applied torque  
 $\Theta(t)$  = rotation of inner cylinder  
 $T_S(t)$  = spring torque  
 $T_D(t)$  = damping torque  
 $I$  = mass moment of inertia of rotating mass

Equations 7, 8, and 9 may be effectively integrated by use of the trapezoidal rule.

At any instant of time during a simulation, the value of the energy ratio should equal one. That is, the work done on the system should equal the sum of the energy lost by the system and the instantaneous energy stored

by the system. A value other than one may indicate either an invalid solution or numerical error.

Assumptions--The simulations of tests involved several significant simplifications or assumptions: a lumped parameter system; a linear, axisymmetric, horizontal displacement distribution in the test soil in horizontal planes; uniform behavior in the vertical direction; independence in the behavior of the soil with respect to the planes on which shear stresses develop; no apparatus friction or viscous damping; and no slippage. Also, we did not model the flow of porewater caused by gradients in excess porewater pressure.

Even though the simple model was reasonably descriptive, because of the simplifying assumptions and because not all important phenomena were modeled, the model was expected to give results which were only qualitatively accurate. However, the level of accuracy provided was judged sufficient and appropriate for establishing feasibility and providing design criteria for a prototype testing system.

Validations--In this subsection, we briefly describe the validations which were carried out for the computer procedures used. The validations are presented in detail in Appendix A. The computer procedures validated included those which were used to simulate impulse and high frequency, cyclic tests for determining the low amplitude dynamic shear modulus and the variation in the dynamic shear modulus with shear strain, and low frequency, cyclic tests for determining the degradation characteristics of clays and the degradation and liquefaction characteristics of sands and silts.

Procedures were validated in various manners. Solutions were tested in the linear range by comparison with closed-form solutions. Because appropriate nonlinear, degrading, closed-form solutions were not found to be available, we validated the nonlinear, degradation, and liquefaction procedures by use of an energy balance (see Solution Check Procedure, pg. 36). We also studied solutions judgmentally to insure that they were reasonable.

### Presentation and Discussion of Results

In this subsection, we present and discuss the main results of our theoretical feasibility study. To determine the theoretical feasibility of the proposed testing system, we simulated representative tests analytically considering expected ranges of selected soil properties. If the behavior of the testing system was predicted to be sensitive to a soil property in a clear, physically reasonable manner, then it was concluded that, theoretically, the soil property could be inferred from test results and therefore, that the testing system is a theoretically feasible means for determining this property. In the subsections that follow, we first discuss model parameters common to most simulations and then, we discuss, by property, the simulations.

Model Parameters Common to Most Simulations--Several model parameters were common to most simulations. All tests were simulated assuming a probe

having dimensions approximately compatible with commonly used drilling equipment. The outer cylinder was assumed to have an inner diameter of 3 in, and the inner cylinder, an outer diameter of 1 in. The active (unshielded) length of the inner cylinder was assumed to be 8 in and the shielded length, 4 in. Thus, the annular element of test soil was assumed to be 8 in tall and 1 in thick with an inner radius of 1/2 in. We roughly estimated a value of  $0.00028 \text{ lb-sec}^2\text{-ft}$  for the mass moment of inertia of the rotating mass. Referring to Fig. 12, for mass moment of inertia calculations, we assumed a 12 in long steel (weight per unit volume = 487 pcf) inner cylinder having an outer radius of 1/2 in and a wall thickness of 1/16 in, and, arbitrarily, a solid aluminum (weight per unit volume = 169 pcf) instrumented head having a height of 1/2 in and a diameter of 3 in. The test soil considered to be effectively rotating with the inner cylinder was assumed to be a cylindrical volume of soil (total weight per unit volume = 122 pcf) having a length of 8 in, a thickness of 1/2 in, and an inner radius of 1/2 in. We did not consider variations in the total weight per unit volume of the soil in our predictions because variations in this parameter were expected to have little effect on conclusions.

Low Amplitude Dynamic Shear Modulus--To determine the theoretical feasibility of the proposed testing system for determining the low amplitude dynamic shear modulus, we considered soil properties ranging from those expected in a uniform, saturated, loose sand deposit at a shallow depth of 5 ft, to those expected in a uniform, dry, dense sand deposit at a depth of 50 ft. This range of properties is expected to cover reasonably well the properties in deposits of clays and silts at similar depths. The depths considered cover the shallower layers of a deposit. These layers usually experience the greatest activity during earthquakes and therefore, require the most accurate definition for earthquake analyses. The lower bound of the range for the low amplitude dynamic shear modulus was calculated to be  $5.14 \times 10^5$  psf while the upper bound was calculated to be  $5.86 \times 10^6$  psf. These bounds were calculated assuming a depth, effective unit weight, void ratio, and coefficient of earth pressure at rest of 5 ft, 56 pcf, 0.85, and 0.6, respectively, for the lower bound, and 50 ft, 122 pcf, 0.35, and 1.0, respectively, for the upper bound. The equation used to calculate the low amplitude dynamic shear modulus is presented in Ref. 15. A value of viscous damping corresponding to 2% of critical damping was assumed. This is representative of sands (25).

We simulated both low amplitude impulse tests and low amplitude, high frequency, cyclic tests. The simulations of the impulse tests are discussed first, after which the simulations of the high frequency, cyclic tests are discussed.

For the simulations of low amplitude impulse tests, we considered a torsional impulsive loading having a rectangular shape and a duration greater than 1/2 the natural period of the system. Thus, the impulsive loading was of long duration (6). The response of the inner cylinder to this type of loading was a decaying rotational oscillation. The amplitude of the loading was 0.015 ft-lb. This induced only linear elastic behavior in the test soil for the range of low amplitude dynamic shear moduli considered. The duration of all loadings was 1.7 ms.

Results are presented in Fig. 14. Figure 14(a) gives samples of the predicted measured quantities while Fig. 14(b) gives selected parameters of predicted measured quantities. The selected parameters include the peak and the frequency of the cyclic rotation of the inner cylinder. The peak rotation, in all cases, was the initial peak.

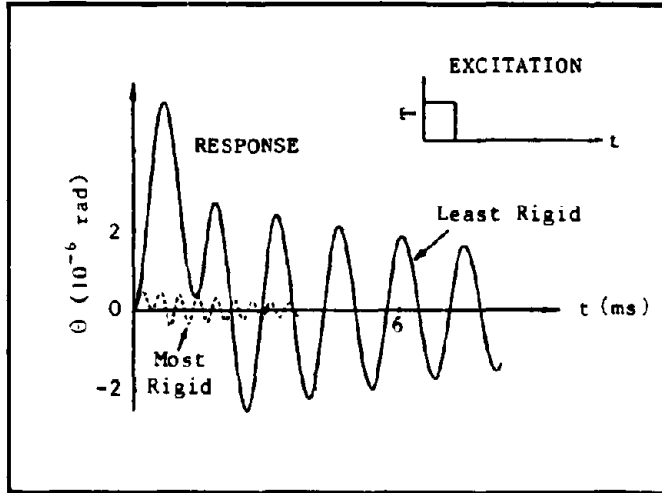
The results of the study indicate that, during low amplitude impulse tests, the behavior of the testing system will be sensitive to the low amplitude dynamic shear modulus in a clear, physically reasonable manner. Referring to Fig. 14(b), the frequency of the oscillation of the inner cylinder was predicted to be about 3 times larger when testing the most rigid sand than when testing the least rigid sand while the amplitude of the peak rotation of the inner cylinder was predicted to be about 10 times larger when testing the least rigid sand than when testing the most rigid sand. In fact, the peak rotation was predicted to be significantly more sensitive to the low amplitude dynamic shear modulus than the shear wave velocity (theoretically proportional to square root of low amplitude dynamic shear modulus) measured in widely used seismic wave propagation tests (in our example case, about 3 times more sensitive).

The results of this study are physically reasonable. One would expect, for a given low amplitude loading, the peak rotation of the inner cylinder to be greater and the frequency of oscillation to be less, when testing less rigid sand. Thus, it was concluded that conducting impulse tests using the proposed testing procedure is a theoretically feasible means for determining the low amplitude dynamic shear modulus.

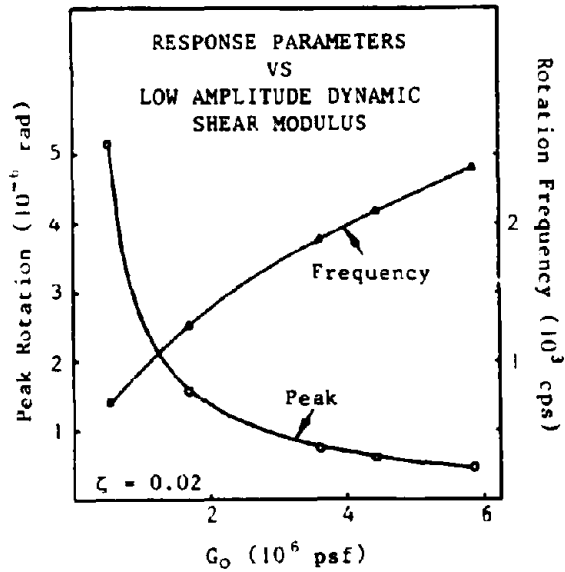
For the simulations of low amplitude, high frequency, cyclic tests, we considered a sinusoidal torque excitation. The response of the inner cylinder to this loading was a cyclic rotation consisting of a decaying transient component and a steady state component. For a test soil of given properties, frequency response curves were developed in the vicinity of the damped natural frequency. The frequency response curves were developed by maintaining the amplitude of the loading while varying the frequency. The frequency response curves were based only on the steady state component of the response. The amplitude of the loadings was 0.001 ft-lb. This induced only linear elastic behavior for the range of low amplitude dynamic shear moduli considered.

Results are presented in Fig. 15. Figure 15(a) gives samples of predicted measured quantities while Fig. 15(b) gives selected parameters of the predicted measured quantities. The selected parameters include the damped natural frequency of the cyclic rotation of the inner cylinder and the amplitude of this rotation at the damped natural frequency.

The results of the study indicate that, during low amplitude, high frequency, cyclic tests, the behavior of the testing system will be sensitive to the low amplitude dynamic shear modulus in a clear, physically reasonable manner. Referring to Fig. 15(b), the damped natural frequency of the oscillation of the inner cylinder was predicted to be about 3 times larger when testing the most rigid sand than when testing the least rigid sand and

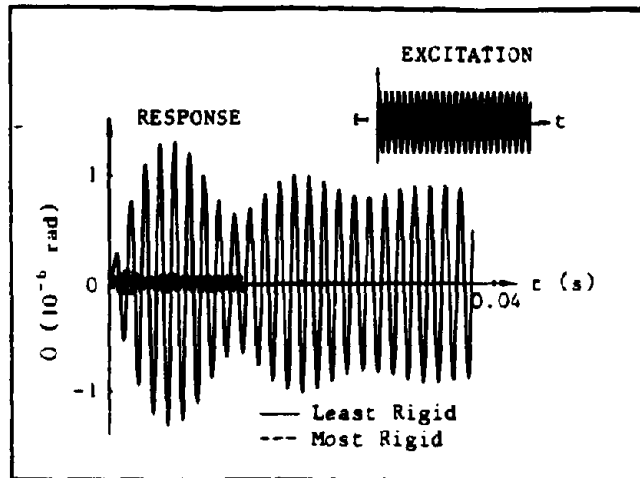


(a) Samples of Predicted Measured Quantities

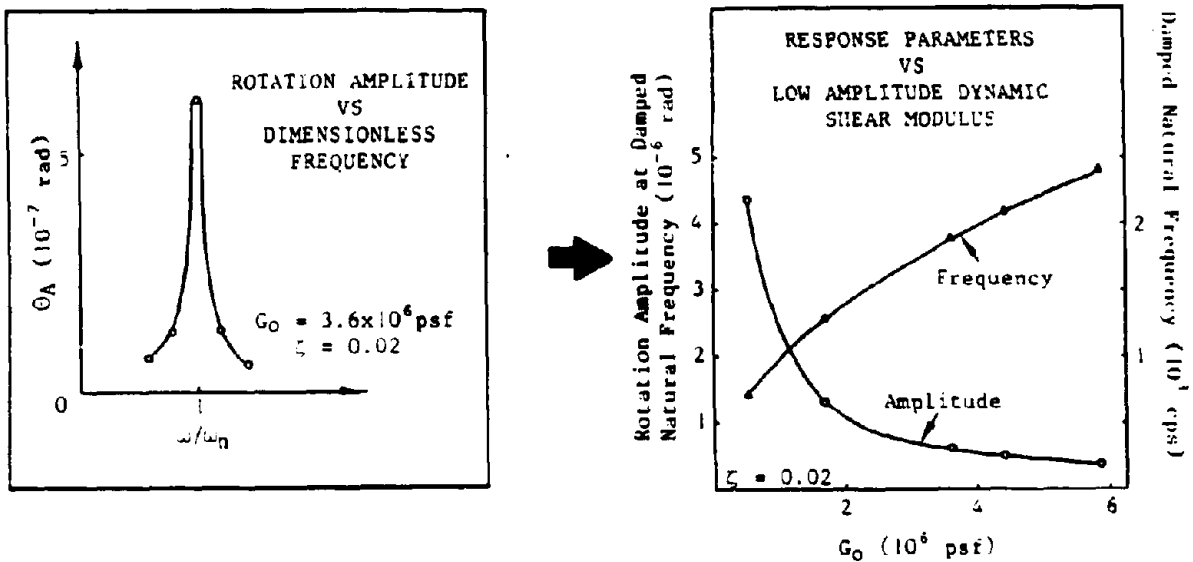


(b) Parameters of Predicted Measured Quantities

Figure 14: Results from Simulations of Low Amplitude Impulse Tests - Low Amplitude Dynamic Shear Modulus Study



(a) Samples of Predicted Measured Quantities



(b) Parameters of Predicted Measured Quantities

Figure 15: Results from Simulations of Low Amplitude, High Frequency, Cyclic Tests - Low Amplitude Dynamic Shear Modulus Study

the amplitude of the cyclic rotation of the inner cylinder at the damped natural frequency was predicted to be about 10 times larger when testing the least rigid sand than when testing the most rigid sand.

The results of this study are physically reasonable. One would expect, for a given low amplitude loading, the amplitude of the cyclic rotation of the inner cylinder at the damped natural frequency to be less and the damped natural frequency to be greater when testing more rigid sand. Thus, it was concluded that conducting high frequency, cyclic tests using the proposed testing procedure is a theoretically feasible means for determining the low amplitude dynamic shear modulus.

Based on our experiences in analytically simulating low amplitude impulse tests and low amplitude, high frequency, cyclic tests, we concluded that the impulse test is a preferable test for determining the low amplitude dynamic shear modulus. With the need to carry out a frequency sweep, the high frequency, cyclic test is somewhat more complex than the impulse test. Also, with the impulse test, it would be necessary to carry out simulations only for a very short duration to obtain the information required. In contrast, because of the time needed to reach steady state conditions, with the high frequency, cyclic test it would be necessary to carry out simulations for a relatively long duration.

Variation in the Dynamic Shear Modulus with Shear Strain--To determine the theoretical feasibility of the testing system for determining the variation in the dynamic shear modulus with shear strain, we varied the variation in dynamic shear modulus with shear strain without varying other parameters. The test soil was considered to have the same shear stress-strain behavior for low levels of strain but we varied shear stress-strain behavior for high levels of strain. To do this, we considered the test soil to have a single low amplitude dynamic shear modulus and shear stress-strain curve shape. However, we varied the shear strength over a range that could be realistically expected for the selected low amplitude dynamic shear modulus. Figure 16 presents the upper and lower bounds for the shear stress-strain skeleton curves used for our study.

For the study, we assumed properties expected in sand deposits. However, results are expected to apply equally to silts and clays. The low amplitude dynamic shear modulus for each stress-strain curve was  $2 \times 10^6$  psf. The Ramberg-Osgood parameters defining the shape of the curves were  $\alpha = 1$ ,  $C_1 = 0.8$ , and  $R = 5$ . The upper bound shear strength was calculated to be 1500 psf while the lower bound was calculated to be 500 psf. The low amplitude dynamic shear modulus and the shear strengths were calculated assuming the following: depth = 6 ft, void ratio = 0.35, coefficient of earth pressure at rest = 1.0, effective unit weight of soil = 122 pcf, and effective angle of internal friction = 42 deg for the lower bound shear stress-strain curve, and depth = 77.5 ft, void ratio = 0.85, coefficient of earth pressure at rest = 0.6, effective unit weight of soil = 56 pcf, and effective angle of internal friction = 32 deg for the upper bound shear stress-strain curve. The equations used to calculate the low amplitude dynamic shear moduli and the shear strengths are presented in Refs. 15 and 16. The shear strengths were averages of the shear strengths estimated separately for horizontal and vertical planes. Intermediate values of strength were also considered. The selected Ramberg-Osgood shape parameters

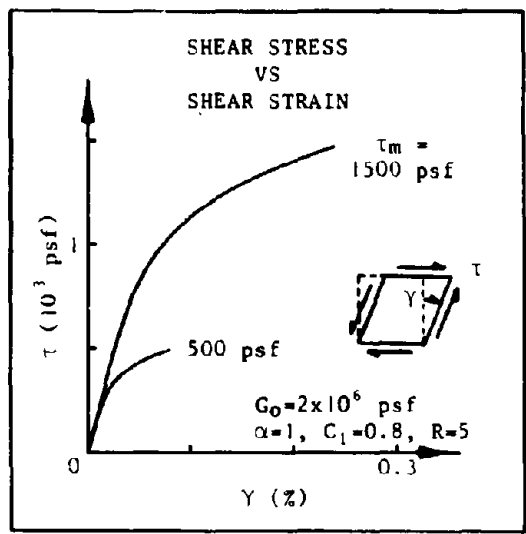


Figure 16: Bounds for Skeleton Shear Stress-Strain Curves Considered - Variation in Dynamic Shear Modulus with Shear Strain Study

give stress-strain curves that closely match experimental data for sands (24). A value of viscous damping corresponding to 2% of critical damping was assumed. This value is representative of sands (25).

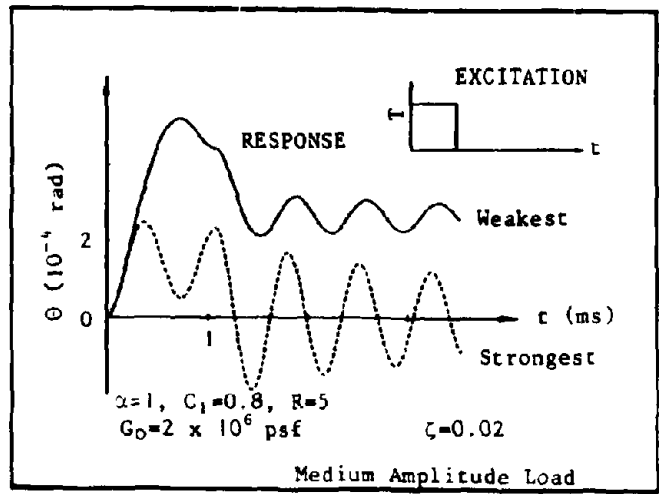
We simulated both impulse tests and high frequency, cyclic tests. The simulations of impulse tests are discussed first, and then, the simulations of high frequency, cyclic tests are discussed.

For the simulations of the impulse tests, we considered an impulsive loading having a rectangular shape. The response of the inner cylinder to this loading was a decaying, cyclic rotation. To study the effects of loading amplitude, we considered two different amplitudes for the torsional impulsive loading: a medium amplitude of 2.7 ft-lb, and a relatively high amplitude of 5.2 ft-lb. These amplitudes were intended to induce shear strains on the order of 0.05% and 0.15%, respectively, in the test soil having a medium strength of 1000 psf. The duration of all the loadings was 1.1 ms which, in each case, exceeded the time of occurrence of the first peak of the rotation of the inner cylinder.

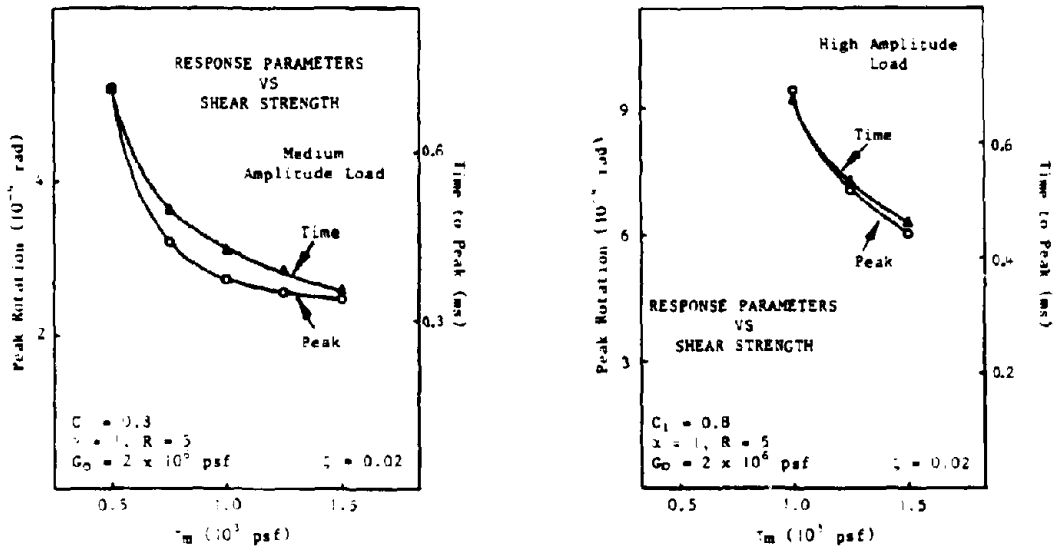
Results are presented in Fig. 17. Figure 17(a) gives samples of the predicted measured quantities while Fig. 17(b) gives selected parameters of the predicted measured quantities for the two amplitudes of loading. The selected parameters include the peak rotation of the inner cylinder and the time to this peak. The peak rotation of the inner cylinder, in all cases, was the initial peak. The time to this peak was used as a measure of the apparent natural period of the nonlinear system for the level of strain induced; the greater the time to this peak, the greater was the apparent natural period of the cyclic rotation of the inner cylinder. Results were not plotted for simulations in which the strength of the test soil was exceeded.

The results of the study indicate that, during impulse tests which induce nonlinear shear stress-strain behavior in the test soil, the behavior of the testing system will be sensitive to the variation in the dynamic shear modulus with shear strain in a clear, physically reasonable manner. For example, referring to Fig. 17(b), for the medium amplitude of loading, the peak rotation and the time to this peak were predicted to be about 2 times larger when testing the weakest sand than when testing the strongest sand. Similar behavior was also predicted for the high amplitude of loading. Additionally, an increase in the peak rotation of the inner cylinder and an increase in the time to this peak were predicted, for each case considered, as the amplitude of the loading was increased.

The results of this study are physically reasonable. For loadings which induce nonlinear shear stress-strain behavior, one would expect the peak rotation of the inner cylinder and the time to this peak to increase with decreases in the shear rigidity of the test soil at high strains. Additionally, one would expect the peak rotation of the inner cylinder and the time to this peak to increase with increases in the amplitude of loading when testing a given soil at strains for which the soil behavior is



(a) Samples of Predicted Measured Quantities



(b) Parameters of Predicted Measured Quantities

Figure 17: Results from Simulations of Impulse Tests - Variation in Dynamic Shear Modulus with Shear Strain Study

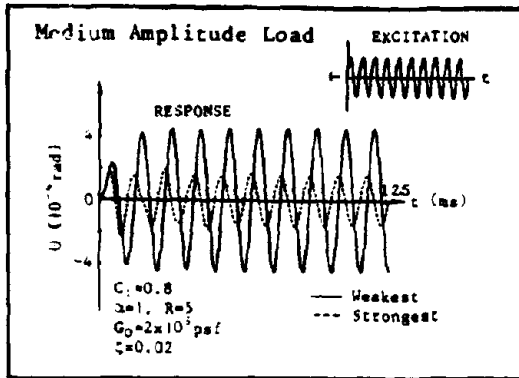
nonlinear. Thus, it was concluded that conducting impulse tests at higher amplitudes of loading using the proposed testing procedure is a theoretically feasible means for determining the variation in the dynamic shear modulus with shear strain.

For the simulations of high frequency, cyclic tests for determining the variation in the dynamic shear modulus with shear strain, we considered a sinusoidal torque excitation. The response of the inner cylinder to this loading was a cyclic rotation consisting of a decaying transient component and a steady state component. For a test soil of given properties, frequency response curves were developed in the vicinity of the apparent natural frequency to determine useful response parameters. The frequency response curves were developed by maintaining the amplitude of the loading while varying the frequency. The frequency response curves were based only on the steady state component of the response. Two amplitudes of loading were selected: a medium amplitude of 2.2 ft-lb and a relatively high amplitude of 4.8 ft-lb. These amplitudes were intended to induce shear strains on the order of 0.05% and 0.15%, respectively, in the test soil having a medium strength of 1000 psf, at the apparent natural frequency. These strains corresponded approximately to those induced in the simulations of impulse tests discussed previously in this subsection.

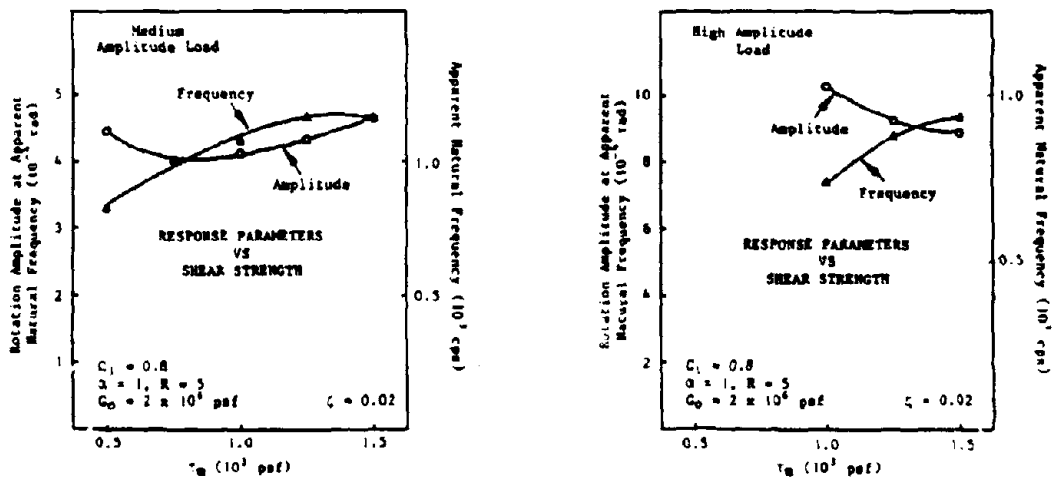
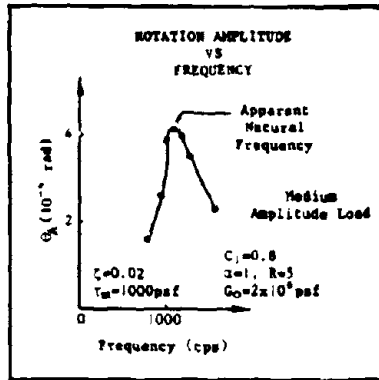
Results are presented in Fig. 18. Figure 18(a) gives samples of the predicted measured quantities while Fig. 18(b) gives selected parameters of the predicted measured quantities for the two different levels of loading. The selected parameters include the apparent natural frequency of the cyclic rotation of the inner cylinder and the amplitude of the cyclic rotation of the inner cylinder at the apparent natural frequency.

The results indicate that, during high frequency, cyclic tests which induce nonlinear shear stress-strain behavior in the test soil, some parameters describing the behavior of the testing system will be sensitive to the variation in the dynamic shear modulus with shear strain, while, under some conditions, other parameters may not. The behavior of the testing system was physically reasonable. For example, referring to Fig. 18(b), for the medium amplitude of loading, the apparent natural frequency of the cyclic rotation of the inner cylinder was predicted to be about 1.5 times greater while the amplitude of the cyclic rotation of the inner cylinder at the apparent natural frequency was predicted to be slightly larger when testing the strongest soil than when testing the weakest soil. A similar trend was predicted for the apparent natural frequency for the high amplitude of loading; however, the amplitude of the rotation of the inner cylinder was predicted to be about 1.2 times smaller when testing the strongest soil than when testing the weakest soil for which data was plotted. Additionally, a decrease in the apparent natural frequency of the cyclic rotation of the inner cylinder and an increase in the amplitude of the cyclic rotation of the inner cylinder at the apparent natural frequency were predicted as the amplitude of the loading was increased for any given set of soil properties.

The results are physically reasonable. For loadings which induce nonlinear shear stress-strain behavior, one would expect decreases in the apparent natural frequency of the cyclic rotation of the inner cylinder with



(a) Samples of Predicted Measured Quantities



(b) Parameters of Predicted Measured Quantities

Figure 18: Results from Simulations of High Frequency, Cyclic Tests - Variation in Dynamic Shear Modulus with Shear Strain Study

decreases in shear strength while holding other parameters describing stress-strain behavior constant. The decrease in shear stiffness and the increase in hysteretic damping accompanying the decrease in shear strength would both contribute to a reduction in the apparent natural frequency. The insensitivity predicted for the amplitude of the cyclic rotation of the inner cylinder at the apparent natural frequency when considering the loading having medium amplitude was the result of the compensating effects of changes in shear stiffness and corresponding changes in hysteretic damping. For sinusoidal torque loads at the apparent natural frequency, decreases in shear stiffness would be expected to result in increases in the amplitude of the cyclic rotation of the inner cylinder while the corresponding increases in hysteretic damping would be expected to result in compensating decreases in this amplitude. The relative magnitudes of these compensating effects would be expected to vary with strain. Thus, the relationship between the amplitude of the cyclic rotation of the inner cylinder and the variation in the dynamic shear modulus with shear strain is predicted to be complex and may not show obvious trends. Finally, one would expect the predicted decreases in the apparent natural frequency of the cyclic rotation of the inner cylinder and increases in the amplitude of the cyclic rotation of the inner cylinder at the apparent natural frequency with increases in the amplitude of the loading, assuming a given set of soil properties. Thus, because at least one parameter of the response of the testing system was predicted to be sensitive to the variation in the dynamic shear modulus with shear strain in a clear, physically reasonable manner, we concluded that conducting high frequency, cyclic tests using the proposed testing procedure is a theoretically feasible means for determining the variation in the dynamic shear modulus with shear strain.

Based on our experiences in simulating impulse tests and high frequency, cyclic tests which induce high levels of shear strain, we concluded that the impulse test would be a preferable test for determining the variation in the dynamic shear modulus with shear strain. With the need to carry out a frequency sweep, the high frequency, cyclic test is somewhat more complex than the impulse test.

Degradation Characteristics of Clays--To determine the theoretical feasibility of the proposed testing system for determining the degradation characteristics of clays, a range of soil conditions was established by varying the degradability of the test soil while maintaining constant the parameters describing the undegraded shear stress-strain behavior (behavior expected during first cycle of loading). Thus, elements of soil at a single depth in uniform, saturated deposits were considered. We did not vary depth since behavior for different depths was expected to be qualitatively similar.

The degradability of the soil was varied by assuming three different degradation parameter functions (20). These functions, which describe cyclic degradation characteristics, are shown in Fig. 19. The functions describe the characteristics of a highly degradable, a moderately degradable, and a nondegradable clay. The average degradation parameter curve presented by Idriss et al. in Fig. 12 of Ref. 20, was used to describe the degradation characteristics of the highly degradable soil while 0.5 times this function was used to describe the degradation characteristics of the moderately

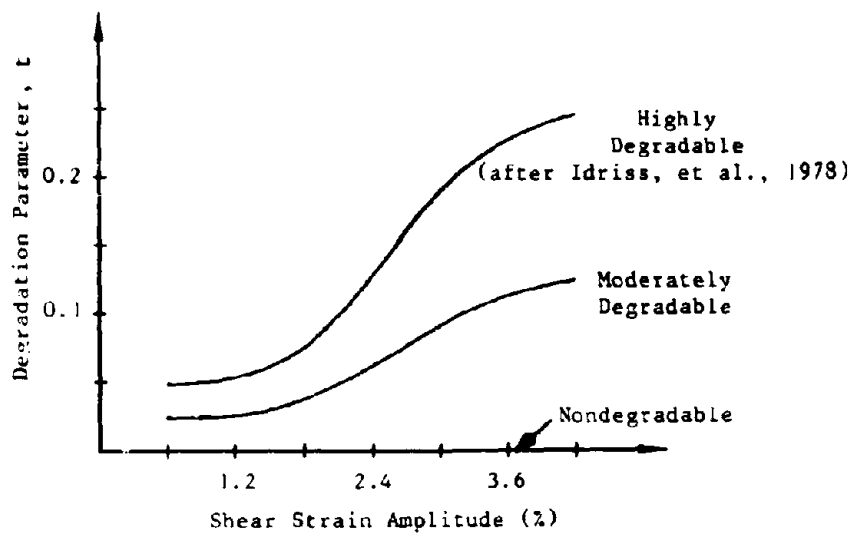


Figure 19: Range of Clay Degradation Parameter Functions Used - Degradation Characteristics of Clays Study

degradable soil. The base curve was converted to terms of shear strain from terms of normal strain (20) by assuming Poisson's ratio = 0.5 and linear elastic behavior. The degradation parameter function for the nondegradable clay was zero over the entire range of shear strain.

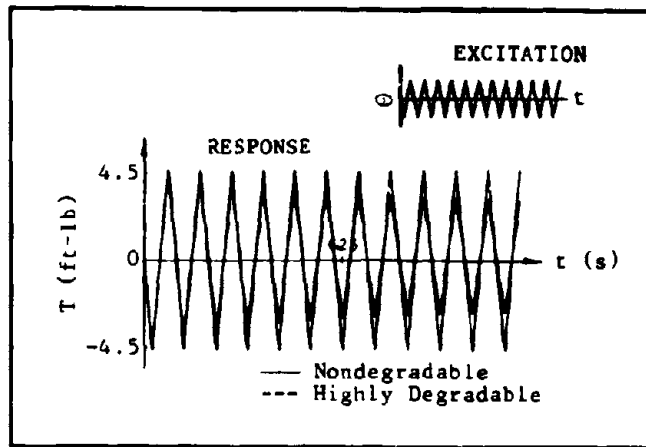
The low amplitude dynamic shear modulus and shear strength were calculated to be 720,000 psf and 660 psf, respectively. The depth, effective unit weight, void ratio, coefficient of earth pressure at rest, effective angle of internal friction, and cohesion were assumed to be 50 ft, 44 pcf, 1.3, 0.6, 28 deg, and 0 psf, respectively. The equations used to calculate the low amplitude dynamic shear modulus and the shear strength are presented in Ref. 15. The shear strength was the average of the shear strengths estimated separately for horizontal and vertical planes. Since solutions were obtained by the static procedure, we did not assume a value for viscous damping.

Guided by current laboratory practice for determining clay degradation characteristics (20), we considered a low frequency, cyclic excitation having a uniform rotation amplitude. The inner cylinder responded by developing the low frequency, cyclic torque needed to maintain the imposed rotation. Three amplitudes of rotation were considered: a high amplitude equal to 0.02 rad, a medium amplitude equal to 0.01 rad, and a low amplitude equal to 0.004 rad. These amplitudes, intended to induce various levels of degradation, were predicted to cause cyclic shear strains in the test soil along the wall of the inner cylinder having amplitudes of 3%, 1.8%, and 0.6%, respectively.

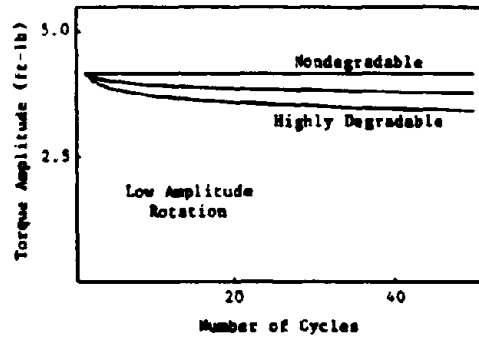
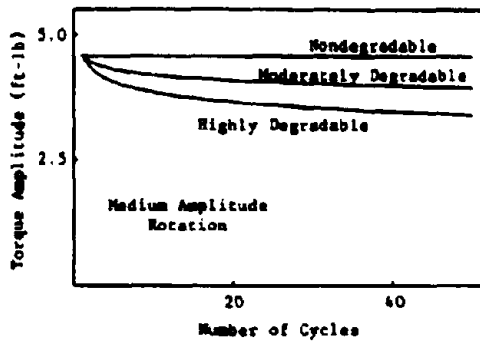
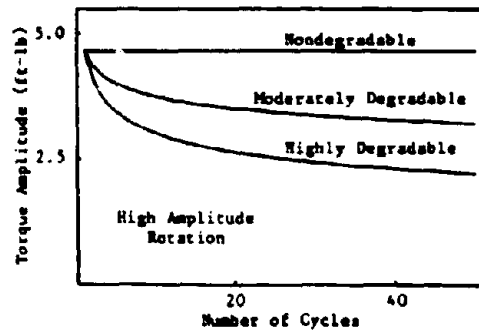
Results are presented in Fig. 20. Figure 20(a) gives samples of the predicted measured quantities. Figure 20(b) gives a selected parameter of the predicted measured quantities as a function of the number of cycles of loading for the various levels of degradability and the various amplitudes of excitation considered. The selected parameter was the amplitude of the cyclic torque developed by the inner cylinder, averaged over each cycle.

The results of the study indicate that the behavior of the testing system will be sensitive to the degradation characteristics of a clay in a clear, physically reasonable manner. For example, referring to Fig. 20(b), with the high rotation amplitude imposed on the inner cylinder, the amplitude of the cyclic torque developed by the inner cylinder was predicted to be about 50% less after 50 cycles of loading when testing the highly degradable clay than when testing the nondegradable clay, and about 30% less when testing the moderately degradable clay. Qualitatively similar behavior was predicted for the other amplitudes of loading. Also, as shown in Fig. 20(b), it was predicted that, when testing the highly degradable clay, the amplitude of the torque developed by the inner cylinder would decrease by about 50% in 50 cycles at the high amplitude of rotation, by about 25% at the medium amplitude, and by about 20% at the low amplitude. Qualitatively similar behavior was predicted for the clay having medium degradability while degradation was not predicted for the nondegradable clay.

The results of the study are physically reasonable. Because the test soil will be more susceptible to degradation when it is more degradable and subjected to larger loads, one would expect the amplitude of the cyclic torque developed by the inner cylinder to be less after a given number of



(a) Samples of Predicted Measured Quantities



(b) Parameter of Predicted Measured Quantities

Figure 20: Results from Simulations of Low Frequency, Cyclic, Controlled-Rotation Tests - Degradation Characteristics of Clays Study

cycles of rotation when testing a more degradable clay at a given amplitude of rotation and when testing a clay of given degradability at higher amplitudes of rotation. Thus, it was concluded that the proposed testing procedure is a theoretically feasible means for determining the degradation characteristics of clays.

Degradation and Liquefaction Characteristics of Sands and Silts--To determine the feasibility of the proposed testing system for obtaining the degradation and liquefaction characteristics of sands and silts, we modeled the degradation and liquefaction characteristics of the test soil analytically and by the use of published test data (see Solution Procedures, pg. 36). The published test data was used to more fully take into account the restraining effect of dilation.

The range of soil conditions considered for the study based on the analytical model was established by varying the degradation and liquefaction characteristics of the test soil. Also, we varied the undegraded shear stress-strain behavior (behavior expected during first cycle of loading) to be consistent with the degradation and liquefaction characteristics of the test soil. Elements of sand at a single depth in uniform, saturated deposits were considered. We did not vary depth since behavior for different depths was expected to be qualitatively similar. Also, silts were expected to behave similarly to the sands.

The test soil was assumed to have high, medium, and low resistance to degradation and liquefaction. The parameters defining the three models are presented in Table 1. Values for the parameters defining the degradation and liquefaction characteristics,  $C_1$ ,  $C_2$ ,  $C_3$ ,  $C_4$ ,  $k_2$ ,  $m$ , and  $n$ , were obtained from Ref. 23. The low amplitude dynamic shear moduli were calculated using the equation presented in Ref. 15. Strengths were estimated iteratively such that the sands having low, medium, and high resistance to degradation and liquefaction showed approximately the same resistance to initial liquefaction, under cyclic simple shear loading, as freshly deposited Monterey No. 0 test sand (see Ref. 28) at relative densities of 54%, 75%, and 90%, respectively. For the strength estimates, we constructed a simple model to simulate cyclic simple shear tests. We iteratively assumed shear strengths until the behavior predicted with this model agreed reasonably well with the data presented in Ref. 28. Figure 21 shows comparisons between the behavior predicted by our simple shear model at the final stage of iteration and that observed during the tests reported by Seed. Because of the approximate nature of our study, we did not distinguish between initial liquefaction and shear failure (see Analytical Modeling, pg. 32).

The range of soil conditions considered for the study based on the published test data was also established by varying the degradation and liquefaction characteristics of the test soil. Elements of sand at a single depth in uniform, saturated deposits were considered. We did not vary depth since behavior for different depths was expected to be qualitatively similar. Silts were expected to behave similarly to the sands. The degradation and liquefaction characteristics of the test soil were varied by varying the relative density. Figure 11 presents the published test data (see Solution Procedures, pg. 36). In this special case of freshly deposited and identically prepared samples of sand tested in the same pressure environment, relative density essentially determines degradation and liquefaction characteristics. Broad ranges of degradation

Parameters	Low Resistance Sand	Medium Resistance Sand	High Resistance Sand
$z$ (ft)	25	25	25
$G_{mo}$ (psf)	1,550,000	1,700,000	1,810,000
$I_{mo}$ (psf)	800	1200	1400
$\bar{\gamma}$ (pcf)	63	66	68
$e$	0.66	0.59	0.54
$D_r$ (%)	54	75	90
$K_0$	0.50	0.45	0.40
$\zeta$	0.02	0.02	0.02
$C_1^1$	0.666	0.52	0.346
$C_2^1$	1.968	2.518	3.536
$C_3^1$	4.761	4.569	3.707
$C_4^1$	3.865	3.706	3.025
$m^1$	0.43	0.43	0.43
$n^1$	0.62	0.62	0.62
$k_2^1$	0.0025	0.0025	0.0025

<sup>1</sup>After Martin et al., (1981)

Table 1: Parameters Defining Analytically-Based Models - Degradation and Liquefaction Characteristics of Sands and Silts Study

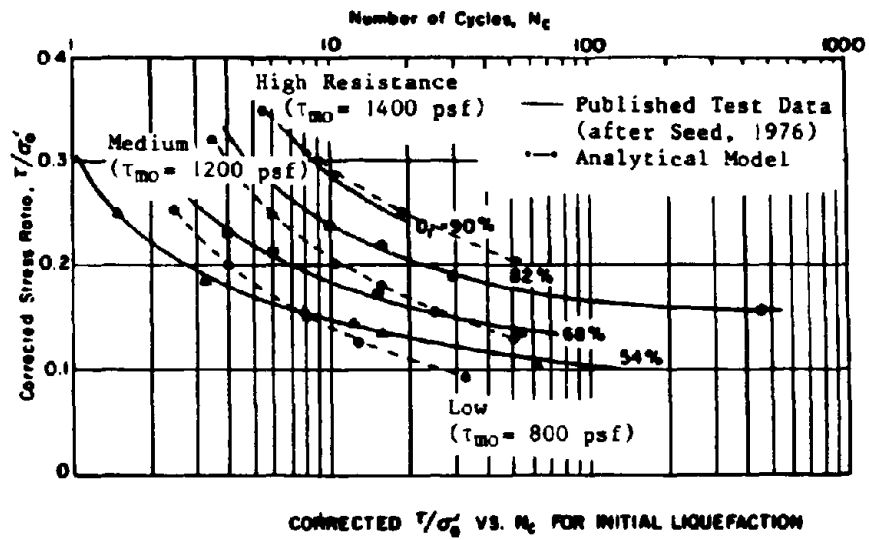


Figure 21: Resistance to Initial Liquefaction Under Cyclic Simple Shear Loading

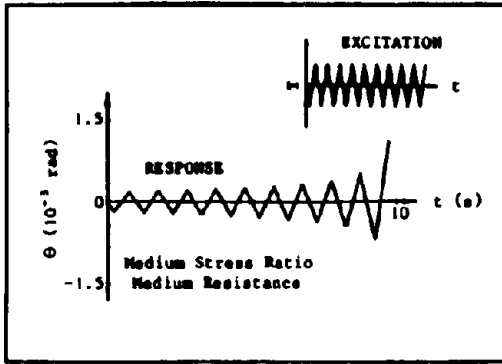
and liquefaction characteristics were assumed. The sand was considered to have relative densities ranging from 40% (very little resistance to liquefaction and degradation) to 100% (highly resistant to liquefaction and degradation). Consistent with the study based on the analytical model, we considered an element of soil at a depth of 25 ft. A single effective unit weight of 60 pcf was assumed.

Guided by current laboratory practice for determining the cyclic degradation and liquefaction characteristics of sands and silts, we considered a low frequency, cyclic, controlled-torque excitation having a uniform amplitude. The response of the inner cylinder was a low frequency, cyclic rotation. When using the analytically-based model, tests were simulated assuming amplitudes of applied torque which induced shear stress ratios ranging in value from 0.075 to 0.40. When using the model based on the published test data, we simulated tests assuming amplitudes of applied torque which induced shear stress ratios ranging in value from 0.15 to 0.40.

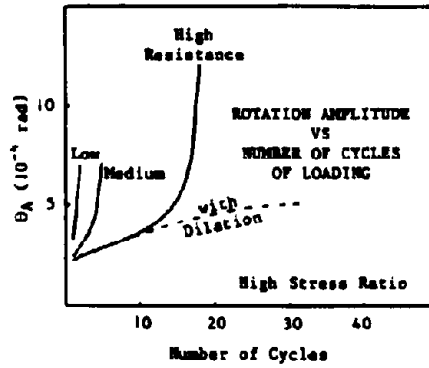
Figures 22 and 23 present results. Figure 22(a) presents samples of predicted measured quantities obtained using the analytically-based model. Figures 22(b) and (c) present a selected parameter of the predicted measured quantities as a function of the number of cycles of loading for the various soil conditions and amplitudes of loading (indicated in Fig. 22 as high, medium, and low stress ratios). The selected parameter was the amplitude of the rotation of the inner cylinder. Expected responses when taking dilation fully into account are sketched in Figs. 22(b) and (c). Figure 23 presents parameters obtained using the model based on the published test data. Figure 23(a) gives the estimated amplitude of the rotation of the inner cylinder after 10 cycles of loading as a function of the amplitude of the applied cyclic torque and relative density. Figure 23(b) gives the estimated limiting amplitude of the cyclic rotation of the inner cylinder as a function of relative density.

The results of the study involving the analytically-based model indicate that the behavior of the testing system will be sensitive to the degradation and liquefaction characteristics of a sand. Referring to Fig. 22, it was predicted that for a medium torque amplitude (medium stress ratio) it will take about 15 times as many cycles of loading for the inner cylinder to reach a rotation amplitude of  $5 \times 10^{-4}$  rad when testing the sand that is highly resistant to degradation and liquefaction than when testing the sand having low resistance. Also, it was predicted that when testing the sand having medium resistance, it will take about 15 times as many cycles for the inner cylinder to develop a rotation amplitude of  $5 \times 10^{-4}$  rad when applying a torque having a low amplitude of 1.4 ft-lb (low stress ratio) as when applying a torque having a high amplitude of 2.9 ft-lb (high stress ratio). Finally, it was predicted that the inner cylinder would develop unrestrained rotations in about 16 times as many cycles of loading when testing the sand having high resistance to liquefaction and degradation at the medium amplitude of loading (medium stress ratio) than when testing the sand having low resistance. Unrestrained rotation of the inner cylinder indicated either liquefaction of the test soil or shear failure.

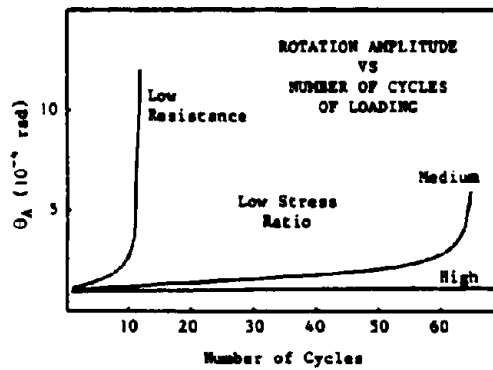
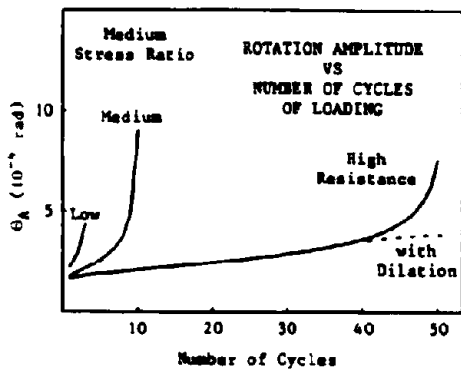
The results of the study are physically reasonable for loose sands and for dense sands at lower levels of excess porewater pressure. In these cases, the amplitude of the cyclic rotation of the inner cylinder would be expected to increase at a



(a) Sample of Predicted Measured Quantities

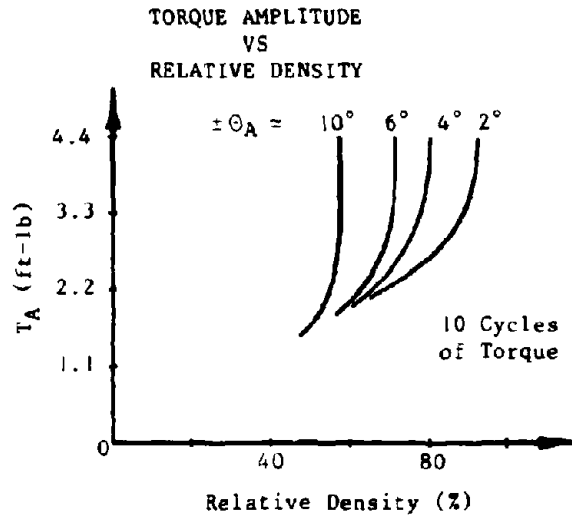


(b) Parameter of Predicted Measured Quantities

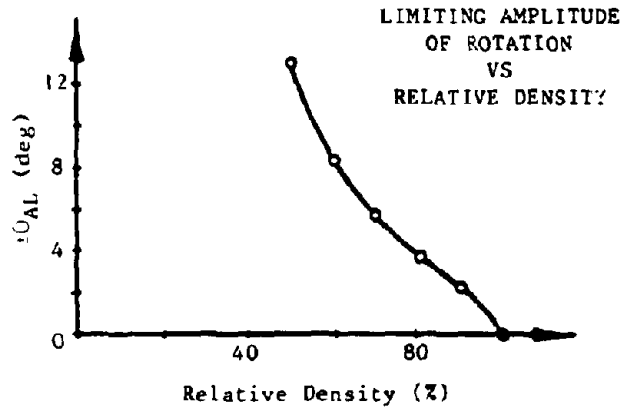


(c) Parameter of Predicted Measured Quantities

Figure 22: Results from Simulations of Low Frequency, Cyclic, Controlled-Torque Tests Using Analytically-Based Model - Degradation and Liquefaction Characteristics of Sands and Silts Study



(a) Estimated Rotation Amplitudes of Inner Cylinder after Applying 10 Cycles of Torque When Testing Freshly Deposited Monterey No. 0 Sand



(b) Estimated Limiting Amplitude of Rotation of Inner Cylinder When Testing Freshly Deposited Monterey No. 0 Sand

Figure 23: Results from Simulations of Low Frequency, Cyclic, Controlled-Torque Tests Using Model Based on Published Test Data - Degradation and Liquefaction Characteristics of Sands and Silts Study

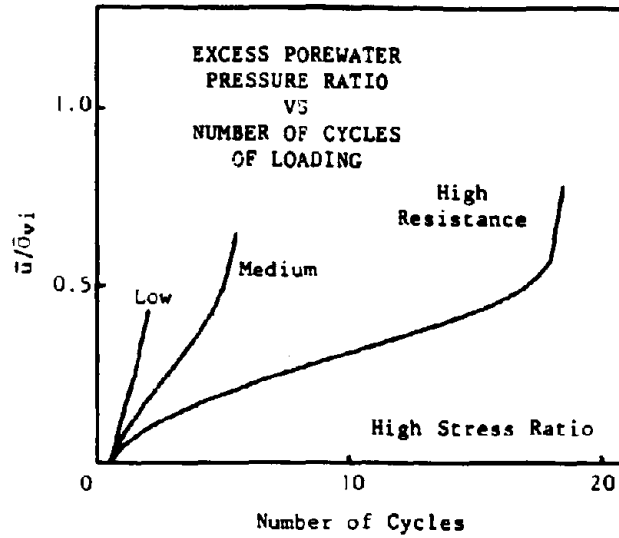
greater rate with an increase in the number of cycles of loading when testing sands less resistant to liquefaction and degradation and when applying higher amplitudes of torque to the inner cylinder. Additionally, when testing loose sands the inner cylinder would be expected to undergo unrestrained rotations if loaded sufficiently.

However, the results are not physically reasonable for dense sands at higher levels of excess porewater pressure. Because of the restraining effect of dilation, the inner cylinder would not be expected to undergo unrestrained rotation when testing a dense sand regardless of the level of excess porewater pressure. Rather, as sketched in Figs. 22(b) and (c), the inner cylinder would be expected to develop a limited amplitude of rotation. As explained in the section entitled PROPOSED METHOD, pg. 22, current, commonly used, state-of-the-art analytical models, such as the one we used, do not model dilation. As a result, we were unable to model effectively the behavior of dense sands at high levels of excess porewater pressure using analytical models. Thus, from the results obtained using the analytically-based model, we were only able to conclude that the proposed testing procedure is a theoretically feasible means for determining the degradation and liquefaction characteristics of looser sands and silts and the degradation characteristics of denser sands and silts at lower levels of excess porewater pressure.

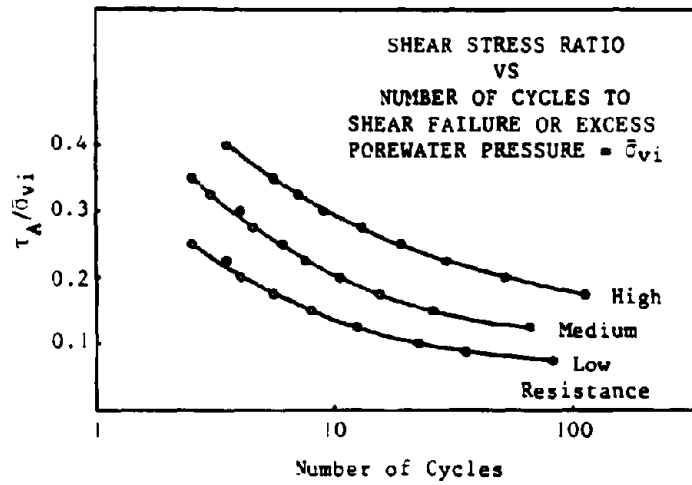
The results of the study involving the published test data indicate that the behavior of the testing system will be sensitive to the degradation and liquefaction characteristics of all sands at higher levels of excess porewater pressure. For example, referring to Fig. 23(a), when applying a cyclic torque having an amplitude of 3.3 ft-lb, it was predicted that, after 10 cycles of loading, the inner cylinder will develop a rotation amplitude when testing a sand having low resistance to liquefaction and degradation (relative density = 55%) about 5 times larger than that developed when testing a highly resistant sand (relative density = 90%). Additionally, referring to Fig. 23(b), the limiting amplitude of the rotation of the inner cylinder was predicted to be about 4 times larger when testing the sand having low resistance to liquefaction and degradation than when testing the highly resistant sand. Also, as shown in Fig. 23(b), with sufficiently large amplitudes of applied torque, virtually unrestrained rotations of the inner cylinder were predicted when testing the sand at relative densities less than about 45%. This indicated liquefaction of the test soil.

These results are physically reasonable. One would expect both the amplitude of the cyclic rotation of the inner cylinder after an arbitrary number of cycles of loading and the limiting amplitude of this rotation to be less when testing sands with greater resistance to liquefaction and degradation. Also, one would expect liquefaction after a sufficient number of cycles of loading at an appropriate amplitude when testing sands having little resistance to liquefaction. Thus, it was concluded that the proposed testing system is a theoretically feasible means for determining the degradation and liquefaction characteristics of sands and silts.

Figures 24 and 25 are presented for demonstrative purposes. These figures show plots of other information that was computed, using the analytically-based model. This type of information could be derived from measured data by soil-probe interaction analysis. Figure 24(a) gives the buildup in the excess porewater pressure within the test soil as a function of the number of cycles of loading at a high shear stress ratio, while Fig.

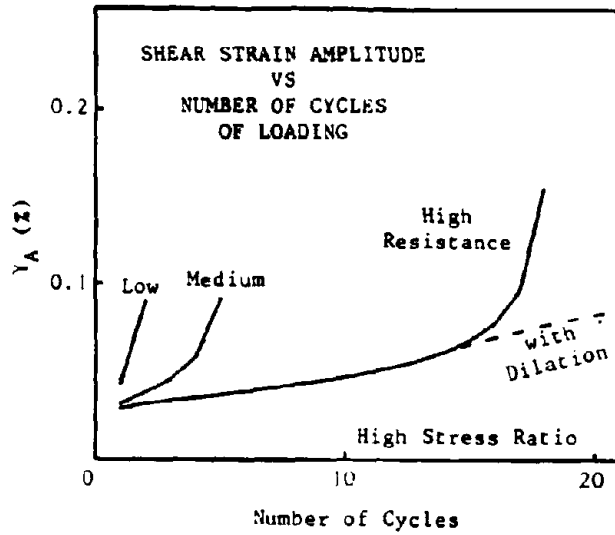


(a) Predicted Derived Information

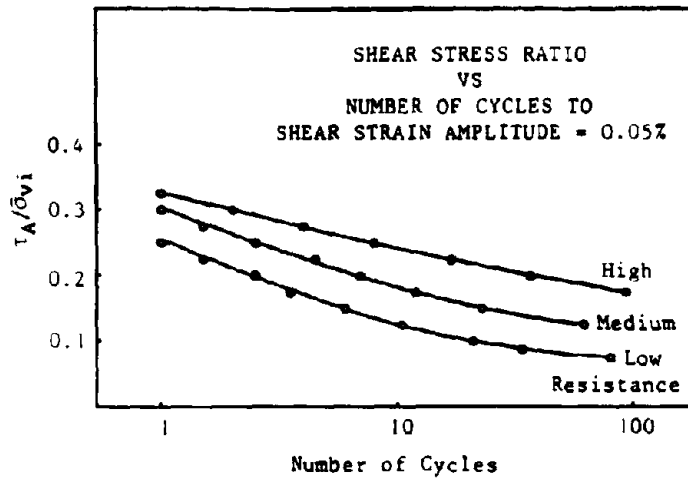


(b) Predicted Derived Information

Figure 24: Results from Simulations of Low Frequency, Cyclic, Controlled-Torque Tests Using Analytically-Based Model - Degradation and Liquefaction Characteristics of Sands and Silts Study



(a) Predicted Derived Information



(b) Predicted Derived Information

Figure 25: Results from Simulations of Low Frequency, Cyclic, Controlled-Torque Tests Using Analytically-Based Model - Degradation and Liquefaction Characteristics of Sands and Silts Study

25(a) similarly gives the amplitude of the cyclic shear strain within the test soil. Such information may be used to develop typical presentations of degradation and liquefaction characteristics such as those shown in Figs. 24(b) and 25(b). Figure 24(b) presents the shear stress ratio as a function of the number of cycles of loading required to cause the excess porewater pressure to rise to the level of the initial effective vertical stress (liquefaction in looser sands) or to cause shear failures for the various soil conditions. Figure 25(b) presents similar information in terms of a specified level of the amplitude of the cyclic shear strain rather than a specified level of excess porewater pressure.

### Conclusions

In this subsection, we itemize the main conclusions resulting from the theoretical feasibility study. These conclusions directly relate to the objectives presented in the subsection entitled Objectives, pg. 28.

1) The proposed testing system is a theoretically feasible means for determining the low amplitude dynamic shear modulus, the variation in the dynamic shear modulus with shear strain, the degradation characteristics of clays, and the degradation and liquefaction characteristics of sands and silts.

2) The theoretical feasibility study served as a basis for the preliminary design criteria needed to conduct an operational feasibility study for determining the operational feasibility of a laboratory research prototype testing system and to develop a preliminary design for such a system.

3) Based on the results of the theoretical feasibility study, an initial testing methodology was established for Phase II research involving the laboratory testing of a research prototype testing system. The impulse test was selected as the preferable test for determining dynamic shear moduli. Using conventional practice as a guide, the low frequency, cyclic, controlled-rotation test was selected as the initial testing mode for determining the degradation characteristics of clays, while the low frequency, cyclic, controlled-torque test was selected as the initial testing mode for determining the degradation and liquefaction characteristics of sands and silts.

4) The analytical procedures, developed as part of the theoretical feasibility study, will serve as simple, but effective means for qualitatively checking, during Phase II research, the results from laboratory tests involving a research prototype testing system, and developmental results from descriptive soil-probe interaction analysis procedures, to be constructed as part of Phase II research.

5) We found two unexpected results in the theoretical feasibility study. The peak rotation of the inner cylinder during long duration impulse tests for determining the low amplitude dynamic shear modulus was predicted to be significantly more sensitive to the low amplitude dynamic shear modulus than the shear wave velocity. Laboratory testing would be required to confirm this finding. Also, the results of our study indicate that the impulse test may be preferable to the high frequency, cyclic test for determining dynamic shear moduli.

## Supplementary Theoretical Feasibility Study

### Introduction and Summary

We conducted a cursory supplementary theoretical feasibility study in addition to our proposed theoretical feasibility study. The purpose of this supplementary study was to estimate roughly the rotational flexibility of the inner cylinder, as configured in the preliminary design of the testing system, relative to the rotational flexibility of the test soil. The estimate was made to determine whether special attention would be required as a result of such relative flexibility. For our theoretical feasibility study, we assumed rigid behavior for the inner cylinder. Rigid behavior is desired mainly so that the measured rotational motions will be due entirely to the rotation of the test soil. Because of project limits, we estimated the rotational flexibility of the inner cylinder relative to that of the test soil only during low frequency, cyclic, controlled-torque tests for determining the degradation and liquefaction characteristics of sands and silts. This mode of testing is expected to be the main capability of the proposed testing system.

The results of our cursory study indicate that the inner cylinder, as configured in the preliminary design of the testing system, may be rotationally flexible relative to the test soil during the initial cycles of loading. However, the inner cylinder was predicted to be rotationally rigid in comparison to the degraded test soil during the later cycles of loading.

Based on the results of the study, we concluded that the estimated rotational flexibility of the inner cylinder would increase uncertainty in inferring soil properties from test results. Nevertheless, because of the many promising mitigating steps which could be taken, if necessary, to reduce the uncertainty caused by flexibility of the inner cylinder, we feel that the proposed testing system will serve its stated purpose well and will advance our ability to determine in situ cyclic and dynamic soil properties.

We provide details in the remaining subsections. We state the objective and procedures of the supplementary theoretical feasibility study and present and discuss results, mitigating steps, and conclusions.

### Objective

The objective of this supplementary study was to provide a rough estimate of the rotational flexibility of the inner cylinder, as configured in the preliminary design of the testing system (see report from Sweet & Aiken, Inc., in Appendix C), relative to the rotational flexibility of the test soil. The estimate was made to help determine whether any special attention should be directed toward the issue of the rotational flexibility of the inner cylinder. Rigid behavior is desired, mainly, so that the measured rotational motions will be entirely due to the rotation of the test soil. The study was conducted considering only the low frequency, cyclic, controlled-torque test for determining the degradation and liquefaction characteristics of sands and silts. This testing mode is expected to be the main capability of the proposed testing system.

## Procedures

In this subsection, we discuss the procedures used to estimate the rotational flexibility of the inner cylinder relative to that of the test soil during low frequency, cyclic, controlled-torque tests. This relative flexibility was estimated for the initial cycle of loading, before significant degradation of the test soil is expected to have taken place. Estimates were also made for the ultimate cycle of loading during which the test soil is expected to have either liquefied or developed limited cyclic deformations. However, for the ultimate cycle of loading we estimated the rotational stiffness of the inner cylinder relative to that of the test soil. Estimates were made assuming expected ranges of soil conditions and applied torque. In our estimates, we did not consider the rotational flexibility of the inactive portion of the inner cylinder. Since this portion will not interact with the test soil, the effects of the rotational flexibility of this portion could be taken into account quite accurately.

The rotational flexibility of the inner cylinder relative to that of the test soil during the initial cycle of loading,  $F_i$ , was estimated using the following relationship:

$$F_i = \frac{Tl / \left[ \frac{\pi}{32} (D_o^4 - D_i^4) G_i \right]}{-\left( \frac{r_o - r_i}{r_o} \right) \left[ \frac{T/2\pi r_i^2 l}{(G_{mo}/\tau_{mo}) (-T/2\pi r_i^2 l) - G_{mo}} \right]} \quad (11)$$

where

- $r_i$  = outer radius of inner cylinder
- $r_o$  = inner radius of outer cylinder
- $D_o$  = outer diameter of inner cylinder
- $D_i$  = inner diameter of inner cylinder
- $G_i$  = shear modulus of inner cylinder
- $l$  = active length of inner cylinder
- $G_{mo}$  = undegraded low amplitude dynamic shear modulus of test soil
- $\tau_{mo}$  = undegraded shear strength of test soil
- $T$  = applied torque

Equation 11 gives the ratio of the static twist of the active portion of the flexible inner cylinder alone, caused by a static torque acting throughout the cylinder, to the static rotation of a rigid inner cylinder embedded in the undegraded test soil, caused by the same torque. Thus, the flexible inner cylinder and the test soil were considered independently. Also, rotations estimated for the rigid inner cylinder were caused entirely by the rotation of the test soil. A derivation for Eq. 11 is presented in Appendix B, pg. B-4.

The following equation was used to estimate the rotational stiffness of the inner cylinder relative to the rotational stiffness of the test soil during the ultimate cycle of loading,  $S_u$ :

$$S_u = - \frac{(\frac{r_o - r_i}{r_o}) [\gamma_{ruA}(r_i)]}{T_1 / [\frac{\pi}{32} (D_o^4 - D_i^4) G_i]} \quad (12)$$

where  $\gamma_{ruA}(r_i)$  = amplitude of cyclic shear strain developed in test soil along wall of inner cylinder during ultimate cycle of loading

Equation 12 gives the ratio of the amplitude of the low frequency, cyclic rotation of the inner cylinder caused by a cyclic torque assuming the inner cylinder to be rigid and embedded in fully degraded test soil, to the static twist of the flexible inner cylinder alone, caused by a torque equal in value to the amplitude of the cyclic torque and acting throughout the cylinder. Thus, the flexible inner cylinder and the test soil were considered independently. Also, rotations estimated for the rigid inner cylinder were caused entirely by the rotation of the test soil. A derivation for Eq. 12 is presented in Appendix B, pg. B-6.

To apply Eq. 12, the amplitude of the cyclic shear strain developed in the test soil along the wall of the inner cylinder during the ultimate cycle of loading,  $\gamma_{ruA}(r_i)$ , was estimated using the published test data presented by Seed (28) and shown in Fig. 11(a). This figure gives, as a function of relative density, the limiting amplitudes of shear strain that developed in samples of sand in response to cyclic shear stresses applied to the samples. The data and the use of the data are discussed more fully in the subsection entitled Solution Procedures, pg. 36. In using Eq. 12, we assumed that the limiting strains were independent of the applied stresses (28). Thus, the applied torque did not affect our predictions of the rotations developed by the test soil during the ultimate cycle of loading.

#### Presentation and Discussion of Results

In this subsection, we present and discuss the results of our study of the rotational flexibility of the inner cylinder relative to that of the test soil. To estimate both the rotational flexibility and stiffness of the inner cylinder relative to the test soil, we assumed a steel inner cylinder having an active length of 8 in, an outer diameter of 1 in, and a wall thickness of 1/16 in. These dimensions were based roughly on the configuration of the inner cylinder in the preliminary design of the testing system (see report from Sweet & Aiken, Inc., Appendix C).

The soil properties considered correspond to those expected in a loose, uniform, saturated sand deposit having low resistance to degradation and liquefaction and those expected in a dense, uniform, saturated sand deposit having high resistance to degradation and liquefaction. The following conditions were assumed for the loose and dense deposits, respectively: coefficient of earth pressure at rest = 0.6 and 0.4, effective angle of internal friction = 32 deg and 41 deg, void ratio = 0.85 and 0.54, and the effective unit weight = 56 and 68 pcf. Properties were obtained for depths of about 5 and 75 ft. For these depths, the strengths of the loose deposit

were estimated to be 100 and 1450 psf, and the strengths of the dense deposit were estimated to be 200 and 3600 psf, respectively. Also, for these depths the low amplitude dynamic shear moduli were estimated to be 514,000 and 1,990,000 psf for the loose deposit and 723,000 and 3,100,000 psf for the dense deposit, respectively. The shear strengths for the loose deposit and shear moduli for both deposits were calculated using expressions presented in Refs. 15 and 16. These shear strengths were averages of the shear strengths estimated separately for horizontal and vertical planes. The strengths for the dense deposit were estimated by calibrating a simple shear model to test data presented by Seed (28) (see Degradation and Liquefaction Characteristics of Sands and Silts, pg. 53). Torques representing various levels of applied shear stress ratio,  $\tau_{rA}(r_i)/\bar{\sigma}_{vi}$ , were considered. An amplitude of cyclic shear strain equal to 40% was taken to represent liquefaction (see Fig. 11(a)).

Summaries of results are provided in Table 2. Table 2(a) provides the rotational flexibility of the active portion of the inner cylinder, relative to that of the test soil, during the initial cycle of loading for the various soil and test conditions considered. Table 2(b) provides the rotational stiffness of the active portion of the inner cylinder, relative to that of the test soil, during the ultimate cycle of loading for the various soil and test conditions considered.

The results of the cursory study indicate that during the initial cycles of loading during low frequency, cyclic, controlled-torque tests for determining the degradation and liquefaction characteristics of sands and silts, the inner cylinder of the testing system may be rotationally flexible relative to the test soil. This relative flexibility may be a source of uncertainty in inferring soil properties from test results. This relative flexibility, and the uncertainty it may introduce, is predicted to be greatest when testing stiff, dense sand deposits at great depth using low levels of excitation. The rotational flexibility of the inner cylinder was predicted to decrease relative to the test soil with higher levels of excitation because higher torques caused decreases in the stiffness of the nonlinear test soil but not of the linear inner cylinder.

The results also indicate that, under all conditions, the inner cylinder will be rotationally very rigid in comparison to the test soil during the ultimate cycle of loading when the test soil has fully degraded. Thus, the rotational flexibility of the inner cylinder relative to that of the test soil should not be a large source of uncertainty in inferring soil properties from the later, more important, stages of a cyclic test.

#### Mitigating Steps

In this subsection, we discuss some of the steps which could be taken, if necessary, to decrease uncertainty introduced into test results by rotational flexibility of the inner cylinder. Generally, such uncertainty may be reduced by reducing the rotational flexibility of the inner cylinder relative to that of the test soil and by taking into account the rotational flexibility of the inner cylinder in the interpretation of test results.

There are a number of ways to greatly reduce the rotational flexibility of the inner cylinder relative to that of the test soil. The most promising

		Depth (ft)	
		5	75
Shear Stress Ratio	0.05	1.0	3.5
	0.15	0.7	2.3

Loose Sand

		Depth (ft)	
		~5	75
Shear Stress Ratio	0.2	1.2	4.5
	0.4	0.7	3.0

Dense Sand

(a) Relative Rotational Flexibility,  $F_i$ , - Initial Cycle of Loading

		Depth (ft)	
		5	75
Shear Stress Ratio	0.05	13,000	900
	0.15	4,000	300

Loose Sand

		Depth (ft)	
		~5	75
Shear Stress Ratio	0.2	500	27
	0.4	250	14

Dense Sand

(b) Relative Rotational Stiffness,  $S_u$ , - Ultimate Cycle of Loading

Table 2: Rotational Flexibility and Stiffness of Active Portion of Inner Cylinder Relative to Rotational Flexibility and Stiffness of Test Soil

methods appear to be reducing the length of the inner cylinder or appropriately increasing the diameters and wall thicknesses of the inner and outer cylinders. Consistent with other in situ testing methods, testing may be optimized by the use of differently sized systems for different conditions. Additionally, for greater certainty in results from earlier stages of loading, the rotational flexibility of the inner cylinder could be reduced relative to that of the test soil by conducting tests at higher levels of excitation.

The most promising means of taking the rotational flexibility of the inner cylinder into account when interpreting soil properties from test results is directly modeling the rotational flexibility of this cylinder in the soil-probe interaction analysis. This is expected to be effective because it is not expected to be difficult to describe, in reasonably complete and accurate detail, the flexibility of the inner cylinder and the interaction of the flexible inner cylinder with the test soil. The inner cylinder will have a relatively simple geometry and relatively simple material properties, and the predominate stresses developed in the inner cylinder and the test soil during testing are expected to be simple torsional shear stresses. To additionally account for the rotational flexibility of the inner cylinder, greater weight could be placed on data obtained during the later stages of a cyclic test.

#### Conclusions

In this subsection, we present the conclusions arising from the study of the rotational flexibility of the inner cylinder relative to that of the test soil. The conclusions apply only to low frequency, cyclic, controlled-torque tests for determining the degradation and liquefaction characteristics of sands and silts.

1) The inner cylinder of the proposed testing system, as configured in the preliminary design, may be rotationally flexible relative to the test soil during the initial cycles of loading. This relative rotational flexibility is expected to be greater when testing denser soils at greater depths and when applying lower levels of excitation. This relative flexibility will be a source of uncertainty when inferring soil properties from test results.

2) The inner cylinder was predicted to be rotationally very rigid in comparison to the test soil, under all conditions considered, during the ultimate cycle of loading when the test soil has fully degraded. Thus, a relatively high degree of certainty is expected when inferring soil properties from test results obtained during the later stages of loading.

3) Uncertainty in the interpretation of test results, caused by the rotational flexibility of the inner cylinder relative to that of the test soil, may be reduced considerably by reducing this relative rotational flexibility. The most promising methods for reducing relative flexibility include decreasing the length of the inner cylinder or appropriately increasing the diameters and thicknesses of the inner and outer cylinders. Consistent with other in situ testing procedures, testing may be optimized by use of differently sized systems for different conditions. Additionally, to reduce relative flexibility, tests may be carried out at higher levels of excitation.

4) Uncertainty in the interpretation of test results, caused by the rotational flexibility of the inner cylinder relative to that of the test soil, may also be reduced considerably by accounting for the rotational flexibility of the inner cylinder in the interpretation of test results. The most promising method for doing this is to directly model the rotational flexibility of the inner cylinder in the soil-probe interaction analysis used to infer soil properties. Also, greater weight could be placed on data obtained during the later stages of a test.

5) Prior to developing a final design for a laboratory research prototype testing system, modest analytical studies should be conducted to optimize the dimensions of the probe.

6) Because of the many promising mitigating steps which could be taken, if necessary, to reduce the uncertainty in test results caused by the rotational flexibility of the inner cylinder, the proposed testing system is expected to serve its stated purpose well and to advance our ability to determine in situ cyclic and dynamic soil properties.

#### Operational Feasibility Study

##### Introduction and Summary

An operational feasibility study was conducted to determine the operational feasibility of a laboratory research prototype testing system. This system will be functionally similar to the field system scheduled for development during Phase III. Since our firm did not have the necessary expertise, we arranged for the mechanical engineering design firm of Sweet & Aiken, Inc., (Sweet & Aiken) to conduct the study. Studies were carried out to determine the operational feasibility of a laboratory testing system for determining 1) the low amplitude dynamic shear modulus and the variation in the dynamic shear modulus with shear strain by impulse test, 2) the cyclic degradation characteristics of clays by low frequency, cyclic, controlled-rotation test, and 3) the cyclic degradation and liquefaction characteristics of sands and silts by low frequency, cyclic, controlled-torque test. Based on the results of our theoretical feasibility study, these three testing modes were judged to be the most promising modes of testing.

Results from the operational feasibility study indicate that a laboratory testing system is operationally feasible. The main components of the system, which satisfy reasonably well specified design criteria, were found to be either available or readily producible and it was determined that these components could be assembled into a convenient, workable arrangement. The design criteria, developed by our firm as part of our theoretical feasibility study, specified mechanical, excitation, and measurement requirements. The operational feasibility study resulted in a preliminary design for a laboratory research prototype testing system.

Not all specified criteria were satisfied; however, the resulting

consequences are not expected to be severe. For example, Sweet & Aiken was unable to find a transducer capable of measuring accurately the smallest predicted angles of the rotation of the inner cylinder that might occur during low frequency, cyclic, controlled-torque tests for determining degradation and liquefaction characteristics of sands and silts. However, it appears that we will be able to measure reasonably small angles. Thus, the potential increase in uncertainty in inferring soil properties from test results was judged to be only modest.

Sweet & Aiken estimated a cost of \$78,260 for the detailed design and construction of a laboratory research prototype testing system. This is a conservative estimate. Based on our experiences, we feel the estimated cost is consistent with that of the design and construction of comparable testing systems.

Details are provided in the remaining subsections. We state the objectives and procedures of the operational feasibility study, define the main components of the laboratory research prototype testing system, present and discuss our specified design criteria, present and discuss results from the operational feasibility study conducted by Sweet & Aiken, and present conclusions. In discussing the operational feasibility study, we concentrate on the geotechnical aspects of the testing system. The report from Sweet & Aiken, which summarizes the firm's work and is included in Appendix C, concentrates on the operational aspects of the testing system. Thus, the two reports are intended to complement each other.

### Objectives

The main objective of the operational feasibility study was to determine the operational feasibility of a laboratory research prototype testing system for determining 1) the low amplitude dynamic shear modulus and the variation in the dynamic shear modulus with shear strain by impulse test, 2) the cyclic degradation characteristics of clays by low frequency, cyclic, controlled-rotation test, and 3) the cyclic degradation and liquefaction characteristics of sands and silts by low frequency, cyclic, controlled-torque test. These three testing modes were judged to be the most promising modes of testing based on the results of the theoretical feasibility study. The laboratory research prototype testing system will be functionally similar to, but somewhat simpler than, the field system scheduled for development during Phase III. If successful, the operational feasibility study was to result in a preliminary design for a laboratory research prototype testing system. A secondary objective of the operational feasibility study was to develop an accurate cost estimate for the detailed design and construction of the laboratory research prototype testing system.

### Procedures

The operational feasibility of the laboratory research prototype testing system was determined by determining whether the main components (see Main Components, pg. 71), which satisfy specified design criteria, were available, and whether these components could be assembled into a convenient, workable arrangement. If it was found that the required components were available and could be assembled into a convenient, workable arrangement, then, we concluded that the laboratory research prototype testing system is operationally feasible.

First, our firm specified design criteria for the testing system including mechanical, excitation, and measurement requirements. Then, Sweet & Aiken conducted the study to determine the operational feasibility of the laboratory system for determining 1) the low amplitude dynamic shear modulus and the variation in the dynamic shear modulus with shear strain by impulse test, 2) the cyclic degradation characteristics of clays by low frequency, cyclic, controlled-rotation test, and 3) the cyclic degradation and liquefaction characteristics of sands and silts by low frequency, cyclic, controlled-torque test.

The following main tasks were performed as part of the operational feasibility study: 1) the evaluation and selection of the excitation systems, 2) the evaluation and selection of the measurement systems, 3) the design of the configuration of the probe (including sizing of main components and selection of seals, bearings, and materials), 4) the design of the vertical pressure system, 5) the development of a preliminary design layout, 6) the optimization of cylinder wall friction, 7) the evaluation and selection of the power and support cables, 8) the identification of problem areas, and 9) the development of an accurate cost estimate for the detailed design and construction of a laboratory system.

#### Main Components

The main components of the laboratory research prototype testing system considered in the operational feasibility study were those components which were judged essential to the performance of the stated functions of the testing system and were not obviously feasible. These components included mechanical, excitation, and measurement components and are expected to resemble closely the corresponding components of a field unit. The main mechanical components considered were the inner cylinder, the outer cylinder, the shield, the vertical pressure system, the sealing systems, and the bearing systems. The main excitation components considered included the power, control, and drive components required to provide the selected excitations. The main measurement components considered included the sensing, transmission, display, and recording components required to measure, transmit, display, and record appropriate excitation and response information. Components, which were not strongly addressed in the operational feasibility study, included a laboratory penetration system and an air pressure system for the probe. These items were considered feasible.

#### Design Criteria

In this subsection, we present the design criteria specified for the design or the selection of the main components of the laboratory research prototype testing system. We specified mechanical, excitation, and measurement requirements. The specified criteria, which are preliminary criteria, are summarized in Table 3. In the following subsections, we present the mechanical and the excitation and measurement requirements.

Mechanical Requirements--The mechanical requirements cover those specifications which affect the design or selection of the mechanical systems, including the vertical pressure system. The following items were specified: the sizes and geometries for the inner and outer cylinders, the

Mechanical Requirements

	Dimensions				Penetration Forces			Maximum Differential Lateral Pressure (psf)
	Outer Diameter (in)	Wall Thickness (in)	Length Below Piston (in)	Active Shielded Length (in)	Bearing Friction (lb)	Skin Friction (lb)	Total (lb)	
Outer Cylinder	3	1/12	12	N/A	4500	9500	14,000	30,000
Inner Cylinder	1	1/16	12	8	1500	2500	4000	30,000

Maximum Environmental Fluid Pressure: 100,000 psf

Range of Differential Vertical Pressures to Be Applied and Measured by Vertical Pressure System: 0 - 6000 psf

Excitation and Measurement Requirements

Mode	Excitation			Torque Amplitude Range (ft-lb)	Rotation Amplitude Range (deg) pk to pk	Rotation Frequency (cps)	Acceleration Amplitude Range @ 1 inch radius (g)	Maximum Power (hp)	
	Form	Period (sec)	Duration						
Controlled-Torque Cyclic Test	sine wave	0.1 - 50	≤100 cycles	0.1 - 15	0.002-30	0.001-15	0.02-10	N/A	0.20
Controlled-Rotation Cyclic Test	sine wave	0.1 - 50	≤100 cycles	0.1 - 15	0.4-3.0	0.2-1.5	0.02-10	N/A	0.03
Impulse Test	rectangular impulse	N/A	≥0.0002 s	0.01 - 20	N/A	N/A	400-2400	±0.3 - ±210	0.20

Table 3: Preliminary Design Criteria

maximum penetration forces, the desired wall characteristics of the inner and outer cylinders, the maximum differential lateral pressures acting on the inner and outer cylinders, the maximum water pressure, and the range of differential vertical pressures to be applied by the vertical pressure system. These items are discussed in the following paragraphs. Specifications are summarized in Table 3.

The sizes and geometries for the inner and outer cylinders were specified with the primary objective of developing a probe which is compatible with commonly used offshore drilling equipment. The field probe is intended to be lowered with a wireline through a drillstring, latched to the drillbit, and then operated (4). Thus, the outer diameter of the outer cylinder was specified to be 3 in. Larger systems could be developed specifically for onshore use. The diameter specified for the inner cylinder was judgmentally selected to be large enough to provide sufficient contact with the test soil and to allow soil to intrude into the inner cylinder during penetration, yet small enough to provide a sufficiently large and reasonably undisturbed sample. To avoid excessive disturbance to the test soil, the wall thickness of the outer cylinder was specified to be the same as that of normal, thin-walled, 3 in diameter sampling tubes. The wall thickness of the inner cylinder was specified to be even thinner to minimize disturbance to the test soil, to facilitate the intrusion of soil into the inner cylinder, and to minimize the amount of soil displaced by this cylinder. Also, we specified that the volume inside the inner cylinder should be large enough to prevent the development of significant confining pressure within the soil inside this cylinder. This feature was intended to help reduce the effect of the soil within the inner cylinder on the motion of this cylinder during testing. The active length (unshielded length) of the inner cylinder was specified to be 8 in, so that samples will have a length comparable to the length of samples for laboratory testing (~6 in) with additional length to allow for end effects. The 4 in length specified for the shield was judged sufficient to place the excitation at a depth below the base of the borehole where the soil is expected to be relatively undisturbed by the drilling process. The total length specified for the outer cylinder was equal to the sum of the shielded and unshielded lengths of the inner cylinder. The penetrating edges of both cylinders were specified to be sharpened in a manner that would minimize disturbances to the test soil during penetration. Additionally, the penetrating edges of the inner cylinder were specified to be jugged inward to divert soil entering the inner cylinder away from the wall of this cylinder during penetration. This feature is intended to help minimize the effects of the soil within the inner cylinder on the rotation of this cylinder during testing and also, to prevent the plugging of the soil within this cylinder during penetration due to wall friction.

We specified the following conservative maximum axial forces that might normally be developed during penetration: inner cylinder - 4000 lb, outer cylinder - 14,000 lb, and total - 18,000 lb. These forces correspond to penetration forces that might normally be developed in a dry, dense sand deposit at a depth of 50 ft or in a saturated, dense sand deposit at a depth of about 80 ft. Based on our experiences, we feel these specifications adequately cover penetration into the layers in which the greatest activity is expected to take place during earthquakes. Reasonable bending forces which may occur during penetration were covered partially by conservatism in our estimates of penetration forces and partially by conservatism in design (see report

from Sweet & Aiken, Appendix C). The following were assumed in calculating maximum penetration forces: a uniform, dry deposit of dense sand, depth = 50 ft, effective unit weight of soil = 122 pcf, coefficient of earth pressure at rest = 5, cohesion = 0 psf, effective angle of internal friction of soil = 45 deg, and effective angle of friction between the soil and the cylinder (clean steel) = 11 deg. The bearing capacities of the penetrating edges were roughly estimated assuming the edges to be blunt and to act as long footings. We used Meyerhof's conservative (maximum) bearing capacity factors (32):  $N_\gamma = 280$  and  $N_q = 130$ .

We specified the maximum differential lateral pressure which might act on either of the two cylinders conservatively as 30,000 psf. For this specification we assumed the conditions itemized in the preceding paragraphs. The maximum differential lateral pressure acting on the inner cylinder was expected to occur immediately following the penetration of the probe and the application of vertical pressure to the test soil. At this stage, the test soil would experience full lateral pressure while the soil within the inner cylinder would be expected to experience very little lateral pressure. The maximum differential lateral pressure acting on the outer cylinder was expected to occur during low frequency, cyclic, controlled-torque tests in loose sands or silts at the occurrence of liquefaction. At this time, the test soil within the outer cylinder would bear negligible effective lateral stress, while the soil surrounding the outer cylinder would bear the original high lateral stress.

The maximum water pressure under which the testing system should operate was specified as 100,000 psf. This corresponds to a depth, in salt water, of about 1500 ft.

The differential vertical pressure to be applied by the vertical pressure system was specified to range from 0 to 6000 psf. The maximum pressure corresponds to the effective pressure developed in a uniform, dense, saturated deposit of sand at a depth of about 80 ft. Two modes of operation were specified for the vertical pressure system (see PROPOSED METHOD, pg. 22). In one mode, the constant pressure mode, the vertical pressure acting on the test soil is to remain constant throughout testing. In the second mode, the constant volume mode, the position of the piston of the vertical pressure system is to remain substantially fixed once an appropriate vertical pressure has been applied. We also requested that the feasibility of a piston system capable of operating along the entire length of the inner and outer cylinders be addressed (see PROPOSED METHOD, pg. 19).

We specified various characteristics for the inner and outer cylinders. For both the outside of the inner cylinder and the inside of the outer cylinder, we specified that the surface friction should be minimized in the vertical direction but that the traction should be maximized in the horizontal direction by providing appropriately sized vertical grooves along these surfaces. Thus, disturbance to the test soil during penetration caused by surface friction would be minimized while the tendency for slip between the test soil and the cylinder walls during testing would also be minimized. The outside surface of the outer cylinder was specified to have vertical grooves to provide more effective anchoring to the surrounding soil during

testing without causing excessive penetration force. The inside surface of the inner cylinder was specified to be smooth and to have a minimum of friction to minimize the effect of the soil within the inner cylinder on the motion of this cylinder during testing.

We specified that frictional torques developed by the sealing systems and the bearings supporting the inner cylinder be kept to an absolute minimum. This was to minimize the effects of bearing and seal friction relative to the effects of soil properties on the rotation of the inner cylinder during testing. For a similar reason, we specified that sources of viscous damping be minimized.

Excitation and Measurement Requirements--In this subsection, we present and discuss the requirements for the excitation and measurement systems for the most promising testing modes. The specified criteria were developed as part of our theoretical feasibility studies. To develop the criteria, we evaluated the behavior of the testing system considering upper and lower bounds for the appropriate soil properties. The specified preliminary design criteria are summarized in Table 3.

To determine the low amplitude dynamic shear modulus and the variation in the dynamic shear modulus with shear strain, an impulsive torque will be applied to the inner cylinder, as shown in Fig. 5(a). The cylinder is expected to respond by developing a high frequency, decaying rotational vibration. The torque and angular acceleration will be measured. We specified excitation and measurement requirements that would provide the properties of interest over a practical range of soil conditions. The range was roughly bounded at the soft end by conditions in a loose, uniform, saturated sand deposit at a shallow depth of 5 ft and at the stiff end by conditions in a dense, uniform, dry sand deposit at a significant depth of 50 ft. The corresponding range of properties is expected to cover the properties of most clay and silt deposits at comparable depths. Properties were calculated as described in the subsections entitled Low Amplitude Dynamic Shear Modulus, pg. 39, and Variation in the Dynamic Shear Modulus with Shear Strain, pg. 43. A mass moment of inertia of  $0.00028 \text{ ft-lb-sec}^2$  was calculated for the rotating mass.

To determine the degradation characteristics of clays, a low frequency, cyclic rotation having a uniform amplitude will be applied to the inner cylinder. In response, the inner cylinder is expected to develop the cyclic torque required to maintain the selected rotation. The torque and angular displacement will be measured. We provided excitation and measurement specifications that would result in a system that could provide degradation characteristics over a practical range of soil conditions. The range was roughly bounded at the soft end by conditions in a uniform, saturated, highly degradable deposit of clay at a depth of 5 ft, and at the stiff end by conditions in a uniform, saturated, nondegradable deposit of clay at a depth of 100 ft. Properties were calculated for these depths as described in the subsection entitled Degradation Characteristics of Clays, pg. 49. It was not necessary to consider a mass moment of inertia for the rotating mass since we used the static procedure to obtain solutions (see Solution Procedures, pg. 33).

To determine the degradation and liquefaction characteristics of sands

and silts, a low frequency, cyclic torque having a uniform amplitude will be applied to the inner cylinder, as shown in Fig. 5(b). The cylinder is expected to respond by developing a cyclic rotation. The torque and angular displacement will be measured. We provided excitation and measurement specifications that would result in a system that could provide degradation and liquefaction characteristics over a practical range of soil conditions. The range was roughly bounded at the soft end by conditions, at a depth of 5 ft, in a loose, uniform, saturated sand deposit having low resistance to degradation and liquefaction and at the stiff end by conditions, at a depth of 75 ft, in a dense, uniform, saturated sand deposit having high resistance to degradation and liquefaction. Properties were calculated for these depths as described in the subsection entitled Degradation and Liquefaction Characteristics of Sands and Silts, pg. 53. It was not necessary to consider a mass moment of inertia for the rotating mass since we used the static procedure to obtain solutions (see Solution Procedures, pg. 33).

#### Presentation and Discussion of Results

In this subsection, we present and discuss the results of the operational feasibility study conducted by Sweet & Aiken, concentrating on the geotechnical aspects of the testing system. Using the design criteria provided by our firm, Sweet & Aiken carried out the tasks itemized in the subsection entitled Procedures, pg. 71. In Appendix C, we present the report from Sweet & Aiken, which presents the results of the operational feasibility study, concentrating on the operational aspects of the testing system.

The results of the operational feasibility study indicate that a laboratory research prototype testing system is operationally feasible. The main components, which satisfy reasonably well our design criteria, were found to be either available or readily producible, and it was found that these components could be assembled into a convenient, workable arrangement. Thus, Sweet & Aiken developed a preliminary design for a laboratory research prototype testing system and provided a cost estimate for the detailed design and construction of such a system.

In the following subsections, we present the preliminary design of the laboratory research prototype testing system and the sequence of steps in the operation of the system. Then, we discuss the mechanical components, systems, and features, and the excitation and measurement systems of the preliminary design. Also, the cost estimate for the laboratory system is presented and discussed.

Preliminary Design of Laboratory Research Prototype Testing System--The preliminary design of the laboratory research prototype testing system consists of specified mechanical, hydraulic, and electronic components conceptually assembled into one possible arrangement. The preliminary design is presented and discussed in the report from Sweet & Aiken. Drawing 850227-10, attached to the report, is an engineering drawing showing the main components of the probe of the testing system arranged in a convenient, workable manner. Figure 2.1 in the report presents a schematic diagram of the drive and measurement systems while Fig. 3.1 presents a schematic diagram of the hydraulic circuitry for the excitation system. Sketch A-1 in the Appendix of the report from Sweet & Aiken presents a sketch showing accessory electronic components arranged in a circuit.

Operation of Laboratory Testing System--To carry out a laboratory test using a system corresponding to that of the preliminary design, the probe would be carefully penetrated into the test soil to the proper depth. The penetration force would then be relieved and the shield raised a small amount to free the inner cylinder. Then, an appropriate vertical pressure would be applied to the test soil using the vertical pressure system. The vertical pressure system would be set to operate in either the constant pressure or the constant volume mode (see PROPOSED METHOD, pg. 22). A test would be conducted by selecting and activating the desired excitation and displaying and recording the measured quantities. Recorded test results would be processed appropriately.

Mechanical Components, Systems, and Features--The mechanical components, systems, and features of the preliminary design of the laboratory research prototype testing system satisfy reasonably well the mechanical requirements specified in the subsection entitled Mechanical Requirements, pg. 71. The mechanical components, systems, and features are discussed, in detail, in the following paragraphs.

The mechanical components satisfy most specified size and geometry requirements. The only departure from specifications occurred as a result of the shield. To provide an adequately thick inner cylinder, an adequately thick shield, and adequate clearance between the cylinder and the shield, as shown in the engineering drawing, it was necessary to constrict the inner cylinder above the region of the bottom of the shield. The inside of the constriction was provided with jugged edges. These edges are intended to funnel soil in the inner cylinder away from the walls above the constriction to minimize the influence of the soil within the inner cylinder on the motion of this cylinder and to prevent the plugging of soil within the inner cylinder during penetration.

The mechanical components, including the inner cylinder, the retractable shield, and the outer cylinder, were designed to withstand the specified maximum penetration forces and maximum differential lateral pressures. Additionally, there should be enough reserve strength in these components to withstand reasonable bending loads developed during penetration.

The probe was designed to operate under the specified maximum water pressure. The main systems which will enable satisfactory operation under this pressure include the sealing systems and a chamber air pressure system. The most important seal separates the instrumented head from the environmental fluids below. The seal can operate effectively only under a small pressure differential; thus, the chamber above the seal will be pressurized with air. This seal is the only seal which will provide resistance to the rotation of the inner cylinder, as may be seen in the engineering drawing. Effects of the seal on the motion of the inner cylinder during testing could be taken into account, if necessary, in soil-probe interaction analyses (see PROPOSED METHOD, pg. 21). The seal is a low friction seal estimated to develop a resisting torque of less than 0.15 in-lb. Air will be used, instead of a liquid, to provide the required pressure differential across the seal to minimize extraneous damping of vibrations during impulse tests. Air will be provided, at a controlled pressure, to the upper chamber of the laboratory system by a laboratory source through an air line.

The mechanical systems should perform required functions to specifications. The vertical pressure system, shown in the engineering drawing, will be provided with the selectable capability to maintain either a constant pressure on the top of the test soil or the position of the piston after application of a selected pressure. Hydraulic fluid will be introduced into the chamber at the top of the piston and the pressure or volume of the fluid will be controlled remotely.

The mechanical features of the testing system should provide specified performance characteristics. The cylinder walls will be provided with several specified features. The outside surface of the outer cylinder will be grooved vertically providing an effective reaction anchor to the surrounding soil. Both the inside surface of the outer cylinder and the outside surface of the inner cylinder will be grooved vertically and covered with a thin coat of polytetrafluoroethylene (PTFE), a low friction material. The coefficient of friction between PTFE and soil was estimated by Sweet & Aiken to be about 0.09. Thus, friction will be very low in the vertical direction to minimize disturbance to the test soil during penetration, while traction will be maximized in the tangential direction to minimize slip between the cylinders and the test soil during testing. The inside wall of the inner cylinder will be smooth and coated with PTFE to minimize friction. This will help minimize the effect of the soil inside the inner cylinder on the motion of this cylinder and the tendency of the soil to form a plug within the inner cylinder during penetration. Sweet & Aiken estimate that the PTFE coating should survive numerous tests without excessive wear. PTFE coats may be reapplied when desired. To avoid excessive difficulties with abraded cylinder coatings or grooves, the inner and outer cylinders will be removable and exchangeable. This capability would also prove useful in providing different grades of cylinder grooving for different grades of soil.

The positioning bearings, required to position the inner cylinder, were given special attention. To minimize the effects of bearing friction on the interpretation of test results, these bearings were placed above both the torque and motion measurement transducers in the preliminary design. While bearing friction will still effect behavior somewhat, this arrangement will help isolate the effects of soil properties on the behavior of the inner cylinder. Special precision bearings were selected to serve as positioning bearings to minimize friction and thus, the effects of the bearings on the motion of the inner cylinder. Sweet & Aiken indicated that the coefficient of friction of these bearings is 0.00018.

Excitation and Measurement Systems--The selected excitation and measurement systems satisfy most of the preliminary design criteria specified in the subsection entitled Excitation and Measurement Requirements, pg. 75. In the following paragraphs, we discuss the selected excitation and measurement systems.

To determine the low amplitude dynamic shear modulus and the variation in the dynamic shear modulus with shear strain, an impulsive torque will be applied to the inner cylinder, as shown in Fig. 5(a). In response, the inner cylinder is expected to rotate with a high frequency, decaying oscillation. The selected excitation system includes hydraulic motors and the equipment

required to control and operate the motors. The selected measurement systems include torque transducers, accelerometers, and the equipment required to operate these components.

Not all specified criteria were satisfied; however, the resulting consequences are not expected to be severe. The specified upper level of torque was not satisfied. We conservatively specified the highest level of torque to be applied to the inner cylinder to be 20 ft-lb. The motor and torque transducer systems selected have upper limits of about 17 ft-lb. Components could have been selected with higher limits but we preferred sacrificing increased capacity for greater accuracy at lower torques. The relatively small reduction in torque capacity should limit only moderately the capabilities of the testing system. We would probably not be able to define shear moduli at larger strains for stiffer soils at greater depths. This is not a serious limitation because, generally, it is the softer soils at shallower depths that pose the greatest threat during earthquakes.

Secondly, the response time for the servovalve which will control the motor is longer than ideal for producing an impulsive loading. Thus, we will not be able to apply loads as quickly as desired. As a result, the vibratory component of the response of the inner cylinder to a load of given amplitude may not be as pronounced as if the load were applied instantaneously. The manufacturer of the servovalve states, in the literature provided by Sweet & Aiken, that the time to develop 90% of the output in response to a step input of current is 0.0025 sec. The vibration frequencies of the inner cylinder during impulse tests were estimated to range from 700 (soft soil) to 2400 cps (stiff soil) when testing soils in the linearly elastic range and from 400 (soft soil) to 1400 cps (stiff soil) when testing soils well into the nonlinear range. Therefore, the ideal of an impulsive loading is approached more closely when testing softer soils at higher strains. Since softer soils driven to higher strains seem to cause the most problems during earthquakes, the proposed testing system would be expected to provide the greatest accuracy in defining shear moduli when testing the soils of greatest concern. If necessary, steps could be taken toward approaching more closely the ideal of an impulsive loading. One possibility includes reducing the natural frequency of the rotating mass either by shortening the active length of the inner cylinder or by increasing the mass moment of inertia of the inner cylinder.

Finally, neither a single motor nor a single torque transducer appears to be capable of satisfying specified criteria over the entire range. Thus, motors and torque transducers having different capacities will be interchanged in the laboratory research prototype testing system to provide the desired capabilities. Sweet & Aiken provided literature from a manufacturer describing a single motor, currently being developed, which may be able to satisfy our criteria. If we are unable to provide a single probe for field use that covers the entire range of interest, then, consistent with current practice, we plan to offer different probes covering different ranges.

To determine the degradation characteristics of clays, a low frequency, cyclic rotation having a uniform amplitude will be applied to the inner cylinder. In response, the cylinder is expected to develop the low frequency, cyclic torque required to maintain the selected rotation. The

selected excitation system includes the previously discussed hydraulic motors and the equipment required to control and operate the motors. The selected measurement systems include angular displacement transducers, the previously discussed torque transducers, and the equipment required to operate these components.

Not all specified criteria were satisfied; however, the resulting consequences are not expected to be severe. Sweet & Aiken was unable to find an available displacement transducer which the firm feels could be used to accurately measure angular displacements as small as those specified. However, Trans-Tek, Inc., (Trans-Tek) indicated that its 600 series angular displacement transducer could be modified and calibrated, for a modest cost, to provide the required small measurements. A letter from Trans-Tek confirming this information is included in the report from Sweet & Aiken. Two interchangeable transducers may be required to cover the specified range of angular displacements.

Also, Sweet & Aiken was unable to find a single torque transducer capable of satisfying the specified criteria over the entire range. Thus, as stated previously, for the laboratory research prototype testing system, interchangeable torque transducers having different capacities will be used.

Finally, Sweet & Aiken was uncertain whether a single hydraulic motor could accurately provide the smallest torques specified. Thus, the lower capacity motor required for impulse tests may also be required for low frequency, cyclic, controlled-rotation tests. The previously described motor which is under development may be able to satisfy the entire range of our criteria for these tests. As mentioned previously, if we are unable to provide a single probe for field use that covers the entire range of interest, then, consistent with current testing practice, we plan to offer different probes having different ranges.

To determine the degradation and liquefaction characteristics of sands and silts, a low frequency, cyclic torque having a uniform amplitude will be applied to the inner cylinder, as shown in Fig. 5(b). In response, the cylinder is expected to develop a low frequency, cyclic rotation. The selected excitation system includes the previously discussed hydraulic motors and the equipment required to control and operate the motors. The selected measurement systems include the previously discussed torque transducers and angular displacement transducers and the equipment required to operate these components.

Not all specified criteria were satisfied; however, the resulting consequences are not expected to be severe. Sweet & Aiken was unable to find a displacement transducer for accurately measuring the smallest angular displacements specified. However, it appears that a transducer could be provided that would accurately measure angles reasonably close to our specified lower limit. We specified that angular displacement amplitudes as low as 0.001 deg should be measured with reasonable accuracy. Trans-Tek indicated, in a letter included in the report from Sweet & Aiken, that a 600 series angular displacement transducer could be modified and calibrated, for a modest cost, to provide an angular displacement transducer with a resolution of 0.001 deg and a range of  $\pm 0.5$  deg. Sweet & Aiken reported that Trans-Tek is certain that measurements down to 0.01 deg could be made

accurately with the testing system, but that measurements below 0.01 deg would be of questionable accuracy.

The consequences of not being able to measure accurately the smallest specified angles are not expected to be severe for several reasons. The conditions under which these small angles are expected are fairly limited. These angles are expected only when applying very low levels of shear stress to the test soil and only during the initial cycles of loading before significant degradation has taken place. To minimize uncertainty in interpreting soil properties, when these conditions occur we would place greater emphasis on behavior during the later stages of tests, during which measurements are more accurate. It would appear that enormously useful information such as the number of cycles to liquefaction or to any reasonable level of specified or limited strain could be defined quite accurately under all conditions with the testing system as currently designed. Thus, we believe that the lower bound of the range for accurate measurements indicated by Sweet & Aiken will lead to reasonably accurate and detailed descriptions of in situ cyclic degradation and liquefaction characteristics. Additionally, improvements in transducer technology may result in improvements in our ability to measure the smallest angles specified.

Two angular displacement transducers will be required in the testing system to carry out low frequency, cyclic, controlled-torque tests. A single Trans-Tek angular displacement transducer calibrated to give high accuracy in the measurement of small angles cannot cover the entire specified range of angular displacements. The entire specified range may occur during a single low frequency, cyclic, controlled-torque test. For example, when testing a loose sand at very low levels of stress, during the initial cycles of loading the inner cylinder will undergo small angular displacements. At a later stage during the test, after significant degradation has occurred, very large, virtually unrestrained, angular displacements may develop. Although Sweet & Aiken does not show two angular displacement transducers in the engineering drawing in their report, the firm indicated that two angular displacement transducers, each calibrated to a different range, may be included in the testing system. Alternatively, low frequency, cyclic, controlled-rotation tests may be carried out to determine the degradation and liquefaction characteristics of sands and silts.

Also, Sweet & Aiken were unable to find a single torque transducer capable of measuring the entire range of torques specified. As mentioned previously, interchangeable torque transducers having different capacities will be used in the laboratory research prototype testing system.

Finally, Sweet & Aiken was uncertain whether a single hydraulic motor could accurately provide the smallest torques specified. Thus, the lower capacity motor required for impulse tests may also be required for low frequency, cyclic, controlled-torque tests. The previously described motor which is under development may be able to satisfy the entire range of torques specified for the low frequency, cyclic, controlled-torque test. As mentioned previously, if we are unable to provide a single probe for field use that covers the entire range of interest, then, consistent with current testing practice, we plan to offer different probes having different ranges.

Cost Estimate--Sweet & Aiken estimated a cost of \$78,260 for a

complete laboratory research prototype testing system. The estimate includes estimated costs for detailed design, purchases, manufacture, and construction. Individual costs are itemized in the report from Sweet & Aiken. The cost estimate is conservative. For the cost estimate, Sweet & Aiken assumed that all electronic components will be purchased. It is likely that we will rent many of these components for Phase II research leading to a considerable reduction in cost.

### Conclusions

In this subsection, we itemize the main conclusions resulting from the operational feasibility study. These conclusions directly relate to the objectives presented in the subsection entitled Objectives, pg. 70.

1) Based on the results of the operational feasibility study conducted by the mechanical engineering firm of Sweet & Aiken, we concluded that a laboratory research prototype testing system for determining the low amplitude dynamic shear modulus and the variation in the dynamic shear modulus with shear strain by impulse test, the degradation characteristics of clays by low frequency, cyclic, controlled-rotation test, and the degradation and liquefaction characteristics of sands and silts by low frequency, cyclic, controlled-torque test is operationally feasible.

2) Sweet & Aiken developed a preliminary design for a laboratory research prototype testing system.

3) Sweet & Aiken estimated a cost of \$78,260 for the design and construction of a complete laboratory research prototype testing system.

4) Not all specified criteria were satisfied by the preliminary design; however, the consequences are not expected to be severe and improvements are expected with advances in related technology. It appears that we will be unable to measure the smallest angles predicted during low frequency, cyclic, controlled-torque tests for determining the degradation and liquefaction characteristics of sands and silts. Thus, we may be unable to determine, as accurately as desired, soil behavior during the initial cycles of loading from tests conducted at lower levels of load. Also, it appears that we will not be able to apply loads as rapidly as desired during impulse tests. Thus, we may not observe as pronounced a vibratory response from the inner cylinder as would be expected during ideal impulse tests. Finally, to satisfy specified design criteria, some components of the laboratory research prototype testing system will have to be interchanged. If we are unable to provide a single probe for field use that covers entirely the range of interest, then, consistent with current testing practice, we plan to offer different probes covering different ranges. Each of the concerns identified is a product of limitations in current technology. Therefore, advances in appropriate technology may be expected to reduce or eliminate each of these concerns.

### ESTIMATE OF FEASIBILITY

In this section, we provide our opinion concerning the feasibility of the proposed in situ testing system. First, we provide our general opinion, and then, we provide supporting details.

Based on the results of the feasibility studies discussed herein, we have concluded that the proposed in situ testing system is feasible. Ultimately, the system is expected to effectively provide information on in situ cyclic and dynamic soil properties to the level of accuracy and detail appropriate for the intermediate and final stages of the analysis and design of important structures located in seismically active areas. The Phase I studies indicate that a laboratory research prototype testing system is theoretically, operationally, and economically feasible. Since the additional equipment required for a field system is reasonably conventional, and since the additional problems that could be encountered in the field appear to be either small or surmountable, we believe that an in situ field testing system is feasible.

Much research and development will be required before the full potential of the system can be realized. This is consistent with comparable testing systems. Much effort will be needed because the problem of determining in situ cyclic and dynamic soil properties is not a simple one, because the testing system is relatively complex, and because the testing system has considerable safety and economic implications. As a result of our Phase I work we have already identified several areas in which work is required. We expect to identify more areas during later stages of work.

The theoretical and operational feasibility studies presented herein indicate that a laboratory research prototype testing system is theoretically, operationally, and economically feasible. To determine the theoretical feasibility of the laboratory testing system, we analytically simulated tests considering expected ranges of the soil properties of interest. The behavior of the testing system was predicted to be sensitive to each soil property considered in a clear, physically reasonable manner. As a result, we concluded that each soil property considered could be inferred from this behavior and therefore, that the testing system is a theoretically feasible means for determining each property. A simple analytical model was used to simulate tests. In practice, we feel that we will be able to infer the soil properties of interest to the required level of detail and accuracy by analytically simulating tests using descriptive analytical procedures. Powerful analytical procedures are available which are expected to be capable of describing, accurately and in detail, the geometry and performance of tests and most of the important phenomena occurring during tests. Also, results obtained using a testing system somewhat similar, in principle, to ours (5) roughly support our estimate of the theoretical feasibility of the proposed testing system.

Prior to and during the Phase I theoretical feasibility studies, areas were identified in which future research and development could improve the effectiveness of the proposed testing system. For example, advancing our ability to describe the effects of dilation on shear stress-strain behavior during cyclic loading is expected to improve our ability to accurately infer, from test results, the behavior of dense sands under cyclic loads.

Similarly, optimizing the dimensions of several of the components of the probe is expected to improve our ability to accurately infer, from test results, all properties of interest.

We arranged for the mechanical engineering firm of Sweet & Aiken, Inc., to determine the operational feasibility of the laboratory research prototype testing system. Sweet & Aiken found that the main components, which satisfy reasonably well specified mechanical, excitation, and measurement requirements, are either available or could be produced at modest cost. Sweet & Aiken also found that these components could be assembled into a convenient, workable arrangement. Thus, we concluded that the laboratory research prototype testing system is operationally feasible. The many operating laboratory systems (37) which are similar, in principle, to our system, and which measure similar parameters at comparable magnitudes support this conclusion.

During the Phase I operational feasibility study, several areas were identified in which future development could improve the effectiveness of the proposed testing system. For example, improvements in the ability to measure small values of angular displacement would be expected to improve our ability to infer the cyclic degradation and liquefaction characteristics of sands and silts. Such improvements may realistically be expected as a result of motivation by fields such as robotics for which small precision measurement systems are required.

To help us determine the economic feasibility of the proposed testing system, Sweet & Aiken provided a cost estimate for the detailed design and construction of a laboratory research prototype testing system. In view of potential benefits and considering the estimated cost for the development of comparable testing systems, the laboratory research prototype testing system was judged to be economically feasible.

We believe that a field in situ testing system will also be theoretically, operationally, and economically feasible. A field system is expected to be theoretically feasible because the principle of operation of the field system will be identical to that of the laboratory research prototype testing system. However, under severe conditions, for example, when testing offshore in high sea states, behavior may differ somewhat from behavior under milder conditions. This may occur as a result of additional disturbance induced into the test soil due to wave and current-induced movement of the probe. A number of steps are routinely taken to reduce such movements during offshore undisturbed sampling and cone penetrometer and remote vane testing (4). Continued advancement in this area is expected. Additionally, it is expected that other steps unique to our testing system could be taken to further reduce the effects of such movements. Such difficulties are not expected during onshore tests.

We feel that a field testing system is operationally feasible because the additional components which may be required for a field testing system are considered to be existing or feasible technology. At this time, though other modes of operation may be possible, we intend for the field probe to be lowered with a wireline through a drillstring, latched to the drillbit, and then operated. The additional components which may be required include a penetration system, a drillbit latching system, a downhole electronics

package, an umbilical, and a winch. Such components have been used successfully with other in situ geotechnical testing systems (4) and also, as indicated in the report from Sweet & Aiken in Appendix C, in other comparable applications.

Also, we feel that a field testing system is operationally feasible because the additional problems which we expect to encounter in the field are expected to be either small or surmountable. Several problems may be encountered. These include problems caused by a corrosive environment, mechanical noise, and rocks.

As indicated by Sweet & Aiken, the effects of a corrosive environment can be minimized by proper maintenance, care, and selection of materials.

Mechanical noise, which may be present in the field, is expected to have the greatest effect on the interpretation of results from tests involving excitations and responses having small magnitudes. A number of seismic field tests, which involve the measurement of small quantities comparable in magnitude to the quantities to be measured by the proposed system (10) (17) (26) (34) (37), have been successfully carried out. Our proposed testing system is primarily intended to provide information on the in situ shear stress-strain behavior of a soil at higher amplitudes of strain. We do not expect major difficulties from mechanical noise during higher amplitude tests. Intuitively, it would appear that general mechanical noise would not create large problems with the proposed testing system. Vertical disturbances would not be expected to be sensed. Horizontal disturbances which do not tend to significantly rotate the inner cylinder would be similarly sensed by the two accelerometers and it would appear that the electrical signals arising from such disturbances could be made to cancel each other. Also, Stokoe et al. (33) have measured noise at the bottom of an offshore borehole. They found that horizontal motions due to noise were significantly less than vertical motions due to noise. Should mechanical noise present problems, one possible solution is special signal processing (33).

Rocks may damage the inner and outer cylinders during penetration. To minimize this difficulty, we plan to include the feature of removable and exchangeable cylinders in a field testing system. Also, we are considering a larger, somewhat stronger probe for use in coarser deposits.

We feel that a field testing system is economically feasible because neither the additional equipment required for a field testing system, nor the additional difficulty which may be encountered in the field is expected to present an unusually large, excessive cost. As stated previously, much of the additional equipment required for the field is relatively conventional and all of this equipment has been used either for in situ geotechnical testing or for other comparable applications. Also, as implied previously, we do not believe that particularly unusual measures will be required to minimize or avoid the problems which may be encountered in the field. Finally, the benefits of a working field system are expected to greatly exceed the overall cost. For example, based on our experiences, we believe that the cost saving alone involved in basing the design of a single major structure on appropriately accurate and detailed information on in situ cyclic and dynamic soil properties could far exceed the cost of the development of the testing system.

#### REFERENCES

1. Anderson, D.G. and Espana, C., "Evaluation of In Situ Testing Methods for High-Amplitude Dynamic Property Determination," prepared by Fugro, Inc., Long Beach, California, for the Electric Power Research Institute, EPRI NP-920, November, 1978.
2. Arulmoli, K., Arulanandan, K., and Seed, H.B., "A New Method for Evaluating Liquefaction Potential," Journal of Geotechnical Engineering, Vol. 111, No. 1, Jan., 1985.
3. Briaud, J.-L., Lytton, R.L., and Hung, J.-T., "Obtaining Moduli from Cyclic Pressuremeter Tests," Journal of Geotechnical Engineering, ASCE, Vol. 109, No. 5, May, 1983, pp. 657-665.
4. Briaud, J.-L. and Meyer, B., "In Situ Tests and Their Application in Offshore Design," Proceedings of the Conference on Geotechnical Practice in Offshore Engineering, ASCE Specialty Conference, Univ. of Texas, Austin, Texas, April 27-29, 1983, pp. 244-266.
5. Castro, G., Shields, D.R., and France, J.W., "Field Index Test for Estimating Liquefaction Potential," Report No. NSF/CEE-82122, prepared by Geotechnical Engineers, Inc., Winchester, MA, for the National Science Foundation, Mar., 1982.
6. Clough, R.W. and Penzien, J., Dynamics of Structures, McGraw-Hill, Inc., New York, 1975.
7. Crandall, S.H., Dahl, N.C., and Lardner, T.J., An Introduction to the Mechanics of Solids, McGraw-Hill, Inc., New York, 1972.
8. De Alba, P., Baldwin, K., Janoo, V., Roe, G., and Celikkol, B., "Elastic-Wave Velocities and Liquefaction Potential," Geotechnical Testing Journal, GTJODJ, Vol. 7, No. 2, June, 1984, pp. 77-87.
9. De Domenico, U.S. Patent 4,353,247, Awarded 1982.
10. Dobry, R., Stokoe, K.H., Ladd, R.S., and Youd, T.L., "Liquefaction Susceptibility from S-Wave Velocity," ASCE Convention and Exposition, Preprint No. 81-544-1, October 26-31, 1981.
11. Esashi, Y., Yoshida, Y., and Nishi, K., "An Exploratory Method for Dynamic Properties of Ground Through Borehole Wall," Sixth World Conference on Earthquake Engineering, Vol. 6, New Delhi, India, Jan., 1977, pp. 147-152.
12. Finn, W.D.L., "Dynamic Response Analyses of Saturated Sands," Soil Mechanics-Transient and Cyclic Loads, John Wiley and Sons, New York, 1982, pp. 105-131.
13. Finn, W.D.L., Bhatia, S.K., and Pickering, D.J., "The Cyclic Simple Shear Test," Soil Mechanics-Transient and Cyclic Loads, John Wiley and Sons, New York, 1982, pp. 583-607.
14. Hardin, B.O., U.S. Patent 3,643,498, Awarded 1971.

15. Hardin, B.O. and Drnevich, V.P., "Shear Modulus and Damping in Soils: Design Equations and Curves," Journal of the Soil Mechanics and Foundations Division, ASCE, Vol. 98, SM7.
16. Henke, R., "Numerical Procedure for Predicting the Torsional Dynamic Response of Solid Media," dissertation presented to the University of Michigan, Ann Arbor, MI, in partial fulfillment of the requirements for the degree of Doctor of Philosophy, 1980.
17. Henke, R., Richart, F.E., Jr., and Woods, R.D., "Nonlinear Torsional Dynamic Response of a Footing," Journal of Geotechnical Engineering, Proc. ASCE, Vol. 109, No. 1, January, 1983, pp. 72-88.
18. Henke, R. and Wylie, E.B., "Torsional Dynamic Response of Solid Media," Journal of the Engineering Mechanics Division, Proc. ASCE, Vol. 108, No. EM1, Feb., 1982, pp. 73-94.
19. Henke, R., Wylie, E.B., and Richart, F.E., Jr., "Torsional Dynamic Response of Solid Systems," Journal of the Engineering Mechanics Division, Proc. ASCE, Vol. 108, No. EM6, December, 1982, pp. 1067-1085.
20. Idriss, I.M., Dobry, R., and Singh, R.D., "Nonlinear Behavior of Soft Clays During Cyclic Loading," Journal of the Geotechnical Engineering Division, Proc. ASCE, Vol. 104, No. GT12, December, 1978, pp. 1427-1447.
21. Idriss, I.M., Dobry, R., Singh, R.D., and Doyle, E.H., "Behavior of Soft Clays under Earthquake Loading Conditions," Proceedings, Offshore Technology Conference, OTC 2671, Dallas, Texas, 1976.
22. Martin, G.R., Finn, W.D.L., and Seed, H.B., "Fundamentals of Liquefaction Under Cyclic Loading," Journal of the Geotechnical Engineering Division, Proc. ASCE, Vol. 101, No. GT5, May, 1975, pp. 423-437.
23. Martin, G.R., Lam, I.P., McCaskie, S.L., and Tsai, C.-F., "A Parametric Study of an Effective Stress Liquefaction Model," International Conference on Recent Advances in Geotechnical Earthquake Engineering and Soil Dynamics, University of Missouri-Rolla, 1981, pp. 699-705.
24. Richart, F.E., Jr., "Some Effects of Dynamic Soil Properties on Soil-Structure Interaction," Journal of the Geotechnical Engineering Division, Proc. ASCE, Vol. 101, No. GT12, December, 1975, pp. 1193-1240.
25. Richart, F.E., Jr., Hall, J.R., Jr., and Woods, R.D., Vibrations of Soils and Foundations, Prentice-Hall, Englewood Cliffs, NJ, 1970, 414 pp.
26. Robertson, P.K., Campanella, R.G., Gillespie, D., and Rice, A., "Seismic CPT to Measure In-Situ Shear Wave Velocity," Measurement and Use of Shear Wave Velocity for Evaluating Dynamic Soil Properties, Proceedings, ASCE Convention, Denver, Colorado, May 1, 1985, pp. 34-48.
27. Sasaki, Y. and Koga, Y., "Vibratory Cone Penetrometer to Assess the Liquefaction Potential of the Ground," Wind and Seismic Effects, Proceedings, 14th Joint Panel Conference of U.S.-Japan Cooperative Program in Natural Resources, National Bureau of Standards Special Publication 651, April, 1983, pp. 541-555.

28. Seed, H.B., "Evaluation of Soil Liquefaction Effects on Level Ground During Earthquakes," State-of-the-Art Paper, Liquefaction Problems in Geotechnical Engineering, Preprint 2752, ASCE Annual Convention, Sept. 27-Oct. 1, 1976, Philadelphia, PA, pp. 1-104.
29. Seed, H.B. and Idriss, I.M., Ground Motions and Soil Liquefaction During Earthquakes, Earthquake Engineering Research Institute Monograph, 1982, 134 pp.
30. Shannon and Wilson, Inc., and Agbalian Associates, "Determination of Soil Liquefaction Characteristics by Large-Scale Laboratory Tests," Report No. NUREG-0027, prepared by Shannon and Wilson, Inc., Seattle, Washington, and Agbalian Associates, El Segundo, California, for the U.S. Nuclear Regulatory Commission, Washington, D.C., May, 1975.
31. Sidey, R., Marti, J., Rodriguez, L., and White, D., "Borehole Shear Device Feasibility and Preliminary Studies," Report prepared by Dames and Moore, Los Angeles, CA, for the Air Force Weapons Laboratory, Kirtland Air Force Base, NM, Aug., 1980.
32. Sowers, G.B. and Sowers, G.F., Introductory Soil Mechanics and Foundations, The Macmillan Company, New York, 1970.
33. Stokoe, K.H., II, Arnold, E.J., Hoar, R.J., Shirley, D.J., and Anderson, D.G., "Development of a Bottom-Hole Device for Offshore Shear Wave Velocity Measurement," Proceedings, Offshore Technology Conference, OTC 3210, Houston, TX, May, 1978, pp. 1367-1380.
34. Stokoe, K.H., II, and Nazarian, S., "Use of Rayleigh Waves in Liquefaction Studies," Measurement and Use of Shear Wave Velocity for Evaluating Dynamic Soil Properties, Proceedings, ASCE Convention, Denver, Colorado, May 1, 1985, pp. 1-17.
35. Streeter, V.L., Wylie, E.B., and Richart, F.E., Jr., "Soil Motion Computations by Characteristics Method," Journal of the Geotechnical Engineering Division, Proc. ASCE, Vol. 100, No. GT3, March, 1974, pp. 247-263.
36. Terzaghi, K. and Peck, R.B., Soil Mechanics in Engineering Practice, John Wiley and Sons, Inc., New York, 1967.
37. Woods, R.D., "Measurement of Dynamic Soil Properties," Proceedings of the ASCE Geotechnical Engineering Division Specialty Conference, Volume 1, Pasadena, CA, June 19-21, 1978.
38. Wiegel, R.L., Editor. Earthquake Engineering, Prentice-Hall, Englewood Cliffs, New Jersey, 1970.
39. Wylie, E.B. and Henke, R., "Nonlinear Soil Dynamics by Characteristics Method," Proceedings of the 2nd U.S. National Conference on Earthquake Engineering, Earthquake Engineering Research Institute, Stanford University, Stanford, CA, 1979, pp. 563-572.

APPENDICES

## Appendix A - Validation of Computer Procedures

In this appendix, we present, in outline form, the validations of the computer procedures used in the theoretical feasibility study for simulating 1) impulse tests for determining the low amplitude dynamic shear modulus, 2) high frequency, cyclic tests for determining the low amplitude dynamic shear modulus, 3) impulse tests for determining the variation in the dynamic shear modulus with shear strain, 4) high frequency, cyclic tests for determining the variation in the dynamic shear modulus with shear strain, 5) low frequency, cyclic, controlled-torque tests for determining the degradation and liquefaction characteristics of sands and silts, and 6) low frequency, cyclic, controlled-rotation tests for determining the degradation characteristics of clays.

- 1) Validation of computer procedure for simulating impulse tests for determining the low amplitude dynamic shear modulus.

Validation Procedure: Compared computer solution with closed-form analytical solution (6).

Parameters:  $G_0 = 1.72 \times 10^5$  psf,  $K_{T0} = 1.88 \times 10^4$  ft-lb/rad,  $I = 2.8 \times 10^{-4}$  lb-ft-sec<sup>2</sup>,  $C_T = 0$  ft-lb-sec/rad,  $\alpha = 1$ ,  $R = 3$ ,  $C_1 = 0.8$ ,  $\tau_m = 6.6 \times 10^5$  psf, computational time step =  $1 \times 10^{-5}$  sec.

Excitation: Rectangular, impulsive torque which induced only linear behavior; amplitude = 10 ft-lb, duration =  $6.5 \times 10^{-4}$  sec.

Response: Decaying, cyclic, rotations.

Results: As shown in Figs. A-1(a) and (b), computed responses agree closely with theoretical responses. Also, as shown in Fig. A-1(c), energy balance requirements are satisfied.

Conclusion: The procedure for simulating impulse tests for determining the low amplitude dynamic shear modulus is valid.

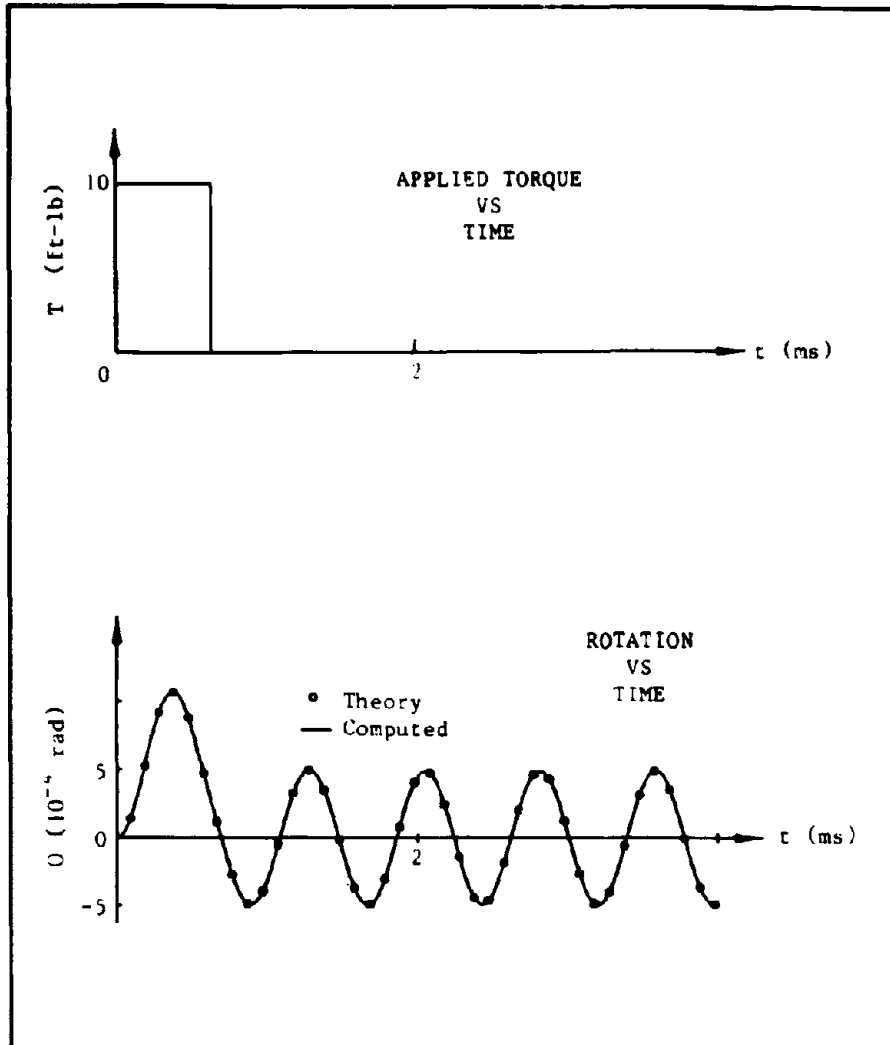
- 2) Validation of computer procedure for simulating high frequency, cyclic tests for determining the low amplitude dynamic shear modulus.

Validation Procedure: Compared computer solution with closed-form analytical solution (6).

Parameters:  $G_0 = 5.14 \times 10^5$  psf,  $K_{T0} = 5610$  ft-lb/rad,  $I = 2.8 \times 10^{-4}$  lb-ft-sec<sup>2</sup>,  $C_T = 0.50$  ft-lb-sec/rad,  $\alpha = 1$ ,  $R = 5$ ,  $C_1 = 0.8$ ,  $\tau_m = 100$  psf, computational time step =  $3.5 \times 10^{-5}$  sec.

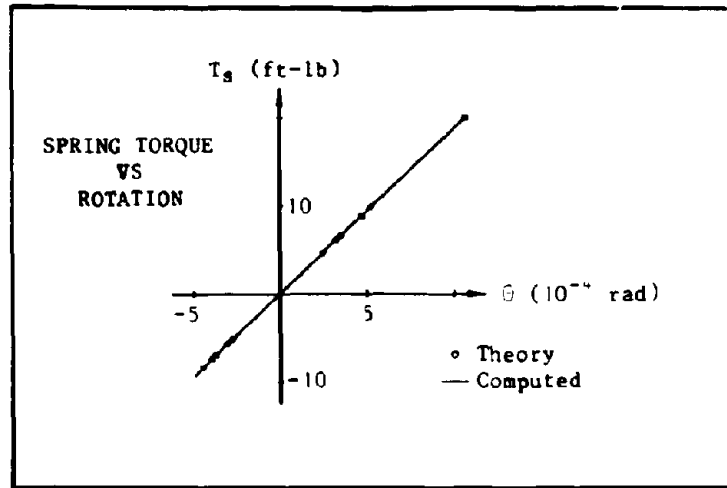
Excitation: High frequency, sinusoidal torque which induced only linear behavior; amplitude = 0.015 ft-lb, frequency = 570 cps.

Response: Decaying transient and steady state, high frequency, cyclic rotations.

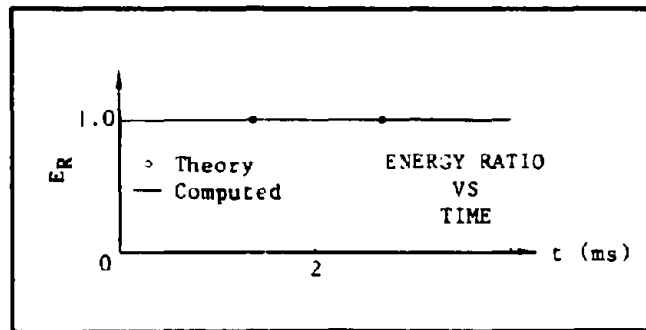


(a) Excitation/Response

Figure A-1: Validation of Computer Procedure for Simulating Impulse Tests for Determining the Low Amplitude Dynamic Shear Modulus



(b) Spring Torque-Rotation Behavior



(c) Energy Ratio

Figure A-1: Validation of Computer Procedure for Simulating Impulse Tests for Determining the Low Amplitude Dynamic Shear Modulus

Results: As shown in Figs. A-2(a) through (c), all computed responses agree closely with theoretical responses. Also, as shown in Fig. A-2(d), energy balance requirements are satisfied.

Conclusion: The procedure for simulating high frequency, cyclic tests for determining the low amplitude dynamic shear modulus is valid.

- 3) Validation of computer procedure for simulating impulse tests for determining the variation in the dynamic shear modulus with shear strain.

Validation Procedure: Obtained computer solution, checked energy balance and torque-rotation behavior, and judgmentally checked solution.

Parameters:  $G_0 = 2 \times 10^6$  psf,  $K_{T0} = 2.2 \times 10^4$  ft-lb/rad,  $I = 2.8 \times 10^{-4}$  lb-ft-sec<sup>2</sup>,  $C_T = 0.1$  ft-lb-sec/rad,  $\alpha = 1$ ,  $R = 5$ ,  $C_1 = 0.8$ ,  $T_m = 1000$  psf, computational time step =  $8.9 \times 10^{-6}$  sec.

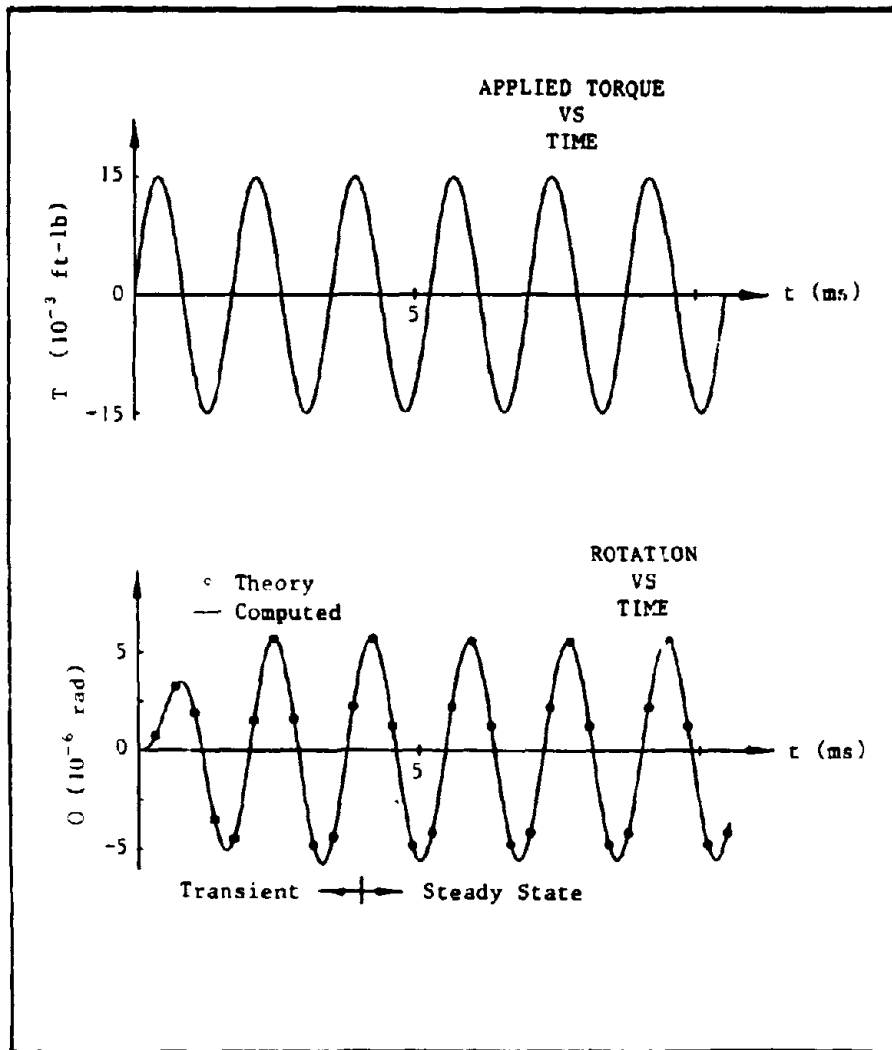
Excitation: Rectangular, impulsive torque which induced nonlinear behavior; amplitude = 5.2 ft-lb, duration =  $1.1 \times 10^{-3}$  sec.

Response: Decaying, cyclic rotations and permanent rotation.

Results: As shown in Fig. A-3(d), energy balance requirements are satisfied. Checking the solution judgmentally, as seen in Fig. A-3(a), during the initial period of higher amplitudes of motion, the apparent natural frequency was lower than during the subsequent period of lower amplitude motions. This is to be expected with a test soil that decreases in stiffness with increasing shear strain. As would be expected, the frequency of the later, lower amplitude free-vibrations corresponds closely to the damped natural frequency of the system at low amplitudes of rotation. The rate of decay of these free-vibrations corresponds to that expected of a system having the specified level of viscous damping. Also, as shown in Fig. A-3(a), permanent rotation, expected when testing a nonlinear, inelastic soil at high levels of strain, was predicted. As shown in Fig. A-3(b), the computed, nonlinear spring torque-rotation curve agrees closely with that estimated directly using Ramberg-Osgood stress-strain equations (24). Differences between these curves were found to decrease with decreases in the computational time step. The computed damping torque-rotational velocity curve, shown in Fig. A-3(c), is linear with the correct slope.

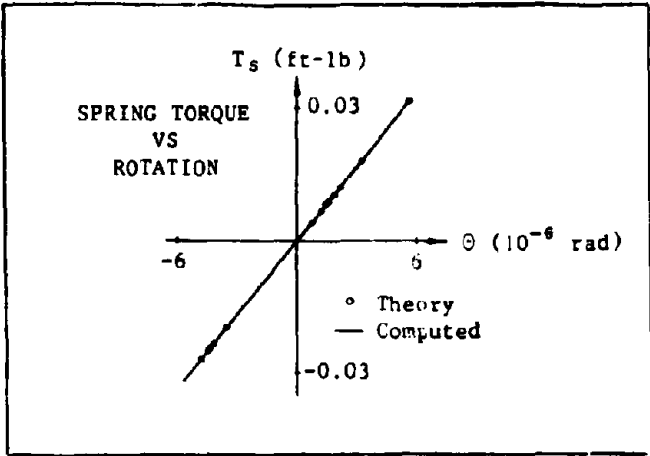
Conclusion: The procedure for simulating impulse tests for determining the variation in the dynamic shear modulus with shear strain is valid.

- 4) Validation of computer procedure for simulating high frequency, cyclic tests for determining the variation in the dynamic shear modulus with shear strain.

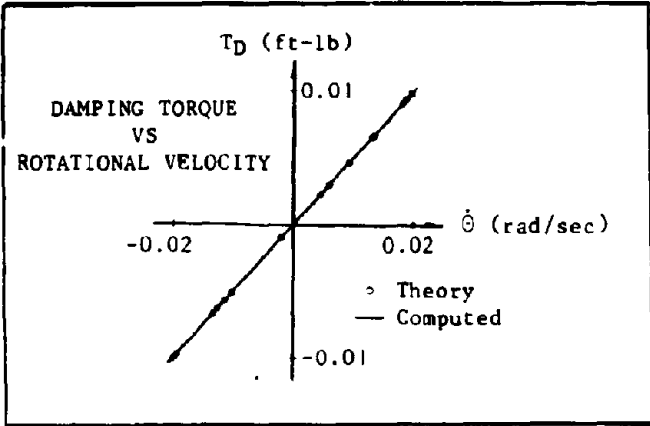


(a) Excitation/Response

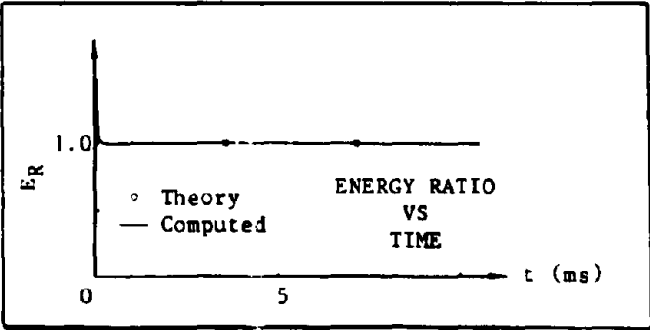
Figure A-2: Validation of Computer Procedure for Simulating High Frequency, Cyclic Tests for Determining the Low Amplitude Dynamic Shear Modulus



(b) Spring Torque-Rotation Behavior

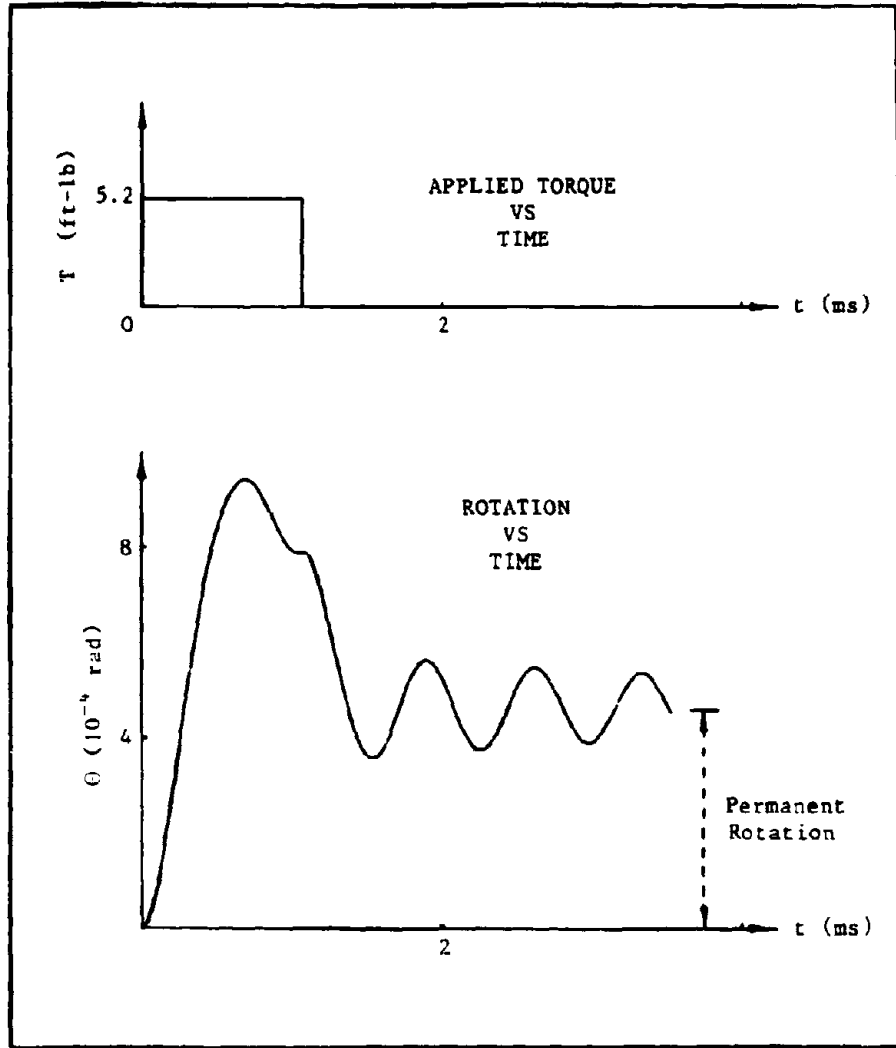


(c) Damping Torque-Rotational Velocity Behavior



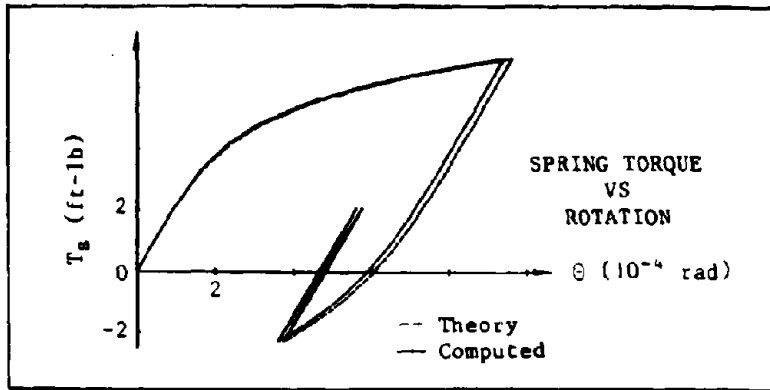
(d) Energy Ratio

Figure A-2: Validation of Computer Procedure for Simulating High Frequency, Cyclic Tests for Determining the Low Amplitude Dynamic Shear Modulus

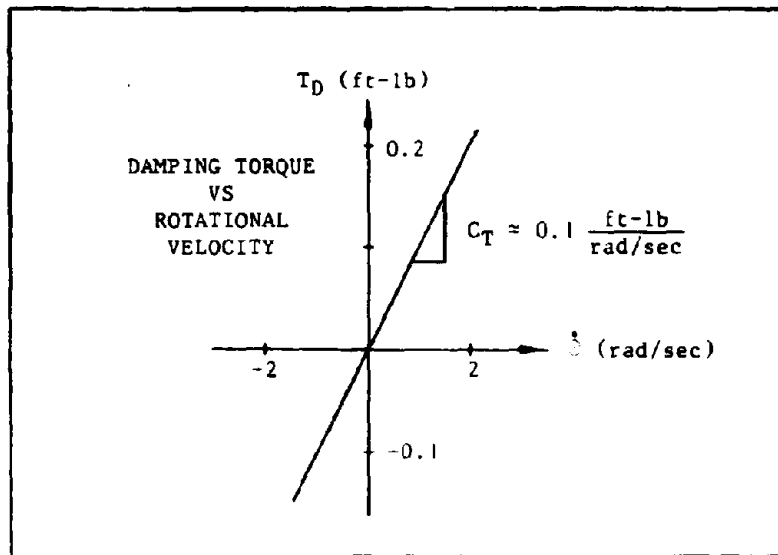


(a) Excitation/Response

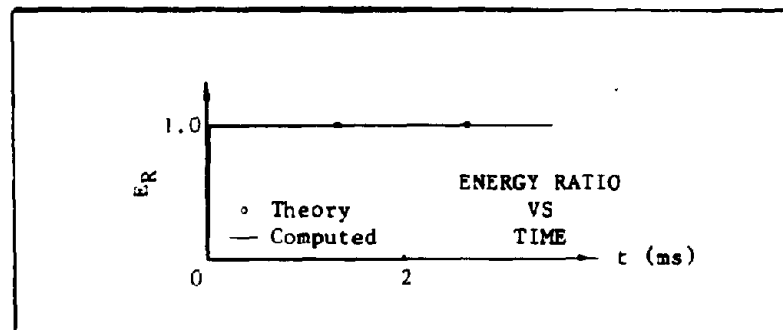
Figure A-3: Validation of Computer Procedure for Simulating Impulse Tests for Determining the Variation in Dynamic Shear Modulus with Shear Strain



(b) Spring Torque-Rotation Behavior



(c) Damping Torque-Rotational Velocity Behavior



(d) Energy Ratio

Figure A-3: Validation of Computer Procedure for Simulating Impulse Tests for Determining the Variation in Dynamic Shear Modulus with Shear Strain

**Validation Procedure:** Obtained computer solution, checked energy balance and torque-rotation behavior, and judgmentally checked solution.

**Parameters:**  $G_0 = 5.14 \times 10^5$  psf,  $K_{T_0} = 5610$  ft-lb/rad,  $I = 2.8 \times 10^{-4}$  lb-ft-sec<sup>2</sup>,  $C_T = 0.5$  ft-lb-sec/rad,  $R = 5$ ,  $\alpha = 1$ ,  $C_1 = 0.8$ ,  $\tau_m = 100$  psf, computational time step =  $1.8 \times 10^{-5}$  sec.

**Excitation:** High frequency, sinusoidal torque which induced nonlinear behavior; amplitude = 2.7 ft-lb, frequency = 570 cps.

**Response:** Decaying transient and steady state, high frequency, cyclic rotations.

**Results:** As shown in Fig. A-4(d), energy balance requirements are satisfied. Checking the solution judgmentally, as seen in Fig. A-4(a) and as would be expected, the frequency of the response, under steady state conditions, is equal to that of the excitation. As shown in Fig. A-4(b), the computed, nonlinear spring torque-rotation curve agrees closely with the curve estimated directly using Ramberg-Osgood stress-strain equations (24). Differences between these curves were found to decrease with decreases in the computational time step. The computed, linear damping torque-rotational velocity curve, shown in Fig. A-4(c), is linear with the correct slope.

**Conclusion:** The procedure for simulating high frequency, cyclic tests for determining the variation in the dynamic shear modulus with shear strain is valid.

- 5) Validation of computer procedures for simulating low frequency, cyclic, controlled-torque tests for determining the degradation and liquefaction characteristics of sands and silts.

#### Dynamic Solution Procedure

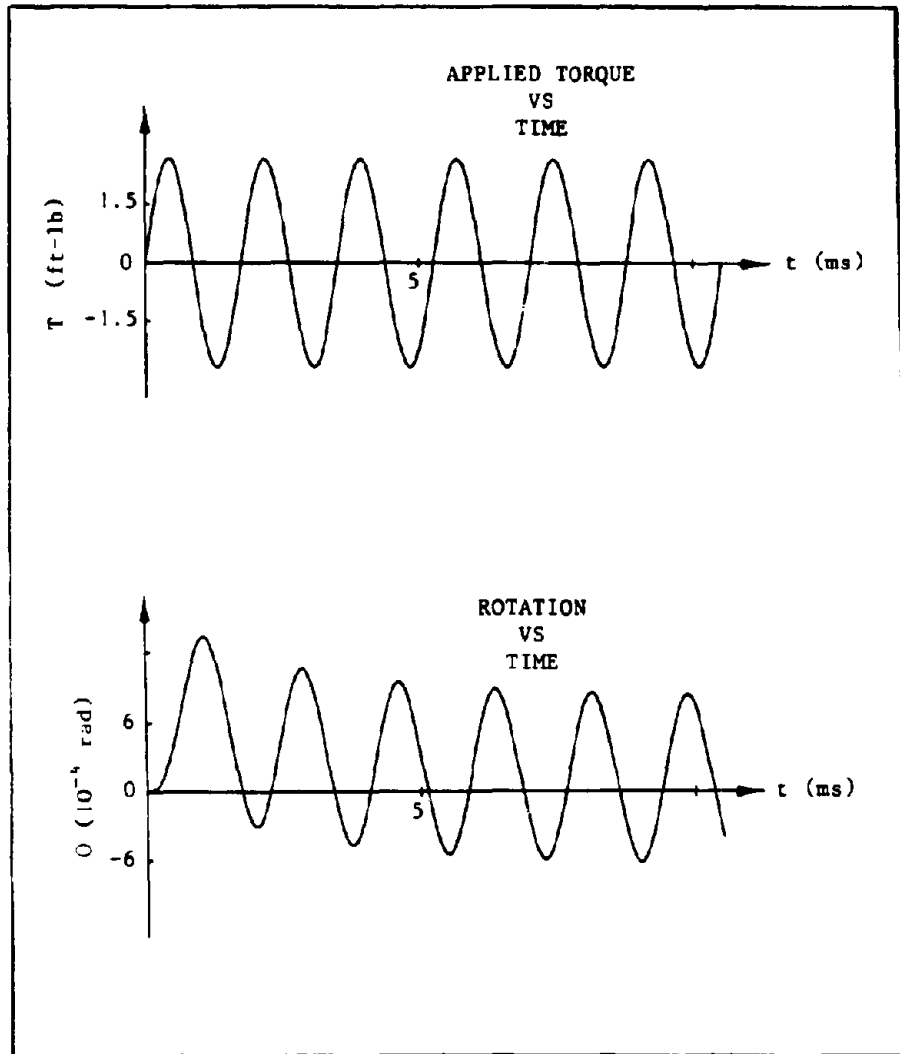
**Validation Procedure:** Obtained computer solution, checked energy balance and torque-rotation behavior, and judgmentally checked solution.

**Parameters:**  $G_{m0} = 1.55 \times 10^6$  psf,  $K_{T_0} = 1.7 \times 10^4$  ft-lb/rad,  $I = 2.8 \times 10^{-4}$  lb-ft-sec<sup>2</sup>,  $C_T = 0.09$  ft-lb-sec/rad,  $\tau_{m0} = 800$  psf,  $C_1 = 0.666$ ,  $C_2 = 1.968$ ,  $C_3 = 4.761$ ,  $C_4 = 3.865$ ,  $k_2 = 0.0025$ ,  $m = 0.43$ ,  $n = 0.62$ , computational time step =  $8 \times 10^{-5}$  sec.

**Excitation:** Low frequency, sinusoidal torque; amplitude = 1.7 ft-lb, frequency = 1 cps.

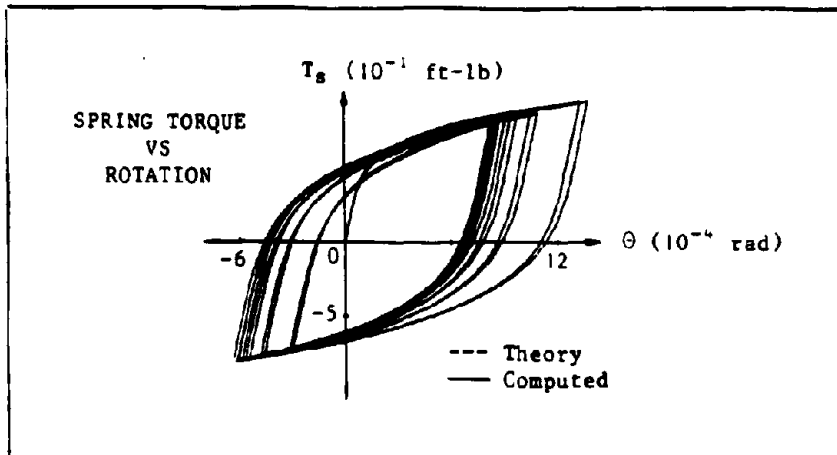
**Response:** Negligible transient rotation and low frequency, cyclic rotation having an amplitude which increased with an increase in the number of cycles of loading.

**Results:** As shown in Fig. A-5(d), energy balance requirements are

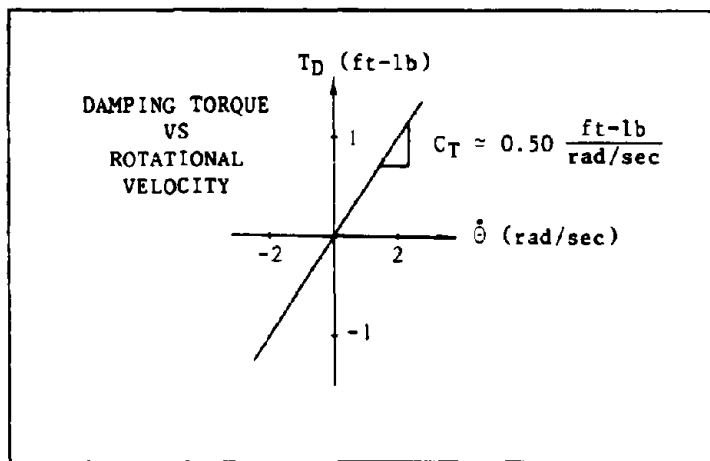


(a) Excitation/Response

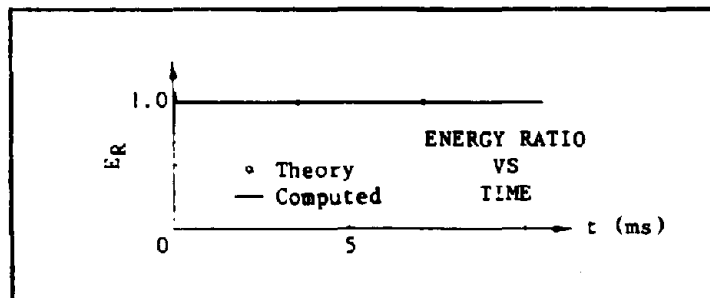
Figure A-4: Validation of Computer Procedure for Simulating High Frequency, Cyclic Tests for Determining the Variation in Dynamic Shear Modulus with Shear Strain



(b) Spring Torque-Rotation Behavior

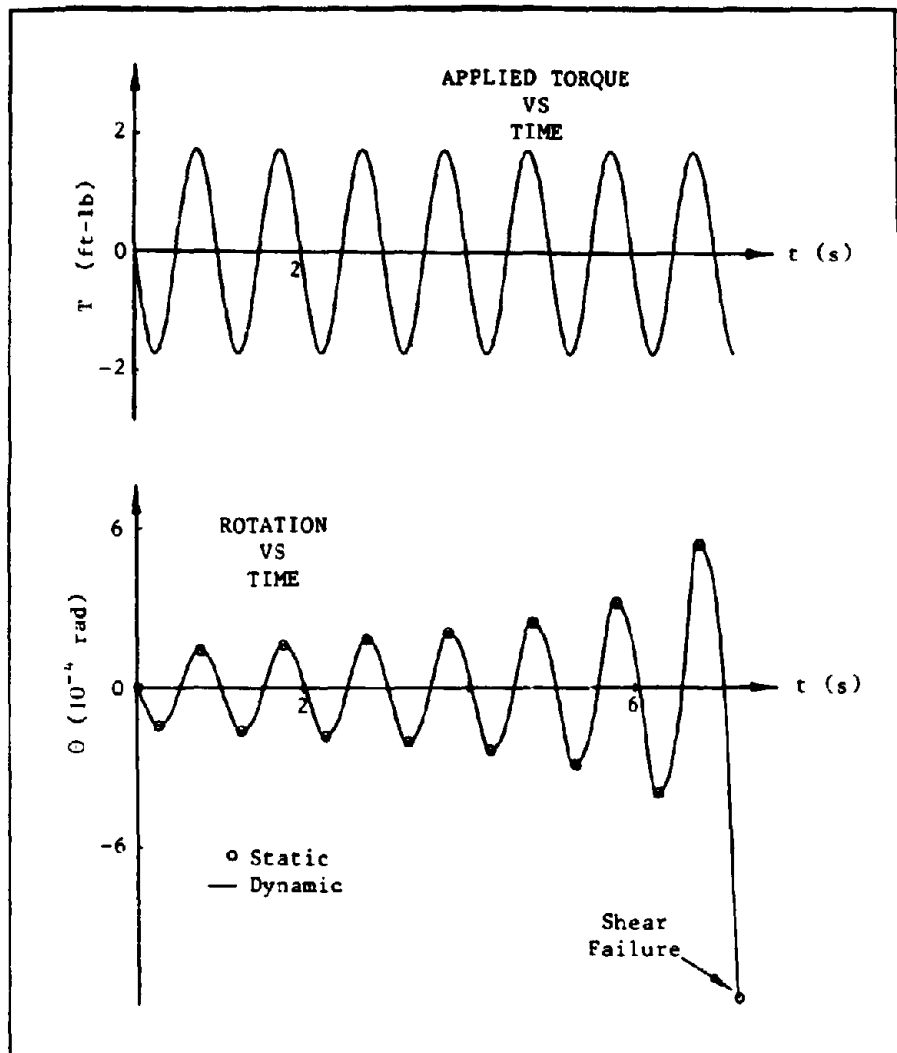


(c) Damping Torque-Rotational Velocity Behavior



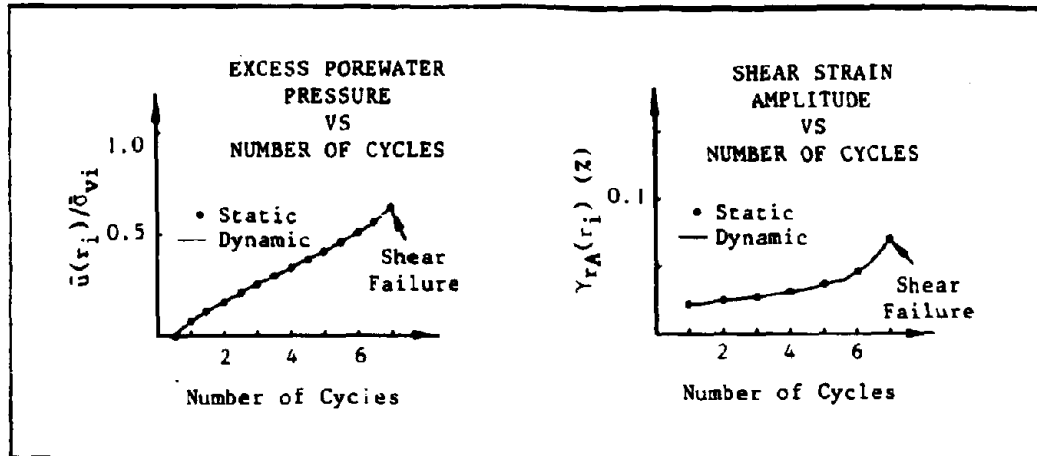
(d) Energy Ratio

Figure A-4: Validation of Computer Procedure for Simulating High Frequency, Cyclic Tests for Determining the Variation in Dynamic Shear Modulus with Shear Strain

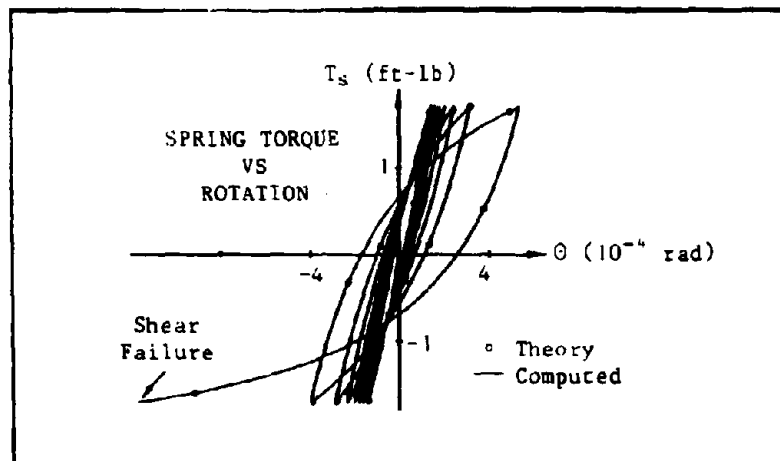


(a) Excitation/Response

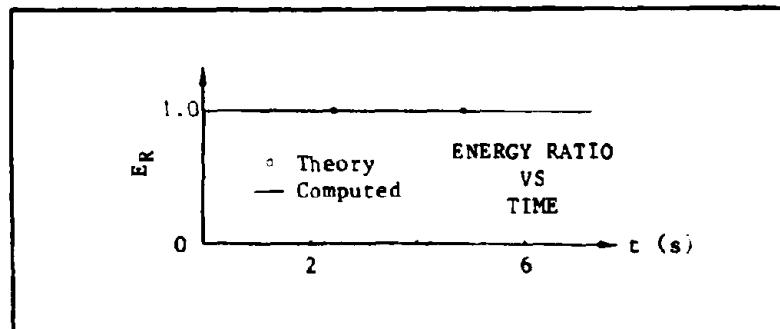
Figure A-5: Validation of Computer Procedures for Simulating Low Frequency, Cyclic, Controlled-Torque Tests for Determining Degradation and Liquefaction Characteristics of Sands and Silts



(b) Excess Porewater Pressure and Shear Strain Histories



(c) Spring Torque-Rotation Behavior



(d) Energy Ratio

Figure A-5: Validation of Computer Procedures for Simulating Low Frequency, Cyclic, Controlled-Torque Tests for Determining Degradation and Liquefaction Characteristics of Sands and Silts

satisfied. Checking the solution judgmentally, as seen in Figs. A-5(a) and (b), the amplitude of the cyclic rotation, the excess porewater pressure ratio, and the amplitude of the cyclic shear strain increased in the manner expected with an increase in the number of cycles of loading. A shear failure of the test soil was predicted during the 8th cycle of loading. As shown in Fig. A-5(c), the computed spring torque-rotation curve shows the expected degradation and agrees closely with the curve estimated directly using hyperbolic stress-strain equations (12). The effects of viscous damping were found to be negligible because of the low excitation and response frequencies considered.

Conclusion: The dynamic solution procedure for simulating low frequency, cyclic, controlled-torque tests for determining the degradation and liquefaction characteristics of sands and silts is valid.

#### Static Solution Procedure

Validation Procedure: Using static procedure, obtained computer solution and compared solution to above-discussed dynamic computer solution.

Parameters:  $G_{m0} = 1.55 \times 10^6$  psf,  $K_{T0} = 1.7 \times 10^4$  ft-lb/rad,  $\tau_{m0} = 800$  psf,  $C_1 = 0.666$ ,  $C_2 = 1.968$ ,  $C_3 = 4.761$ ,  $C_4 = 3.865$ ,  $k_2 = 0.0025$ ,  $m = 0.43$ ,  $n = 0.62$ .

Excitation: Cyclic torque having a uniform amplitude; amplitude = 1.7 ft-lb.

Response: Cyclic rotation having an amplitude which increased with an increase in the number of cycles of loading. The static procedure was programmed to give response parameters only at every half-cycle.

Results: As shown in Fig. A-5(a), the peaks of the cyclic rotation, computed using the static solution procedure, agree quite well with those computed using the validated dynamic procedure. Additionally, as shown in Fig. A-5(b), the histories of the excess porewater pressure ratio and the amplitude of the cyclic shear strain, computed using the static solution procedure, agree quite well with those computed using the dynamic procedure. Finally, as implied by Fig. A-5(a), the peaks of the torque-rotation history, computed using the static procedure, agree well with those computed using the dynamic procedure.

Conclusions: The static solution procedure for simulating low frequency, cyclic, controlled-torque tests for determining the degradation and liquefaction characteristics of sands and silts can provide good approximations of dynamic solutions when excitation frequencies are low. The static solution procedure for simulating such tests is valid.

- 6) Validation of computer procedure for simulating low frequency,

cyclic, controlled-rotation tests for determining the degradation characteristics of clays.

#### Dynamic Solution Procedure

Based on our experiences with the dynamic solution procedure for simulating low frequency, cyclic, controlled-torque tests for determining the degradation and liquefaction characteristics of sands and silts, and considering the reasonable similarity between the characteristics of clays and those of sands and silts, we decided that it was unnecessary, for the theoretical feasibility study, to develop a dynamic solution procedure for simulating low frequency, cyclic controlled-rotation tests for determining the degradation characteristics of clays.

#### Static Solution Procedure

Validation Procedure: Obtained computer solution, checked torque-rotation behavior, and judgmentally checked solution. An energy balance was not carried out because the energy balance is not an effective method for checking static solutions.

Parameters:  $G_{m0} = 7.2 \times 10^5$  psf,  $K_{T0} = 7900$  ft-lb/rad, degradation parameter curve for highly degradable clay (see Fig. 19, pg. 50),  $T_{m0} = 660$  psf.

Excitation: Cyclic rotation having uniform amplitude; amplitude = 0.02 rad.

Response: Cyclic torque having an amplitude which decreased with an increase in the number of cycles of loading. The static procedure was programmed to give response parameters only at every half-cycle.

Results: As shown in Fig. A-6, the peaks of the cyclic torque decrease with an increase in the number of cycles of loading as would be expected. Additionally, the peaks of the cyclic torque computed using the static solution procedure, agree closely with those estimated directly using hyperbolic stress-strain equations (12). This also implies that the spring torque-rotation peaks obtained using the static solution procedure agree closely with those estimated directly using hyperbolic stress-strain equations (12).

Conclusions: Based on our experiences in validating the procedures for simulating tests for determining the degradation and liquefaction characteristics of sands and silts, the static solution procedure was judged to be an effective means for simulating low frequency, cyclic, controlled-rotation tests for determining the degradation characteristics of clays. The static solution procedure for simulating such tests is valid.

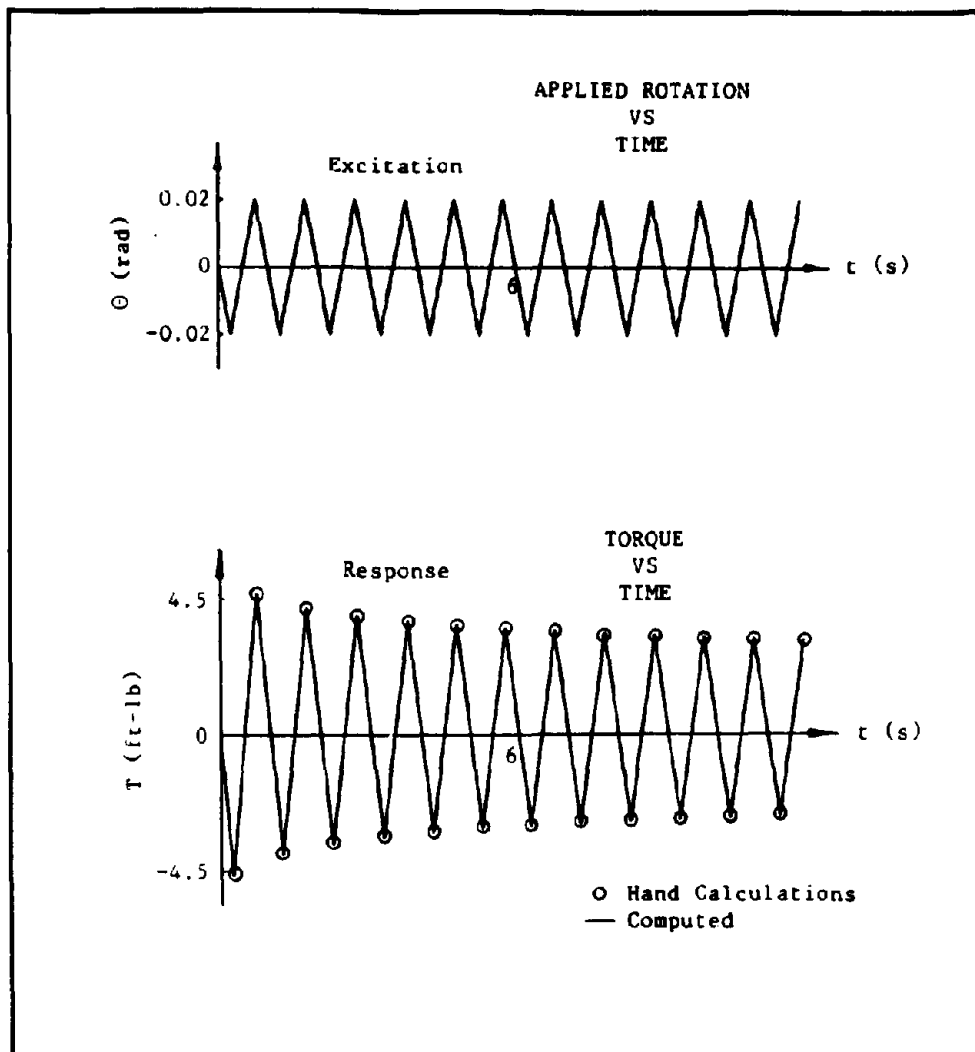


Figure A-6: Validation of Computer Procedure for Simulating Low Frequency, Cyclic, Controlled-Rotation Tests for Determining the Degradation Characteristics of Clays

### Appendix B - Derivations for Key Relationships

In this appendix, we present our derivations for 1) the equation relating the spring torque,  $T_s$ , to the corresponding shear stress developed in the test soil along the wall of the inner cylinder,  $\tau_{rs}(r_i)$ , and related equations, 2) the equation relating the rotation of the inner cylinder,  $\theta$ , to the shear strain developed in the test soil along the wall of the inner cylinder,  $\gamma_r(r_i)$ , 3) the equation for the tangent spring stiffness,  $K_T$ , of the single-degree-of-freedom system, 4) the equation defining the rotational flexibility of the inner cylinder relative to the rotational flexibility of the test soil during the initial cycle of loading,  $F_i$ , and 5) the equation defining the rotational stiffness of the inner cylinder relative to the rotational stiffness of the test soil during the ultimate cycle of loading,  $S_u$ .

- 1) Derivation for the equation relating the spring torque,  $T_s$ , to the corresponding shear stress developed in the test soil along the wall of the inner cylinder,  $\tau_{rs}(r_i)$ , and related equations.

From Fig. 9 and basic principles of mechanics, we may derive the following relationship assuming a uniform distribution of shear stress in the vertical direction within the test soil:

$$T_s = -\tau_{rs}(r_i)Ar_i \quad (B-1)$$

where  $A$  = surface area of active (unshielded) portion of inner cylinder  
 $r_i$  = outer radius of inner cylinder

Using basic geometry and rearranging terms, Eq. B-1 may be rewritten as follows:

$$\tau_{rs}(r_i) = -\frac{T_s}{2\pi r_i^2 l} \quad (B-2)$$

where  $l$  = length of active portion of inner cylinder

We may infer, from Eq. B-2 the equation of interest:

$$\Delta\tau_{rs}(r_i) = -\frac{\Delta T_s}{2\pi r_i^2 l} \quad (1)$$

If viscous damping and inertia forces are negligible,  $T \approx T_s$ , and  $\tau_r(r_i) \approx \tau_{rs}(r_i)$  and we may rewrite Eq. B-2 as follows:

$$\tau_r(r_i) = - \frac{T}{2\pi r_i^2 l} \quad (B-3)$$

where  $T$  = torque applied to inner cylinder  
 $\tau_r(r_i)$  = shear stress in test soil along wall of inner cylinder

Equation B-3 may be rearranged and rewritten in terms of the amplitudes of cyclic quantities,  $T_A$  and  $\tau_{rA}(r_i)$ , giving the following expression of interest:

$$T_A = -2\pi r_i^2 l \bar{\sigma}_{vi} \left( \frac{\tau_{rA}(r_i)}{\bar{\sigma}_{vi}} \right) \quad (2)$$

where  $\bar{\sigma}_{vi}$  = initial effective vertical stress  
 $\tau_{rA}(r_i)/\bar{\sigma}_{vi}$  = shear stress ratio

- 2) Derivation for the equation relating the rotation of the inner cylinder,  $\Theta$ , to the shear strain developed in the test soil along the wall of the inner cylinder,  $\gamma_r(r_i)$ .

Assuming an axisymmetric, linear, horizontal displacement distribution in the test soil, as shown in Fig. 10, we may write the following equation:

$$u(r) = \frac{r_0 - r}{r_0 - r_i} u(r_i) \quad (B-4)$$

where  $u(r)$  = horizontal displacement of test soil  
 $r$  = radius  
 $r_0$  = inner radius of outer cylinder  
 $r_i$  = outer radius of inner cylinder

From basic principles of mechanics (16):

$$\gamma_r(r) = \frac{\partial u(r)}{\partial r} - \frac{u(r)}{r} \quad (B-5)$$

where  $\gamma_r(r)$  = shear strain in horizontal planes

Applying Eq. B-5 to Eq. B-4 leads to:

$$\gamma_r(r) = -\left(\frac{r_o}{r_o - r_i}\right) \frac{u(r_i)}{r} \quad (\text{B-6})$$

Evaluating Eq. B-6 along the wall of the inner cylinder gives:

$$\gamma_r(r_i) = -\left(\frac{r_o}{r_o - r_i}\right) \frac{u(r_i)}{r_i} \quad (\text{B-7})$$

The following equation is based on the assumption that slip does not occur between the test soil and the wall of the inner cylinder:

$$u(r_i) = \Theta r_i \quad (\text{B-8})$$

where  $\Theta$  = rotation of inner cylinder

Substituting Eq. B-8 into Eq. B-7 gives:

$$\gamma_r(r_i) = -\left(\frac{r_o}{r_o - r_i}\right) \Theta \quad (\text{B-9})$$

We may infer from Eq. B-9 the equation of interest:

$$\Delta\gamma_r(r_i) = -\left(\frac{r_o}{r_o - r_i}\right) \Delta\Theta \quad (3)$$

- 3) Derivation for the equation for the tangent spring stiffness,  $K_T$ , of the single-degree-of-freedom system.

We derived the tangent spring stiffness,  $K_T$ , from the following shear stress-strain relation:

$$G(r_i) = \frac{\Delta\tau_{rs}(r_i)}{\Delta\gamma_r(r_i)} \quad (\text{B-10})$$

where  $G(r_i)$  = shear modulus of test soil along wall of inner cylinder  
 $\tau_{rs}(r_i)$  = shear stress in test soil along wall of inner cylinder  
caused by shear strain  
 $\gamma_r(r_i)$  = shear strain in test soil along wall of inner cylinder  
 $r_i$  = outer radius of inner cylinder

Substituting Eq. 3, pg. B-3, and Eq. 1, pg. B-1, into Eq. B-10 gives the following equation:

$$G(r_i) = \frac{1}{2\pi r_i^2 l} \frac{(r_o - r_i)}{r_o} \frac{\Delta T_s}{\Delta \theta} \quad (B-11)$$

The term  $\Delta T_s / \Delta \theta$  in Eq. B-11 may be recognized as the tangent spring stiffness,  $K_T$ , of the single-degree-of-freedom system. Substituting  $K_T$  for  $\Delta T_s / \Delta \theta$  in Eq. B-11 and rearranging terms gives the equation of interest:

$$K_T = \frac{2\pi r_i^2 r_o l}{r_o - r_i} G(r_i) \quad (4)$$

- 4) Derivation for the equation for the rotational flexibility of the inner cylinder relative to the rotational flexibility of the test soil during the initial cycle of loading,  $F_i$ .

We defined the rotational flexibility of the inner cylinder relative to the rotational flexibility of the test soil during the initial cycle of loading,  $F_i$ , as:

$$F_i = \frac{\theta_i}{\theta_{si}} \quad (B-12)$$

where  $\theta_i$  = static twist of active portion of flexible inner cylinder due to static torque,  $T$ , acting throughout cylinder  
 $\theta_{si}$  = static rotation of rigid inner cylinder embedded in undegraded test soil due to static torque,  $T$

To determine  $\theta_i$ , we considered the following expression (7), giving the static twist between the ends of a circular shaft,  $\bar{\theta}$ , caused by a static torque,  $\bar{T}$ , acting throughout the shaft:

$$\bar{\theta} = \frac{\bar{T}L}{G\bar{I}} \quad (B-13)$$

where  $\bar{G}$  = shear modulus of shaft  
 $\bar{L}$  = length of shaft  
 $\bar{J}$  = polar moment of inertia of cross section of shaft

For a hollow, circular shaft, (7),

$$\bar{J} = \frac{\pi}{32} (\bar{D}_o^4 - \bar{D}_i^4) \quad (B-14)$$

where  $\bar{D}_o$  = outer diameter of shaft  
 $\bar{D}_i$  = inner diameter of shaft

Substituting Eq. B-14 into Eq. B-13 and writing the resulting expression in terms of the variables used in the theoretical feasibility study, an expression may be obtained for the static twist between the ends of the active portion of the flexible inner cylinder caused by a static torque, T, acting throughout the inner cylinder:

$$\Theta_i = \frac{Tl}{\frac{\pi}{32} (D_o^4 - D_i^4) G_i} \quad (B-15)$$

where  $G_i$  = shear modulus of inner cylinder  
 $l$  = active length of inner cylinder  
 $D_o$  = outer diameter of inner cylinder  
 $D_i$  = inner diameter of inner cylinder

To determine  $\Theta_{gi}$ , we assumed the static torque, T, to be applied to a rigid inner cylinder embedded in the undegraded test soil. The shear strain developed in the undegraded test soil along the wall of the inner cylinder,  $\gamma_r(r_i)$ , as a result of the applied torque, T, may be estimated using the following relationship based on hyperbolic shear stress-strain relationships (12):

$$\gamma_r(r_i) = - \frac{\tau_r(r_i)}{\frac{G_{mo}}{\tau_{mo}} \tau_r(r_i) - G_{mo}} \quad (B-16)$$

where  $\tau_r(r_i)$  = shear stress in test soil along wall of inner cylinder caused by applied torque T  
 $G_{mo}$  = undegraded low amplitude shear modulus  
 $\tau_{mo}$  = undegraded shear strength

The shear stress,  $\tau_r(r_i)$ , induced in the test soil as a result of the applied torque, may be estimated using Eq. B-3. Equation B-16 is valid only for positive shear strains. A similar equation is used for negative

shear strains.

Using Eq. B-9, the static rotation of the rigid inner cylinder,  $\Theta_{si}$ , resulting from the applied torque, T, may be estimated in terms of the shear strain developed in the test soil along the wall of the inner cylinder,  $\gamma_r(r_i)$ , as:

$$\Theta_{si} = -\left(\frac{r_o - r_i}{r_o}\right) \gamma_r(r_i) \quad (B-17)$$

Appropriately combining Eq. B-3, Eq. B-16, and Eq. B-17, we may obtain the following expression for the static rotation of the rigid inner cylinder embedded in undegraded test soil due to torque T:

$$\Theta_{si} = -\left(\frac{r_o - r_i}{r_o}\right) \left[ \frac{T/2\pi r_i^2 l}{(G_{mo}/\tau_{mo}) (-T/2\pi r_i^2 l) - G_{mo}} \right] \quad (B-18)$$

Equation B-15 and Eq. B-18 may be substituted into Eq. B-12 giving the desired expression for  $F_i$ :

$$F_i = \frac{Tl / \left[ \frac{\pi}{32} (D_o^4 - D_i^4) G_i \right]}{-\left(\frac{r_o - r_i}{r_o}\right) \left[ \frac{T/2\pi r_i^2 l}{(G_{mo}/\tau_{mo}) (-T/2\pi r_i^2 l) - G_{mo}} \right]} \quad (11)$$

- 5) Derivation for the equation for the rotational stiffness of the inner cylinder relative to the rotational stiffness of the test soil during the ultimate cycle of loading,  $S_u$ .

We defined the rotational stiffness of the inner cylinder relative to the rotational stiffness of the test soil during the ultimate cycle of loading,  $S_u$ , when the test soil has either liquefied or stabilized at some limiting cyclic deformation as:

$$S_u = \frac{\Theta_{suA}}{\Theta_i} \quad (B-19)$$

where  $\Theta_i$  = static twist of active portion of flexible inner cylinder due to torque, T, acting throughout cylinder  
 $\Theta_{suA}$  = amplitude of low frequency (inertia and viscous damping forces negligible), cyclic rotation of rigid inner cylinder embedded in fully degraded test soil caused by low frequency, cyclic torque having amplitude, T.

The quantity  $\Theta_i$  may be determined using Eq. B-15. To determine  $\Theta_{suA}$ , we assumed that the cyclic torque having an amplitude  $T$  was sufficient to induce either liquefaction in loose soils or limiting deformations in dense soils. Using Eq. B-9, we may write the following expression giving  $\Theta_{suA}$  in terms of the peak shear strain developed in the test soil along the wall of the inner cylinder during the ultimate cycle of loading,  $\gamma_{ruA}(r_i)$ , when the soil has fully degraded:

$$\Theta_{suA} = -\left(\frac{r_o - r_i}{r_o}\right) [\gamma_{ruA}(r_i)] \quad (B-20)$$

Substituting Eq. B-15 and Eq. B-20 into Eq. B-19, gives the desired expression for  $S_u$ :

$$S_u = -\frac{\left(\frac{r_o - r_i}{r_o}\right) [\gamma_{ruA}(r_i)]}{T1 / \left[ \frac{\pi}{32} (D_o^4 - D_i^4) G_i \right]} \quad (12)$$

Appendix C - Report on Operational Feasibility  
Study from Sweet & Aiken

In this appendix, we present the entire report on the operational feasibility study from Sweet & Aiken, Inc. The report includes a presentation and discussion of the operational aspects of the proposed testing system, an engineering drawing presenting a preliminary design of a laboratory research prototype testing system, and an appendix which includes discussions of electronic equipment and provides appropriate literature from manufacturers.

**PRELIMINARY DESIGN OF A PROTOTYPE IN SITU TESTING TOOL**

**Prepared For  
DYNAMIC IN SITU GEOTECHNICAL TESTING  
Houston, Texas**

**Prepared By**  
*William B. Aiken*  
**William B. Aiken, P.E.  
SWEET & AIKEN, INC.  
13810 Champion Forest Drive, Suite 235  
Houston, Texas 77069  
713/580-8455**



**July, 1985**

## **PRELIMINARY DESIGN OF A PROTOTYPE IN SITU SOIL TESTING TOOL**

### **1.0 INTRODUCTION**

A prototype tool has been designed for in situ measurement of cyclic and dynamic soil properties. The final field tool is intended to be used to test soil on dry land or on the ocean floor. The prototype has most of the important features of a field tool, but is intended to be used primarily for laboratory testing.

This report summarizes the tool. A discussion of mechanical aspects and explanations of modifications and special features are included in this report. A discussion of electronic systems is provided in two reports from an independent consultant, included in the Appendix.

The preliminary design criteria for the tool are presented in Table 1.1, and were taken from documents provided by Dynamic In Situ Geotechnical Testing, Inc.

In operation the tool will be pushed into the soil to be tested. The test specimen will be an annular volume of soil captured between an inner barrel and an outer barrel. The outer barrel will remain stationary with the surrounding soil and the inner barrel will be rotated in various fashions.

Excitation and Measurement Requirements

Mode	Torque Amplitude Range (ft-lb)		Excitation			Rotation Amplitude Range (deg) pk to pk single pk	Rotation Frequency (cps)	Acceleration Amplitude Range @ 1 inch radius (g)	Maximum Power (hp)
	Form	Period (sec)	Duration (sec)	Range (deg)	pk to pk				
Torque-Controlled Cyclic Test	0.1 - 15	sine wave	0.1 - 50	≤ 100 cycles	0.002-30	0.001-15	0.02-10	N/A	0.20
Rotation-Controlled Cyclic Test	0.1 - 15	sine wave	0.1 - 50	≤ 100 cycles	0.4-3.0	0.2-1.5	0.02-10	N/A	0.03
Impulse Test	0.01 - 20	rectangular impulse	N/A	≥ 0.0002 s	N/A	N/A	400-2400	± 0.3 - ± 210	0.20

Mechanical Requirements

	Dimensions				Penetration Forces			
	Outer Diameter (in)	Wall Thickness (in)	Length Below Piston (in)	Active Length (in)	Shielded Length (in)	Bearing Friction (lb)	Skin Friction (lb)	Total (lb)
Outer Barrel	3	1/12	12	N/A	N/A	4500	9500	14,000
Inner Barrel	1	1/16	12	8	4	1500	2500	4000

Maximum Environmental Fluid Pressure: 100,000 psf

Range of Differential Vertical Pressure to Be Applied by Piston: C - 6000 psf

Table 1.1: Preliminary Design Criteria (Includes All Revisions)

The tool was designed for testing in two modes:

1. Impulse Testing
2. Cyclic Testing.

For the impulse mode, a step torque will be input to the inner barrel. The torque will be held constant for a fraction of a second and rapidly released. The inner barrel will be allowed to freely vibrate in response to the impulse. The tool will measure the input torque and the rotational response of the inner barrel.

Cyclic testing can be done in two different ways. In one way a cyclic rotation can be input to the inner barrel. The response will be the cyclic torque necessary to generate this motion. In the other way, a cyclic torque will be input to the inner barrel and the response will be the resulting cyclic rotation. Torques and rotational motions will be measured when testing in either way.

The limits of penetration forces, environmental pressure, applied pressure, torque, rotation, power, acceleration, time duration, and frequency are presented in Table 1.1. Manufacturer's literature on all available components are presented in the Appendix. Calculations are provided in Section 7.0.

## 2.0 DESCRIPTION OF TOOL

Figure 2.1 is a schematic diagram of the drive and measurement systems while Drawing 850227-10 shows a full scale assembly drawing of the prototype in situ soil testing tool. The overall length excluding a latch/penetration device is 44 inches, and the outer diameter is 3 inches. These dimensions are such that the tool will fit inside a standard coring bit for testing ocean floor soil.

The soil test specimen is contained between the outer barrel and the inner barrel. Its dimensions are

Outer Diameter	-	2.833 inches
Inner Diameter	-	1.000 inch
Length	-	8.000 inches.

The tool captures an additional 4 inches of soil above the test specimen. This soil is expected to be disturbed and is not intended to be tested; it is isolated from the rotating inner barrel by a shield which remains stationary and does not touch the rotating inner barrel.

The tool simulates the overburden effect of the soil removed from the borehole by applying a force to the top of the soil specimen. The force is applied hydraulically through the vertical pressure piston. The pressure will be measured by a pressure transducer.

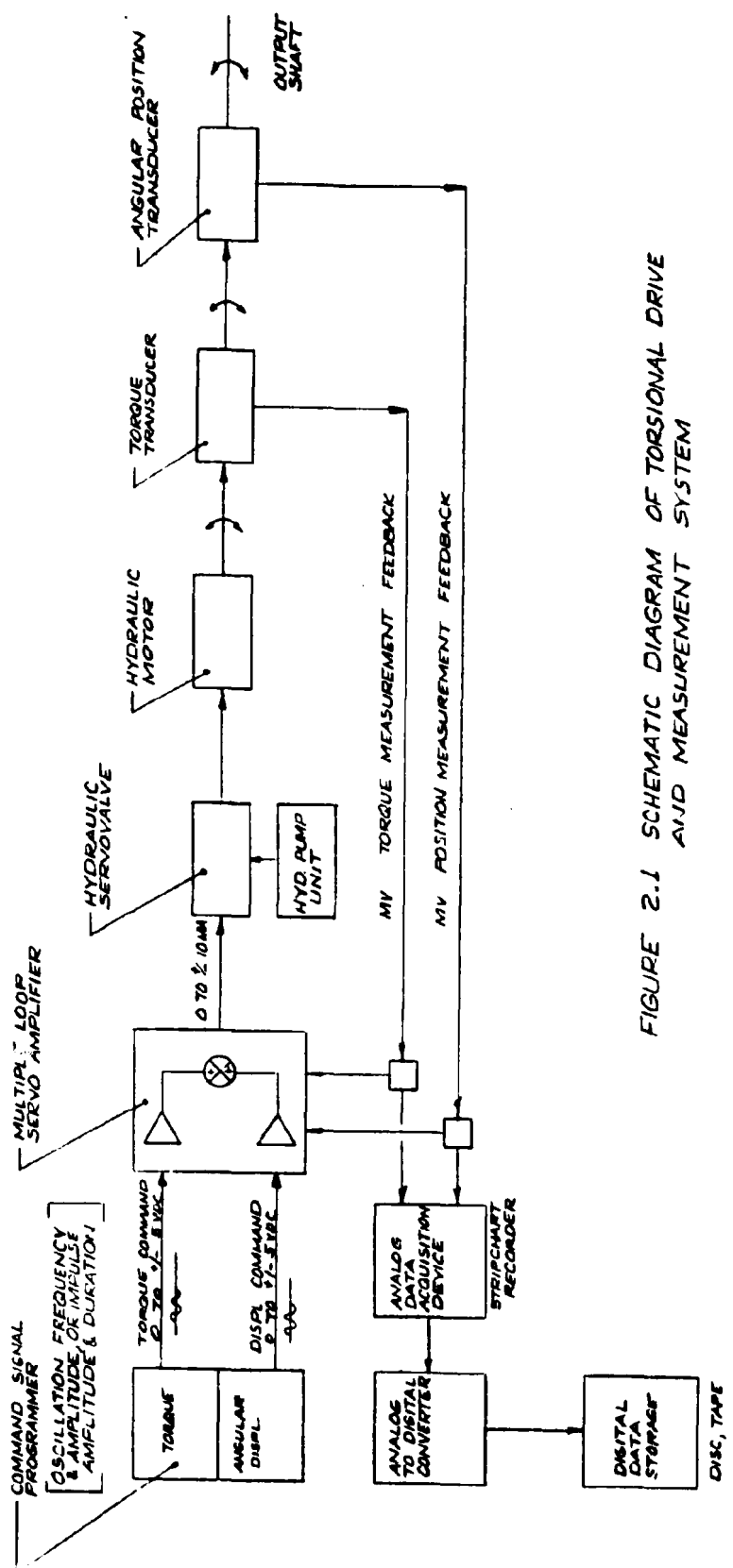


FIGURE 2.1 SCHEMATIC DIAGRAM OF TORSIONAL DRIVE AND MEASUREMENT SYSTEM

REV. NO.	REV. DATE	REV. BY	REV. FOR
B	7/15/65		REV. NOTES
A	5/1/65		PRELIM. RELEASE
1			
2			
3			
4			
5			
6			
7			
8			
9			
10			
11			
12			
13			
14			
15			
16			
17			
18			
19			
20			
21			
22			
23			
24			
25			
26			
27			
28			
29			
30			
31			
32			
33			
34			
35			
36			
37			
38			
39			
40			
41			
42			
43			
44			
45			
46			
47			
48			
49			
50			
51			
52			
53			
54			
55			
56			
57			
58			
59			
60			
61			
62			
63			
64			
65			
66			
67			
68			
69			
70			
71			
72			
73			
74			
75			
76			
77			
78			
79			
80			
81			
82			
83			
84			
85			
86			
87			
88			
89			
90			
91			
92			
93			
94			
95			
96			
97			
98			
99			
100			

BOATMAN ENGINEERS CORPORATION  
HOUSTON, TEXAS

SWEET & AIKEN, INC.  
SYSTEM BLOCK DIAGRAM

531-01

The lower ends of the inner and outer barrels are designed with tapers that drive the displaced soil away from the test specimen. The soil displaced by the outer barrel is forced into the surrounding soil; the soil displaced by the hollow inner barrel is forced inside the inner barrel. Jutted edges are provided in this barrel to force soil away from the wall of this barrel. The volume of space inside the inner barrel and the soil holding chamber was designed to hold all soil displaced by the inner barrel and shield. The various surfaces of the barrels will be treated for different characteristics. Relief ports are provided for soil chambers to prevent porewater pressure build-up during penetration.

The force necessary to drive the inner barrel into the soil is larger than the transducers and bearings can support. Thus, the inner barrel driving force is transferred to the shield through a load shoulder. Then it is transferred to the outer barrel through a pins where it combines with the outer barrel driving force and is transferred to the coring tool.

It is probable that the inner barrel will be transversely loaded during the driving operation. This may induce excessive shear and bending on the inner barrel and transducers, unless lateral support is provided. The tool was designed with two lateral support shoulders: one at the lower end of the shield and one at the upper end of the

shield. These support shoulders are designed so that reasonable bending loads will not damage the tool.

The lateral supports can induce frictional resistance to rotation that might be of the same order of magnitude as the input torque. Since torque is measured above the supports, the support induced torque would contaminate the test results. To alleviate this problem the shield was designed so that it could be moved axially upward after the driving operation, eliminating all contact with the inner barrel.

Excessive transverse forces developed during actual testing, <sup>(WH)</sup> may cause the inner barrel to contact the shield. This will prevent the completion of the test; however, it should also prevent damage to the transducers due to excess bending. This is not expected to occur under normal conditions.

The only component that will touch the inner barrel below the transducers is a lip seal between the inner barrel and outer barrel. This seal is necessary to keep the in situ fluid away from the transducers and bearings. The seal used is a Parker U packing seal designed to reduce contact forces to a minimum. The pressure differential across the seal will be kept below 10 psi. This low pressure, along with the low friction features of the seal, should reduce signal contamination by seal contact to less than 0.15 inch lbs.

One important requirement of the oscillating components for testing in the impulse mode is that they be underdamped. Underdamped behavior was promoted by limiting contact with stationary parts to a bare minimum and enclosing all but the inner barrel in air instead of oil. During testing the only contacts between moving and stationary parts are in the hydraulic motor, at the two tapered roller bearings, and at the lip seal.

Measurement transducers are located between the inner barrel and the drive shaft. These transducers measure inner barrel rotation, torque on the inner barrel, and rotational acceleration of the inner barrel.

Based on the search conducted for the preliminary design, it was concluded that the torque range requirements are too large for a single torque transducer. Thus, for the prototype system, two interchangeable transducers will be used: a low range torque transducer and a high range torque transducer. Small torques will be measured using a Lebow Model 2127 torque transducer, and large torques will be measured using a Lebow Model 2102 torque transducer. A second Lebow Model 2127, with a lower capacity, could be used for accuracy in the lowest torque range. Separate tools would be considered for field use.

Angular acceleration will be measured using two PCB

Piezotronics model 303A quartz accelerometers. The two accelerometers are mounted on the inner barrel 180 degrees apart at a known radial distance from the centerline. They measure linear acceleration which is converted to rotational acceleration using the kinematic relationships between rectilinear and angular motion. Using two accelerometers avoids imbalance and more accurately provides rotational motion.

Angular rotation will be measured using a Trans-Tek Series 604 angular displacement transducer. The housing of the transducer will be connected to the outer barrel and the transducer shaft will be connected to the main shaft.

Inner barrel excitation is provided by a miniature orbit type hydraulic motor manufactured by Lamina. This motor will run with equal torque in either direction and is instantly reversible. Its housing is sleeved into the outer barrel and its shaft is sleeved into the drive shaft. Based on the search conducted for the preliminary design, it was concluded that, just as with the torque transducers, the torque range requirements may be too large for a single motor. Thus, for the laboratory prototype, two interchangeable motors may be required. For the field, two tools may be required. The small torques will be provided by a Model A-25F motor, and the large torques will be provided by a Model A-50F motor.

The torque or rotation output of the motor is to be controlled by a Moog type 30 Series 30 servovalve. The position of the valve stem will be controlled by a signal from the torque transducer or angular rotation transducer. It will compare the signal with the desired value. If the signal is too low, the valve will open and if it is too high, the valve will close. The test operator will control the servovalve through a Moog series F120 rack mounted electronics package.

### 3.0 DESCRIPTION OF COMPONENTS

#### 3.1 Outer Barrel

The outer barrel serves as the housing for the test specimen and all internal components of the soil testing tool. The removable lower end of the outer barrel contains the test specimen. The upper portion contains the internal components and will connect, in the field model, to the coring bit or thread into a pipe.

The outer barrel has a uniform diameter of 3 inches, is 44 inches long, and is made of type 410 stainless steel. The lower portion has a nominal wall thickness of 1/12 inch and is 12 inches long.

Type 410 is a general purpose stainless steel that has good

corrosion resistance, is strong enough to resist penetration forces, is readily available, and is low cost compared to most other stainless steels. The upper end is made of annealed 410 having a minimum tensile strength of 75 ksi and a minimum yield strength of 35 ksi. The lower end is made of quenched and tempered type 410 having a minimum tensile strength of 110 ksi and a minimum yield strength of 85 ksi.

The lower end, containing the soil specimen, will be hydraulically pushed at a controlled rate into the soil formation. It has special inside and outside surface treatments so that disturbances are minimized and it properly interacts with the surrounding soil and the test specimen.

It is necessary that the outside surface provides reasonably low axial resistance with the soil to reduce the penetration force. More importantly, it must have high rotational resistance so that it helps transfer the driver reaction torque to the surrounding soil. These characteristics are developed by machining axial grooves all around the outer circumference of the lower end. Cylinders with different groove dimensions would be used for different soils.

The inner surface must be as frictionless as possible in the axial direction. This minimizes disturbances to the test specimen. As with the outer surface, this surface must have a high rotational resistance to minimize slip between the

outer barrel and the soil specimen. These characteristics are achieved by machining axial grooves along the inside of the lower end and coating the surface with a polytetrafluoroethylene (PTFE) coating. This will produce a surface coefficient of friction of less than 0.090.

PTFE is a fluoroplastic having excellent chemical inertness, good high and low temperature stability, and very low friction. The static coefficient of friction decreases with increasing load. Thus, PTFE bearing surfaces do not seize, even under extremely high loads. PTFE is relatively soft and is not resistant to wear unless improved by compounding the resins with inorganic fibers or particulate materials. Most PTFE coating companies include proprietary additives to improve wear characteristics. These improved PTFE coatings will allow numerous in situ soil tests before wear makes them nonfunctional. When this occurs, the barrels can be returned to the coating company for recoating.

The lower end of the outer barrel is provided with a taper so that displaced soil will be pushed into the surrounding soil instead of into the test soil.

A fluid relief port is provided at the top of the lower end of the outer barrel so that entrapped fluid will displace during penetration. A filter stone will be provided in the port to prevent the escape of soil.

### 3.2 Inner Barrel

The inner barrel is the lowermost portion of the oscillating components. It forms the inside of the soil test specimen and transfers the input torques and rotations to the specimen. It has a 1 inch outer diameter at the lower end, a 1.8 inch diameter at the upper end, and is about 18 inches long. The lower end adjacent to the soil test specimen has a wall thickness of 1/16 inch and is threaded into the upper section for easy removal for repairing or recoating.

The inside of the inner barrel is hollow to reduce the amount of soil displaced during penetration. The lower end has a taper to drive the displaced soil inside the bore instead of outside to the test specimen. The top of this taper is jugged to minimize contact between the tool surface and the soil inside the bore. A second jugged taper is provided near the base of the shield where the inner cylinder is constricted. The top end has a larger bore to provide room for the soil displaced by its wall. A relief port is provided at the uppermost part of the inner barrel wall to allow entrapped fluid to escape during penetration. A filter stone will be provided in the port to prevent the escape of soil.

The outside surface of the inner barrel must have the same

characteristics as the inside surface of the outer barrel; thus, it has the same surface treatments. The outside surface is axially grooved and coated with PTFE resin so that it will properly transfer driver actions to the test specimen, but will not excessively disturb the test specimen during penetration. The inside surface is to be machined to a 16 RMS finish and coated with PTFE resin so that interaction with the entrapped bore soil is minimized. Durability characteristics described for the outer barrel coatings also apply to the inner barrel coatings.

The inner barrel is made of quenched and tempered type 410 stainless steel having a minimum tensile strength of 110 ksi and a minimum yield strength of 85 ksi. This material has adequate strength to resist the penetration force, is hard enough to resist damage from soil contact, and is corrosion resistant.

### 3.3 Vertical Pressure System

A hydraulic piston is provided in the top of the annular space between the inner and outer barrels. This piston may be pressurized after penetration to simulate the vertical in situ force removed by the coring operation.

The outside diameter is 2.833 inches, the inside diameter is 1.0 inch, and the length is 0.75 inch. The piston is made of

annealed type 410 stainless steel for its corrosion resistance.

The pressure area of the piston is the same as the cross sectional area of the soil specimen; thus, the applied soil pressure is approximately the same as the hydraulic pressure applied to the piston. The pressure is monitored by a pressure transducer located at the top of the tool. This transducer is described in Section 3.5 of this report.

The vertical pressure system is designed either to provide a constant pressure on the specimen regardless of the soil movement or to remain stationary during testing. A valve is provided to control the vertical pressure system mode. Thus, in the constant pressure mode, with the valve open, if the soil specimen contracts during testing, the piston is compliant and will move down so that the pressure remains constant. In the stationary mode, after pressurizing the piston, the valve is closed so that the piston remains stationary regardless of the soil movement.

### 3.4 Shield

A 12 inch long soil specimen is trapped between the inner and outer barrels. Of this, the lower 8 inches is considered the test specimen and the top 4 inches is probably disturbed and not intended to be tested. A stationary shield is provided

between the oscillating inner cylinder and the top 4 inches of the soil specimen. This shield prevents the inner cylinder movements from being transferred to the inner surface of the disturbed part of the soil specimen.

Another function of the shield is to react the penetration forces and transmit them directly to the outer barrel so that they do not damage the transducers or bearings. The axial penetration force on the lower end of the inner barrel is transferred to a bearing shoulder located on the lowermost end of the shield. It passes axially up the shield to the three radial pins connecting the shield and outer barrel.

It is very likely that transverse forces will act on the inner barrel during penetration due to nonuniform soil properties. This causes an end moment as well as transverse shear forces. These actions are transferred to the shield by circumferential bearing areas located at the bottom of the shield and near the top of the shield. Thus, reasonable transverse forces may be sustained.

Since the input torques may be very small, it is necessary that contact between the shield and inner barrel be eliminated during testing. This is achieved by applying 400 psi hydraulic pressure to the bottom face of the shield flange. The pressure forces the ~~two~~ <sup>three</sup> ~~two~~ <sup>(113)</sup> connecting pins out of engagement on the shield and slowly drives the shield upward

3/32 inch where it contacts a landing surface on the inner barrel. This axial movement disengages the shield bearing surfaces from contact with the inner barrel leaving enough clearance between the shield and inner cylinder to prevent contact under normal conditions. The shield can be reengaged in two ways. It can be moved back into position by hand after disassembling the tool. Alternatively, a second hydraulic line can be provided to apply pressure to the upper face of the shield flange so that the shield can be driven downward until the connecting pins reengage. The second method would be preferred in a field tool.

### 3.5 Transducers

The tool incorporates three types of transducers to measure actions and motions input to the inner barrel. These include an angular displacement transducer, a torque transducer, and two accelerometers. The angular displacement transducer will mainly provide measurements during low frequency cyclic tests; whereas, the accelerometers will provide measurements during impulse tests. The torque transducer will provide measurements during both tests.

A Trans-Tek series 604 angular displacement transducer is attached to the upper end of the inner barrel. It measures the angular position of the inner barrel relative to the outer barrel and converts it into a DC voltage directly

proportional in amplitude and polarity to displacement from the electrical null position. It is a precision differential capacitor device and has integral voltage regulation, oscillator, demodulator and output buffer. The DC output can be fed directly into voltmeters, recorders, A/D converters or other devices. The standardized output allows interchanging units without system recalibration. A locking wedge is provided between the inner barrel and shield at the upper support surface. The locking wedge prevents rotation of the inner cylinder and shaft to prevent deviations from zeros during running and penetration. The lock is disengaged when the shield is moved out of contact with the inner barrel.

Standard series 604 transducers are designed to measure a 60 degree rotation range. This is much larger than required for the in situ soil testing tool which requires a maximum peak to peak rotation range of 30 degrees and a minimum range of 0.002 degree. Trans-Tek specifies factory calibration to any specified output sensitivity and Trans-Tek technical experts are certain the series 604 can be calibrated to accurately read rotations down to 0.01 degree with a resolution of 0.001 degree. Accuracy below 0.01 degree is questionable. The range would be  $\pm 0.5$  degree. As indicated in a letter from Trans-Tek included in the Appendix, they are willing to make the necessary modifications at a reasonable cost.

The full range of rotations can be measured with a single

tool using two angular displacement transducers in series. One would be calibrated for the large rotations and the other for the smaller rotations. All but the very smallest rotations (less than 0.01 degree) would be accurately measured with this system. The full scale assembly drawing shows only a single angular displacement transducer. The Trans-Tek series 604 meets all other requirements including pressure and temperature requirements.

The shaft of the angular displacement transducer fits into a precision hole in the upper end of the inner barrel. It is held in place with a small set screw. The body is attached to the outer barrel with three mounting brackets bolted to the three tapped holes in the bottom face of the transducer. These brackets pass through slots in the shaft coupler to the outer barrel.

The two accelerometers are PCB Piezotronics model 303A. They are quartz sensors having built in electronics so they can operate over a coaxial or two conductor cable; one lead conducts both signal and power.

The two accelerometers are mounted 180 degrees apart on angle brackets attached to the shaft coupler just above the angular displacement transducer. They are oriented to measure tangential acceleration at a radius of 0.75 inch. These transducers meet all requirements, including pressure and

temperature requirements.

The torque transducer is mounted between the motor shaft and the angular displacement transducer. A Lebow model 2127 with a 50 in-oz capacity will be used to measure torques less than 0.26 ft-lbs and a Lebow model model 2102-200 will be used to measure torques between 0.26 and about 17 ft-lbs. If necessary, a Lebow model 2127 with a 10 in-oz capacity can be used to measure very small torques more accurately. The upper limit is somewhat less than specified by the client, but was judged acceptable by the client. These are all in-line reaction torque devices using foil type strain gages to measure torsional shear strains. They produce minimal friction error.

The model 2127 has a flange at one end with 3 holes for boltup. This end will attach to the shaft coupler. The other end has a shaft that will fit into a mating hole in the lower end of the drive shaft. It will be held rigidly to the drive shaft with a small set screw.

The higher torque transducer has different end fittings. Both ends of this transducer have four drilled and tapped holes for flanges. For the prototype tool, a flange adapter will be necessary to make the high torque transducer interchangeable with the low torque transducer.

Both torque transducers have lead terminal boxes extending radially outward. Since these boxes will interfere with the outer barrel they will be removed and pigtail lead wires will be draped out of the main body. The torque transducers satisfy all requirements including temperature and pressure requirements.

The tool will also include three pressure transducers. These will be used to measure the differential pressure between the vertical pressure piston and ambient, between the transducer/bearing chamber and ambient, and between the space under the shield flange and the ambient. If the upper face of the shield flange is pressurized, a fourth pressure transducer will be used. All transducers will be Entran model EPX101 strain gage sensors that can be specified with a pressure range from 5 to 5000 psi. These pressure transducers meet all requirements. They will be threaded into a mounting plate attached to the inner barrel above the driver.

### 3.6 Drive Shaft

The drive shaft connects the driver to the transducers. It is guided by two tapered roller bearings. It is about 7 inches long and has a maximum diameter of 1.25 inches. It is made out of annealed type 410 stainless steel having a minimum ultimate strength of 75 ksi and a minimum yield strength of 35 ksi. The shaft is very lightly stressed during

operation; thus the material was selected solely for availability, cost, and corrosion resistance.

The lower end of the shaft has a precision drilled hole for the torque transducer shaft and the upper end has a precision drilled hole for the motor shaft. Both ends have radial drilled and tapped holes for set screws to hold in the mating shafts.

### **3.7 Drive Shaft Coupler**

The drive shaft coupler is used to connect the inner barrel to the torque transducer. The lower end is provided with a female thread which connects with a mating male thread on the top end of the inner barrel. A set screw will prevent unthreading during tests. The top end has drilled and tapped holes for bolts which connect it to the torque transducer and accelerometers.

The drive shaft coupler is made out of annealed type 410 stainless steel. This material was chosen for its availability, cost, and corrosion resistance.

### **3.8 BEARINGS**

The bearings supporting the shaft that drives the torque and angular displacement transducers are single row, straight

bore Timken precision bearings, identified by the number 07100-07196.

The approximate 4.5 inch spacing of the bearings in the "indirect" installation mode provides high shaft stability and accurate alignment with the axis of the tool. The tapered roller bearing elements not only minimize shaft axial movement, but also are ideal for oscillatory service of the type anticipated for the tool. Each bearing has a coefficient of friction of approximately 0.00018. The torsional resistance of the bearings will not contaminate the torque measurements of the tool since the torque transducer is between the soil test specimen and the bearings.

The very low radial and thrust loads that will be imposed on the bearings in the anticipated application of the tool should insure long bearing life provided lubrication is adequate and the operating environment is clean.

### 3.9 SEALS

The single dynamic seal isolating the transducers, accelerometers, motor, servovalve, and other components from the environment in which the tool is operating is a Parker 8500 series U-ring. Parker's identifying number is 8506-0175.

The very low friction characteristics of the Parker seal result from its cross sectional design and from the seal material. The cross section is a nominal "U" shape, but actually resembles a truncated "Y". This shape provides almost knife edge contacts between the sealing edges and the sealing surfaces. The seal material is a very low friction polyurethane compound having optimum wear and abrasion resistance.

As stated previously, the pressure differential across the seal will be kept below 10 psi. The upper chamber of the tool will be pressurized with air to 10 psi above ambient using a standard air line and surface control unit. The pressure will be monitored with a pressure transducer described in Section 3.5.

All other seals are conventional "O" ring seals used as static or gasket type seals or as piston seals. There is nothing unique or unusual about these "O"-ring type seals.

### 3.10 Hydraulic Motor

As stated previously in Section 2.0, excitation of the inner barrel comes from a miniature, high torque, medium speed orbit type hydraulic motor built by Lamina under license from Char-Lynn, a division of Eaton Corporation. Also as stated previously, two sizes of this motor will be required to

handle the range of torque requirements: the A-25F model for the lower torque range and the A-50F model for the higher torque range.

These motors will run in each direction with equal torque and are instantly reversible. Maximum torque output is 100 inch pounds for the A-25F model and 200 inch pounds for the A-50F model. As with the torque transducers, this maximum torque is slightly less than that specified by the client, but was judged to be adequate by the client. Otherwise the motors meet all requirements including temperature and pressure requirements.

Mounting in the prototype tool will require some modification, including turning down the mounting flange diameter, turning down the shaft diameter, and changing the hydraulic ports as illustrated in the assembly drawing.

### 3.11 Hydraulic Controller

A Moog standard series 30 servovalve provides control of torque output and of rotation. The torque transducer sends a signal to the servovalve, which will compare the signal with the desired torque value and make the required adjustment. Similarly, the angular displacement or rotation transducer will send a signal to the servovalve giving the measured angular displacement for comparison with the desired value

and correction if required. The frequency response of the servovalve is satisfactory for low frequency cyclic tests. During impulse tests, in which an impulsive rectangular torque will be applied, an accumulator will be used to insure constant pressure, and thus, constant torque. This is needed because the servovalve could not follow the high frequency fluctuations that would otherwise develop.

The servovalve does not have as rapid a rise time as desired by the client. As indicated in the manufacturer's specifications the approximate time to develop 90% output in response to a step input of current is 0.0025 second. The client has accepted this limitation. Additionally, the servovalve does not appear to satisfy environmental pressure requirements. Moog provides special designs for high pressure applications and such a design may be required. Alternatively, in the field unit, the controller may be placed in the low pressure environment of the downhold electronics package (see Appendix for discussion of electronics package). The standard servovalve will satisfy all other requirements including temperature requirements. The servovalve can be mounted on a plate in the interior of the tool as indicated in the assembly drawing.

The servovalve can be controlled by the operator using a Moog series F120 rack mounted electronics package. The package will consist of an F120<sup>7</sup>-101 modular cage with the following

**electronic cards:**

**F128-201 Power Supply**

**F122-202 Servo Amplifier**

**F123-202 Test Module**

**F123-206 Signal Generator.**

### **3.12 Hydraulic Drive Schematic**

Figure 3.1 shows a schematic layout of the hydraulic drive system for operation of the tool. This schematic diagram illustrates the functions of the various components and how they relate to each other.

For the laboratory prototype, the Moog servovalve and the Lamina motor will be housed in the tool. All other hydraulic components will be outside the tool for convenience. For the field tool, the accumulator will also be housed in the tool. Including the accumulator in the tool is feasible. The remaining hydraulic components are standard and pose no feasibility problems for remote operation over 1500 of cable.

### **3.13 Power and Support Cable**

It will be necessary to support the field tool from the surface with a cable, and to run electrical wires, hydraulic lines and a pneumatic line from the surface to the tool. The

- 1 OIL RESERVOIR
- 2 PUMP & ELECTRIC MOTOR
- 3 RELIEF VALVE
- 4 PUMP UNLOADING VALVE
- 5 ACCUMULATOR
- 6 FLOW CONTROL VALVE
- 7 PRESSURE FILTER
- 8 HOSE
- 9 QUICK DISCONNECTS
- 10 SERVOVALVE, MOOG SERIES 30
- 11 MINIATURE HYDRAULIC MOTOR
- 12 DISPLACEMENT TRANSDUCER (ANGULAR)
- 13 TORQUE TRANSDUCER

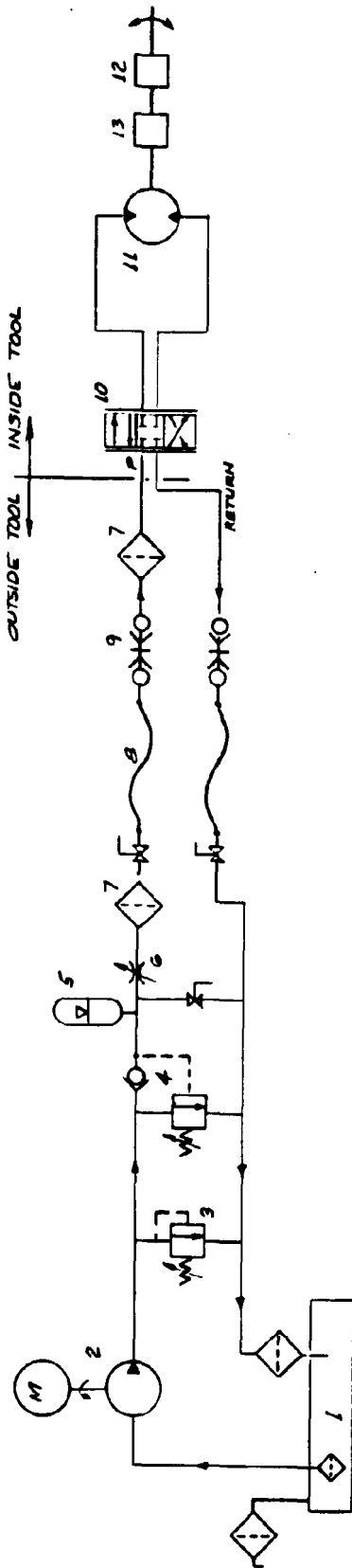


FIG. 3.1 HYDRAULIC CIRCUIT DIAGRAM FOR TORSIONAL DRIVE SYSTEM

REV	DATE	BY	CHKD	APP'D	DESCRIPTION
B	7/23				ADD NOTE
A	6/15/58				PRELIM RELEASE
BOATHMAN ENGINEERS CORPORATION HOUSTON, TEXAS					
SWEET & AIKEN, INC. HYDRAULIC SYSTEM SCHEMATIC					
					531-02

field tool will use a single umbilical with all the wires, hoses, and support cable contained within an overall jacket. There are several local cable companies that routinely manufacture custom cables like this.

For the laboratory prototype a hand made umbilical will be formed by strapping or taping the hoses and electrical wires together.

Electrical noise is a source of potential problem especially while taking small readings when the electrical signals will be very small. It will be necessary to shield all sensor cables and eliminate any sources of electrical noise while testing.

### **3.14 Latching and Penetration Systems**

Based on my experiences, I believe that a drill string latching unit and a controlled-rate penetration system for a field tool will involve only current technology, and thus, should not present any feasibility problems.

### **3.15 Electronic Systems**

Required electronic systems were established by Lionel Milberger, a consultant. His work is discussed in two brief reports given in the Appendix. Cost estimates are included.

#### 4.0 POTENTIAL PROBLEMS

The major source of potential problems is the very small rotations required to be measured by the tool. Based on the study, it was concluded that probably the smallest angular displacement that can accurately be measured with the tool is 0.01 degrees; thus, it seems that the requirements for the torque-controlled cyclic tests cannot be fully satisfied. Rectilinear capacitance transducers and LVDT devices were considered but rejected because they are extremely sensitive to electrical noise and temperature effects. Optical encoders were also considered. A standard optical encoder was not found that would meet the criteria of the in situ test tool. However, an optical encoder could probably be designed that would meet the criteria. This is a very definite possibility for the field units.

#### 5.0 POTENTIAL IMPROVEMENTS

The most important improvement would be replacement of the angular displacement transducer with a transducer that could measure smaller angles. Optical encoders are devices currently under development that might do this. These are relatively small displacement transducers that measure light passing through a perforated target. As the measured displacement changes more or fewer perforations are exposed or covered. The perforations are calibrated to measure

displacement.

Other developments in control and measurement technology, motivated by the robotics industry, may improve tool design. One example is a miniature servovalve/oscillator unit currently being developed by Moog. This would replace both the servovalve and hydraulic motor incorporated in the prototype design. Manufacturer's information on this unit is provided in the Appendix. It is very possible that a single Moog servovalve/oscillator that meets the criteria of the in situ test tool will be available when the field units are designed.

Another improvement which seems to be feasible will be to modify the vertical pressure piston so that it can be at the bottom of the inner barrel prior to penetration and will apply a load to the soil specimen as the tool penetrates.

## 6.0 COST ESTIMATE FOR LABORATORY PROTOTYPE TESTING SYSTEM

Detail Design and Drafting.....	\$16900.00
Machined Components.....	12500.00
Four Pressure Transducers.....	1860.00
Angular Displacement Transducers	
Small Angles.....	1500.00
Large Angles.....	300.00
Two Accelerometers.....	900.00
Hydraulic Components (Including	
Servovalve, Two Motors,	
Controller, and, Misc. Items)....	13000.00
Accessory Electronic Equipment.....	20400.00
Torque Transducers	
High Torque.....	1400.00
Low Torque - 10.....	2300.00
Low Torque - 50.....	2300.00
Two Roller Bearings.....	100.00
Seals.....	50.00
Miscellaneous Hardware.....	350.00
Laboratory Penetration System.....	4400.00
	-----
Total Cost Estimate.....	\$78260.00

## 7.0 CALCULATIONS

WBA  
7/1/85

## 1.0 ANALYSIS OF PENETRATION LOAD STRESSES

### 1.1 PENETRATION LOADS

$F_0$  = MAXIMUM PENETRATION FORCE ON  
OUTER BARREL (AXIAL)

$$F_0 = 14,000 \text{ lbs} \Rightarrow \begin{array}{l} 4500 \text{ lbs FROM BEARING} \\ 9500 \text{ lbs FROM SKIN FRICTION} \end{array}$$

$F_I$  = MAXIMUM PENETRATION FORCE ON  
INNER BARREL (AXIAL)

$$F_I = 4000 \text{ lbs} \Rightarrow \begin{array}{l} 1500 \text{ lbs FROM BEARING} \\ 2500 \text{ lbs FROM SKIN FRICTION} \end{array}$$

### 1.2 AXIAL STRESSES IN BARRELS (LOWER END)

$S_{AI}$  = MAXIMUM AXIAL STRESS IN INNER BARREL

$$S_{AI} = \frac{F_I}{A_{MIN}}$$

$A_{MIN}$  = MINIMUM CROSS SECTIONAL AREA

$A_{MIN}$  OCCURS IN UPPER SECTION COINCIDENT TO  
SHIELD, WHERE

$$D_o = 1.000 \text{ in (OUTSIDE DIA.)}$$

$$D_i = 0.875 \text{ in}$$

$$W_T = 0.0625 \text{ in (WALL THICKNESS)}$$

$$A_{MIN} = \frac{\pi}{4} (1.000^2 - 0.875^2)$$

$$A_{MIN} = 0.1841 \text{ in}^2$$

WST  
7/1/85

1.2

$$S_{AZ} = \frac{4000}{0.1841}$$

$$S_{AZ} = 21,730 \text{ PSI}$$

R = RATIO OF STRESS TO YIELD STRENGTH

$$S_y = 85,000 \text{ PSI} \quad (\text{YIELD STRENGTH})$$

$$R = \frac{21,730}{85,000}$$

$$R = 0.256 \Rightarrow \text{OK}$$

$S_{AO}$  = MAXIMUM AXIAL STRESS IN OUTER BARREL

$$S_{AO} = \frac{F_o}{A_{MIN}}$$

$A_{MIN}$  OCCURS AT LOWER SECTION OF OUTER BARREL  
WHERE,

$$D_o = 3 \text{ in}$$

$$D_i = 2.833 \text{ in}$$

$$W_T = 0.0833 \text{ in}$$

$$A_{MIN} = \frac{\pi}{4} (3^2 - 2.833^2)$$

$$A_{MIN} = 0.765 \text{ in}^2$$

$$S_{AO} = \frac{14,000}{0.765}$$

WGA 1.3  
7/2/95

$$S_{AO} = 18,299 \text{ PSI}$$

$$S_y = 85,000 \text{ PSI}$$

$$R = \frac{18,299}{85,000}$$

$$R = 0.2153 \Rightarrow \text{OK}$$

### 1.3 STABILITY OF BARRELS

$L_c$  = CRITICAL BUCKLING LENGTH

$$L_{cr}^* = \sqrt{\frac{\pi^2 EI}{F}} \Rightarrow \text{CONSERVATIVELY ASSUMES PINNED ENDS}$$

WHERE,

$$E = \text{YOUNG'S MODULUS} = 29 \times 10^6 \text{ PSI}$$

$$I = \text{MOMENT OF INERTIA} = \frac{\pi}{64} (D_o^4 - D_i^4)$$

$$F = \text{AXIAL FORCE}$$

FOR THIN OUTER BARREL

$$I = \frac{\pi}{64} (3^4 - 2.933^4)$$

$$I = 0.0141 \text{ in}^4$$

\* PG 49 OF THEORY OF ELASTIC STABILITY, BY S TIMOSHENKO  
MCGRAW-HILL, 2ND EDITION.

WBA 1.4  
7/2/87

$$L_{CR} = \sqrt{\frac{(\pi)^2 (29 \times 10^6) (0.8141)}{(14,000)}}$$

$$L_{CR} = 129.0 \text{ inches} \gg L = 12 \text{ in}$$

FOR INNER BARREL

$$I = \frac{\pi}{64} (1^4 - 0.875^4)$$

$$I = 0.02031 \text{ in}^4$$

$$L_{CR} = \sqrt{\frac{(\pi)^2 (29 \times 10^6) (0.02031)}{(40000)}}$$

$$L_{CR} = 38.1 \text{ in} > L = 12 \text{ in} \text{ (INNER BARREL LENGTH + SHIELD LENGTH)}$$

∴ BARRELS WILL NOT BUCKLE

1.4 AXIAL STRESS IN SHIELD

$S_A$  = AXIAL STRESS IN SHIELD

$$S_A = \frac{F_z}{A_{MIN}}$$

$A_{MIN}$  = SAME AS INNER BARREL

$$A_{MIN} = 0.1941 \text{ in}^2$$

WBA  
7/3/95

1.5

$$S_m = \frac{4000}{0.1841}$$

$$S_m = 21,727 \text{ PSI}$$

$$S_y = 85,000 \text{ PSI}$$

$$R = \frac{21,727}{85,000}$$

$$R = 0.256 \Rightarrow \text{OK}$$

1.5 BEARING STRESS BETWEEN SHIELD & LOCK PIN

$S_B =$  BEARING STRESS

$$S_B = \frac{F_L}{3A_p} \Rightarrow \text{FACTOR OF 3 FOR 3 PINS}$$

WHERE,

$A_p =$  PROJECTED AREA OF PIN INSERT  
INTO SLEEVE FLANGE (DIAMETER =  $D_p$ )

$$A_p = D_p L$$

$$D_p = 0.200 \text{ in} \quad L_p = 0.080 \text{ in}$$

$$A_p = (0.200)(0.080)$$

$$A_p = 0.0160 \text{ in}^2$$

7/3/95  
WBT

1.6

$$S_B = \frac{4000}{(3)(.0160)}$$

$$S_B = 83,333 \text{ PSI}$$

$$S_y = 85,000 \text{ PSI}$$

$$R = \frac{83,333}{85,000}$$

$$R = 0.980 \Rightarrow \text{OK FOR BRG STRESS}$$

1.6 BEARING STRESS OF LOCK PIN ON OUTER BARREL  
INSERT

$S_B =$  BEARING STRESS

$$S_B = \frac{F_i}{3 A_p}$$

$A_p =$  PROJECTED AREA OF PIN WITH  
DIAMETER  $D_p$  AND ENGAGEMENT  
LENGTH,  $L$

$$D_p = 0.325 \text{ in} \quad L = 0.1 \text{ in}$$

$$A_p = D_p L$$

$$A_p = (.325)(0.1)$$

$$A_p = 0.0325 \text{ in}^2$$

7/3/85  
WBT

1.7

$$S_B = \frac{4000}{(3)(.0325)}$$

$$S_B = 41,026 \text{ PSI}$$

$$S_y = 85,000 \text{ PSI}$$

$$R = \frac{41,026}{85,000}$$

$$R = 0.483 \Rightarrow \text{OK}$$

### 1.8: SHEAR STRESS IN SHIELD LOCK PIN

$S_S$  = SHEAR STRESS IN LOCK PINS

$$S_S = \frac{F_1}{3A_S} \Rightarrow \text{FACTOR OF 3 FOR 3 PIN/INSERT ASSEMBLIES}$$

$A_S$  = CROSS SECTIONAL AREA OF EACH PIN AT NOSE DIAMETER  $D_p = 0.200 \text{ in}$

$$A_S = \frac{\pi}{4} D_p^2$$

$$A_S = \left(\frac{\pi}{4}\right)(.200)^2$$

$$A_S = 0.0314 \text{ in}^2$$

$$S_S = \frac{4000}{(3)(0.0314)}$$

$$S_S = 42,463 \text{ PSI}$$

7/3/25 1.9  
WBT

$$S_y = 140,000 \text{ PSI}$$

$$R = \frac{42,463}{140,000}$$

$$R = 0.303 \Rightarrow \text{OK}$$

1.9 AXIAL STRESS IN TOP OF LOWER BARREL  
(ASSUMES ALL PENETRATING FORCE GOES UP  
THRU BARREL)

$S_A =$  AXIAL STRESS

$$S_A = \frac{F_0 + F_I}{A_{MIN}}$$

$A_{MIN} =$  MIN. CROSS SECTIONAL AREA

$$A_{MIN} = \frac{\pi}{4} (D_o^2 - D_i^2)$$

$$D_o = 3 \text{ in} \quad D_i = 2.7 \text{ in}$$

$$A_S = \frac{\pi}{4} (3^2 - 2.7^2)$$

$$A_S = 1.343 \text{ in}^2$$

$$S_A = \frac{4000 + 14,000}{1.343}$$

$$S_A = 13,403 \text{ PSI}$$

$$S_y = 35,000 \text{ PSI}$$

$$R = \frac{13,403}{35,000} = 0.383 \therefore \text{OK}$$

## 2.0 ANALYSIS OF PRESSURE TO OPEN SHIELD LOCK PINS & RESULTING STRESSES

### 2.1 PRESSURE TO OPEN, $P_2$

$$P_2 = \frac{F_0}{A_R}$$

$F_0$  = FORCE REQUIRED TO COMPRESS RUBBER CYLINDER OF DIAMETER  $D_R$  AND LENGTH  $L_R$  A DISTANCE  $S$

$$D_R = 0.200 \text{ in}$$

$$L_R = 0.15 \text{ in}$$

$$S = 0.08 \text{ in}$$

ASSUMING ELASTIC BEHAVIOR,

$$\frac{F_0}{A_R} = E \frac{S}{L_R}$$

$A_R$  = CROSS SECTION OF RUBBER

$$A_R = \frac{\pi}{4} D_R^2$$

$$A_R = \left(\frac{\pi}{4}\right) (0.200)^2$$

$$A_R = 0.0314 \text{ in}^2$$

$E$  = COMP. MODULUS OF RUBBER

$$E = 1000 \text{ PSI (CONTROLLABLE BY RUBBER TYPE & DIAMETER)}$$

WBA  
7/4/85

2.2

$$F_0 = \frac{(1000)(0.00)(.0314)}{(0.15)}$$

$$F_0 = 16.7 \text{ lbs}$$

$A_p$  = PRESSURE AREA ON INSERT HAVING PRESSURE DIAMETER  $D_p = 0.325 \text{ in}$

$$A_p = \frac{\pi}{4} D_p^2$$

$$A_p = \left(\frac{\pi}{4}\right)(.325)^2$$

$$A_p = 0.0830 \text{ in}^2$$

$$P_F = \frac{16.7}{.0830}$$

$$P_F = 201 \text{ PSI}$$

∴ USE OPENING PRESSURE OF 400 PSI

## 2.2 SHEAR STRESS ON LOCK PIN INSERT THREADS

$S_s$  = SHEAR STRESS IN THREADS DUE TO PRESSURE,  $A_s$

$$S_s = \frac{F_0}{A_s}$$

WHERE,

$F_0$  = PRESSURE FORCE

$$F_0 = P_F A_p$$

WAS  
7/5/95

2.3

$$F_0 = (400)(0.093)$$

$$F_0 = 33.2 \text{ lbs}$$

$A_s$  = SHEAR AREA OF THREAD

$$A_s \geq 0.3 \pi D_T L_T$$

WHERE,

$$D_T = \text{NUM. THRD. DIA.} = 0.5 \text{ in}$$

$$L_T = \text{THTD ENGAGEMENT LENG} = 0.25 \text{ in}$$

$$A_s \geq (0.3)(\pi)(0.5)(0.25)$$

$$A_s = 0.1179 \text{ in}^2$$

$$S_s \leq \frac{33.2}{0.1179}$$

$$S_s \leq 282 \text{ PSI}$$

$$S_y = 35,000 \text{ PSI}$$

$$R = \frac{282}{35,000}$$

$$R = .0081 \quad \text{OK}$$

USA  
2/5/25

2.4

### 2.3 BEARING STRESS BETWEEN SHIELD & OUTER BARREL

$S_B$  = BEARING STRESS

$$S_B = \frac{F_P}{A_B}$$

WHERE,  $F_P$  IS THE AXIAL FORCE CAUSED BY PRESSURE ACTING ON PRESSURE AREA  $A_P$ . BOUNDED BY SEAL DIAMETERS  $D_o$  &  $D_i$ . AND  $A_B$  IS THE BEARING AREA.

$$D_o = 2.4 \text{ in}$$

$$D_i = 1.09 \text{ in}$$

$$A_P = \frac{\pi}{4} (D_o^2 - D_i^2)$$

$$A_P = \frac{\pi}{4} (2.4^2 - 1.09^2)$$

$$A_P = 3.608 \text{ in}^2$$

$$F_P = P_i A_P$$

$$F_P = (400)(3.608)$$

$$F_P = 1443 \text{ lbs}$$

$A_B$  IS AN ANNULAR AREA BOUNDED BY DIAMETERS  $D_o$  &  $D_i$

$$D_o = 2.37 \text{ in}$$

$$D_i = 2.17 \text{ in}$$

WSP  
7/17/25

25

$$A_B = \frac{\pi}{4} (D_o^2 - D_i^2)$$

$$A_B = \frac{\pi}{4} (2.35^2 - 2.19^2)$$

$$A_B = 0.571 \text{ in}^2$$

$$S_B = \frac{1443}{0.571}$$

$$S_B = 2527 \text{ PSI}$$

$$S_y = 35,000 \text{ PSI}$$

$$R = \frac{2527}{35,000}$$

$$R = 0.0722 \Rightarrow \text{OK}$$

#### 2.4 HOOP STRESS IN THIN CYLINDER

$S_H$  = HOOP STRESS DUE TO EXTERNAL PRESSURE,  $P_2$

$$S_H = \frac{P_2 D_o}{2 W_t}$$

WHERE,

$D_o$  = OUTSIDE DIAMETER = 1 in

$W_t$  = WALL THICKNESS = 0.0625 in

$$S_H = \frac{(400)(1)}{(2)(.0625)}$$

$$S_H = -3200 \text{ PSI}$$

WBA  
7/5/95

26

$$S_y = 85,000 \text{ PSI}$$

$$R = \frac{3200}{85,000}$$

$$R = 0.0376 \Rightarrow \text{OK}$$

$\delta$  = RADIAL DEFORMATION DUE TO  $S_H$

$$\delta = \frac{S_H D_o}{2E}$$

$$E = \text{YOUNG'S MODULUS} = 29 \times 10^6 \text{ PSI}$$

$$\delta = \frac{(-3200)(1)}{(2)(29 \times 10^6)}$$

$$\delta = 0.000055 \text{ in} \Rightarrow \text{OK FOR SEALS}$$

2.5 HOOP STRESS IN OUTER BARREL DUE TO  $P_i$

$$S_H = \frac{P_i D_i}{2 W_T}$$

$$D_i = \text{INSIDE DIAMETER} = 2.4 \text{ in}$$

$$W_T = \text{WALL THICKNESS} = 0.32 \text{ in}$$

$$S_H = \frac{(400)(2.4)}{(2)(0.32)}$$

$$S_H = 1500 \text{ PSI}$$

$$S_y = 35,000 \text{ PSI}$$

$$R = \frac{1500}{35,000} = 0.0429 \Rightarrow \text{OK}$$

e47

7/9/87  
WST

3.1

### 3.0 ANALYSIS OF STRESSES DUE TO DIFFERENTIAL LATERAL PRESSURES

#### 3.1 PRESSURE

$\Delta P =$  PRESSURE DIFFERENTIAL ACROSS WALLS OF INNER & OUTER CYLINDERS (POSITIVE TOWARD  $\phi$ )

$$\Delta P_{max} = 30,000 \text{ PSF} = 209 \text{ PSI}$$

#### 3.2 HOOP STRESS IN OUTER BARREL

$S_H =$  HOOP STRESS

$$S_H = - \frac{\Delta P D_o}{2 W_T}$$

$D_o =$  OUTSIDE DIA. = 3.0 in

$W_T =$  WALL THICKNESS = 0.0933 in

$$S_H = \frac{-(209)(3.0)}{(2)(0.0933)}$$

$$S_H = -3744 \text{ PSI}$$

$$S_y = 87,000 \text{ PSI}$$

$$R = \frac{3744}{87,000}$$

$$R = 0.0441 \Rightarrow \text{OK}$$

7/19/95  
WBT

3.2

$\delta =$  RADIAL DISP

$$\delta = \frac{S_H A_0}{2E}$$

$$\delta = \frac{(3744)(3)}{(7)(29 \times 10^9)}$$

$$\delta = 0.000194 \text{ in} \Rightarrow \text{OK}$$

### 3.3 HUMP STRESS IN INNER BARREL

$S_H =$  HUMP STRESS

$$S_H = -\frac{\Delta P A_0}{2W_T}$$

$D_0 =$  OUTSIDE DIAMETER = 1.0 in

$W_T =$  WALL THICKNESS = 0.0625 in

$$S_H = -\frac{(209)(1.0)}{(2)(0.0625)}$$

$$S_H = -1664 \text{ PSI} \Rightarrow \text{OK}$$

4.0 ANALYSIS OF ALLOWABLE SHEAR AND BENDING ON INNER BARREL WITH SHIELD ENGAGED

$F_s$  = ALLOWABLE SHEAR ON EACH SUPPORT SURFACE OF SHIELD

$$F_s = S_B A_P$$

WHERE,

$S_B$  = ALLOWABLE BEARING STRESS ON PROJECTED AREA

$$S_B = 0.25 S_y \Rightarrow \text{CONSERVATIVE}$$

$$S_B = (0.25)(85,000)$$

$$S_B = 21,250 \text{ PSI}$$

$A_P$  = PROJECTED AREA

$$A_P = D_c L_c$$

$$D_c = \text{CONTACT DIAMETER} = 0.95 \text{ in}$$

$$L_c = \text{LENGTH OF CONTACT SURFACE} = 0.09 \text{ in}$$

$$A_P = (0.09)(0.95)$$

$$A_P = 0.068 \text{ in}^2$$

$$F_s = (21,250)(0.068)$$

$$F_s = 1445 \text{ lbs}$$

WBA  
7/23/05

4.

M = ALLOWABLE BENDING MOMENT ON  
INNER BARREL

$$M = F_s L_w$$

WHERE,

$L_w$  = DISTANCE BETWEEN SHIELD CONTACT  
POINTS

$$L_w = 7.9 \text{ in}$$

$$M = (1445)(7.9)$$

$$M = 11416 \text{ in-lbs} = 951 \text{ FT-lbs}$$

WPA  
7/24/95

S.

## S.O. FRICTIONAL RESISTANCE OF LIP SEAL

$T_s$  = TORSIONAL RESISTANCE OF PARKER SEAL

$$T_s = F_R R_s$$

WHERE,

$F_R$  = RADIAL FORCE OF SEAL ON COUPLER

$R_s$  = SEAL I.R. = 0.875 in

$$F_R = 2\pi R_s W \Delta P \mu_s$$

WHERE,

$\Delta P$  = PRESSURE DROP ACROSS SEAL = 10 PSI

$W$  = CONTACT WIDTH BETWEEN SEAL LIP & COUPLER

$W \leq 0.03$  in

$\mu_s$  = COEF. OF FRICTION BETWEEN SEAL  
& COUPLER  $\approx 0.08$

$$F_R = (2\pi)(.875)(.03)(10)(.08) = 0.1319 \text{ lbs}$$

$$T_s = (0.1319)(.875) = 0.1155 \text{ in-lbs} = 0.0096 \text{ ft-lbs}$$

**APPENDIX - SUPPLEMENTARY DOCUMENTS**

## TECHNICAL PRODUCTS, INC.

10219 HEDGEWAY DRIVE  
DALLAS, TEXAS 75229  
214-357-9603

1710 DAIRY ASHFORD, SUITE 205  
HOUSTON, TEXAS 77077  
713-493-6520

July 10, 1985

Mr. William B. Aiken, P.E.  
Sweet & Aiken, Inc.  
13810 Champion Forest Drive  
Suite 235  
Houston, TX 77069

Dear Mr. Aiken:

Confirming our past conversations, Trans-Tek will be able to furnish a modified 600 Series angular displacement transducer on a state of the art best effort basis.

The proposed specifications are nominal values which we believe are attainable at a reasonable cost.

SENSITIVITY: 100 millivolts per 0.01 degree  
RANGE: + 0.5 degrees  
OUTPUT: + 5 volts  
POWER: + 15 volts at approximately 30 milliamps

The transducer will not have an electrical zero adjustment on the transducer. Zero output will have to be achieved by the mechanical position of the transducer. Because of the high sensitivity of this device the success of your application will depend on whatever degree of mechanical isolation from extreneous loads your fixture will allow. We also understand that the transducer will not be subject to extremes of temperature, humidity, electromagnetic interference, shock or vibration.

The unit price for this transducer will be approximately \$1500.00 including all materials, calibration, and special engineering charges. Shipment should be about 12 weeks after receipt of a firm order. Should you have any further questions, please do not hesitate to contact us.

Best Regards,



Michael B. Stone

# REACTION TORQUE SENSORS — GENERAL PURPOSE — continued

## Low capacity torque sensors.



Model 2105

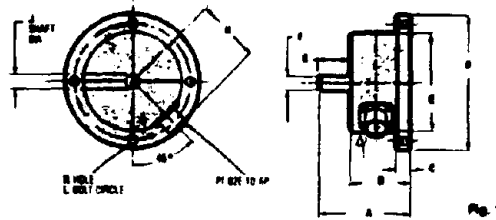
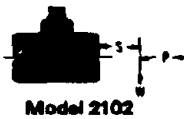


Fig. 1

	A	B	C	D	E	F	G	H	J	K	L	M
2105	2 1/2	1 1/2	3/4	3.491	2 1/2	3/4	3/4	1 1/2	3 7/8	7/8	3.062	45°



Model 2105

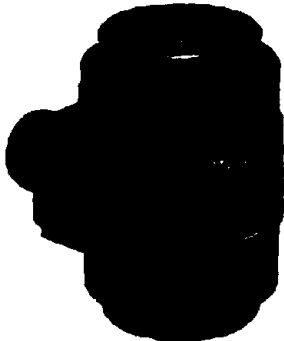


Model 2102

### LOAD CARRYING CAPACITY

W = weight of test device      S = distance to center of gravity of test unit  
W x S = overhung moment  
Do not exceed moment (W x S) or shear (W), whichever value is attained first. P = thrust.

## Small flanged reaction torque sensors.



Model 2102

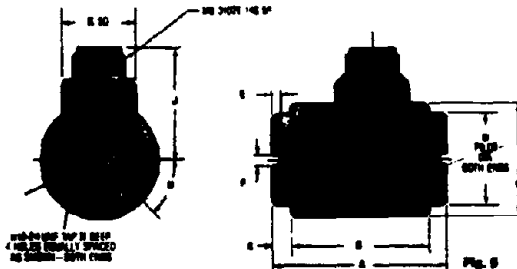


Fig. 2

	A	B	C	D	E	F	G	H	J	K	L	M
2102	3	2 3/4	2	1.625	3/4	2 1/2	3/4	45°	2	1 1/4	1.250	3/4

Specifications	Standard	"H" Option*	Specifications	Standard	"H" Option
Output at rated capacity: millivolts per volt nominal	2 to 2.5	5	Temperature range, useable: °F	-65 to +200	-65 to +200
Nonlinearity: of rated output	±0.1%	±0.15%	Temperature range, useable: °C	-18 to +93	-18 to +93
Hysteresis: of rated output	±0.1%	±0.15%	Temperature effect on output: of reading per °F	±0.002%	±0.003%
Repeatability: of rated output	±0.05%	±0.07%	Temperature effect on output: of reading per °C	±0.0036%	±0.0036%
Zero balance: of rated output	±1.0%	±1.0%	Temperature effect on zero: of rated output per °F	±0.002%	±0.003%
Bridge resistance: ohms nominal	350	350	Temperature effect on zero: of rated output per °C	±0.0036%	±0.0036%
Temperature range, compensated: °F	+70 to +170	+70 to +170	Excitation voltage, maximum: volts DC or AC rms	20	20
Temperature range, compensated: °C	+21 to +77	+21 to +77	Insulation resistance, bridge/case: megohms at 50 VDC	>5000	>5000
Number of bridges	1	1			

44 METRIC DIMENSIONS AND SPECIFICATIONS ARE PURELY MATHEMATICAL CALCULATIONS FROM STANDARD ENGLISH DIMENSION CONTROL DRAWINGS. REQUEST CERTIFIED DRAWINGS BEFORE DESIGNING MOUNTINGS OR FIXTURES. DIMENSIONS AND SPECIFICATIONS ARE SUBJECT TO CHANGE WITHOUT NOTICE.

e55

- FEATURES**
- Reaction measurements eliminate speed limitations
  - Minimal friction error
  - No maintenance of slip rings, bearings, or brushes
  - Compact "low mass" physical size

Model No.	Capacity Oz. In.	Dimensions	Over-Load	Torsional Stiffness	Max. OverTemp Moment W x S	Max. Shear W	Max. Thrust - P
			Oz. In.	Oz. In./Rad*	Oz. In.	Oz.	Oz.
2105-50	50	See Figure 1	75	12,800	100	100	320
2105-100	100		150	18,000	150	220	640
2105-200	200		300	61,500	200	350	880
2105-500	500		750	95,500	250	400	1,600
2105-1000	1,000		1,500	258,000	400	480	2,400

\*NOTE: Torsional stiffness given for sensor less shaft extension(s).

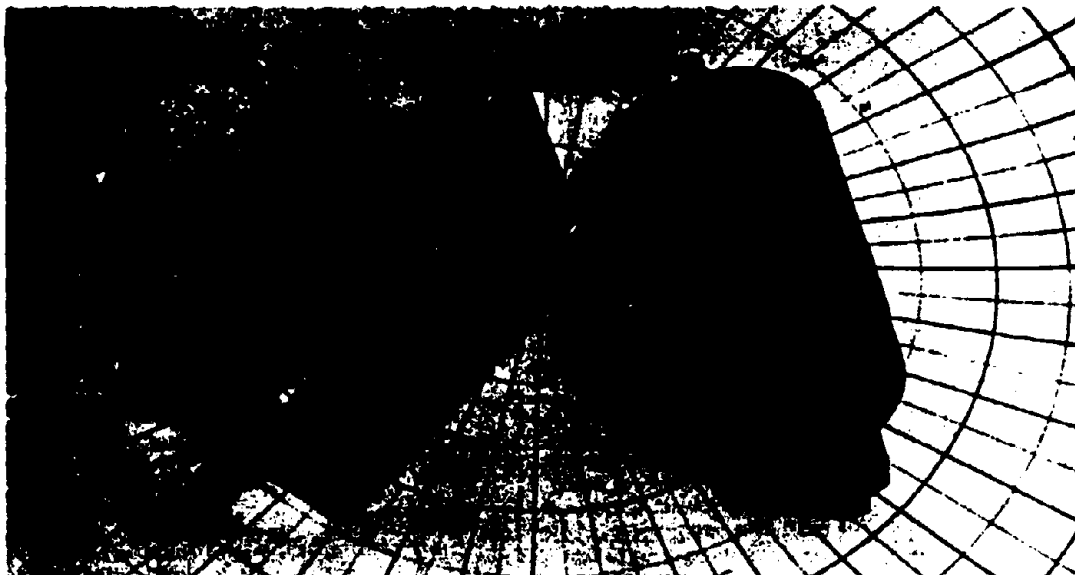
Model No.	Capacity Lbs. In.	Dimensions	Over-Load	Torsional Stiffness	Max. OverTemp Moment W x S	Max. Shear W	Max. Thrust - P
			Lbs. In.	Lbs. In./Rad.	Lbs. In.	Lbs.	Lbs.
2102-50	50	See Figure 5	75	2,300	50	13	200
2102-100	100		150	6,725	100	20	280
2102-200	200		300	18,500	200	28	400
2102-500	500		750	73,500	250	500	500
2102-1K	1,000		1,500	127,000	500	800	680

• SAFETY CONSIDERATIONS: It would be unsafe to operate Eaton® Torque Sensors and Load Cells beyond their Overload or Ultimate Simultaneous Load Limits as defined on page 111 in the Glossary of Terms or, when available, higher than maximum speed. When in doubt consult the factory. Eaton Corporation is not responsible for any property damage or personal injury which may result because of the misapplication of the Transducer.



## ANGULAR DISPLACEMENT TRANSDUCER

SERIES 604



### FEATURES

- $\pm 0.25\%$  zero base — terminal linearity
- 60° linear range
- DC in, DC out
- 100 mv output per degree of rotation
- Infinite resolution
- Precision ball bearings for long life
- Built in voltage regulator
- Can be battery excited
- Shaft rotational speed up to 3000 rpm

### THEORY

Series 604 Angular Displacement Transducers (ADT's) are precision differential capacitors with integral voltage regulation, oscillator, demodulator and output buffer amplifier. The angular position of the shaft is converted into a DC voltage directly proportional in amplitude and polarity to displacement from the electrical null position.

### EASE OF USE

After mechanical installation, connect the transducer to a dual polarity power supply. The 604 series internal voltage regulator allows it to operate from widely ranging, unregulated voltage sources or regulated ones, such as Trans-Tek's D15-100. The high level, DC output can be fed directly into voltmeters, recorders, A/D converters or other devices. The standardized output allows interchanging units without system recalibration.

### APPLICATIONS

Series 604 ADT's are ideal for use in:

- Servo position feedback
- Rotary actuators
- Robotic wrist and elbow position
- Rotary valves, throttle and antenna position
- Torque displacement
- Inclinometers, vertical references
- Positioning optical devices
- Web or film tension control

### CONSTRUCTION

Optimum performance and reliability is obtained by our selection of components and factory calibration. Mechanical parts are machined to exacting tolerances from stable materials and are corrosion protected where required. The shaft is supported by ball bearings for low torque, resistance to side load and to insure a long life.

### INSTALLATION

The precision pilot diameter and tapped mounting holes on the base plate are provided for quick installation. Once mounted, approximate mechanical zero is established by aligning the mark on the shaft midway between the zero and span controls on the cover. The electrical zero adjustment can then be used to correct for small offsets. Electrical connections are via terminal strip, eliminating the need for mating connectors or terminal lugs.

## ELECTRICAL SPECIFICATIONS

MODEL NO.	LINEAR <sup>(1)</sup> DISPL. RANGE	MAX. NON-LIN. <sup>(2)</sup> LINEAR RANGE	USABLE DISPL. RANGE	MAX. NON-LIN. USABLE RANGE	OUTPUT SENSITIVITY	TYP. TEMP. COEF. OF SPAN
0604-0000	± 30°	± 0.25 %	± 35°	± 1.0 %	100mVDC/°	< ± 0.01 % Output/°F
0604-0001	0 to 60° CW	± 0.25 %	- 5° to + 65° CW	± 1.0 %	100mVDC/°	< ± 0.01 % Output/°F
0604-0002	0 to 60° CCW	± 0.25 %	- 5° to + 65° CCW	± 1.0 %	- 100mVDC/°	< ± 0.01 % Output/°F

(1) CW defined as clockwise direction of shaft rotation, when viewed from shaft end.

(2) Zero base terminal average, expressed as max % deviation of total range.

POWER SUPPLY	VOLTAGE	± 14.5 to ± 30VDC unregulated, input polarity protected.	REPEATABILITY	< .02% of range.
	CURRENT	± 20maDC maximum when load current is less than ± 5maDC.	RESOLUTION	Infinite.
OUTPUT	VOLTAGE	Factory calibrated to deliver 100mVDC per degree of rotation unless otherwise ordered.	ZERO CONTROL	10% of total linear range via multi turn pot.
	CURRENT	Load can draw up to ± 5maDC without significant effect on non-linearity; Output is protected against short circuits to power supply lines (50maDC max. short circuit current).	SPAN CONTROL	20% range via multi turn pot.
	RIPPLE	Max. peak-to-peak ripple voltage is 0.5% of total DC voltage over linear range; ripple is at 500KHz nom.	ANGULAR VELOCITY	2% max. attenuation of signal when operating at 10,000°/second.
	IMPEDANCE	Less than 1 ohm when output current is less than ± 5maDC.		

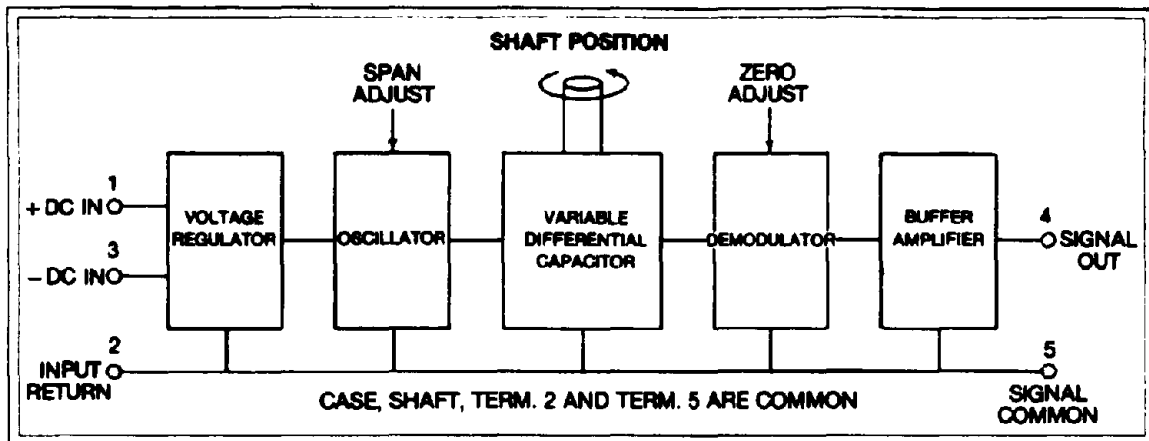
## MECHANICAL SPECIFICATIONS

DISPLACEMENT RANGE	Continuous; there are no stops.	TEMPERATURE	
TORQUE STARTING	5 gram-cm maximum.	OPERATING	0°-70°C
	3.5 gram-cm maximum.	STORAGE	- 55° to + 125°C
MOMENT OF INERTIA (SHAFT)	0.6 gram-cm <sup>2</sup>	MOUNTING	Any position, gravity insensitive
LOAD RADIAL	10 lbs. maximum.	NET WEIGHT	4.3 oz. (120 grams)
	7 lbs. maximum.		
BEARING LIFE ex: 17,000 hours expected at 10 RPM with 10 lb. radial load at shaft end.			

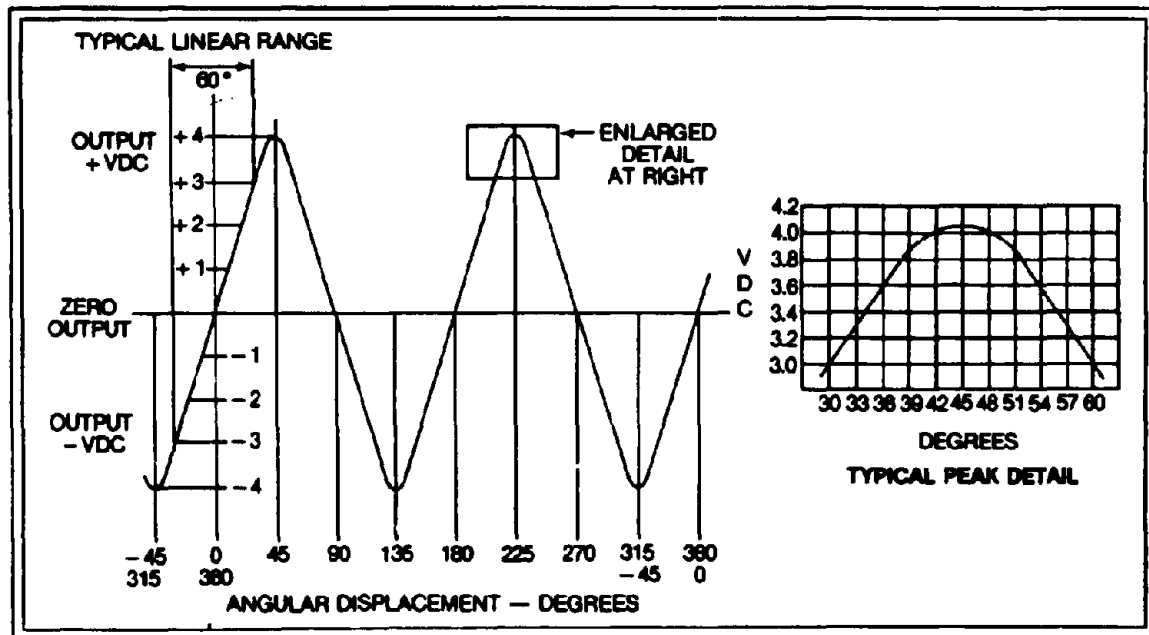
### OPTIONS:

The following options are available at added cost at time of purchase.

1. Factory calibrated to any specified output sensitivity, output voltage limited to ± 8VDC.
2. Calibrated for inverse slope; standard output with reversed shaft rotation.
3. Operation over - 55°C to + 125°C, weight increases to 7.4 oz. (210 grams).



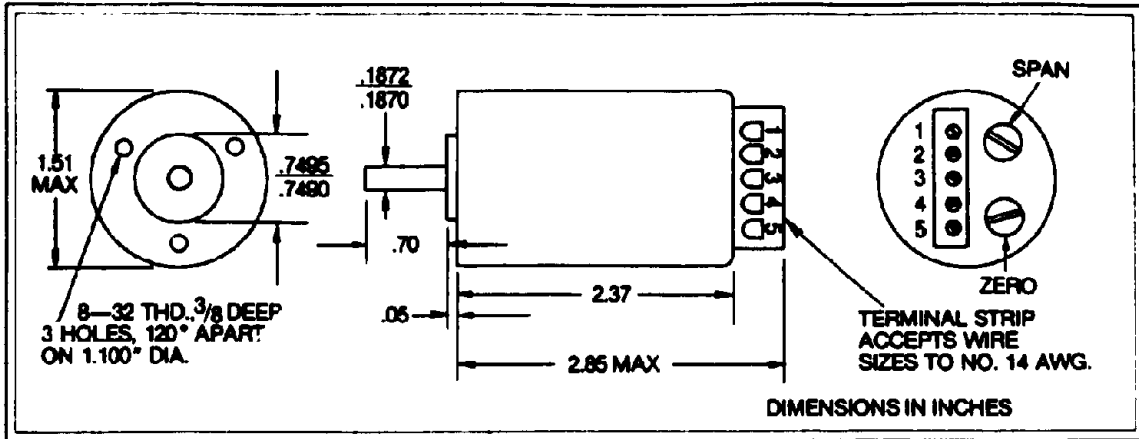
**CIRCUIT BLOCK DIAGRAM**



**OUTPUT FUNCTION**

The illustration above is a plot of output voltage versus shaft position for Model 0604-0000. By definition the output is 0 VDC at the zero position. Rotating the shaft CW provides a positive voltage proportional to the angular displacement from the zero position. CCW rotation from the zero position produces a negative voltage, again proportional to the shaft's position in relation to 0°. The 0604-0001 is designed to provide a 0 to +6 VDC output proportional to a 0° to 60° CW rotation, Model 0604-0002 gives a 0 to -6 VDC output proportional to a 0° to 60° CCW rotation.

# DC-DC ADT



DIMENSIONAL DIAGRAM

## WIRING

TERMINAL	FUNCTION
1.	+ DC input
2.	Input return
3.	- DC input
4.	Signal output
5.	Signal common

NOTE: Case, shaft, and terminals 2 & 5 are common

## CALIBRATION

This Model 0604 ADT has been factory calibrated as noted below. User should check calibration before placing instrument in service. To check calibration, or to recalibrate, proceed as follows:

1. Secure the housing and shaft to a suitable test rig.
2. Power the ADT and allow a 10 minute warmup.
3. Rotate the shaft to the zero position (coarsely identified by aligning mark on end of shaft between zero and span access holes.)
4. The span pot is used to adjust the output for  $6.000 \pm 0.001$  VDC difference between the  $-30^\circ$  and  $+30^\circ$  or  $0^\circ$  and  $60^\circ$  positions, depending on the model. Units ordered with special zero and sensitivity values should be calibrated to these.

## INSTALLATION

The ADT should be mounted and bolted in position with due care taken to avoid damage to the precision ball bearings. Rotate the shaft to the proper zero position, coarsely identified by aligning mark on shaft end to be between ZERO and SPAN controls. After powering the ADT, set the mechanism to be monitored at its zero position, and then lock the ADT shaft to the rotating mechanism. Small misalignments between the ADT zero position and the mechanism zero position can be eliminated by using the ADT ZERO control.

## MODIFICATIONS

Transducers for special applications are available. Consult TRANS-TEK, Incorporated on your particular requirement.

TELEX 9-9207 (TRANS TEK ELLG)

Printed in U.S.A.

## CALIBRATION RECORD

This section will be completed during final inspection.

Model No. \_\_\_\_\_ Date Code \_\_\_\_\_

Serial No. (optional) \_\_\_\_\_

Calibration Temperature \_\_\_\_\_ °F

Calibrated to deliver 0.1000 VDC per degree of rotation with input power  $\pm 14.5$  to  $\pm 15.5$  VDC unless otherwise noted below.

Special Calibration (optional) \_\_\_\_\_

Unit is supplied with following options (checked if applies):

- 1. Special Sensitivity \_\_\_\_\_  
Zero Offset \_\_\_\_\_
- 2. Calibrated for Inverse Slope.
- 3. For  $-55^\circ\text{C}$  to  $+125^\circ\text{C}$  Operation.

## NOTES

All specifications are subject to change without notice. Contact TRANS-TEK for quantity discount prices available on all models. (For areas beyond the United States — contact the international representative)

## ORDER PLACEMENT

Orders should be made out to TRANS-TEK, Incorporated, sent in care of your local TRANS-TEK representative, or directly to Box 338, Ellington, Connecticut 06029.

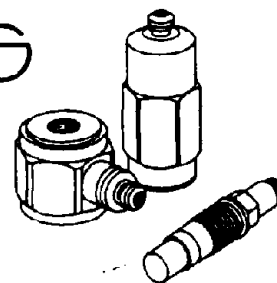
## WARRANTY

All TRANS-TEK transducers are warranted against defective materials and workmanship for one year.

**TRANS-TEK**  
INCORPORATED

Box 338, Route 83, Ellington, Connecticut 06029 (203) 872-8351

# Quartz sensors



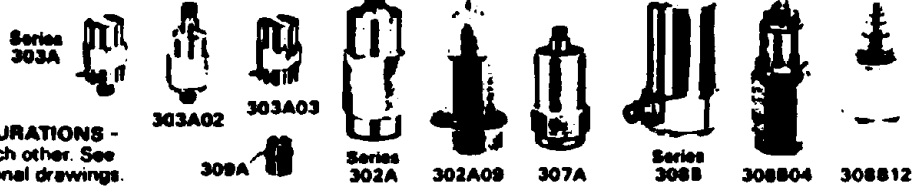
**PCB PIEZOTRONICS, INC.**  
3425 WALDEN AVENUE  
DEPEW, NEW YORK 14043-2495  
TELEPHONE 716-684-0001  
TWX 710-263-1371

**ICP QUARTZ  
ACCELEROMETERS**

with built-in amplifiers<sup>(1)</sup>

**Series 300**

**STANDARD DESIGN CONFIGURATIONS -**  
Photos are not proportional to each other. See  
page following chart for dimensional drawings.



Application	MINIATURE, LOW MASS					GENERAL PURPOSE - HIGH									
	Std Mtg Side Conn	Std Mtg Top Conn	Adv Mtg Side Conn	High Sens 100 mV/g	Out-Grav Weight	Low Strain	Gold In. Lo Strain	Gold In. 10K	Integrat <sup>W</sup> Mag Base 0 Strain	W Sens Lo Mass Gold In	High Sens	High Freq Low Mass	Side Connector		
Model Number (see optional models below specifications)	303A	303A02	303A03	303A11	303A	302A	302A04	302A06	302A09	308B15	308B3	307A	308B	308B3	
Sensitivity Peak <sup>(2)</sup> mV/g	10	10	10	100*	5	10±2%	10±2%	10±2%	10±2%	100±2%*	300±2%*	100±5%*	100±2%	50±2%	
Range (for ±5V out) ±gpk	500	500	500	10 (±1V)	1000	500	500	500	100 (±1V)	50	18	50	50	100	
Range (for ±10V out) <sup>(1)</sup> ±gpk	—	—	—	—	—	1000	1000	1000	—	—	32	100	100	200	
Resolution gpk	01	01	01	005*	02	01	01	01	005	001	0025	005	001	002	
Resonant Freq (mtg) >kHz	70	100*	70	70	120*	45	45	45	20	25	20	>40	25	25	
Freq Range ±5% <sup>(1)</sup> Hz	1 to 10000	1 to 10000	1 to 10000	5 to 10000	5 to 10000	1 to 5000	1 to 5000	1 to 10000	1 to 5000	1 to 3000	1 to 5000	2 to 10000	1 to 3000	1 to 3000	
Freq Range ±10% <sup>(1)</sup> Hz	7 to 20000	7 to 20000	7 to 20000	3 to 20000	7 to 20000	7 to 10000	7 to 10000	—	7 to 10000	7 to 6000	7 to 7000	1.3 to 15000	7 to 6000	7 to 6000	
Overload Recovery μs	10	10	10	10	10	10	10	10	10	10	10	10	10	10	
Discharge Time Constant <sup>(2)</sup> @ 70°F >s	0.5	0.5	0.5	0.2	0.1	0.5	0.5	0.5	0.5	0.5	0.2	0.3	0.5	0.5	
Amplitude Linearity (zero based best straight line) %	1	1	1	1	1	1	1	1	1	1	1	1	1	1	
Output Impedance <ohm	100	100	100	100	100	100	100	100	100	100	100	100	100	100	
Transverse Sens (max) %	5	5	5	5	5	5	5	5	5	5	5	5	5	5	
Strain Sens g/μm/m	05	05	05	05	.005	01	01	01	0*	05	01	1	05	05	
Temperature Range <sup>(4)</sup> °F	-40 to +200	-40 to +200	-40 to +200	-40 to +120	-40 to +150	-100 to +250	-100 to +250	-100 to +250	-100 to +250	-100 to +250	-85 to +175	-100 to +250	-100 to +250	-100 to +250	
Temp Coefficient %/°F	03	03	03	03	05	03	03	03	03	03	03	03	03	03	
Vibration (max) ±gpk	1000	1000	1000	500	1000	2000	2000	2000	1000	1000	100	500	500	1000	
Shock (max) gpk	2000	2000	2000	1000	2000	5000*	5000*	5000	2000	10000	5000	5000	5000*	10000	
Structure (vs. compression)	upright	upright	upright	upright	upright	inverted	inverted	inverted	inverted	upright	inverted	upright	upright	upright	
Size (dia x height) in	.281 x .48	.281 x .61	.281 x .48	.281 x .48	.23 dia x .30	.50 x 1.3	.50 x 1.3	.50 x 1.3	.50 x 1.5	.75 x 1.10	.562 x 1.01	.625 x 1.50	.75 x 1.32	.75 x 1.07	
Weight gm	2*	2.3*	1.9*	2*	1*	25	25	25	38	55*	39*	31	87	55	
Connector	integrat <sup>W</sup> 10' cable	5-44 micro	integrat <sup>W</sup> 10' cable	integrat <sup>W</sup> 10' cable	integrat <sup>W</sup> 8' cable	10-32	10-32	10-32	10-32	10-32	10-32	10-32	10-32	10-32	
Case Material	SS 316	316	316	316	316	316	316	316	316	SS	316	SS	SS	SS	
Sealing	epoxy	epoxy	epoxy	epoxy	epoxy	epoxy	epoxy	epoxy	epoxy	hermetic	hermetic	hermetic	epoxy	epoxy	
Ground Isolation <sup>(5)</sup>	no	no	no	no	no	no	yes	yes	no	yes	no	yes	no	no	
OPTIONAL MODELS (see specific data sheets)				303A13 adhesive mount		302A07 low phase		302A05 non-iso		308B14 low cost non-iso non-herm			308B03 308B10	308B11 hermetic sealed	

NOTES: (\* denotes exceptional characteristic)  
 (1) PCB power units provide 2 to 20 mA from +18 to -28V DC supply. For 10V output, +24 to +28V DC is required. For driving cables longer than 100 ft, use 4 mA.  
 (2) Discharge time constant relates to low frequency response per chart and to transient events lasting up to several percent of discharge TC. For half sine events, discharge TC should be 25 times event duration. Use 4848 or 484802 Series power units to utilize the full transducer discharge TC.  
 (3) Standardized to tolerance indicated nominal otherwise.  
 (4) Special cryogenic models operate to -440°F. Special high temperature to +325°F.  
 (5) Supplied with attached 10 ft ribbon wire termination 10-32 panel connector.



393C



328B



306A



306A06

Series 306A



301A Vibration Calibration Std in 394A03 System (see specific data sheet)

**PCB**  
PIEZOTRONICS

**MOTION**  
shock & vibration

12

H	SENSITIVITY					INDUSTRIAL		TRIAxIAL			SHOCK					
	Top Case Gnd In	High Temp ±325°F	2nd Order LP Filter & Built-in	Seismic		Low Strain	Horn & Seal Gnd In	One Inch Cube	5/8" & Inch Cube	Three 303A's on Block	General Purpose	High g, Low Mass				
	306B12	306006	306036	306002	393C	306004	328B	306A	306A06	303A06	303A02	306A	306A02	306A03	306A04	
%	100 ±5%	100 ±2%	100 ±2%	1000 ±5%	1000	100 ±2%	100 ±5%	10 ±2%*	10	10	10 ±2%	05	1	5	1	
	50	50	50	5	2.5 ±2.5V	50	50	500	500	500	500	100 000*	50 000	10 000	5000	
	100	100	100	10	—	100	100	1000	—	—	1000	—	100 000	20 000	10 000	
	001	001	001	0005	0001*	001	001	01	02	01	01	2	1	2	1	
	30	25	25	25	3.5	25	18	8	28	7	45	60	60	60	60	
	1 to 3000	4 to 3000	1 to 20	2.5 to 3000	025 to 800*	2 to 5000	1 to 3000	1 to 1000	1 to 3000	1 to 1000	05 to 5000	25 to 8000	25 to 8000	25 to 8000	25 to 8000	
	7 to 5000	2 to 6000	7 to 24	1.5 to 5000	01 to 1200	1.3 to 7000	7 to 5000	7 to 3000	7 to 10 000	—	03 to 10 000	1 to 12 000	1 to 12 000	1 to 12 000	1 to 12 000	
	10	10	10	10	10	10	10	10	10	10	10	10	10	10	10	
	0.5	0.2	0.5	0.2	20	0.5	0.5	0.5	0.5	0.5	10	2.0	2.0	2.0	2.0	
	1	1	1	1	1	1	1	1	1	1	1	1	1	1	1	
	100	100	100	100	10 <sup>6</sup>	100	100	100	100	100	100	100	100	100	100	
	5	5	5	5	5	5	5	5	5	5	5	5	5	5	5	
	05	05	05	05	001	01	1	01	05	01	01	2	2	2	2	
to	-100 to +250	-100 to +325*	-100 to +250	-65 to +175	-100 to +200	-100 to +250	-50 to +250	-100 to +250	-100 to +250	-100 to +200	-100 to +175	-100 to +250	-100 to +250	-100 to +250	-100 to +250	
	03	03	03	03	03	03	05	03	03	03	03	03	03	03	03	
	200	500	500	100	100	500	500	1000	1000	1000	2000	100 000	75 000	20 000	10 000	
	5000	5000	5000	200	100	5000	5000	2000	2000	2000	5000	125K anal 30K trans	100K anal 30K trans	50K anal 30K trans	20K anal 20K trans	
	upright	inverted	upright	upright	upright	inverted	upright	inverted	inverted	upright	inverted	inverted	inverted	inverted	inverted	
	75 x 1.73	75 x 1.07	75 x 1.32	75 x 1.32	2.2 dia x 2.2	75 x 2.0	1.0 dia x 2.5	1.0 cube	825 cube	86 cubic envelope	50 x 1.3	312 x 68	312 x 68	312 x 68	312 x 68	
	60	55	95	65	1000	97	180	130	17*	22*	25	4*	4*	4*	4*	
	10-32	10-32	10-32	10-32	10-32	5/16-32 Con-hex	10SL* 4P-20-0A	10-32	integral 8' cable	integral & 10' cable	10-32	10-32	10-32	10-32	10-32	
	SS	SS	SS	SS	SS	SS	316	316	titanium	SS	316	17-4PH	17-4PH	17-4PH	17-4PH	
	hermetic	hermetic	epoxy	epoxy	hermetic*	hermetic	hermetic*	epoxy	epoxy	epoxy	epoxy	epoxy	epoxy	epoxy	epoxy	
	yes*	no	no	no	yes*	no	yes*	no	no	no	no	no	no	no	no	
	306B13 50mV/g		306B31-34 50-100-200 & 500 Hz			306006 base iso		306A02 shock		303A07 100mV/g				306A12	306A13	306A14
														built in second order 10K LP filter		

(6) Accessory isolation pads and studs are available

(7) Calibration furnished to 5% optional calibration available to 10% frequency range

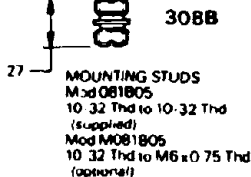
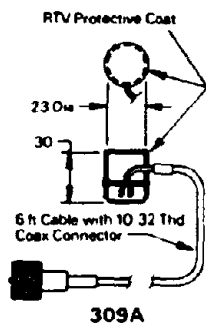
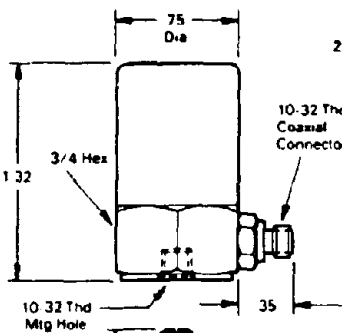
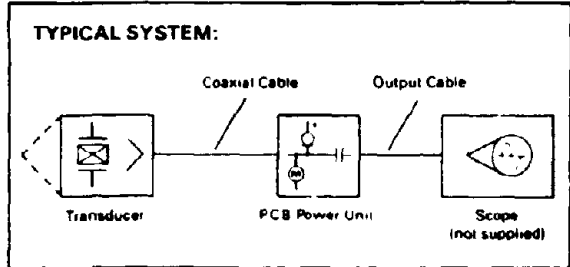
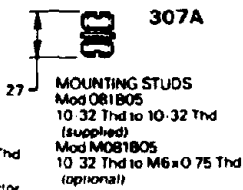
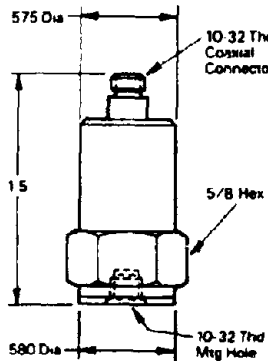
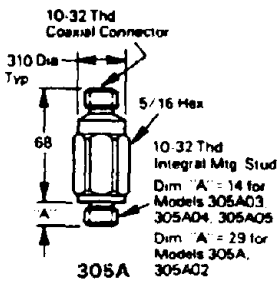
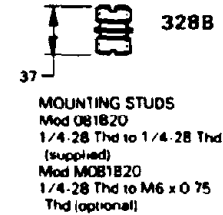
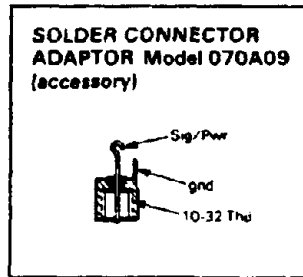
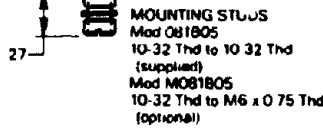
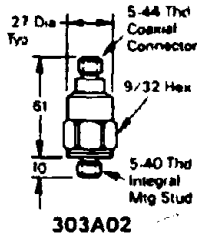
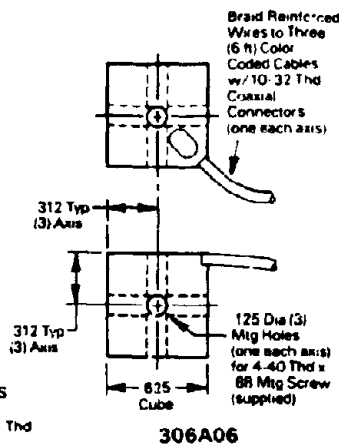
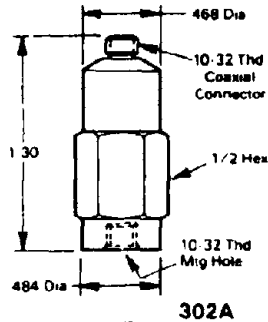
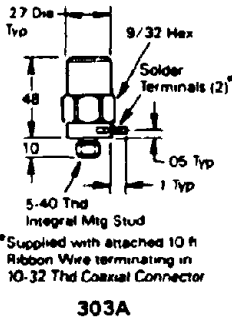
(8) Field repairable solder terminal connection

OPTIONS: Special sensitivities, ranges, electrical isolation, hermetic sealing, low and high pass filtering, case pressure insensitivity, lower frequency response, longer discharge TC, biased and limited output, lower noise, lower temperature electronics to -440°F or higher temperature to +325°F, conventional charge output, solder connector adaptor and thermal jackets

N B S TRACEABLE CALIBRATION CERTIFICATE IN COMPLIANCE WITH MIL STD 45662 FURNISHED WITH EACH ACCELEROMETER

004

**TRANSDUCER CONFIGURATION DIMENSIONS:**  
See specific data sheet for transducers not shown.



**TYPICAL KIT:**

Includes accelerometer, 10 ft input cable, power supply, and 3 ft output cable in a convenient carrying case.

Designate and order as follows

For battery power kit add 'K' to accelerometer Model No. (e.g. K302A).

For line power kit add 'KL' to accelerometer Model No. (e.g. KL302A).

Special length cables to 50 ft supplied in kits at no additional charge, if specified.

**Typical Kit**

MINIATURE 2 GRAM  
**QUARTZ ACCELEROMETER**  
 Series 303A

**PCB**  
 PIEZOTRONICS

**MOTION**  
 shock & vibration

with built-in microelectronics & 10 mV/g sensitivity

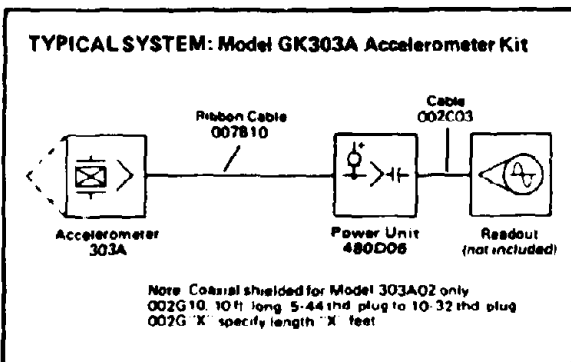
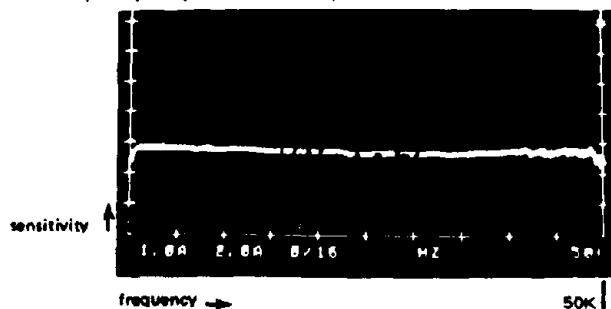
Measure shock and vibration in applications requiring small size, low mass or very high frequency response.

Series 303A Quartz Accelerometers function to transfer shock and vibratory motion into high-level, low-impedance (100 ohm) voltage signals compatible with readout, recording or analyzing instruments. These tiny sensitive (10 mV/g) sensors operate reliably over wide amplitude and frequency ranges under adverse environmental conditions.

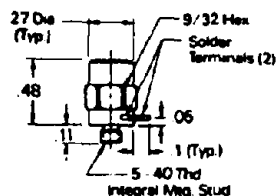
They are structured with permanently polarized compression-mode quartz elements and a microelectronic amplifier housed in a lightweight metal case. Three different case and connector configurations give you a choice in mounting and cabling. The built-in electronics operate over a coaxial or two-conductor cable; one lead conducts both signal and power. Solder terminal versions are normally supplied with a ribbon wire cable (10 ft. long; Model 007B10) attached. Model 303A02 requires Model 002G coaxial cable with a Micro 5-44 connector on one end.

Test results of the behavior of the Model 303A are presented below. Note especially the sharp clean signals free of cable noise and the exceptionally high frequency response. Because of the low mass, Series 303A sensors measure motion of many light structures without appreciably changing the structure or behavior of the test object during the measuring transaction.

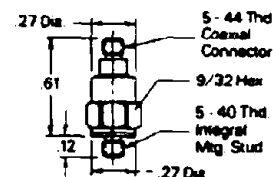
Frequency Response (mounted)



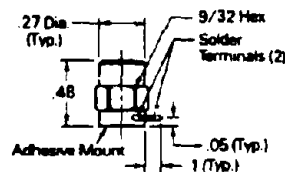
303A  
 Supplied with attached 10' ribbon wire terminating in 10-32 Micro connector



303A02



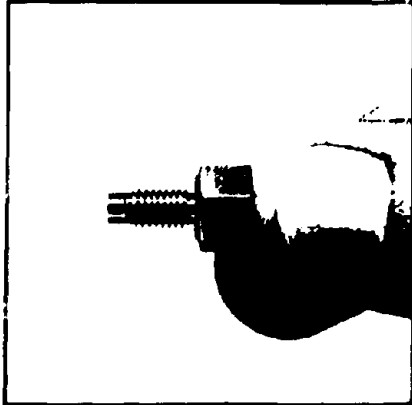
303A03  
 Supplied with attached 10' ribbon wire terminating in 10-32 Micro connector



SPECIFICATIONS: Model No.	303A & 303A03
Range (for ±5 output)	g ±500
Resolution	g 0.01
Sensitivity (nominal)	mV/g 10
Resonant Frequency (mounted)	kHz 70
Frequency Range (±5%)	Hz 1 to 10000
Discharge Time Constant	sec 1
Linearity	% 1
Output Impedance	ohm 100
Output Bias (nominal)	V 11
Overload Recovery	microsec 10
Transverse Sensitivity (max.)	% 5
Strain Sensitivity	g/μin/in 0.05
Temperature Coefficient	%/°F 0.03
Temperature Range (operational to +250°F)	°F -40 to +200
Vibration	g ±1000
Shock (protected)	g 2000
Size (hex. x height)	in 0.28 x 0.48
Weight (approx.)	gm 2
Connector (solder terminals)	2
Case Material	s.s.
Seal	epoxy
Excitation Voltage	V ±18 to 24
Excitation Current (constant)	mA 2 to 20

Notes:

Model 303A02 has a 5-44 micro-connector. Other specifications are the same.  
 Options include 080A15 adhesive mounting base, 080A16 three-axis mounting adaptor (10-32 thread) and triaxial Model 303A06.



## EPX Series Miniature Threaded Pressure Transducers

- 5 PSI to 5000 PSI (.35 BAR TO 350 BAR)
- 10-32 UNF OR M5 METRIC THREADED MOUNT
- O-RING SEAL, STAINLESS STEEL CONSTRUCTION
- STATIC & DYNAMIC PRESSURE

Entran's EPX Miniature threaded pressure sensors represent a unique approach in transducer design based on mounting ease and flexibility of use. Developed with a wide range of applications in mind, the EPX offers an optimum combination of characteristics which permit static and dynamic pressure measurements when small size and ease of attachment are of prime importance.

The EPX has a stainless steel diaphragm construction which eliminates the cracking and shattering problems normally associated with silicon diaphragm transducers. Available in either a 10-32 UNF or M5 metric thread, with built in O-ring seal, it allows simple mounting to test objects or systems. A custom thread length option enables matching the EPX directly to existing requirements and allows specification of the exact transducer length between 0.250" and 1.500" (6.3mm and 40mm), instead of machining the fixture to match the transducer. Another standard option incorporates two varieties of "Welded" diaphragm seals for use in water or corrosive fluids compatible with 304SS. In short, it is possible to customize the transducer directly from this data bulletin without the necessity of complicated special order procedures.

The EPX is a semiconductor strain gage device which combines a fully active Wheatstone bridge with state of the art transducer design. The semiconductor elements are bonded directly to the stainless steel diaphragm thereby providing extremely high frequency response coupled with extremely low sensitivity to extraneous accelerations, vibrations and shocks. Its high output enables the EPX to drive most recorders and data monitoring systems directly, without amplification and costly signal conditioning. The semiconductor circuitry is fully compensated for temperature changes in the environment.

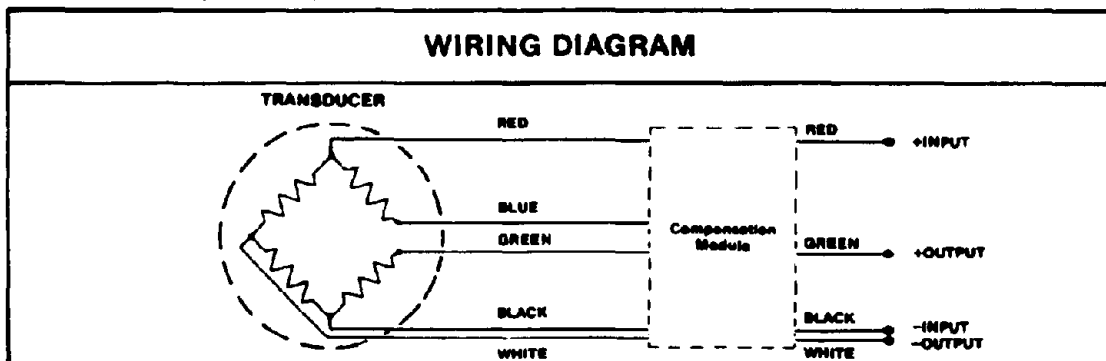
The EPX is ranged for the pressures which are commonly experienced in research, testing and control, from 5 to 5000 psi (.35 to 350 bar) (for ranges higher than 5000 psi or 350 bar, contact Entran directly.) Typical uses have varied in scope from missile engine and skin pressure studies, automotive fuel line and brake hydraulic tests, ship model impact and perturbation studies to chemical process control and general university laboratory research.

SPECIFICATIONS EPX-10												
RANGE	psi	5	10	15	25	50	100	250	500	1000	2500	5000
OVERRANGE	psi	50	50	50	50	100	200	500	1000	2000	4000	6000
SENSITIVITY (nom.)	mV/psi	3	2.5	2	2	1.5	1.2	.5	.25	.12	.05	.025
	mV F.S.	15	25	30	50	75	125	125	125	125	125	125
RES. FREQUENCY nom.		45KHz	50KHz	65KHz	65KHz	75KHz	80KHz	120KHz	150KHz	200KHz	300KHz	450KHz
COMM. NON-LIN. & HYST.		±1% F.S.					±1% F.S.	±½% F.S.				
TEMP. SHIFT	ZERO	±1mV/100°F			±2% F.S./100°F			±1½% F.S./100°F				
	SENS.	±2%/100°F (±3½%/100°F for EPX6-)										
SENS. nom.	% F.S./g	.015	.007	.0048	.003	.0016	.0012	.0006	.0004	.0003	.0002	.0001

<sup>1</sup> Useful Frequency Range to 20% of Resonant Frequency

SPECIFICATIONS COMMON TO ALL RANGES AND THE METRIC SERIES			
	EPX-	EPX6-	CUSTOM OPTIONS* (see Selection Manual)
EXCITATION	10 VDC	6 VDC	3 to 15 VDC or VAC
IMPEDANCE	INPUT	1200 Ω nom. typ. (350 Ω min.)	700 Ω nom. typ. (350 Ω min.)
	OUTPUT	350 Ω nom.	350 Ω nom.
			200 Ω to 2500 Ω nom.
REPEATABILITY	±0.25%	±0.25%	±0.1%
RESOLUTION	INFINITE		
COMPENSATED TEMP.	70°F to 170°F (21°C to 77°C)		Ranges within: -100°F to 450°F -73°C to 230°C
OPERATING TEMP.	-40°F to 250°F (-40°C to 121°C)		-100°F to 500°F (-73°C to 260°C)
ZERO OFFSET ( $\frac{70^\circ\text{F}}{21^\circ\text{C}}$ )	±10mV	±10mV	±1% F.S.

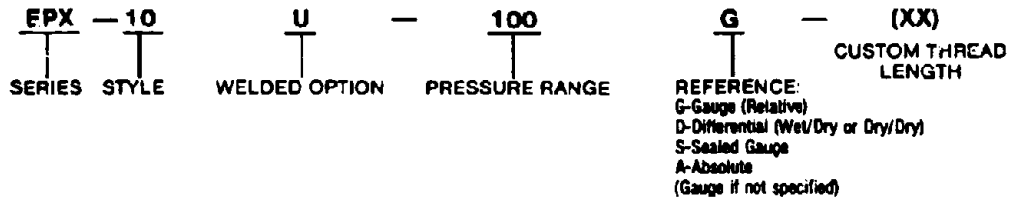
\*Custom options may alter other specifications and are not necessarily available on all models and in all combinations. Contact Entran directly for your specific requirements.





## TO ORDER AN "EPX" SERIES PRESSURE TRANSDUCER

1. Select Desired Input Voltage Option EPX or EPX6.
2. Select Desired Mounting Style in Standard or Metric Versions.
3. Select Welded Version If Required.
4. Select Pressure Range.
5. Specify Pressure Reference Gauge, Absolute, Differential or Sealed Gauge.  
If Not Specified, Unit Will Be Supplied as Gauge.
6. Specify Custom Thread Length If Required.



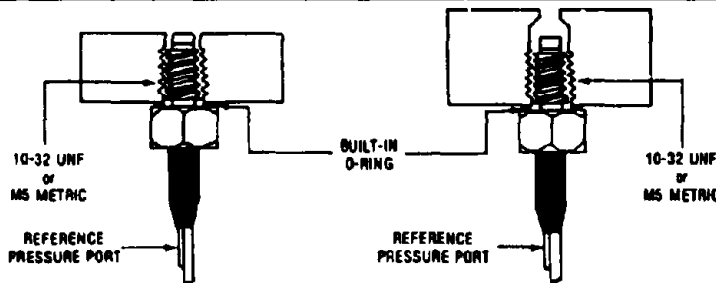
**Examples:** EPX-10-50    Standard 10-32 UNF Thread, 50 PSIG range.  
 EPX-M5-3.5    M5 Metric Thread, 3.5 bar range, relative (gauge).  
 EPX-10U-100A(.37)    Braze Welded 10-32 UNF Version with 100 PSIA range and custom thread length of "X" = 0.37".  
 EPX-M5W-7(10)    Beam Welded M5 Metric Thread with 7 bar range and custom thread length of "X" = 10mm.  
 EPX6-10I-5000    EPX with 6V Excitation option on 10-32 UNF Threaded Housing with Internal Compensation Module, 5000 psig.

ACTUAL SIZE



## TYPICAL INSTALLATION

EPX-10 or EPX-M5



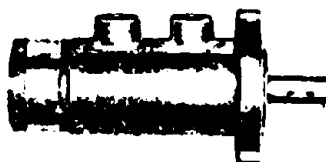
INSTALLATION TORQUE		
Pressure Range	In-Lbs.	Milli-Newton
0 to 50 psi 0 to 3.5 bar	5	0.6
60 to 500 psi 4 to 35 bar	10	1.2
800 to 5000 psi 40 to 350 bar	15	1.8

Specifications subject to change without notice.



## 3HP ORBIT-TYPE HYDRAULIC MOTOR

Medium Speed – High Torque – Miniature Size



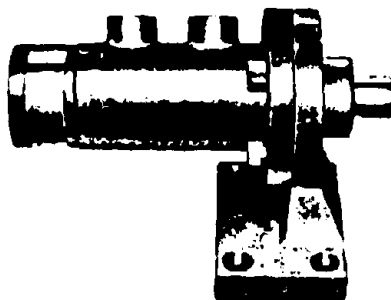
Built by Lamina under license from Char-Lynn, these motors use the Orbit principle to obtain reduced speed on the output shaft with increased torque. Best operation is in a moderate speed range with 4 to 6 GPM. Will run with equal torque in either direction and is instantly reversible.

Body length 5-1/8" on Model A-100; slightly shorter on other models. Front mounting flange 3" diameter. Four mounting holes 11/32" diameter spaced on a 5-hole pattern, with one hole omitted in line with the oil port. Bolt circle 2.375" diameter. Shaft 5/8" diameter x 1-1/8" long with Woodruff keyway. Motor body diameter 1-3/4". Oil ports are straight thread with O-ring seal, 9/16-18. For foot mounted motors see listings below.

Motor shaft will tolerate full side loading but thrust loading should be kept as low as possible. Recommended fluid, Type A transmission fluid or hydraulic oil with viscosity not less than 100 SSU (at 100°F). Four displacements are offered in the chart below. Choose the one which most closely matches load speed and torque requirements.

### Choose From Five Displacements

MODEL No.	A-25F	A-37F	A-50F	A-62F	A-100F
Displacement, Cubic Ins./Rev.	0.81	1.21	1.62	2.03	3.25
Maximum Oil Flow (Supply)	All models 8 GPM				
Maximum Operating Pressure	All Models 1500 PSI				
No Load RPM @ 8 GPM	2272	1517	1137	909	568
Full Load RPM @ 8 GPM	2107	1385	1038	843	519
No Load RPM @ 1 GPM	284	189	142	113	71
Full Load RPM @ 1 GPM	74	21	16	29	8
Maximum HP @ 8 GPM*	All models 3 HP				
Maximum Torque, Inch-Lbs.*	100	150	200	250	400
Approximate Weight	All models 3 1/4 Lbs.				



### Foot Mounted Lamina Motors

To order above motors for foot mounting, add "M" after model number, as A-62FM, etc. Bracket must be specified at time of original order; it cannot be added to flange mounted motors in the field. Centerline height 3 1/4"; Shaft extends 1 1/4" beyond bracket. The weight of motor and foot bracket 5 1/4 lbs.

### ORBIT MOTOR PRINCIPLE

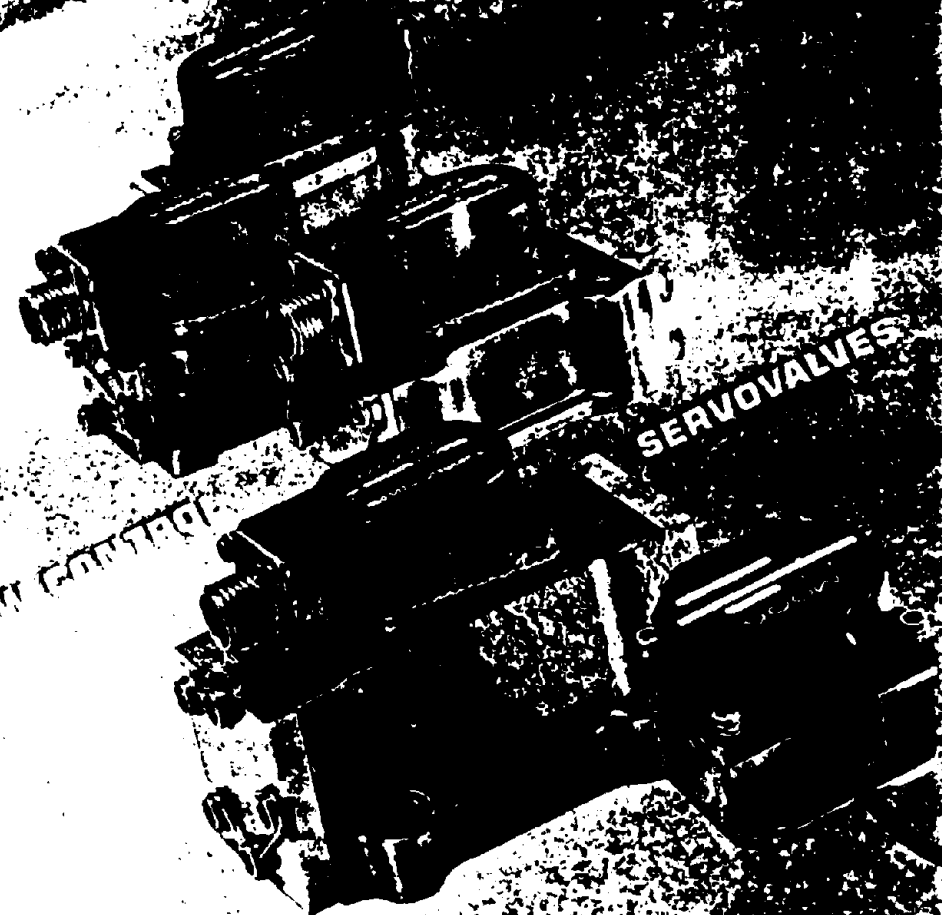
Lamina motors listed above and Char-Lynn ORBIT motors on Pages 96D to 96J obtain their desirable slow speed, high torque characteristic by operating on the ORBIT principle. This gives a built-in speed reduction without the use of external gear boxes or speed reducers. The result is a slow shaft speed at a greater efficiency than could usually be produced by a high speed hydraulic motor operating through an external speed reducer.

\*Note: ORBIT is a registered trademark of Char-Lynn Division, Eaton Corp.

MOOG

TYPE EG ELECTRO HYDRAULIC

SERVOVALVES



Reproduced from  
best available copy.



# TYPE 30 SERVOVALVES

- flow control
- double nozzle
- two stage
- mechanical feedback

## FIVE BASIC SIZES

		PORT CIRCLE DIAMETER		MAX. RATED FLOW		VALVE WEIGHT	
		in.	mm	gpm at 3000 psi	liters/min at 210 bars	lbs	kg
TYPE 30 SERVOVALVES	Series 30	0.480	12.19	3.1	12	0.42	0.19
	Series 31	0.625	15.88	6.8	26	0.81	0.37
	Series 32	0.780	19.81	14	54	0.81	0.37
	Series 34	0.780	19.81	19	73	1.10	0.50
	Series 35	1.000	25.40	44	170	2.13	0.97

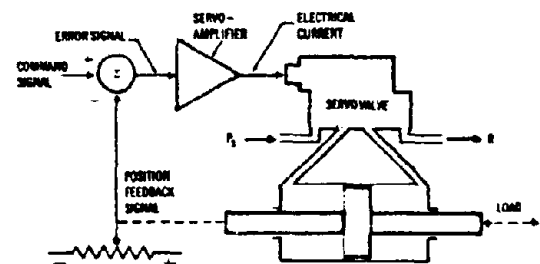
## THIS CATALOG CONTAINS

- general information on Type 30 servovalves
- information on standard valve designs

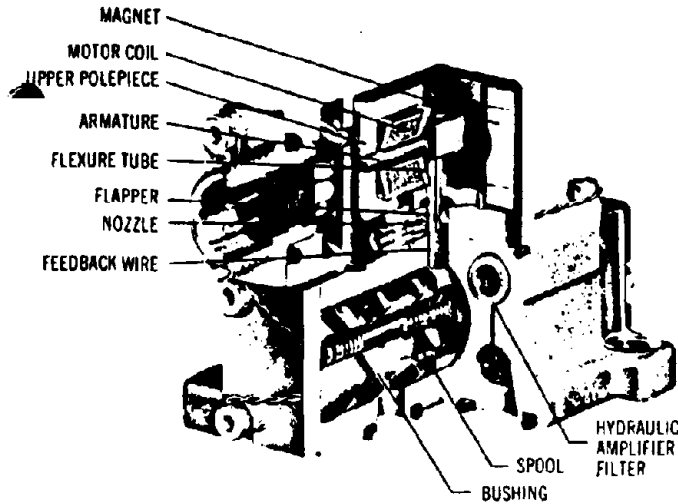
## STANDARD DESIGNS

- are assembled from standard parts
- offer choice of
  - rated flow
  - rated pressure
  - rated current (coil resistance)
  - internal coil connection
  - electrical connector or cable
  - connector or cable location
  - seal compound
- give standard performance (per Moog specification)
- eliminate non-recurring start-up costs
- minimize lead-time; certain models carried in stock

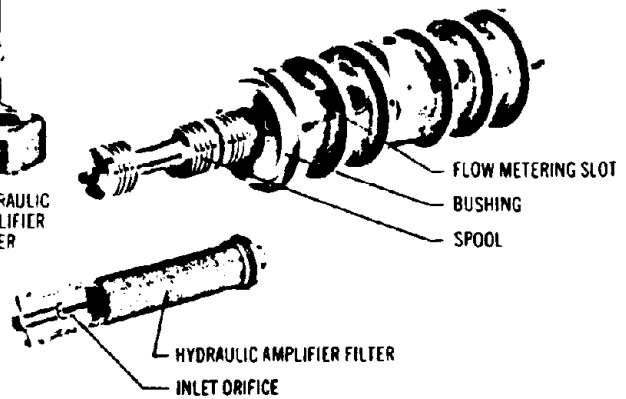
## POSITION SERVO - THE USUAL APPLICATION OF FLOW CONTROL SERVOVALVES



- servovalve supplied with constant pressure  $P_s$  (e.g., 3000 psi or 210 bars)
- servovalve controls flow to and from piston end chambers in response to electrical signal
- piston drives load
- position feedback signal obtained from pot, LVDT, DCDT, etc.
- difference between position command signal and position feedback signal is error signal
- error signal is amplified to drive servovalve
- load moves to reduce error to near zero



# DESIGN FEATURES



## MATERIALS used in Standard Type 30 Servovalves

Body*, end caps and accessories	17-4 PH stainless steel
Spool and bushing*	440-C stainless steel
Filter (35 micron absolute)	Sintered stainless steel wire mesh
Flexure tube	Beryllium copper
Polepieces and armature	4750 Nickel-iron steel
Magnets	Alnico VI
Feedback wire	440-C stainless steel
Torque motor cover	Anodized aluminum alloy

\*The Series 30 has an integral bushing and body made from 440-C.

## QUALITY CONTROL

- conforms to MIL-Q-9858A
- valves assembled and tested in clean room (per FED STD 209 Class 100,000)

## ENVIRONMENTAL CAPABILITY OF STANDARD DESIGNS\*

- meet or exceed MIL-V-27162 (SAE ARP 490C)
- suitable for Type I and II missile and aircraft hydraulic systems per MIL-H-8775C
  - Type I —65°F to +160°F (-54°C to +71°C)
  - Type II —65°F to +275°F (-54°C to +135°C)
- meet or exceed following as tested per MIL-STD-810B
  - high temperature — normal performance at +275°F fluid and ambient with MIL-H-5606 fluid
  - low temperature — normal performance at 0°F fluid and ambient with MIL-H-5606 fluid
  - extreme low temperature — valves will respond to input commands at -65°F fluid and ambient on MIL-H-5606 fluid
  - altitude — normal performance to 100,000 feet altitude
  - random vibration — will withstand 25 g rms (5 to 2000 Hz) 30 minutes per axis
  - sinusoidal vibration — will withstand sweep from 16 g at 25 Hz, to 35 g at 2000 Hz, 30 minutes per axis
  - acceleration — will withstand 50 g any axis
  - shock — will withstand 6 msec sawtooth, 100 g peak, any axis
  - salt spray, fungus, humidity, sand and dust — will withstand all exposures per MIL-STD-810B
  - useful life — >10 years with normal overhaul
  - cyclic life — >10<sup>6</sup> cycles with normal wear

\*Type 30 Servovalves are not necessarily limited by the environments listed. Special designs are available that considerably extend these capabilities.

- rugged, stainless steel body
- one-piece bushing with EDM flow slots\*
  - bushing slip-fit in body bore
  - eliminates bushing land O-rings
  - bushing easily removed for cleaning or replacement
- O-ring sealed spool stops
  - eliminates pressure loading of ends of bushing
- spool bushing tolerances for diametral clearance held within 20 microinches (1/2 μm)
- 20 μm nominal filter (35 μm absolute) for pilot flow
- symmetrical, double nozzle hydraulic amplifier
  - provides consistent performance over wide temperature range
- hydraulic amplifier integrated into main valve body
  - eliminates several O-rings
- torque motor in environmentally sealed compartment
- frictionless, flexure tube supported armature/flapper
  - isolates hydraulic fluid from torque motor
- balanced, double coil, double air gap torque motor
  - reduces temperature centershift
  - minimizes external magnetic fields
  - reduces sensitivity to external magnetic materials or fields
- motor coils have resilient potting
  - cushions coils during thermal and vibration extremes
- mechanical feedback with simple cantilever spring
  - rolling ball contact with spool minimizes wear
  - feedback removable without damage to valve
- locating pin in base of valve prevents improper installation

\*EDM = electric discharge machined  
Series 30 does not have a bushing (slots are EDM'd in valve body)

Design features of Type 30 Servovalves are covered by U. S. Patents 3,023,782; 3,328,423 and 4,017,706 together with corresponding patents in several foreign countries

# SPECIAL DESIGNS

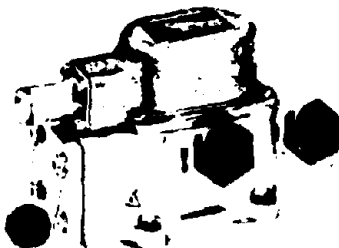
major programs usually warrant a special servovalve design

- special Type 30 valves are designed to satisfy customer specification
  - provides optimum servovalve configuration
  - allows customer configuration control
- may be
 

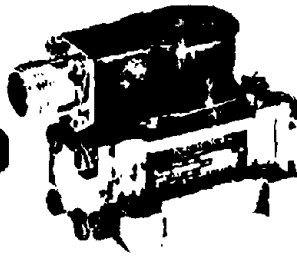
<input type="checkbox"/> special performance	<input type="checkbox"/> special mounting
<input type="checkbox"/> special environments	<input type="checkbox"/> special porting
<input type="checkbox"/> special testing	<input type="checkbox"/> special connector
<input type="checkbox"/> special bias	<input type="checkbox"/> special materials
<input type="checkbox"/> special quality control	<input type="checkbox"/> special handling
- any change from standard is a special
- special designs carry a unique model number, parts list, test procedures, etc.
- special Type 30 designs that require a non-standard manifold pattern will be assigned a Series 33 model number

## UNUSUAL ENVIRONMENTS

- high temperature — to 400°F (200°C) fluid and ambient with Viton seals (limited life)
  - to 650°F (350°C) fluid and ambient with metallic seals, ceramic insulated magnet wire, and special magnetic materials
- high accelerations — to 400 g with special mass balanced armature/flapper and stainless steel flexure tube
- high vibration — to 100 g rms (20-2000 Hz) with silicon damping fluid and armature motion restraint
- high shock — to 5000 g with damping fluid and stainless steel flexure tube
- nuclear radiation — to  $2 \times 10^5$  rads (c) with standard teflon insulated magnet wire; higher radiation levels with ceramic insulation and metallic seals
- external pressurization — to hundreds of psi with special motor cap or with motor cavity vented to pressure equalized return



SPECIAL 33 SERIES FOR SHORT DUTY DURING HIGH ACCELERATION



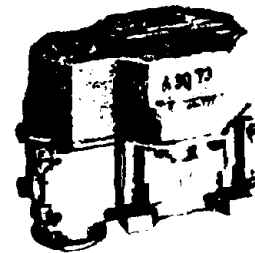
SPECIAL 32 SERIES FOR OPERATION TO 600°F. OIL AND AMBIENT

## SPECIAL BODY CONFIGURATIONS

- diamond port pattern Series 30
- plug-in electrical connector mounted flush with manifold surface
- plug-in hydraulic manifold with annular hydraulic ports



SPECIAL 33 SERIES WITH PLUG-IN MANIFOLD AND THREE-WAY SPOOL



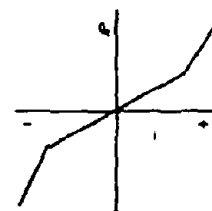
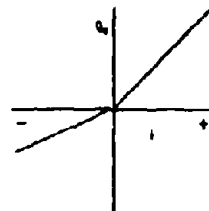
SPECIAL 30 SERIES WITH PLUG-IN ELECTRICAL CONNECTOR

## SPECIAL FLUIDS

- other hydraulic fluids including water
- most fuels, propellants, and oxidizers
- pneumatics

## SPECIAL SPOOL DESIGNS

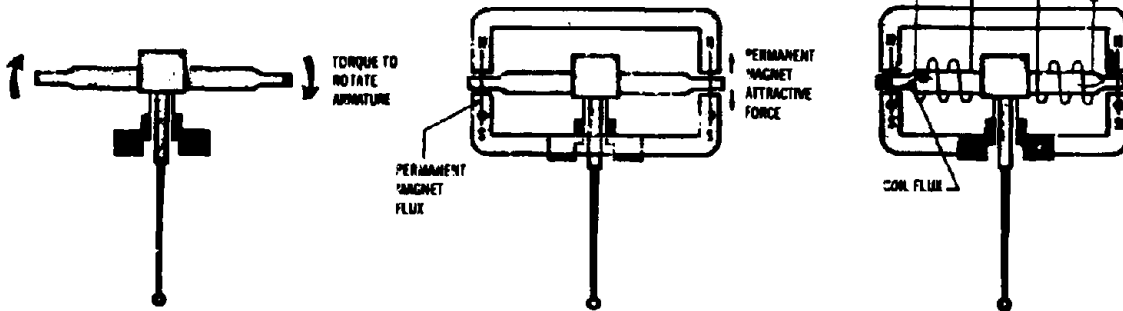
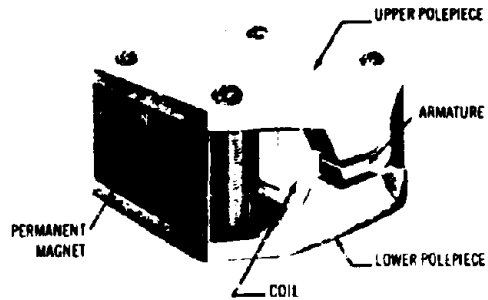
- three-way spools having single control port
- spool stops for limiting maximum flow
  - limit flow usually held to  $\pm 10\%$
- special spool null cuts
  - prescribed amounts of underlap or overlap, symmetrical or unsymmetrical
- graphite impregnation of spool for pneumatic and water applications
- non-linear slot width
  - different flow gain for each valve polarity as used with some three-way actuators
  - stepped width slots for dual flow gain



# OPERATION

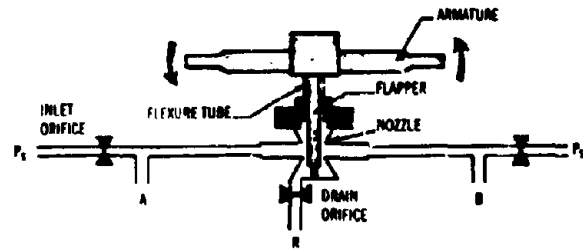
## TORQUE MOTOR

- charged permanent magnets polarize polepieces
- dc current in coils causes increased force in diagonally opposite air gaps
- magnetic charge level sets magnitude of decentering force gradient on armature



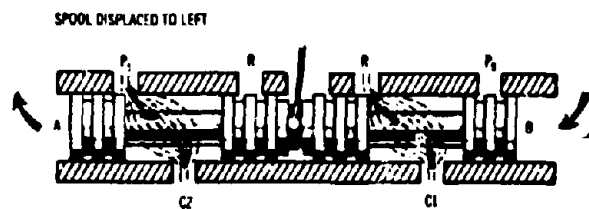
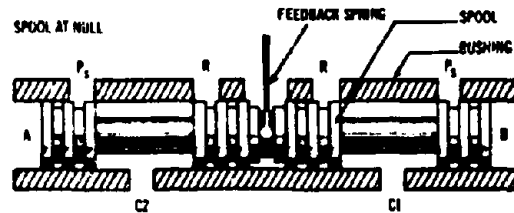
## HYDRAULIC AMPLIFIER

- armature and flapper rigidly joined and supported by thin-wall flexure tube
- fluid continuously flows from pressure  $P_S$  through both inlet orifices, past nozzles into flapper chamber, through drain orifice to return R
- rocking motion of armature/flapper throttles flow through one nozzle or the other
- this diverts flow to A or B (or builds up pressure if A and B are blocked)



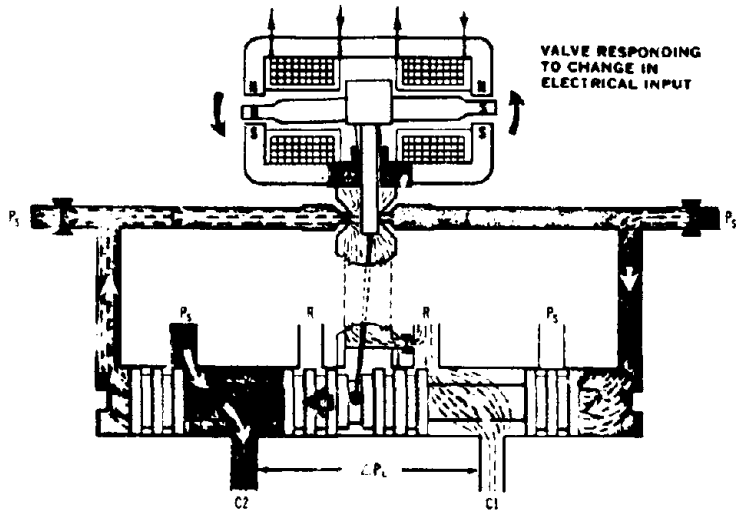
## VALVE SPOOL

- spool slides in bushing (sleeve), or directly in a body bore for Series 30
- bushing contains rectangular holes (slots) or annular grooves that connect to supply pressure  $P_S$  and return R
- at "null" spool is centered in bushing; spool lobes (lands) just cover  $P_S$  and R openings
- spool motion to either side of null allows fluid to flow from  $P_S$  to one control port, and from other control port to R

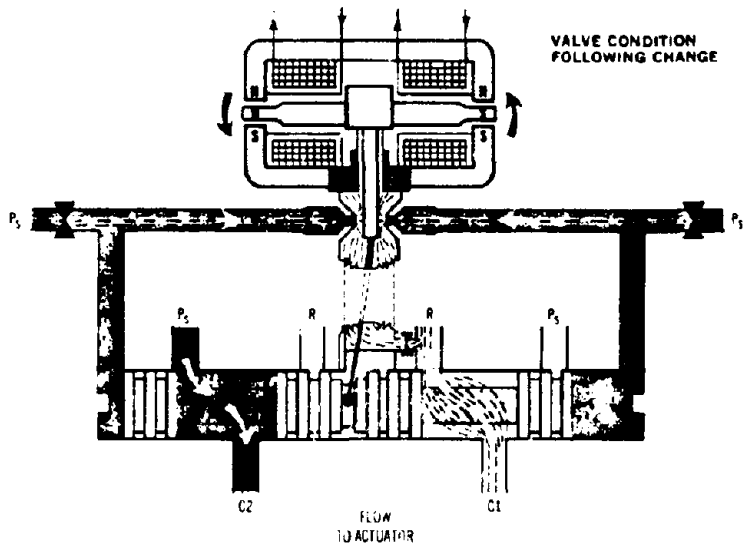


**OPERATION**

- electrical current in torque motor coils creates magnetic forces on ends of armature
- armature and flapper assembly rotates about flexure tube support
- flapper closes off one nozzle and diverts flow to that end of spool
- spool moves and opens  $P_s$  to one control port; opens other control port to R



- spool pushes ball end of feedback spring creating restoring torque on armature/flapper
- as feedback torque becomes equal to torque from magnetic forces, armature/flapper moves back to centered position
- spool stops at a position where feedback spring torque equals torque due to input current
- therefore spool position is proportional to input current
- with constant pressures, flow to load is proportional to spool position



**TYPICAL TYPE 30 SERVOVALVE SIZES**

	Thousandths of an inch	Micro meters
air gap spacing (each gap)	10 to 15	250 to 380
maximum armature motion in air gap	±3	±75
maximum torque on armature	±0.3 in-lbs	±0.03 N·m
inlet orifice diameter	5 to 10	125 to 250
nozzle diameter	10 to 20	250 to 500
nozzle flapper maximum opening	2.4 to 3.0	60 to 75
drain orifice diameter	10 to 15	250 to 380
spool stroke	±10 to ±20	±250 to ±500
spool/bushing radial clearance	0.03 to 0.06	0.7 to 1.5
bushing/body radial clearance	0.08	2.0

# ELECTRICAL CHARACTERISTICS

## STANDARD COIL CONFIGURATIONS

CODE FOR PART NUMBER OF STANDARD VALVE	P	S	D	I	
INTERNAL COIL CONFIGURATION	PARALLEL COILS 	SERIES COILS 	DIFFERENTIAL COILS 	INDIVIDUAL COILS 	
PINS (IF CONNECTOR)	B A	B A	B A C	B A D C	
COLORS (IF CABLE)	grn red	grn red	grn red blu	grn red yel blu	
EXTERNAL CONNECTIONS TO GIVE FLOW OUT	SERIES COILS	Not possible	B+ A-	B+ Tie A,D C-	
	PARALLEL COILS	B+ A-	Not possible	Tie B,D+ Tie A,C-	
	DIFFERENTIAL COILS	Not possible	Not possible	for A+ when current A to B < A to C for A- when current B to A > C to A	Tie A,D for A,D+ when current A to B < D to C for A,D- when current B to A > C to D
	SINGLE COIL	Not possible	Not possible	B+ A- or A+ C-	B+ A- or D+ C-

## ELECTRICAL CONNECTOR

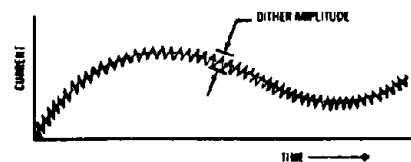
- standard configurations (see table below)
  - Bendix pigmy
  - 18 inch long cable
- special Type 30 connectors
  - connector type and location per specification
  - flush manifold plug-in connector available

COIL CONFIGURATION AVAILABLE	CONNECTOR TYPE	CODE FOR PART NUMBER
P, S, D, I	* PC-02E-8-4P 4 pin screw	4 PC
P, S, D	* PC-02E-8-3P 3 pin screw	3 PC
P, S, D, I	* PT-02E-8-4P 4 pin bayonet	4 PT
P, S, D	* PT-02E-8-3P 3 pin bayonet	3 PT
I	4 wire cable, 18" long	** 4 CA
D	3 wire cable, 13" long	3 CA
P, S	2 wire cable, 18" long	2 CA

\* Bendix Corporation part number  
\*\* only choice for Series 30

## DITHER

- servovalve performance normally measured without dither
  - dither current may be applied to Type 30 Servovalves
  - usually will improve servovalve and actuator threshold
  - will increase spool null leakage
- dither characteristics
  - usually 100 to 400 Hz (selected to suit system)
  - peak-to-peak dither amplitude may be as high as  $\pm 20\%$  servovalve rated current without degradation of valve life

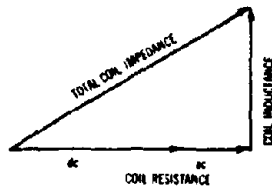


### RATED CURRENT

- choice of coil resistance and coil connections determine valve rated current (see table below)
- other coil resistance and rated current combinations can be supplied for special valves
  - lower rated current can be specified for standard coils, but with corresponding degradation of valve performance
- triple rated current can be supplied indefinitely with no damage to servovalve

### COIL IMPEDANCE

- composed of
  - dc coil resistance
  - ac coil resistance
  - apparent coil inductance
- dc coil resistance
  - nominally equal for both coils, but may vary  $\pm 10\%$  as coils are wound for desired number of turns
  - will vary with temperature (approximately 0.002 ohms/ohm \*F)
- ac coil resistance
  - represents work done in moving armature
  - becomes significant above 200 Hz
- coil apparent inductance
  - includes coil self inductance plus mutual inductance of other coil
    - mutual coupling of coils is approximately 50%
  - will vary considerably with motion of armature (back emf's)
    - affected by valve supply pressure, signal amplitude, and signal frequency
    - may become capacitive at higher frequencies
    - usually specified at 50 Hz with normal operating conditions



### QUIESCENT CURRENT

- may be present with push-pull operation of three and four wire coil configurations
  - signal input current  $i = i_1 - i_2$
  - quiescent current  $i_Q = \frac{i_1 + i_2}{2}$  when  $i_1 = i_2$
  - quiescent current  $i_Q$  should be  $i_R > i_Q > \frac{i_R}{2}$
  - small null shift and gain change may occur with changes in quiescent current amplitude and polarity



### SERVOAMPLIFIER



MODEL 82-300 SERVOCONTROLLER

- should provide dc current into torque motor coils
  - irrespective of coil inductance and resistance
  - requires current feedback amplifier
  - large shunt capacitance at output of amplifier may produce undesirable resonance with servovalve coil impedance
- current feedback amplifier
  - eliminates apparent servovalve gain change due to changes in coil impedance
  - minimizes phase lags due to coil inductance
- standard servovalve drive amplifiers available from Moog
  - rack mounted laboratory units
  - low cost industrial units
  - aerospace units on special order

Model	P			S			D			I		
	Parallel Coils			Series Coils			Differential Coils			Individual Coils		
	Ohms	$i_R$	Ma	Ohms	$i_R$	Ma	Ohms	$i_R$	Ma	Ohms	$i_R$	Ma
0040	20	0.10	50	80	0.36	25	40	0.19	50	40	0.12	50
0080	40	0.18	40	160	0.66	20	80	0.34	40	80	0.22	40
0130	65	0.30	30	260	1.1	15	130	0.58	30	130	0.37	30
0200	100	0.59	20	400	2.2	10	200	1.1	20	200	0.72	20
0500	250	1.1	15	1000	4.1	7.5	500	2.1	15	500	1.3	15
1000	500	2.6	10	2000	9.7	5	1000	5.0	10	1000	3.2	10
1500	750	3.4	8	3000	12.5	4	1500	6.4	8	1500	4.1	8

NOTE: Resistance values at 68°F (20°C)  $\pm 10\%$  tolerance  
 Inductance values are typical for 50 Hz, servovalve pressurized. Inductance is not normally measured on individual servovalves.  
 \* Inductance values per coil with differential operation (Class A push-pull).

# HYDRAULIC CHARACTERISTICS

## SUPPLY PRESSURE

- 500 psi to 4000 psi for standard designs
  - valves are set up and tested at supply pressure specified
  - valves can be used at other supply pressures, but some null shift may occur
- valves supplied for pressures below 500 psi should be specially designed
  - Type 30 Servovalves are usable with supply pressures as low as 50 psi
  - servovalve performance, especially threshold and dynamic response, is degraded with low supply pressure

## PROOF AND BURST PRESSURES

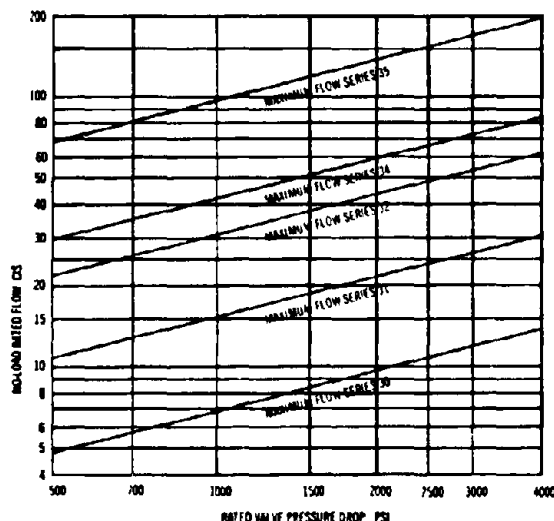
- proof pressure capability:
  - at supply and control ports =  $1.5 P_s$
  - at return port =  $1.0 P_s$
- burst pressure capability:
  - at supply and control ports =  $2.5 P_s$
  - at return port =  $1.5 P_s$  or 5000 psi maximum

## RETURN PRESSURE

- may vary widely with minimal valve null shift
- should never exceed supply pressure to avoid back flowing hydraulic amplifier

## RATED FLOW

- each valve Series covers a range of rated no-load flow to the maximum shown (for MIL-H-5606)

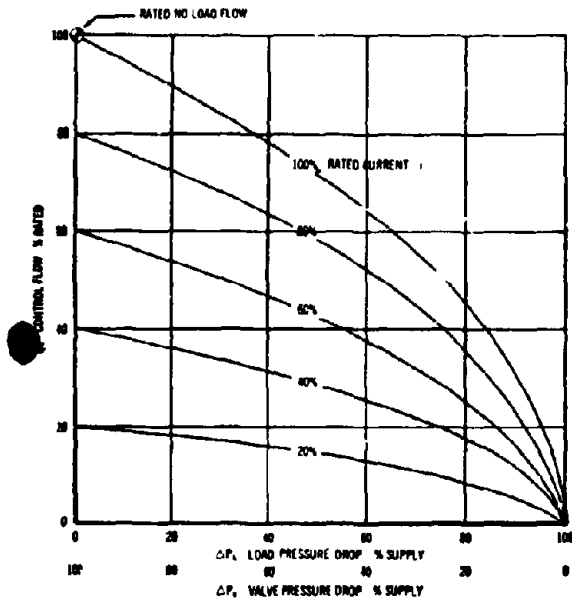


## STANDARD SEALS, FLUIDS, AND TEMPERATURES

O-RING ELASTOMER	RECOMMENDED FLUIDS	RECOMMENDED TEMP. RANGE*	TEST FLUID	CODE FOR PART NO.
Buna N	Petroleum Base Fluids such as MIL-H-5606, MIL-H-6083, DTE, Regal, Brayco  MIL-H-83283 (synthetic hydrocarbon)  Freon 12, 13, 14, 113, 114  Silicone Fluids	-65°F to +275°F	MIL-H-5606	BUN
Fluorocarbon Rubber (Viton)	Petroleum Base Fluids such as Type A Transmission Fluid, JP-4, JP-5  Superrefined Mineral Oils  Silicone Fluids  Silicate Ester Fluids such as MIL-H-8446, MLO-8200, GS-45, MZY  Industrial Phosphate Ester Fluids such as Cellulube, Pydraul, Pyroguard  Di-Ester Base Fluids such as MIL-L-7808, Houghton Safe  Tri-Ester Base Fluids such as Trichloroethylene	-20°F to +400°F	MIL-H-5606	VIT
Ethylene Propylene Rubber	Aircraft Phosphate Ester Fluids such as Skydrol, Hyjet, Aerosafe  Freon 22, 31, 32, 115  Hydrazine** UOMH Water, steam, air	-55°F to +300°F	Hyjet IV	EPR

\* Operating temperature range may be further restricted by fluid.  
 \*\* Standard Type 30 Servovalves are recommended for short term use with this fluid. Special designs with all stainless steel wetted parts are available.

## FLOW-LOAD CHARACTERISTICS



- nominal flow to load

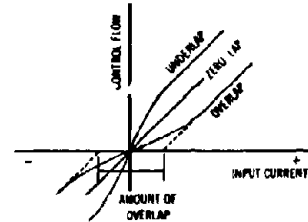
$$Q_V = K i \sqrt{\Delta P_V}$$

where  $Q_V$  = valve flow to load  
 $K$  = servovalve sizing factor  
 $i$  = input current  
 $\Delta P_V$  = valve pressure drop

$$\Delta P_V = (P_S - R) - \Delta P_L$$

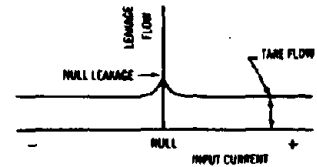
where  $P_S$  = supply pressure  
 $R$  = return pressure  
 $\Delta P_L$  = load pressure drop

- some flow saturation will occur with servovalves having maximum flow capacity
- saturation causes droop at the high end of the flow curve



## SPOOL LAP

- standard servovalves have zero lap within limits of flow linearity shown on Page 12
- prescribed amounts of under or overlap can be specified on special order
  - underlap (or open center)
    - increases flow gain at null
    - reduces valve pressure gain at null
    - increases valve null leakage
  - overlap
    - reduces flow gain at null
    - reduces null leakage flow
    - degrades pressure gain (into a load)



## INTERNAL LEAKAGE

- includes first stage hydraulic amplifier flow, spool null leakage flow, and bushing laminar leakage flow
  - spool null leakage flow is essentially zero when spool is off-null
  - servovalve internal leakage excluding spool null leakage is called Tare Flow
- hydraulic amplifier flow largely determines servovalve frequency response
  - lower flow degrades response
- spool null leakage flow is related to maximum valve flow (slot width) and null cut
  - table gives internal leakage of standard Type 30 Servovalves (with MIL-H-5606)
  - special low leakage versions of the miniature Series 30 available with <0.25 cis at 3000 psi

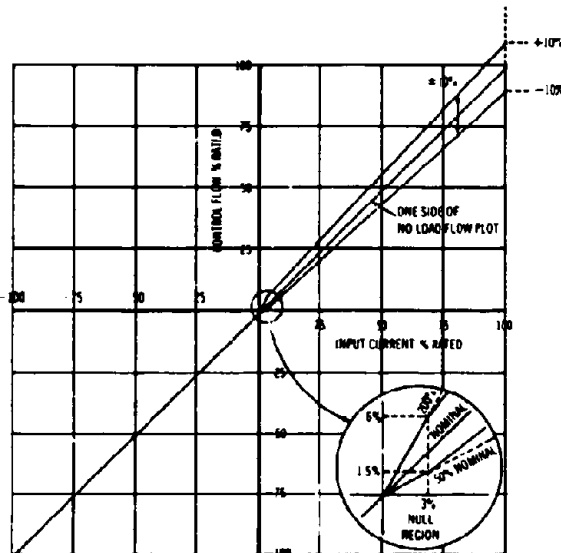
## MAXIMUM LEAKAGE OF STANDARD TYPE 30 SERVOVALVES

VALVE SERIES	TARE LEAKAGE FLOW at 1000 psi	CIS at 3000 psi	SPOOL NULL LEAKAGE FLOW (% rated flow at rated pressure)
30	< 0.20	< 0.35	< 4
31	< 0.25	< 0.45	< 4
32	< 0.28	< 0.50	< 3
34	< 0.35	< 0.60	< 3
35	< 0.45	< 0.75	< 3

# STATIC PERFORMANCE

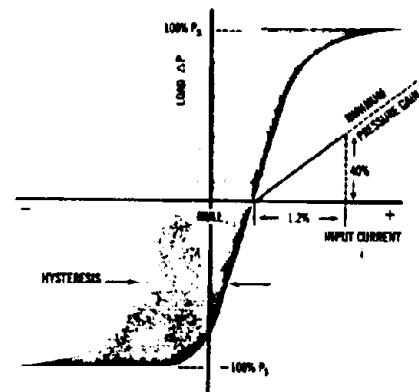
## CONTROL FLOW

- servovalve control flow to the load is nominally proportional to electrical input current
  - standard production acceptance test limits for no load flow shown below
  - limits do not include servovalve hysteresis or null bias
  - limits at  $\pm 100\%$  input for maximum flow designs may be  $+10, -20\%$  due to non-linearities caused by flow saturation



- control flow non-linearity is greatest in null region
  - may be from 50% to 200% nominal gain within range of  $\pm 3\%$  electrical input for standard null cut
  - can be held to closer limits on special order
- maximum valve flow may be 120 to 140% rated flow with oversignal
  - spool stops to limit maximum flow can be provided on special order
- control flow characteristic may change with fluid temperature
  - a  $+100^\circ\text{F}$  temperature rise may cause control flow to increase as much as 3% due to fluid viscosity effects
  - at very high temperatures (over  $400^\circ\text{F}$ ) a  $+100^\circ$  temperature rise may cause control flow to decrease by 3% due to magnetic effects

## PRESSURE GAIN



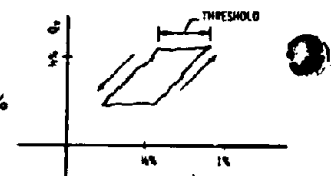
- blocked load  $\Delta P_L$  changes rapidly from  $-P_s$  to  $+P_s$  in null region
  - minimum pressure gain will be  $0.4 P_s / 1.2\% i_R$  for standard servovalves
  - maximum pressure gain may be three times higher
  - pressure gain will degrade with spool null edge wear
- special pressure gain requirements may interact with desired flow gain at null, spool null leakage, and nominal control port pressures at null

## HYSTERESIS

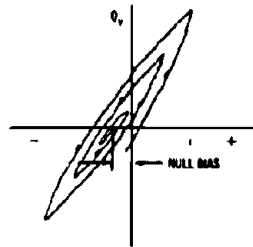
- maximum hysteresis for standard Type 30 Servovalves with normal operation conditions is  $< 3\%$ 
  - hysteresis may increase to 4% at  $-30^\circ\text{F}$
  - hysteresis limit for special high temperature servovalves ( $> 400^\circ\text{F}$ ) is  $< 4\%$

## THRESHOLD

- maximum threshold for standard Type 30 Servovalves with normal operating conditions is  $< \frac{1}{2}\%$  (without dither and with supply pressure greater than 1000 psi)
  - with  $P_s$  below 1000 psi threshold limit is  $< 1\%$
  - threshold limit should be doubled at  $-30^\circ\text{F}$
  - with dither, threshold  $= 0\%$



### NULL BIAS



- electrical input current to give valve null includes both temporary null shifts and permanent changes in null bias
- null bias is measured under standard valve operating conditions (pressures, temperatures, etc.)
- null bias measurements exclude valve hysteresis
- initial servovalve null bias on standard valves (as shipped) is less than 2% rated input
- long-term null bias after exposure to environments and use can be expected to be < 5%

### NULL SHIFT

- change in null bias with environment and operating conditions will vary from unit to unit, but is generally:
 

TEMPERATURE	NULL SHIFT
50°F to 150°F	< 2%
0°F to 200°F	< 4%
ACCELERATION	
TO 40 G SPOOL AXIS	< 0.3%/G
TO 40 G TRANSVERSE AXIS	< 0.1%/G
SUPPLY PRESSURE	
60% TO 110%	< 4%
QUIESCENT CURRENT	
50% TO 200% RATED CURRENT	< 6%
BACK PRESSURE	
0% TO 20% OF SUPPLY	< 4%
- special mass balanced torque motor design available for < 0.06%/g to 400 g
- null shifts are not normally measured during production acceptance testing
- tighter null shift specifications can be imposed by providing 100% valve testing under critical environment

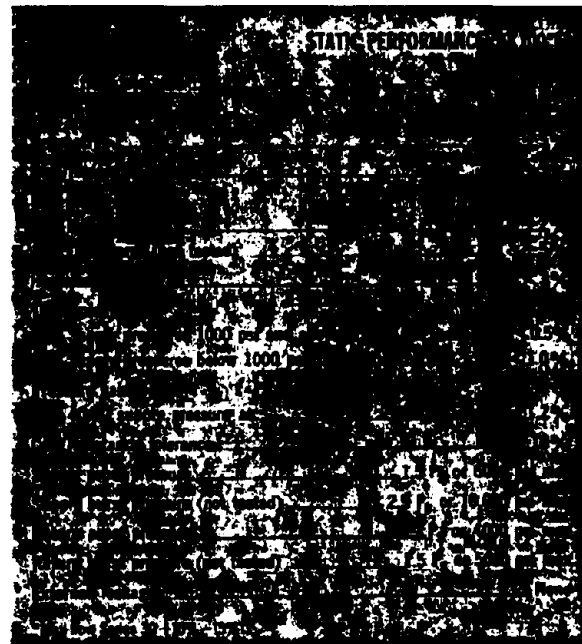
### SPOOL DRIVING FORCE

- hydraulically created force to move spool for standard Type 30 Servovalves is > 1 lb/% input (with 3000 psi supply)
  - spool driving force gradient will be > 0.6 lb/% input for operation at 1000 psi supply
- maximum spool driving force for standard servovalves at 3000 psi supply is

SERIES	MAX. SPOOL FORCE (POUNDS)
30	55
31	55
32	110
34	140
35	160

- special servovalves with lower hydraulic amplifier flow will have higher spool driving force gradients (but lower dynamic response)

### SUMMARY



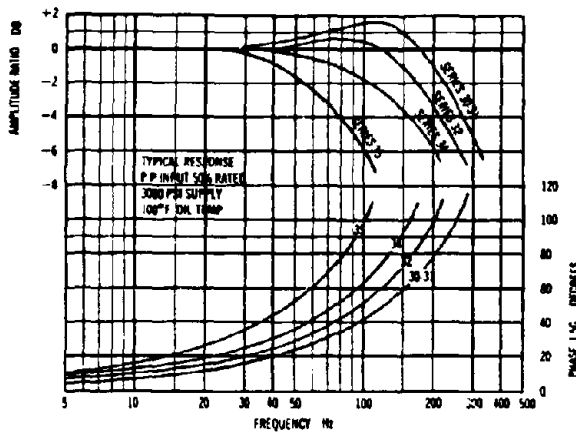
Reproduced from  
best available copy



# DYNAMIC PERFORMANCE

## FREQUENCY RESPONSE

- will depend upon signal amplitude, supply pressure, and internal design configuration
- plot below shows typical response for standard Type 30 Servovalves



- for system design these characteristics can be approximated by

Valve Series	Equivalent First Order Time Constant sec.	Equivalent Second Order Natural Frequency Hz	Damping Ratio
30	0.0015	200	0.5
31	0.0015	200	0.5
32	0.0020	160	0.55
34	0.0029	110	0.6
35	0.0035	90	0.9

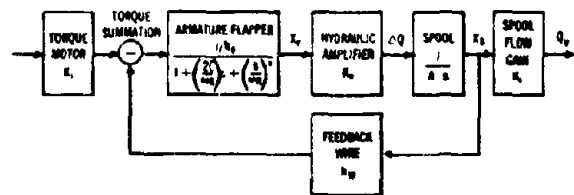
- frequency response of specially designed valves can be improved by
  - increased hydraulic amplifier leakage flow
  - shorter spool stroke (larger slot width)
  - use of stub shafts on spool ends
  - higher rated current (stiffer feedback wire)

## STEP RESPONSE

- time response to step input of current depends on valve design parameters
  - approximate transient response of standard Type 30 Servovalves operating at 3000 psi is
- | Valve Series | Approximate Response Time to 90% Output sec. |
|--------------|--|
| 30           | 0.0025                                       |
| 31           | 0.0025                                       |
| 32           | 0.0045                                       |
| 34           | 0.007  |
| 35           | 0.012  |

## INTERNAL DYNAMICS OF TYPE 30 SERVOVALVES

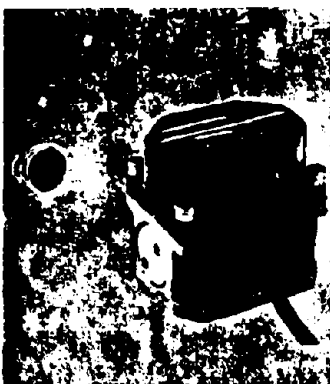
See Technical Bulletin 103 for a discussion of servovalve dynamic characteristics and response measuring techniques.



## TYPICAL PARAMETERS FOR SERIES 31\*

- $I$  = torque motor current  $\pm 10$  ma
- $x_f$  = flapper displacement at nozzles  $\pm 0.0012$  in max.
- $x_s$  = spool displacement  $\pm 0.015$  in max.
- $\Delta Q$  = hydraulic amplifier differential flow  $\pm 0.18$  in<sup>3</sup>/sec
- $Q_v$  = servovalve control flow  $\pm 4$  gpm
- $K_1$  = torque motor gain 0.025 in-lbs/ma
- $K_2$  = hydraulic amplifier flow gain  $150 \frac{\text{in}^3/\text{sec}}{\text{in}}$
- $K_3$  = flow gain of spool/bushing  $1030 \frac{\text{in}^3/\text{sec}}{\text{in}}$
- $A$  = spool end area 0.026 in<sup>2</sup>
- $k_f$  = net stiffness on armature/flapper 115 in-lbs/in
- $k_w$  = feedback wire stiffness 16.7 in-lbs/in
- $b_f$  = net damping on armature/flapper  $0.016 \frac{\text{in-lbs}}{\text{in}/\text{sec}}$
- $I_f$  = rotational mass of armature/flapper  $4.4 \times 10^{-4} \frac{\text{in-lbs}}{\text{in}/\text{sec}^2}$
- $\omega_n = \sqrt{\frac{k_f}{I_f}}$  natural frequency of first stage 814 Hz
- $\zeta = \frac{1}{2} \frac{b_f}{k_f} \omega_n$  damping ratio of first stage 0.4
- $K_v = \frac{K_3 k_w}{k_f A}$  servovalve loop gain 840 sec<sup>-1</sup>

\* Consult factory for parameters of other series valves.



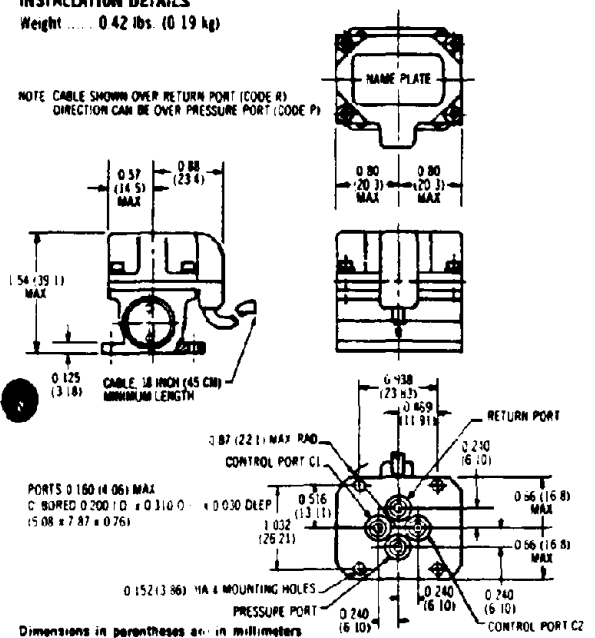
# STANDARD SERIES 30 SERVOVALVES

Standard design valves may be ordered by completing order form (see back cover).

## INSTALLATION DETAILS

Weight ..... 0.42 lbs. (0.19 kg)

NOTE: CABLE SHOWN OVER RETURN PORT (CODE R) DIRECTION CAN BE OVER PRESSURE PORT (CODE P)

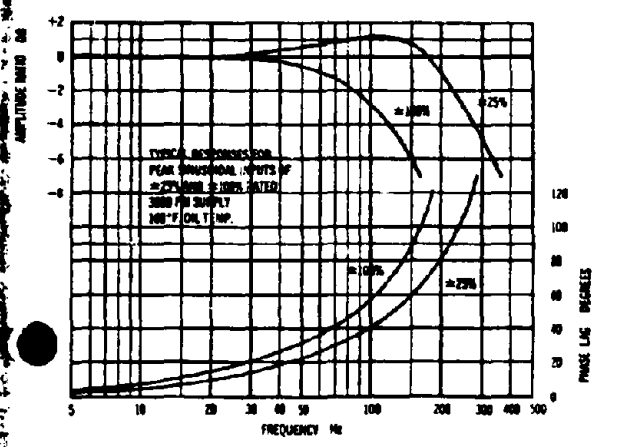


- specify rated control flow in gpm (l/min) or lps (l/s)
- use two digits and decimal point as indicated
- specified flow will be provided for test fluid (see page 10)
- lower rated flows available on special order
- specify supply pressure from 500 to 4000 psi (34.5 to 275.8 bar)
- lower and higher pressures available on special order

Flow Capacity vs. Supply Pressure

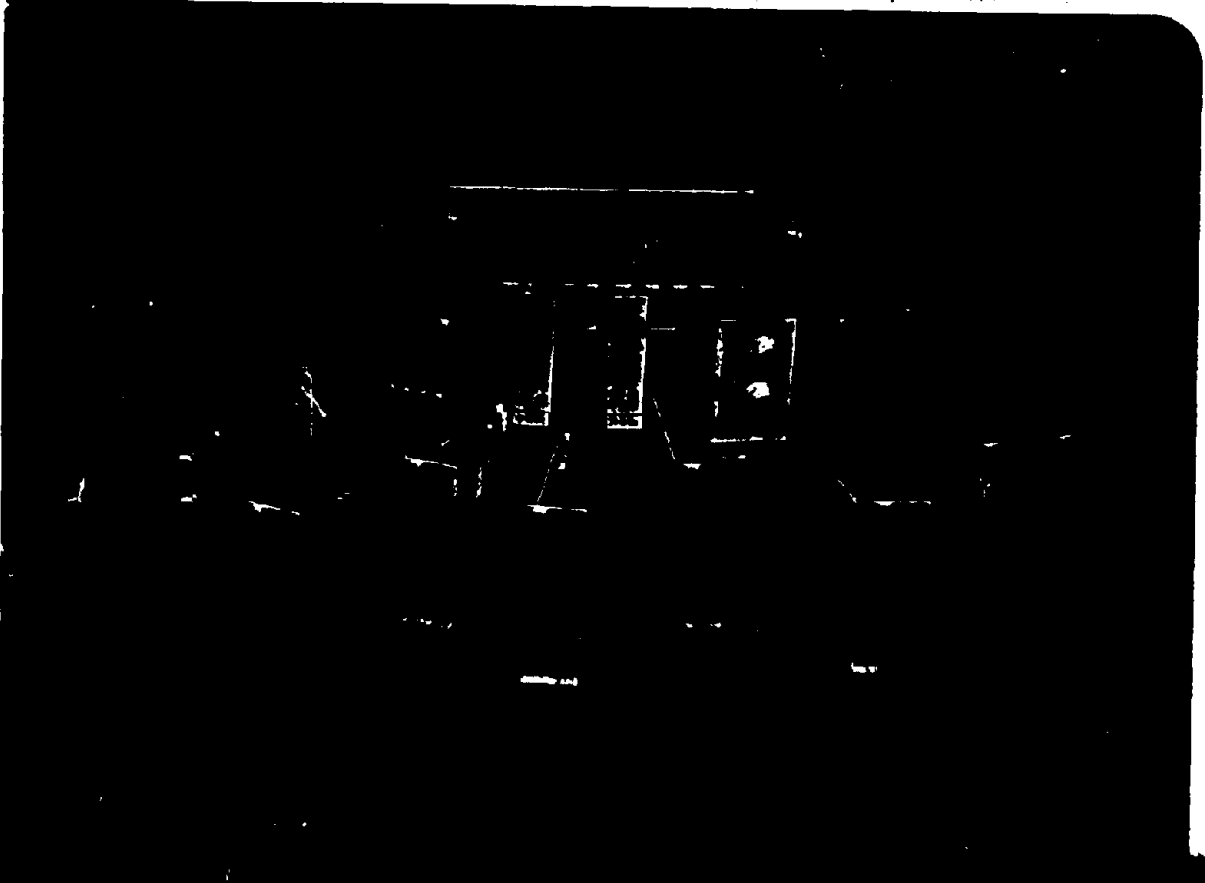
Flow Capacity (gpm)	Flow Capacity (l/min)	Flow Capacity (lps)	Flow Capacity (m³/hr)
1000	37.8	0.63	2.27
1500	56.7	0.945	3.405
2000	75.6	1.26	4.54
2500	94.5	1.575	5.67
3000	113.4	1.89	6.80
3500	132.3	2.205	7.94
4000	151.2	2.52	9.07

Typical frequency response for Standard Series 30 Servovalves shown below



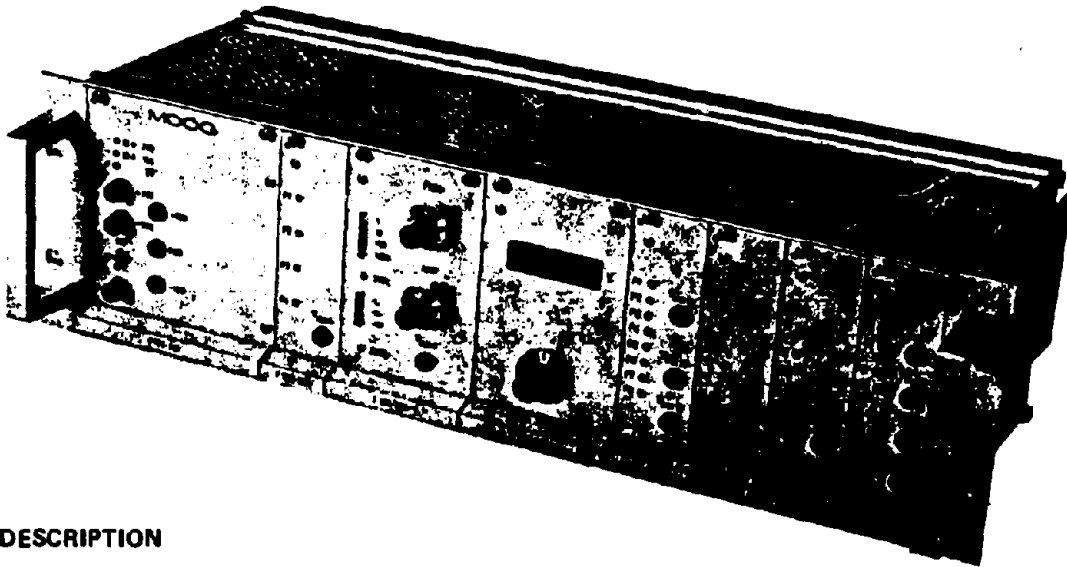
**MOOG**

**F120**



## MOTHER BOARD FRAME

F127-101



### DESCRIPTION

The MOOG rack mount module cage F127-101, is especially designed to accommodate the MOOG plugboards F120. The case will fit the standard 19" equipment racks or cabinets.

The cages are completely assembled with card guides installed for ten modules; one location reserved for the power supply unit.

The motherboard provides large buses for the supply voltages and GND.

The pin of each receptacle is also wired to a terminal strip to allow easy access for external wiring.

The MOOG modules allow access to all controls and test points on the front panel of each module.

### SPECIFICATIONS

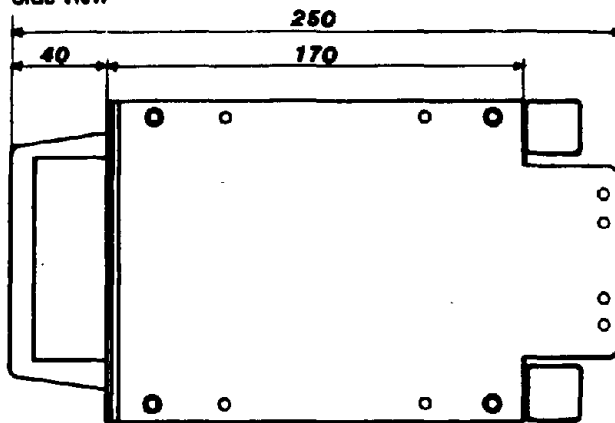
- standard 19" a rack mount module cage
- 1 plugboard location reserved for power supply (DIN 41612 style H)
- 9 plugboard locations (DIN 41612 style C)
- terminal strip for main power supply connection (220/110 VAC)
- terminal strip for output voltage of power supply  $\pm 15$  V,  $\pm 24$  V, and 5 V (option)
- 9 (32 pins) terminal strips, one for each plugboard location
- any supply failure triggers a relay
- contact rating : 0,25 A/24 VDC
- weight : 2,5 kg

# MOTHER BOARD FRAME

F127-101

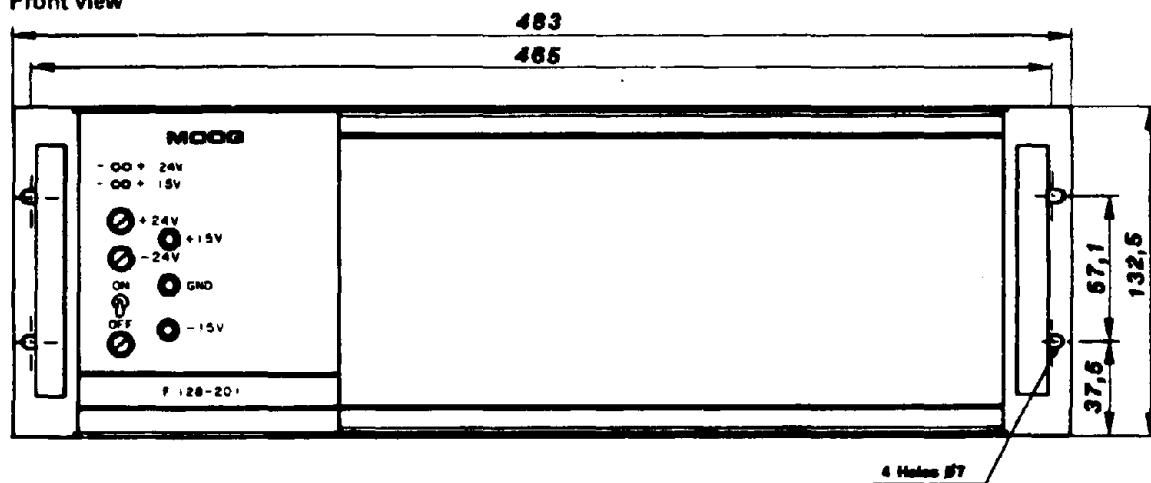
## INSTALLATION

Side view



Dimensions in millimeters

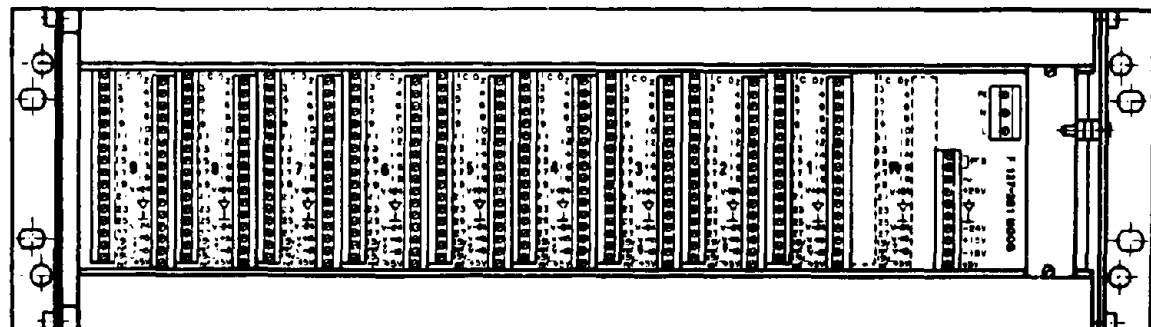
Front view



4 Holes Ø7

## CONNECTING

Rear view



# POWER SUPPLY

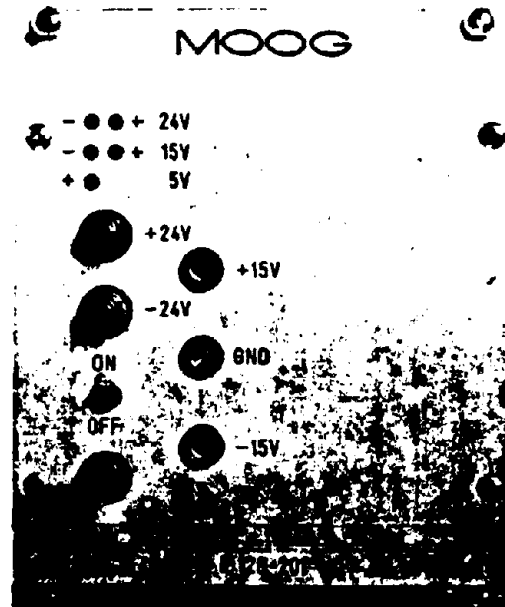
F128-201

## DESCRIPTION

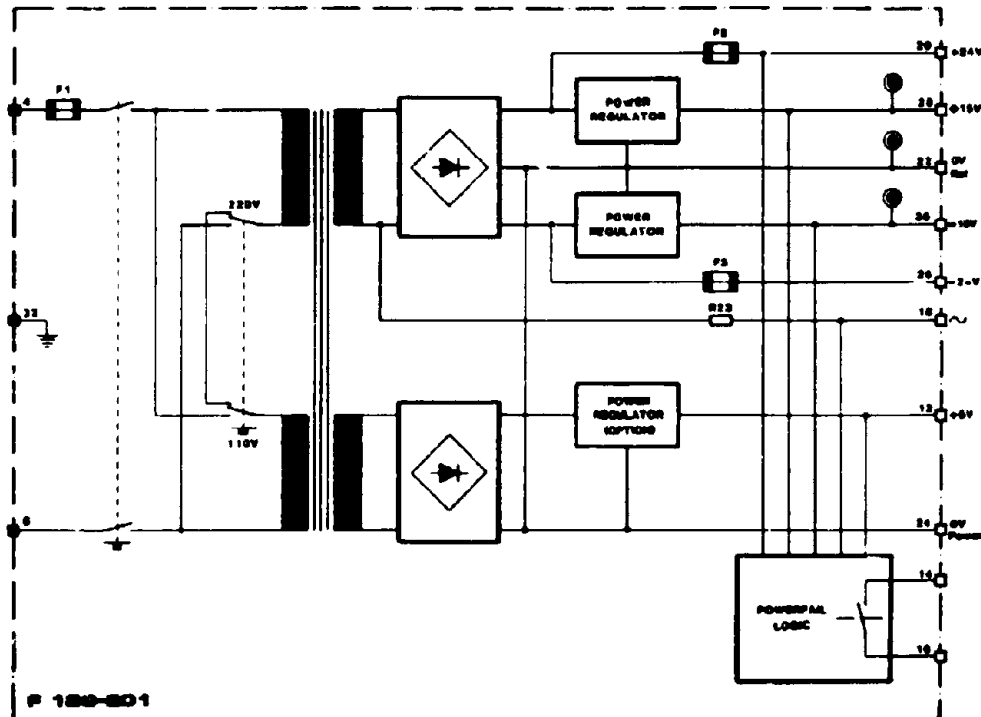
The stabilized, IC regulated power supply F128-201 was designed to operate the cards of the series F120. The entire power supply conveniently mounts in the chassis F127-101. Front panel controls include ON/OFF switch, jacks to measure the regulated 15 V and 5 V (option) outputs and LED indicators to show the presence of all voltages.

## SPECIFICATIONS

- Input voltage range : 210-230 VAC/50 Hz  
option 106-115 VAC/60 Hz
- Output voltage : + 15 VDC stab : 1.0 A max  
- 15 VDC stab : 1.0 A max  
+ 24 VDC not stab : 1.2 A max  
- 24 VDC not stab : 1.2 A max  
+ 5 VDC stab : 1 A max. (optional)  
note : the total source current of  
15 and 24 volt supplies may  
not exceed 1.2 Amp.
- 24 VDC fuses :  
Primary fuse : 1 Amp (slow blowing)
- Power failure detection : 15 V or 5 V supply failure triggers a  
relay contact rating : 0,25 A/24 VDC
- Weight : 1,7 kg
- Test points : jacks provided on front panel for  
GND, + 15 VDC, - 15 VDC,  
(and 5 VDC) outputs.



## BLOCK DIAGRAM



# SERVOAMPLIFIER

F122-202

## DESCRIPTION

The servoamplifier card F122-202, is a differential amplifier with PID control action, which supplies a servovalve with a current proportional to the difference of control and feedback voltage.

Controls to adjust amplifier gain, input sensitivity, null offset as well as test points for input and output signals are located on the front panel to allow fast and easy set up of an electrohydraulic control system.



## SPECIFICATIONS

power supply	$\pm 15$ VDC (stabilized)	input sensitivity	signal Vin 7 + P7
	$\pm 24$ VDC	offset	signal VR7 + P9 (0.. 100%)
input voltage range	pin 3, 20 to 10 VDC	proportional gain	P1 ( $\pm 750$ mV)
	pin 9, 10 to 120 VDC	differential gain	P2 (fine) R6 (coarse)
output capability	max current 50 mA	integral gain	P6, P8
	max voltage 10 V	Other	P5
proportional gain	5 to 200 mA/V	Test points	amplitude P4
linearity	$\pm 3\%$ of full scale	input voltage	frequency P3
temp. coefficient	0.1 mV/deg. C	output voltage	signal of terminal 3 at jack Vin 3
	between 10 to 50 degrees C		signal of terminal 7 at jack Vin 7
	(input resistance of 1000 Ohm		signal of terminal 8 at jack VR7
	and gain of 50 mA/V)		(signal taken after potentiometer
freq. response	-20 dB at 20 Hz		divider)
	with inductive load		
dither	amplitude 0 to 20 mV		
	frequency 20 to 30 Hz		
External control relays		voltage image of	jack 1sv (voltage drop across
consumption	15 mA/24 VDC	servo valve current	R 31 proportional to servovalve
contact rating	2 amp/24 VDC		current, R 31 = 20 Ohm $\pm 1\%$ )

## USE

The servoamplifier F122-202 is used in electrohydraulic control devices to directly drive a servovalve. This card can accommodate servovalves of up to 50 mA rated current.

## FUNCTION

The servoamplifier F122-202 consists of :

- a comparator with adjustable gain
- three amplifiers, comprising PID control action with gain of each amplifier independent of the others
- an output driver stage including an operational amplifier and two power transistors (this output stage employs current feedback to reduce the effects of coil impedance variations due to temperature).

# SERVOAMPLIFIER

F122-202

## INITIAL INSTALLATION

The setpoint voltage is applied to pin 3 of the servoamplifier. This voltage can be taken from a potentiometer supplied by  $\pm 15$  V or by any type of voltage generator as eg. the card F124-202.

The feedback voltage is then applied to pin 7. This voltage is generally derived from some sort of transducer (as eg. position, force) and must be of opposite polarity to the setpoint voltage. Potentiometer P7, is used to adjust the input sensitivity.

An additional input is available, which can accommodate the higher voltages encountered when using a tachometer for measuring speed.

Adjust the loop gain using P2 to the largest possible value to achieve best system performance regarding accuracy and speed. Increasing loop gain is limited by the system becoming unstable.

If integral control action is required, close jumper « I » to activate the integrator and adjust gain using P5 on front panel. Integral control allows to eliminate static errors in control loops. To disable integral control, jumper points 8 and 10 (relay K1 can be used).

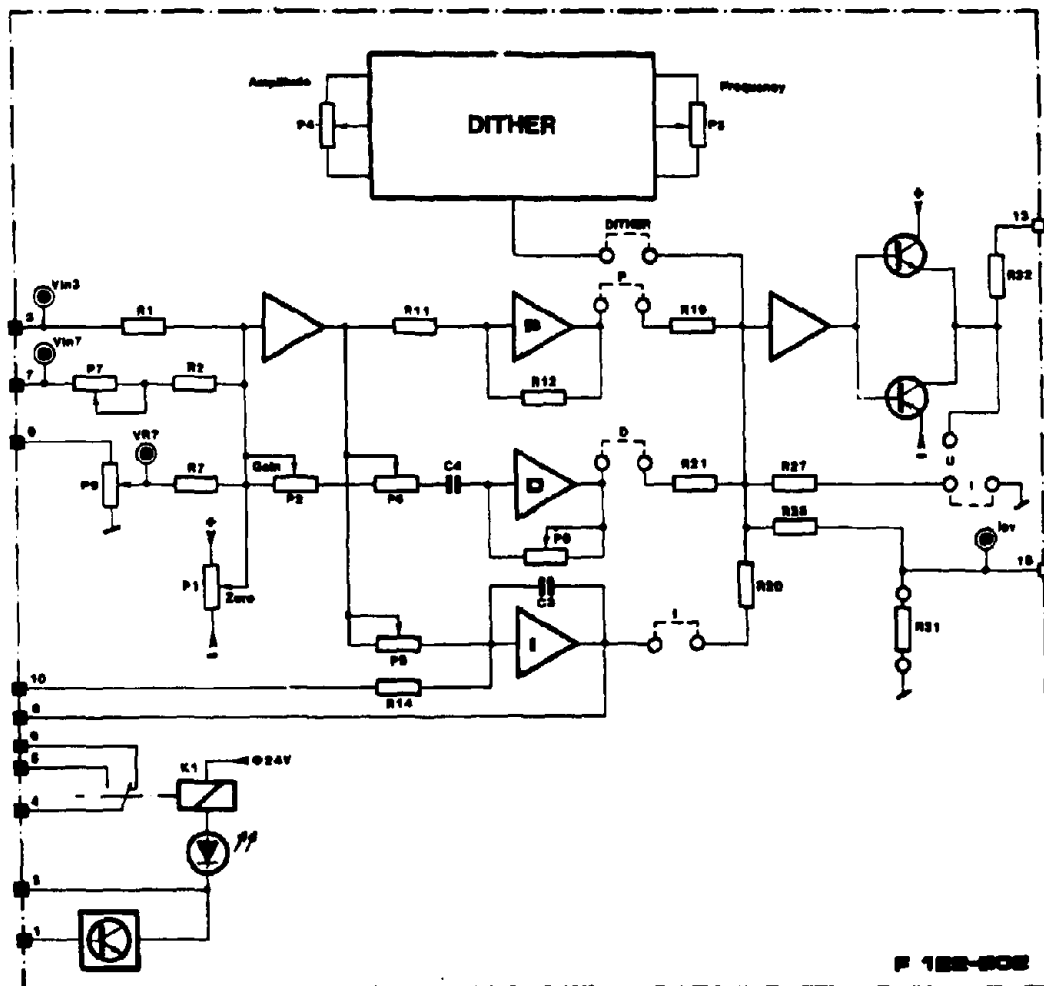
To achieve differential control, close jumper « D » and adjust gain using P6 and P8. Differential control improves system response and damping which has a stabilizing effect on the control element.

To activate the dither, close jumper « DITHER ». Use P4 to adjust dither amplitude and P5 for dither frequency.

To use voltage output close jumper « U ».

To use current output close jumper « I ».

## BLOCK DIAGRAM



# TEST MODULE

# F123-202

## DESCRIPTION

The card F123-202 allows to check twelve different voltages prewired on the mother board terminals. This card facilitates system adjustments, modifications or maintenance.



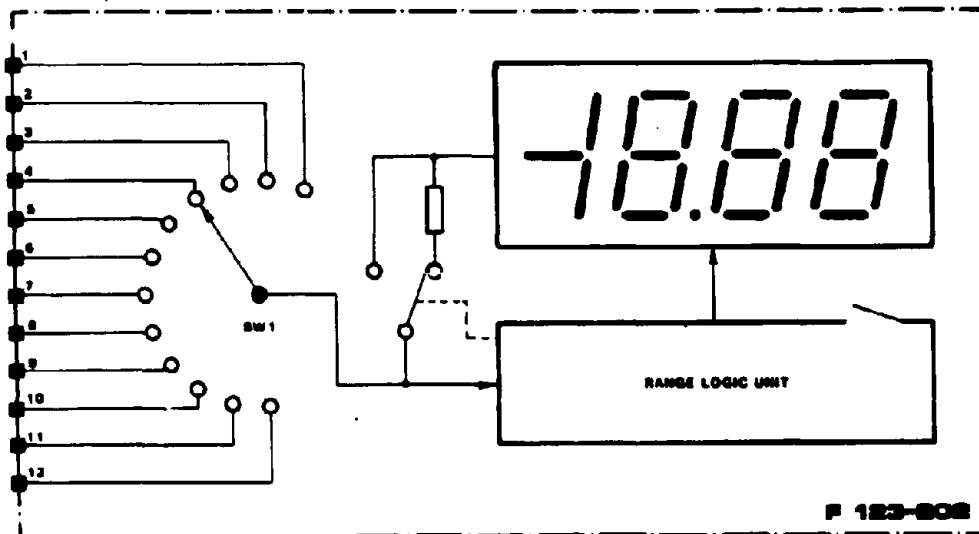
## SPECIFICATIONS

Power supply :  $\pm 15$  V stab. (100 mA each)  
Input Voltage ranges : 0 - 999 mV  
                          : 0 - 10 V  
Resolution : 1 mV  
Input Selection : switch on front panel  
Range Selection : automatic

## USE

This card allows permanent checking or adjustment of up to twelve different system parameters requiring frequent calibration or verification.

## BLOCK DIAGRAM



# ANALOG RAMP GENERATOR

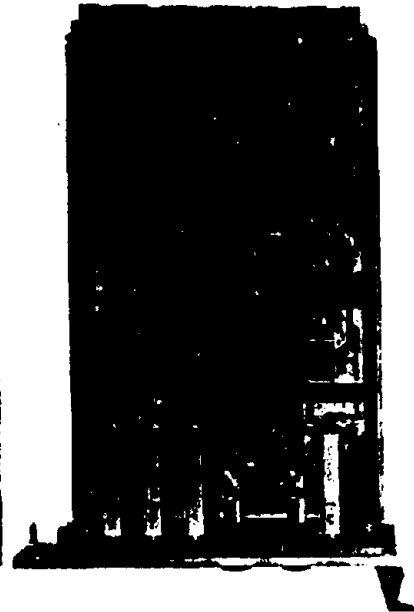
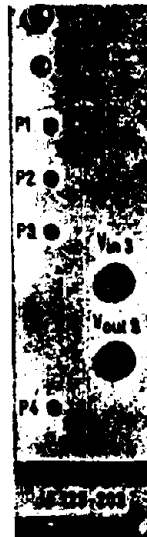
F123-203

## DESCRIPTION

The card F123-203 generates a ramp of adjustable slope. The output voltage of the card is ramped from its current value to the voltage applied to the card input. The slope can be either ascending or descending, depending on whether the input voltage is greater or less than the input voltage. When the ramp is completed, the output voltage is equal to the input voltage in amplitude and sign.

## SPECIFICATIONS

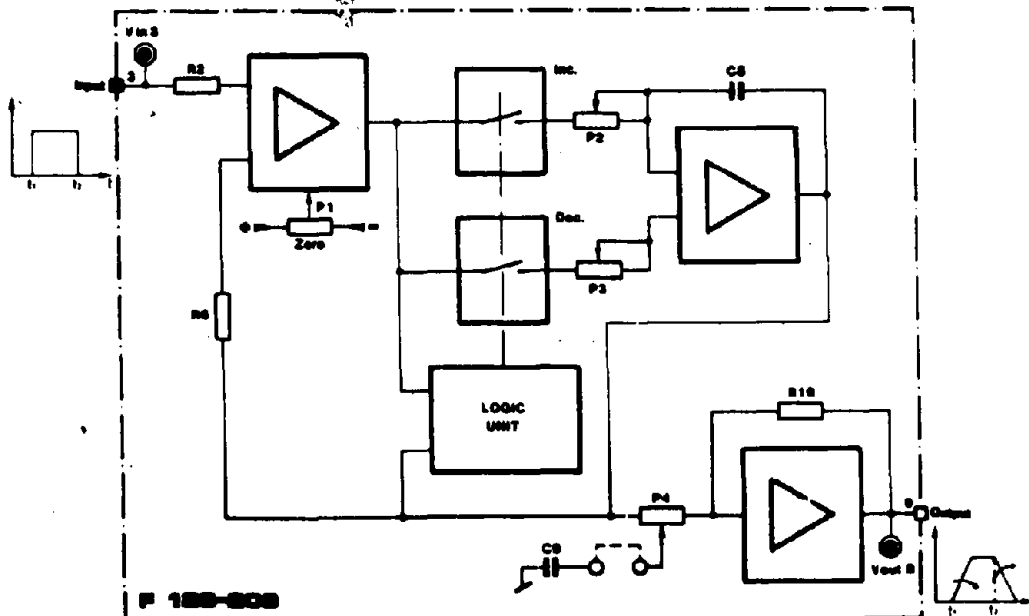
- Power supply :  $\pm 15$  VDC stable 20 mA
- Input voltage :  $\pm 10$  VDC max
- Output voltage :  $\pm 10$  VDC max
- Load impedance :  $\geq 100 \Omega$
- Slope range : 1.5 to 100 V/sec  
 this range may be modified as follows:  
 - by increasing the value of R10 for ascending slope and/or R15 for descending slope  
 - by increasing the value of capacitor C8
- Adjustments :  
 Ascending slope : P2 on front panel or ext. potentiometer  
 Descending slope : P3 on front panel or ext. potentiometer  
 Null shift : P1 on front panel  
 Rounding at end of slope : P4 (by jumper)
- Test points :  
 Input voltage : jack Vin 3 on front panel  
 Output voltage : jack Vout 2 on front panel



## USE

The card F123-203 can be used in a speed control device to allow precise control of acceleration and deceleration. In a position controlling device it allows movement at a constant and adjustable speed.

## BLOCK DIAGRAM



# OSCILLATOR/DEMODULATOR

F123-204

## DESCRIPTION

The card F123-204 is a position demodulator intended for use with a LVDT position encoder. The oscillator circuit generates a sinusoidal waveform to drive the primary coils of the LVDT. The demodulator stage uses the signal returned by the secondary coils to generate a DC voltage directly proportional to the displacement of the core within the LVDT.

## SPECIFICATIONS

Power supply :  $\pm 15$  VDC stab. (25 mA each)

Oscillator output :

- Voltage : 4.5.. 11 Vpp (500 mA)
- Frequency : 0 to 2500 Hz

Demodulator output :

- Voltage : 0 ...  $\pm 10$  VDC adjustable
- Load impedance : 2 kOhm min.

Adjustments

Oscillator :

- Frequency adjustment : P1
- Output voltage : P2

Demodulator :

- Output voltage : P3
- Zero offset : P4

Test points

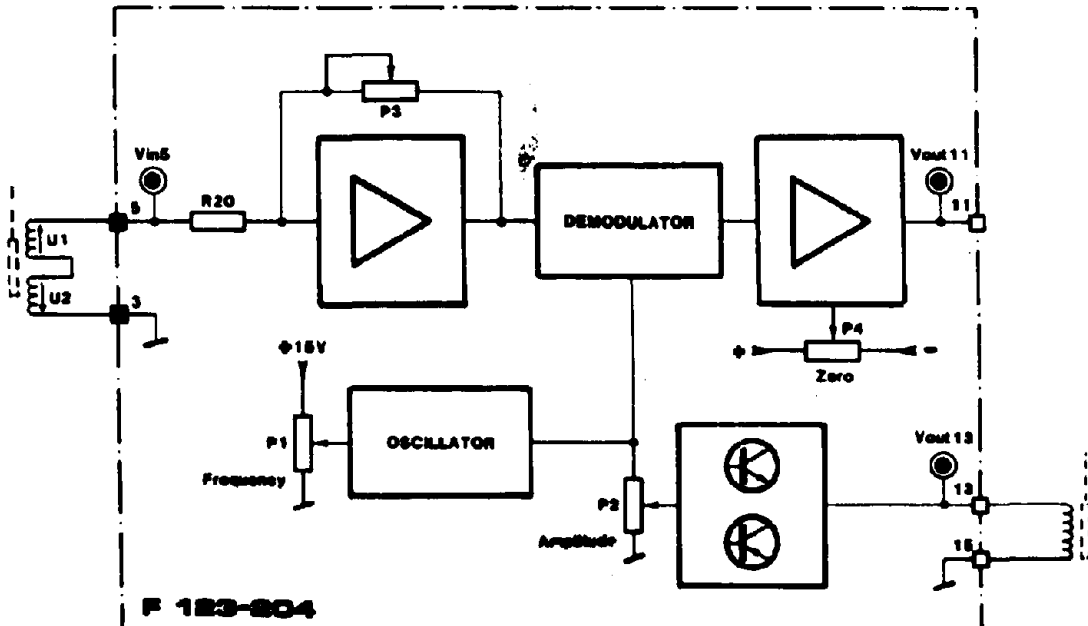
- Oscillator output voltage : jack Vout 13
- Demodulator input voltage : jack Vin 5
- Demodulator output voltage : jack Vout 11



## USE

This card is used in electrohydraulic control loops using LVDT position encoders to supply a continuous voltage in direct proportion to sign and amplitude of the positioning element.

## BLOCK DIAGRAM



# COMPARATOR

F123-205

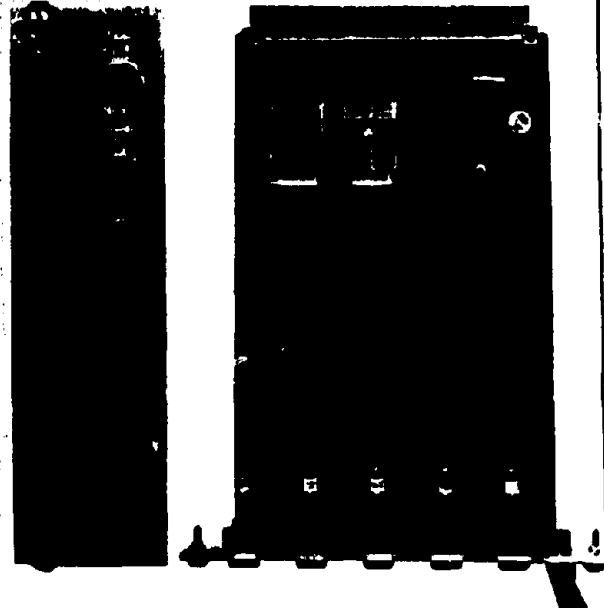
## DESCRIPTION

The F123-205 card can compare two variable analog voltages or can be used as a threshold detector regarding a preset voltage.

The two relays K1 or K2 will be switched according to the result of the comparison.

$K1$  and  $K2$  = OFF for  $U_1 = U_2$   
 $K1$  = ON,  $K2$  = OFF for  $0 < (U_1 - U_2)$   
 $K1$  = OFF,  $K2$  = ON for  $(U_1 - U_2) < 0$

Two adjustable trigger threshold, adjustable hysteresis effect and adjustable delay time are employed to provide reliable switching characteristics.



### SPECIFICATIONS

Power supply: 12V DC  
 Input voltage range: 10V  
 Input resistances: 100 kΩ  
 Relay outputs: 2 SPDT contact  
 Contact rating: 2A/250V AC  
 Time constant: 0 to 10 seconds  
 Trigger threshold: 0 to 10V  
 Adjustments:  
 - Preset voltage: P1 (fine)  
 - Hysteresis: R 25 (fine)  
 - Threshold: P3 (for K1)  
 - Delay time: P2 (fine) range 0.1 to 10 seconds  
 - constant  
 - Delay time annulation: by jumper  
 Test points:  
 - Preset voltage: Jack V<sub>ref</sub>  
 - Error: Jack TP 1  
 - Error delayed: Jack TP 2  
 - Threshold: Jack K1 - TP 1  
 - K2 - TP 2

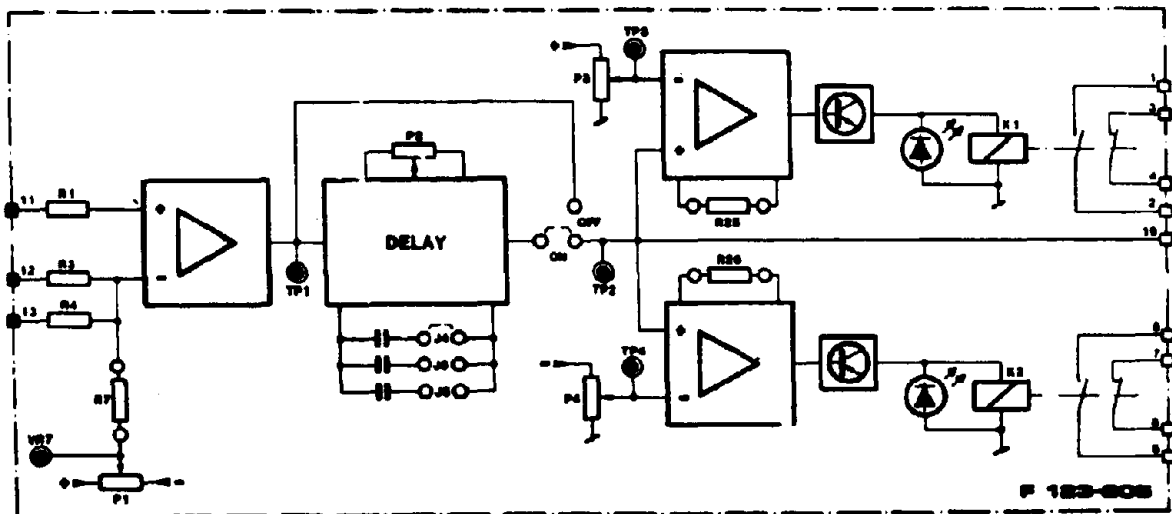
**Indicators**  
 Two LED indicators on front panel show ON/OFF state of relays.

## USE

The F123-205 card has been specially adapted to the use in analogic circuits where it is necessary to monitor the amplitude of a voltage that represents eg. position or speed.

The output of this card can then be used to give an alarm when a preset maximum value has been exceeded or to signal a sequence controller that the set point has been reached.

## BLOCK DIAGRAM



F 123-205

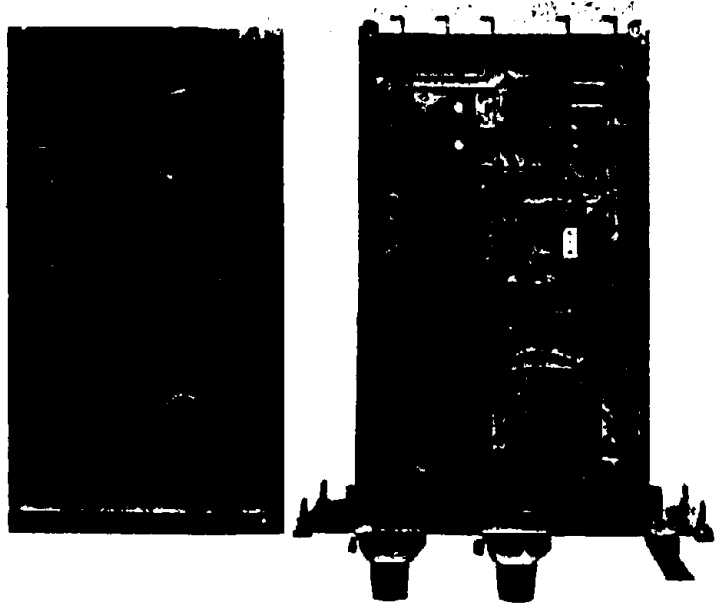
# FUNCTION GENERATOR

F123-206

## DESCRIPTION

The F123-206 card generates a sinusoidal, triangular or square wave voltage of adjustable amplitude and frequency.

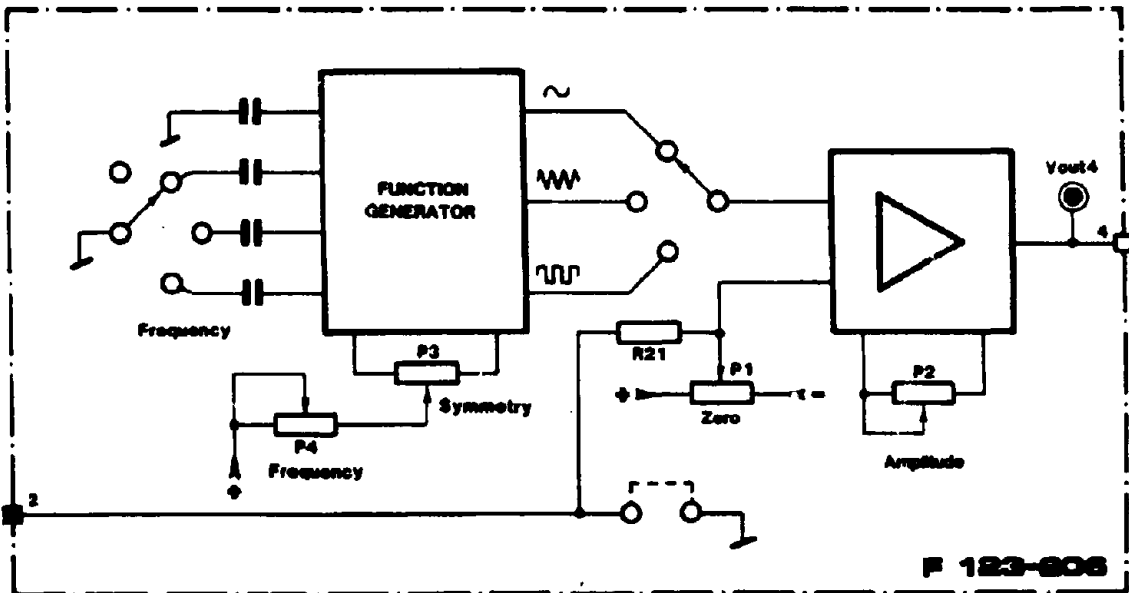
This card can be used as a controller for position, speed, force, for example in automated test stands and fatigue test stands or wherever a set point voltage is required that varies according to sinusoidal, triangular or square wave functions.



## SPECIFICATIONS

Power supply	: $\pm 15$ V stab. (30 mA each)	Test points	
Output signal	: sinus, triangular, square wave voltage	Output voltage	: jack Vout 4
Amplitude	: $\pm 10$ V pp max.	Adjustments	
Load impedance	: $> 2$ kOhm	Waveform selection	: switch
Frequency range	: range A : 0,1 to 1,5 Hz range B : 1 to 15 Hz range C : 10 to 150 Hz range D : 100 to 2000 Hz	Frequency range	: switch
		Frequency adjustment	: 10 turns potentiometer with vernier scale
		Output amplitude	: 10 turns potentiometer with vernier scale
		Null shift adjust.	: P1
		Waveform symmetry	: P3

## BLOCK DIAGRAM



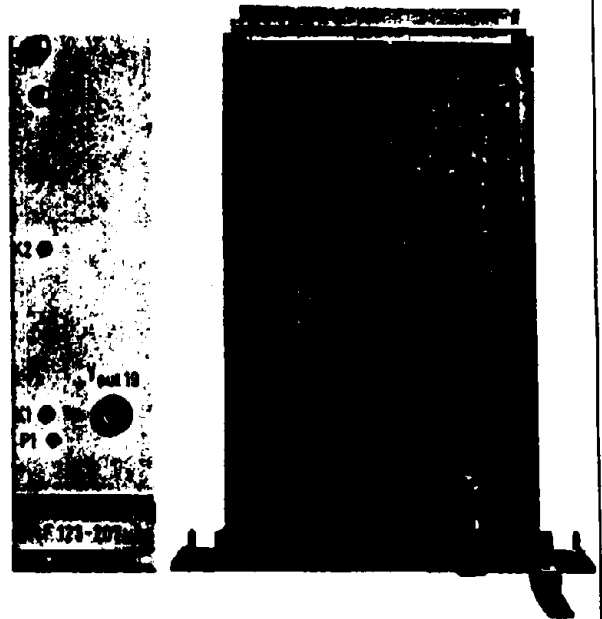
# RELAY CARD

F123-207

## DESCRIPTION

The card F123-207 consists of :

- a potentiometer and resistor voltage divider which allows to adjust an output voltage between + 15 V and -15 V. This output voltage can also be switched by a relay externally controlled.
- A relay with a high contact rating to switch external devices.



## SPECIFICATIONS

- Power supply : ± 15 VDC (lab) + 24 VDC
- Relays : K1 - consumption : 15 mA at 24 V DC contact rating : 0,25A/24 V DC K2 - consumption : 25 mA at 24 V DC contact rating : 2A/24 V DC contacts : 4 x SPDT

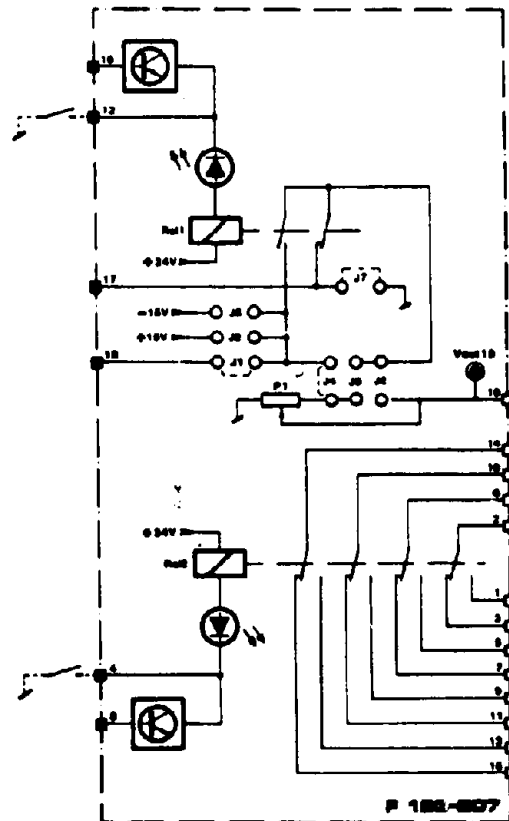
### Adjustments :

- Output voltages : P1 (R1, R2, R3)
- Function selection :
  - jumpers select input voltage for potentiometer : + 15 V (J2), -15 V (J3) or ext. voltages (J1)
  - jumpers select output voltage :
    - J4 - output is potentiometer output direct
    - J5 - output is potentiometer switched by relay
    - J6 - output is input voltage switched by relay

### Test points :

- Potentiometer output voltage : test Vout 19

## BLOCK DIAGRAM

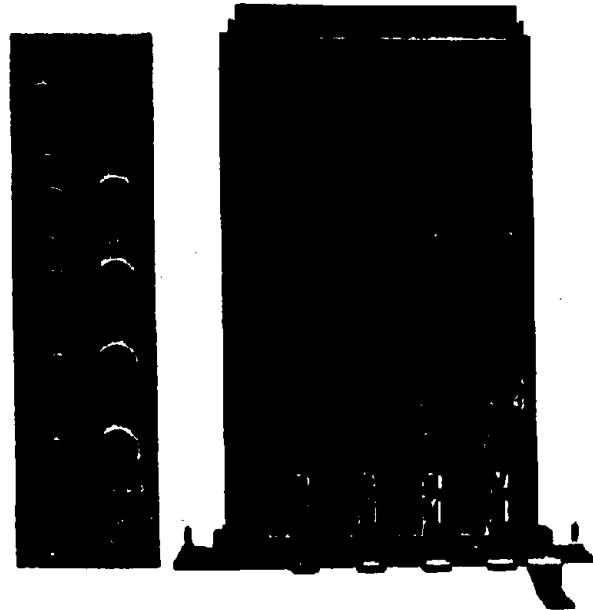


# PERMASET POINT CARD

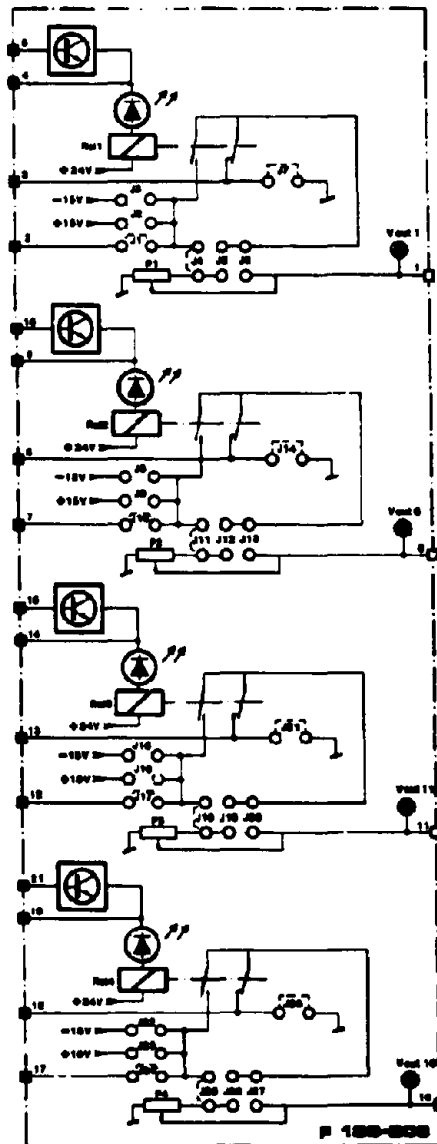
F123-208

## DESCRIPTION

The card F123-208 allows four set point voltages to be set between -15 VDC to + 15 VDC. These voltages can be used as set point values for a control device such as position or velocity controller. The set point voltages can also be switched by relays externally controlled.



## BLOCK DIAGRAM



## SPECIFICATIONS

Power supply :  $\pm 15$  VDC Stab  
 $\pm 24$  VDC

Relays : consumption = 15 mA/24 VDC  
 contact rating = 2 A/24 VDC

### Adjustments :

- Output voltages :
  - potentiometer 1 - P1 (R1-R2-R3)
  - potentiometer 2 - P2 (R6-R7-R8)
  - potentiometer 3 - P3 (R11-R12-R13)
  - potentiometer 4 - P4 (R16-R17-R18)

### Function selection :

- Jumpers select input voltage for each potentiometer + 15 V, -15 V or ext. voltage
- Jumpers select each output voltage :
  - J4, J11, J18, J25 : output is potentiometer output direct
  - J5, J12, J19, J26 : output is potentiometer switched by relay
  - J6, J13, J20, J27 : output is input voltage switched by relay

### Test points :

- Output voltage :
  - potentiometer 1 : jack Vout 1
  - potentiometer 2 : jack Vout 6
  - potentiometer 3 : jack Vout 11
  - potentiometer 4 : jack Vout 16

## SINGLE SIGNAL CONDITIONER

F123-209

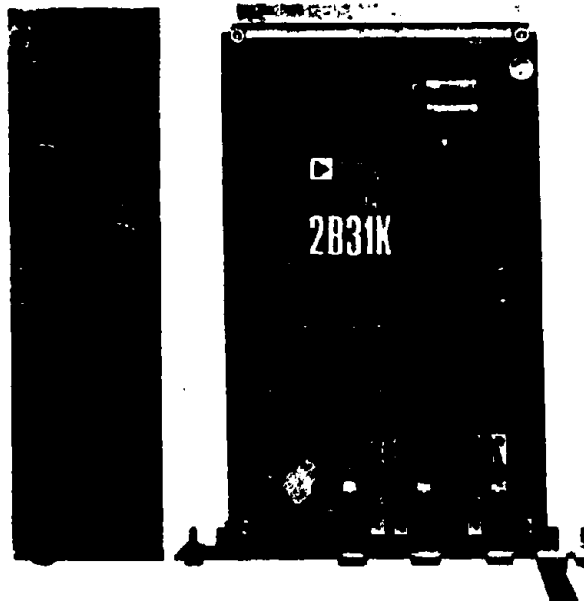
### DESCRIPTION :

The card F123-209 supply sensors like strain gages pressure transducers and load cells with necessary supply voltages and amplifies their output signal.

The supply voltage can be monitored via a remote sense line to provide temperature compensation and compensation of line voltage drop when using excessively long connections between sensor and conditioner card.

Three selectable amplifier ranges allow adaptation to a wide range of sensors.

The output from the sensor can be passed through a low pass filter to provide a smoother signal.



### SPECIFICATIONS

Power Supply : 15 VDC max (10 VDC min)  
Sensor Supply voltage : adj. 9 - 11 VDC  
Output Voltage : adj. 0 - 10 VDC  
Bridge Resistance : 80 - 1000 ohms  
Sensor Ranges : a) 0.75 to 1.5 mV/V  
                  b) 1 to 2 mV/V  
                  c) 1.5 to 3 mV/V  
Filter cut-off Frequency : 2 to 5000 Hz  
Test points :  
Gage Zero Offset : Jack Vout 16  
Unfiltered Output : Jack Vout 18  
Filtered Output : Jack Vout 17

Adjustments  
Sensor Supply Voltage : P1 on front panel  
4 - wire sensor - close jumpers J4, J5  
6 - wire sensor - open jumpers J4, J5  
Remote Sense Offset : P2 on front panel  
Sensor Gain : close J1 to select 0.75 to 1.5 mV/V  
                  close J2 to select 1 to 2 mV/V  
                  close J3 to select 1.5 to 3 mV/V  
Low Pass Filter : R7, R8, R9 (see table 1)  
Offset Output Stage : P3  
Output Voltage Level : P4  
Calibration : resistor R2  
                  Select via jumper J6, J7  
                  activate calibration via switch on  
                  front panel (or ext. contact)

### USE

The card F123-209 is used with pressure transducers or similar gages integrated into a control loop using a servo amplifier card like the F122-202.

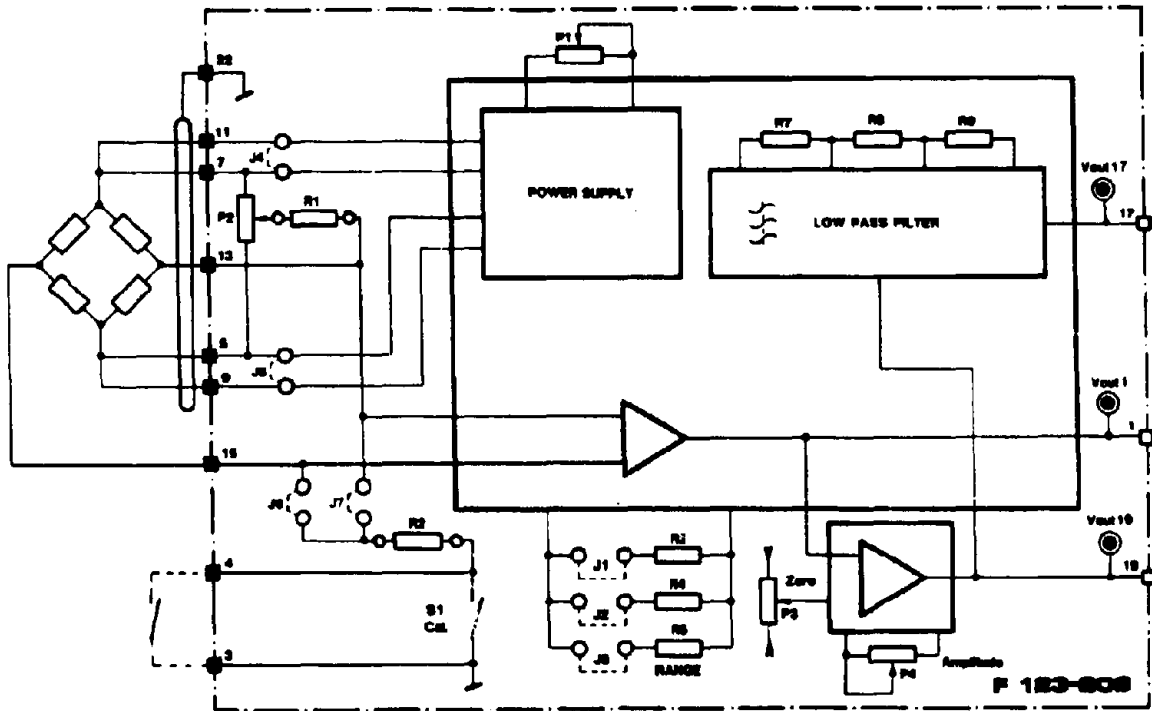
### INITIAL INSTALLATION

- Select the power supply mode of the sensor (4 wires or 6 wires for remote sensing) and adjust the supply voltage to 10 VDC.
- Adjust the sensor zero offset at null pressure.
- Adjust the zero offset of the output stage to read 0 VDC.
- Adjust the output level of the amplifier at max. pressure, or use the calibration resistor.
- Eventually readjust the zero setting of the output stage.

**TABLE 1**  
Filter cut off Frequency

F (HZ)	R9 (KΩ)	R8 (KΩ)	R7 (KΩ)
2	∞	∞	∞
5	1270	2050	383
10	523	806	154
50	40	137	26,7
100	44,2	68,1	13,3
500	8,66	13,3	2,61
1000	4,32	6,65	1,3
5000	0,866	1,33	0,261

**BLOCK DIAGRAM**



# AUXILIARY FUNCTIONS UNIT

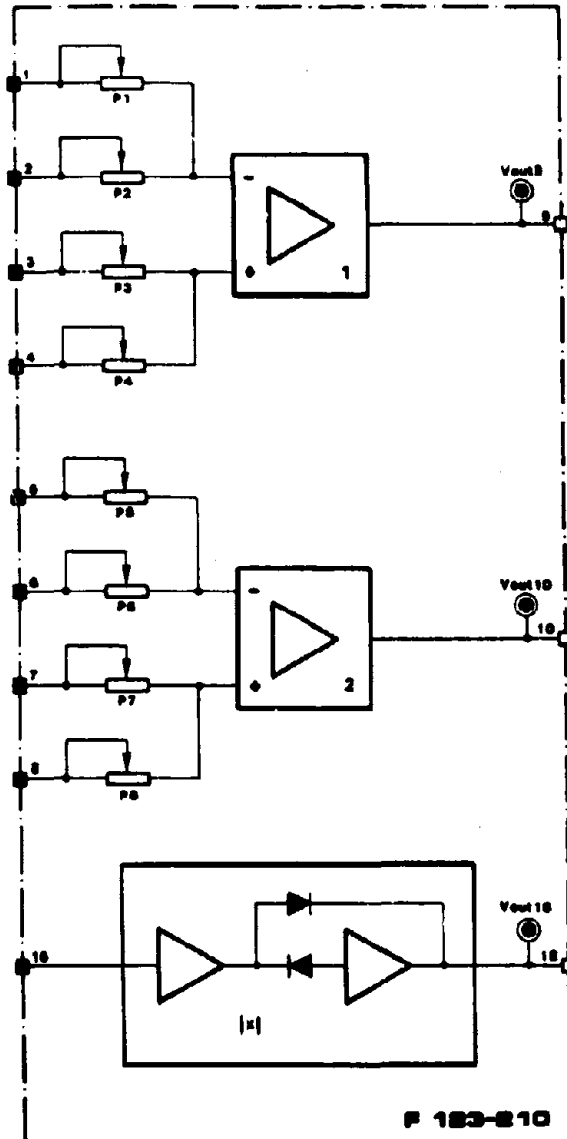
F123-210

## DESCRIPTION

The F123-210 card contains a number of auxiliary analog functions often needed to implement an analog control scheme. This card makes available two amplifiers with 4 inputs each and a precision rectifier.



## BLOCK DIAGRAM



## SPECIFICATIONS

- Power Supply :  $\pm 15$  VDC stab (15 mA each)
- Output Voltages :  $\pm 10$  V max
- Input Impedance : amp 1 = 100 kohm
- : amp 2 = 100 kohm
- : rectifier = 20 kohm
- Load Impedance : 2 kohm min
- Gain : amp 1 and amp 2 =  $\pm 1$
- : rectifier = +1

### Adjustments

- amp 1 gain : P1, P2, P3, P4
- amp 2 gain : P5, P6, P7, P8

### Test Points

- ampli 1 output : jack Vout 9
- ampli 2 output : jack Vout 10
- rectifier output : jack Vout 18

## USE

The amplifiers on this card can be used as either adders, subtractors or inverters needed to complete a control scheme being realized with MOOG standard cards of the series F 120.

The precision rectifier can be used to obtain the magnitude (absolute value) of a voltage, which can then be compared to a fixed voltage for threshold detection using MOOG card F123-205.

## DUAL SIGNAL CONDITIONER

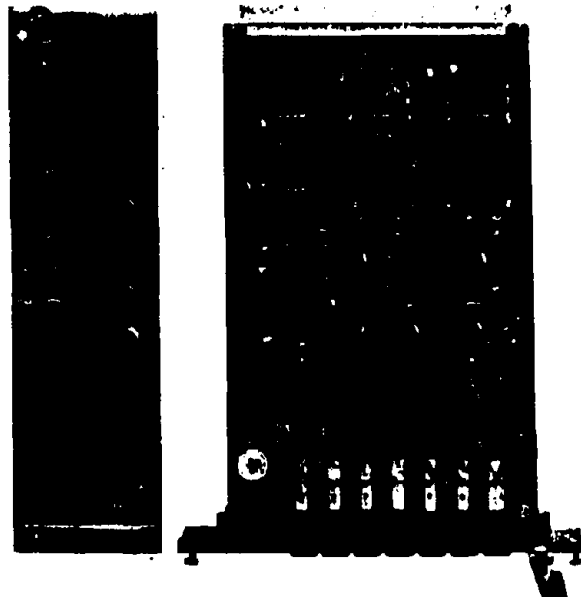
F123-211

### DESCRIPTION

The card F123-211 supplies two sensors like strain gages, pressure transducers and load cells with the necessary supply voltages, amplifies their output signal and delivers an electrical signal proportional to their sum or their difference such as  $\Delta = \pm \alpha P1 \pm \beta P2$ ,  $\alpha$  and  $\beta$  being comprised within zero and one.

Three selectable amplifier ranges allow adaptation to a wide range of transducers.

Trimming potentiometers and test points are located on the front panel.



### SPECIFICATIONS

Power Supply	: $\pm 15$ VDC	Test Points	Output transducer 1	: P1 and - P1
Sensor Supply Voltage	: adj. 0 to 10 Vdc	Output transducer 2	: P2 and - P2	
Output Voltage	: adj. 0 to $\pm 10$ Vdc	Output divided	: $\alpha$ and $\beta$	
Bridge Impedance	: 350 ohms	Output summation	: $\Delta$	
Sensor Ranges	: 0.75 to 1.5 mV/V	Adjustments		
	: 1 to 2 mV/V	Sensor Supply Voltage	: P1	
	: 1.5 to 3 mV/V	Sensor Zero Offset	: P6 and P7	
		Sensor Output Voltage	: P4 and P5	
		Sensor Gain	: close J1-J4 to select 0.75 to 1.5 mV/V	
			: close J2-J5 to select 1 to 2 mV/V	
			: close J3-J6 to select 1.5 to 3 mV/V	

### USE

The card F123-211 is suitable to be used in a control loop using servo-amplifier card like F122-202 in conjunction with two pressure transducers, each output being used differentially or independently.

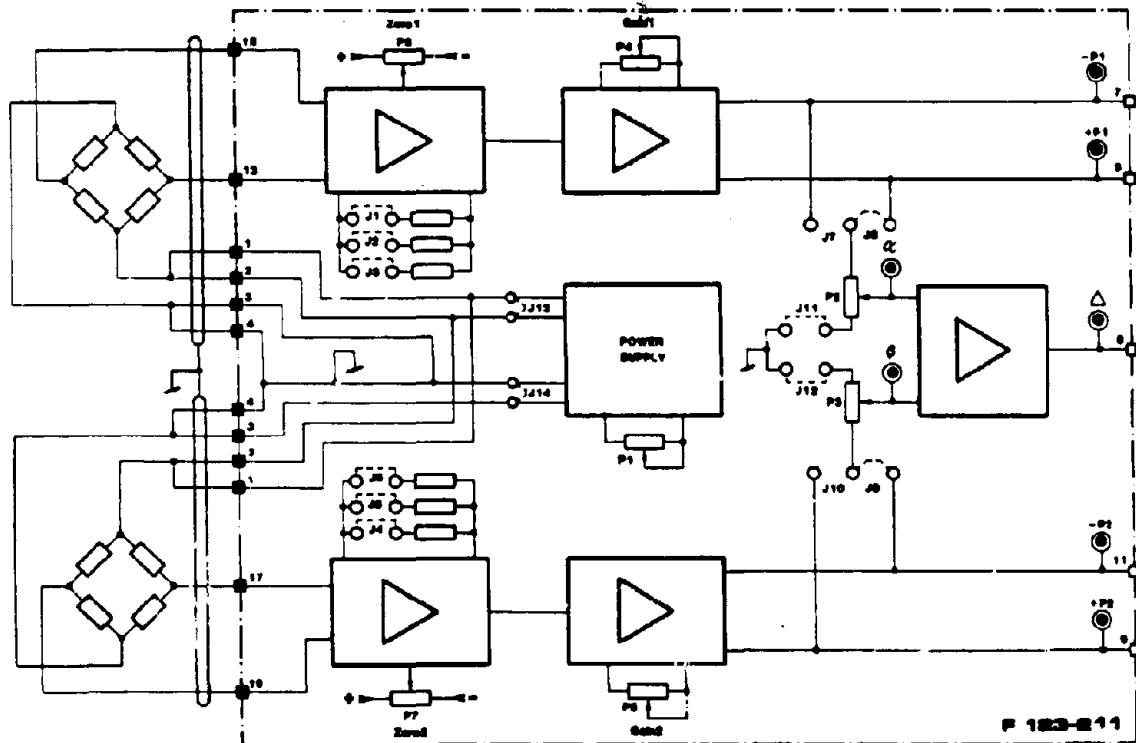
### INSTALLATION

- Connect the sensors (+ excitation : 1-2, - excitation 3-2)
- Select the proper sensor gain
- Adjust the sensor supply voltage by P1
- Adjust each zero offset with a null pressure by P6 and P7
- Adjust each output level by P4 and P5
- If differential output is used, select the mode (close jumper J11 and J12) and adjust the dividers  $\alpha$  and  $\beta$ .

# DUAL SIGNAL CONDITIONER

F123-211

## BLOCK DIAGRAM



# PROGRAMMABLE FUNCTION GENERATOR

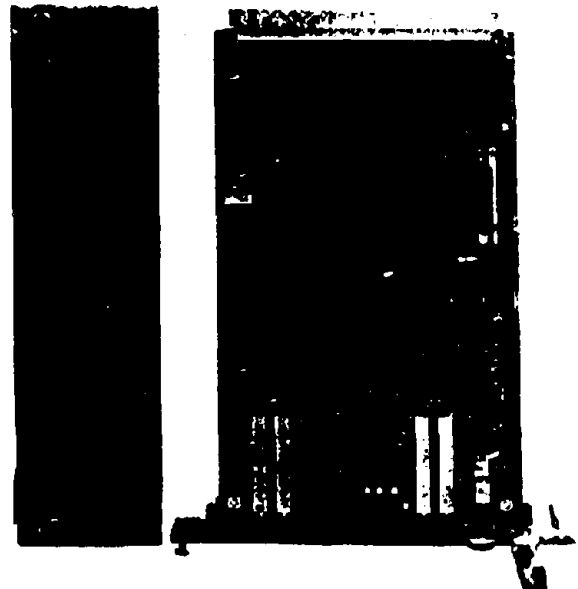
F124-201

## DESCRIPTION

The card F124-201 is a function generator which converts a function stored in PROM memory in digital form to an analog voltage. This allows any type of function once defined and stored into PROM to be used in a control system.

The stored function can be regenerated as either a continuous voltage-time waveform (X-T mode) using a clock frequency or as a voltage-voltage converter (X-Y mode) using an external input voltage.

Several cards F124-201 can be coupled to generate more complex synchronized waveforms.



## SPECIFICATIONS

Power supply :  $\pm 15$  VDC stab (80 mA each)  
+ 5 VDC stab 15 mA  
(internal J 19 external J 20)

Prom :

- type 2704 class J12-J13-J16-J18 (512 samples)
- type 2708 class J11-J13-J16-J17 (1024 samples)
- type 2716 class J11-J14-J15-J17 (1024 samples)

Function resolution :

- 8 bit resolution (0-255)

X-T mode :

- function in PROM regenerated using time base
- range 1 : 0,2 to 2 seconds
- range 2 : 2 to 20 seconds
- range 3 : 20 to 200 seconds
- range 4 : external clock frequency (Frequency 5 KHz)  
(Vpp = 5 V)

X-Y mode :

- function in PROM used as voltage-voltage converter (input voltage range : 0 to + 10 VDC or - 10 to - 10 VDC)

Output voltage :

- 0 to + 10 VDC or - 10 to + 10 VDC

Single/Continuous :

- in X-T mode, stop after one pass thru PROM or generate continuous waveform

Stop :

- in X-T mode, stops clock generator (waveform)

End of cycle :

- in X-T mode a + 5 V pulse of 5 ms duration signals end of pass thru PROM

Test points :

- output full voltage : jack Vout 8
- output adjustable voltage : jack Vout 10

Adjustments :

Frequency :

- P1 on front panel  
(range by ext. switch or jumpers on circuit board)

Amplitude :

- P5 on front panel

Mode selection :

- output voltage : see table 1

- input voltage : see table 1

- X-T, X-Y : see table 1

- single/continuous : switch or ext. signal

- stop X-T : switch or ext. signal

## USE

Especially designed to be used in automatic control of different types of hydraulic devices, the card F124-201 is used as a programmable function generator between classic designs (sine, triangle and squarewave generators) and more evolved systems using microprocessors.



# DIGITAL RAMP GENERATOR

F124-202



## DESCRIPTION

The card F124-202 is a ramp generator with output amplitude and slope being adjustable. The card can produce either symmetrical triangle or sawtooth waveforms. Pressing START does one cycle ; i.e. ramps the output voltage to the set point value and then back to the initial value. The ramp can be stopped at any time by pushing the « STOP » button and then resumed by pressing START again.

To stop the output voltage at the set point value close jumper J3. The descending ramp will start by an external signal (pin 15) or by pushing the START button.

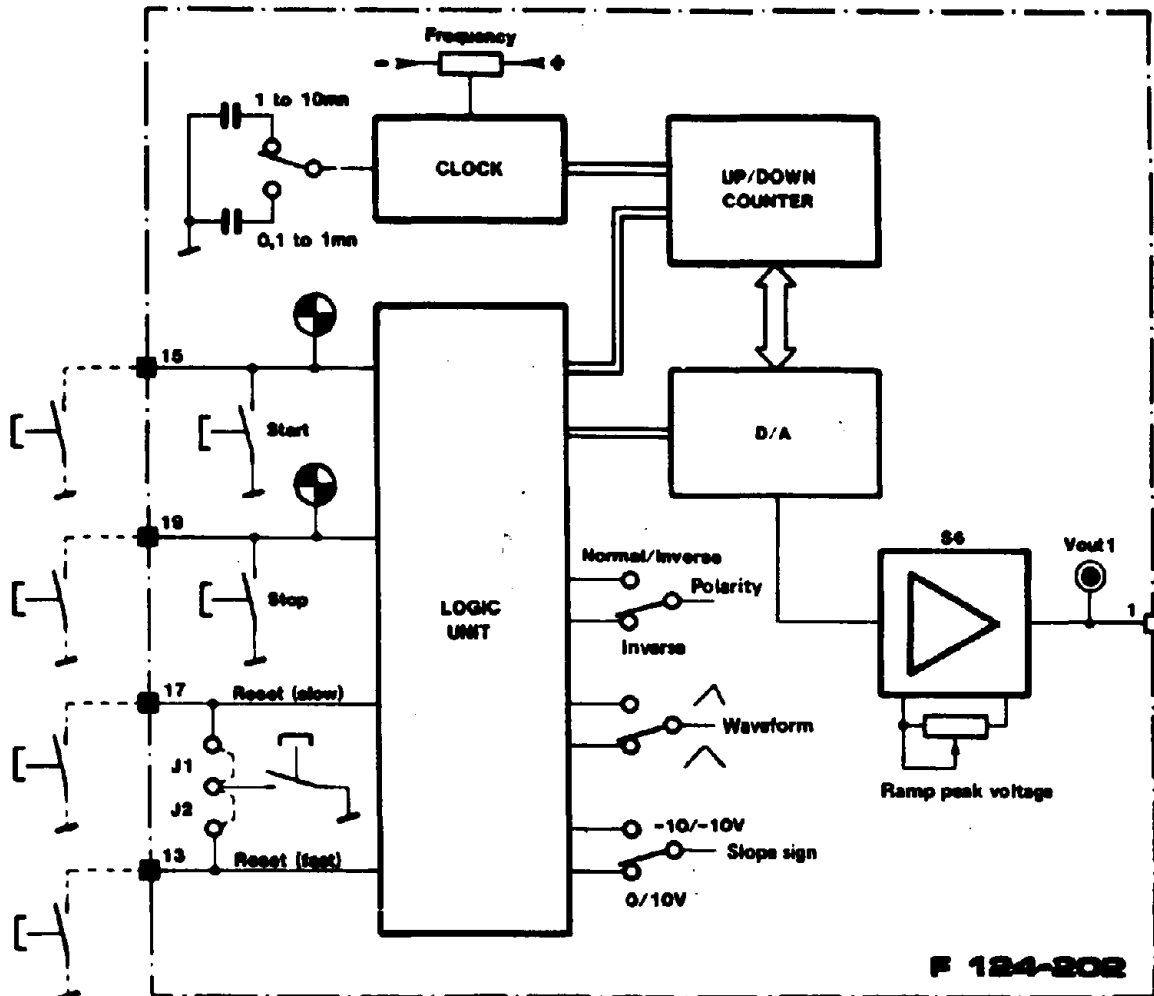
## SPECIFICATIONS

Power supply : ± 15 VDC stab (40 mA)	Output polarity : toggle switch
+ 5 V stab - 10 mA	Stop signal : toggle switch
Output voltage : 0 - 10 V	Waveform : toggle switch selects triangle/sawtooth
Load impedance : 2 k Ohms	Test cycle : push button or ext. contact resets ramp generation to 0
Frequency range : 1 - 80 Hz	Freeze ramp : push button or ext. contact freezes ramp
Test points : direct on board	Start ramp : push button or ext. contact starts ramp
Ramp output voltage : 0 - 10 V	Resume ramp after STOP : push button or ext. contact starts ramp
Adjustments :	
Ramp peak voltage : 10-turn potentiometer	
Slope : 10-turn potentiometer	
Waveform : selected by toggle switch	

## USE

The card F124-202 is an automatic voltage generator for control of speed, position, pressure or force where very slow set point voltage ramps are required.

BLOCK DIAGRAM



# PRESELECTION COUNTER

F124-203

Reproduced from  
best available copy.

## DESCRIPTION

The card F124-203 consists of an up/down counter which can be preset via front panel BCD switches.

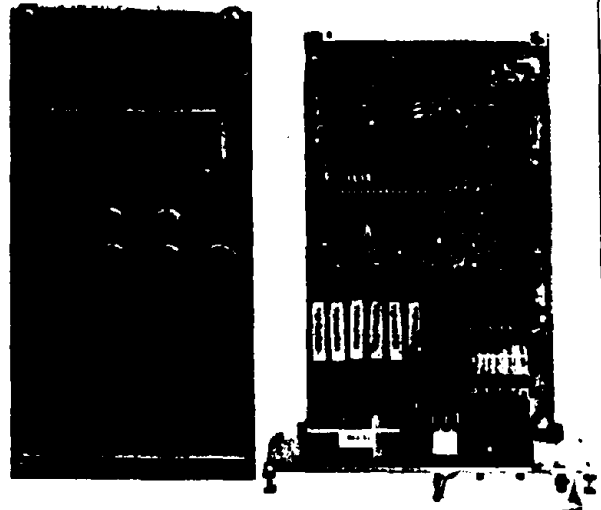
This card then counts the number of preset pulses, either digital (TTL or CMOS compatible) or analog signals via a schmitt-trigger input.

When the final count is reached (0 when counting down from preset value, or preset value when counting up from 0) a relay and an analog switch are toggled.

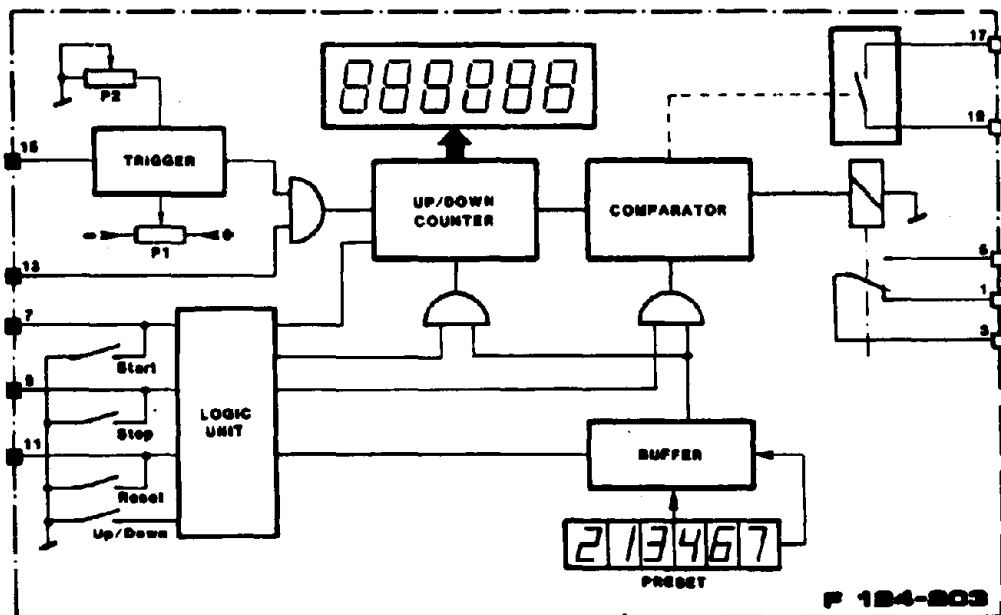
The up/down counter is started, stopped and reset either using the front panel push buttons or via external signals.

## SPECIFICATIONS

Power Supply :  $\pm 15$  V stab (110 mA each)  
 Input sensitivity : pulse (pin 13) 1.5V pp to 10V  
 wave/form signal (pin 15) 0.5V to 10V pp  
 Frequency : 5 KHz max  
 Counter capability : 0 to 999999  
 Contact rating : relay 250 mA/24V AC  
 Resistance 800 ohms max  
 0 ..... 10 V (only positive voltage)  
 Adjustments :  
 Trigger levels : P1 and P2  
 Start : push button in front panel or external contact  
 Stop : push button in front panel or external contact  
 Reset : push button in front panel or external contact  
 Up/Down Selection: switch in front panel  
 Present Value : BCD coded switches on front panel (6 decimals)

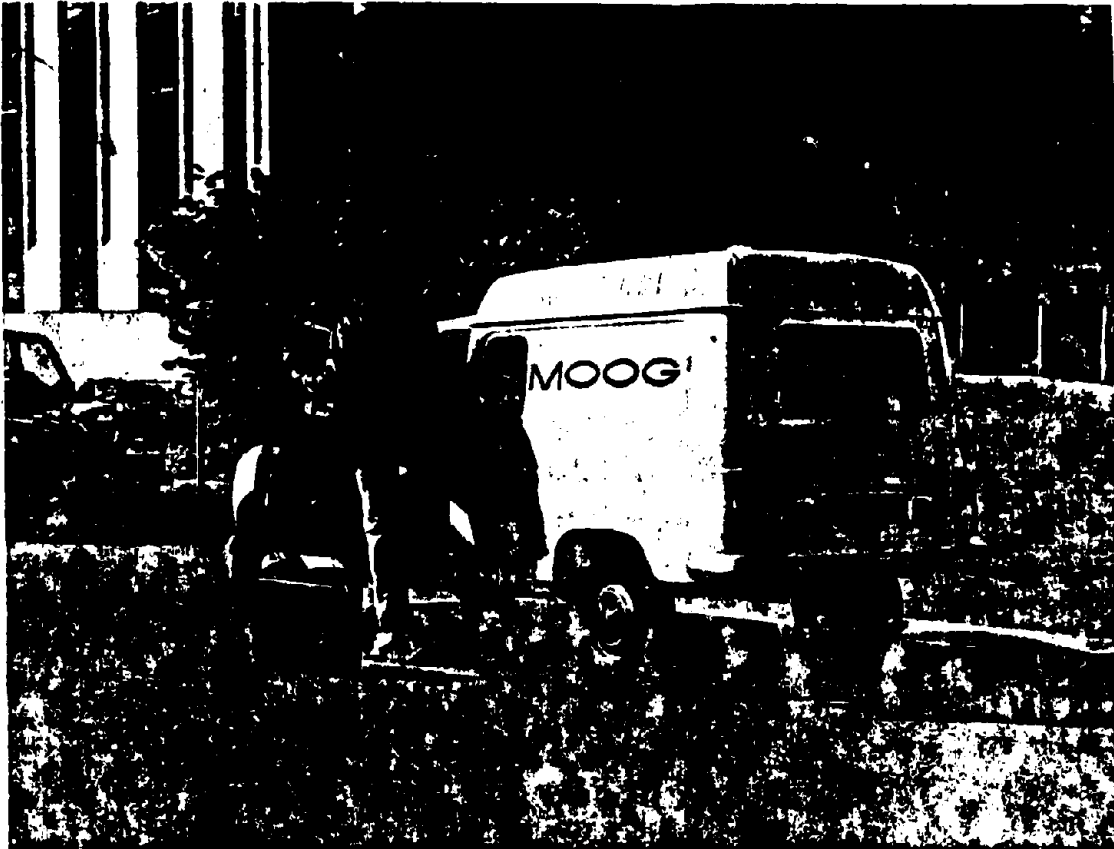


## BLOCK DIAGRAM



## USE

The card F124-203 is especially designed to be used in automatic sequence control, wherever the number of cycles to do are predetermined or the number of cycles executed are to be counted, as for example in fatigue test stands.



# MOOG

## FRANCE

MOOG S.a.r.l.  
38, rue du Morvan  
Sillie 417  
94573 Rungis  
Tel. : (1) 687.33.63  
Twx 200427

## WEST GERMANY

MOOG GmbH  
Hanns-Klemm-Strasse 28  
D-7030 Böblingen  
Tel. : (07031) 6220  
Twx 07285777

## GREAT BRITAIN

MOOG Controls Ltd  
Ashchurch, Tewkesbury  
Glos. GL 208 NA  
Tel. Tewkesbury (0884) 296800  
Twx 43229

## ITALY

MOOG Italiana S.r.l.  
Via dei Cavalli 52  
I-21100 Varese  
Tel. (0332) 261080  
Twx 380582

## SWEDEN

MOOG Sweden AB  
Datavägen 18  
S-43600 Askim, Sweden  
Tel. (031) 681020  
Twx 21178

## JAPAN

MOOG Japan Ltd  
1-6285 Tamura  
Hiratsuka, Japan 254  
Tel. (0463) 55-3615  
Twx 3882-436

## AUSTRALIA

MOOG Australia Ltd  
Gatwick & Kelvin Rds.  
N. Bayswater,  
3153 Victoria/Australia  
Tel. (03) 729.00.44  
Twx 36375

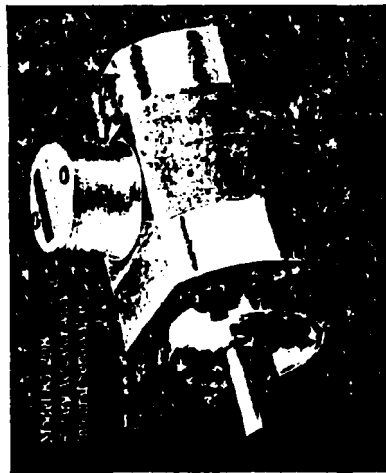
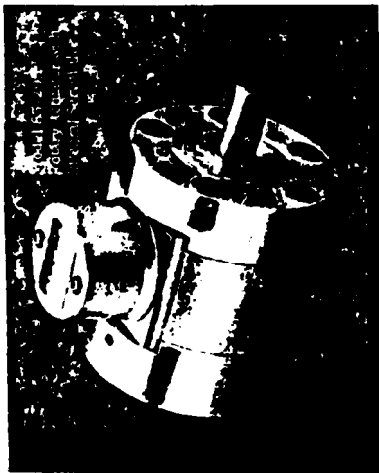
## BRASIL

MOOG do Brasil  
Rua Prof. Campos de Oliveira, 338  
Jurubatuba-Santa Amaro  
Sao-Paulo/S P., Brazil CEP 04675  
Tel. (011) 522.45.10 / 521.65.81  
521.65.44  
Twx 01132874

## U.S.A.

MOOG INC.  
Industrial Division  
Seneca and Jamison Rds  
East Aurora, New York 14052  
Tel. (716) 652-2000  
Twx 7102641442 + 91-399

110



Robot Actuator Specifications	Moog Model 85-285	Moog Model 85-286
Displacement	0.18 IN <sup>3</sup> /RAD	0.35 IN <sup>3</sup> /RAD
Rotation	270 Degrees	270 Degrees
Supply Pressure	2500 PSI Max	2500 PSI Max
Seal Torque at 1000 PSI	100 IN-LB	200 IN-LB
Operating Torque at 1000 PSI	50 IN-LB	100 IN-LB
No Load Velocity	1000 DEG/SEC	800 DEG/SEC
Responsive Parameters	1.0 GPM	1.5 GPM
• Flow at 1000 PSI	100 OHMS	100 OHMS
• Coil Resistance	20 MA	20 MA
• Rated Current	2.6 LBS	4.5 LBS
Actuator Weight		

## MOOG PLANTS AND OFFICES

MOOG ENGINEERING CORPORATION  
 1400 KENNEDY BLVD  
 PITTSBURGH, PA 15205  
 TELEPHONE (412) 781-2000  
 TELETYPE (412) 781-2000  
 CABLE MOOG 1000  
 MOOG ENGINEERING (UK) LTD  
 1000 KENNEDY BLVD  
 PITTSBURGH, PA 15205  
 TELEPHONE (412) 781-2000  
 TELETYPE (412) 781-2000  
 CABLE MOOG 1000



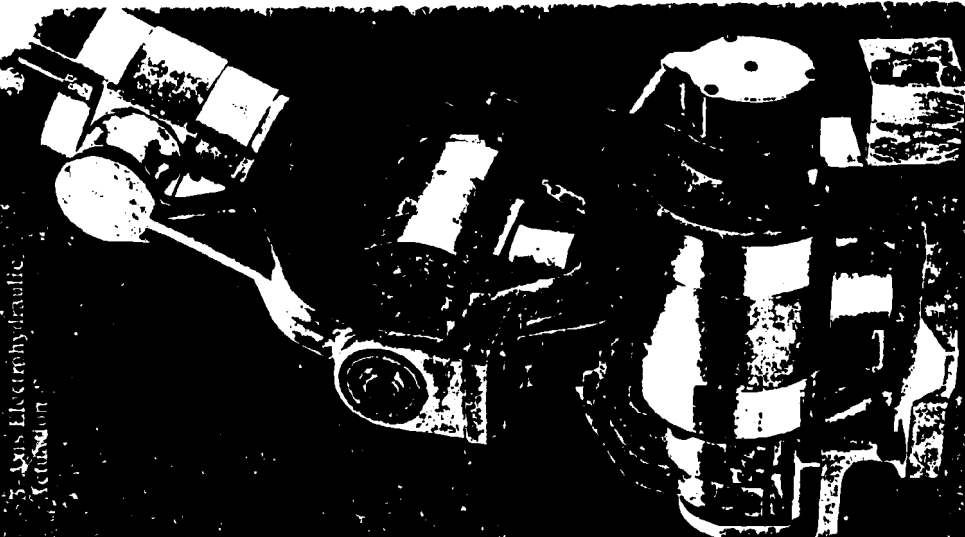
MOOG ENGINEERING CORPORATION  
 1400 KENNEDY BLVD  
 PITTSBURGH, PA 15205  
 TELEPHONE (412) 781-2000  
 TELETYPE (412) 781-2000  
 CABLE MOOG 1000  
 MOOG ENGINEERING (UK) LTD  
 1000 KENNEDY BLVD  
 PITTSBURGH, PA 15205  
 TELEPHONE (412) 781-2000  
 TELETYPE (412) 781-2000  
 CABLE MOOG 1000

## MOOG

MOOG ENGINEERING CORPORATION  
 1400 KENNEDY BLVD  
 PITTSBURGH, PA 15205  
 TELEPHONE (412) 781-2000  
 TELETYPE (412) 781-2000  
 CABLE MOOG 1000

## MOOG Robot Wrist

5 Axis Electrohydraulic  
 Actuation



MOOG



Reproduced from  
 best available copy.

# Moog® Robot Wrist

## FEATURES:

- High Speed, High Performance
- Compact, Sturdy, Light Weight
- Long Life, No Leakage
- No External Plumbing or Cables
- Intrinsically Safe Design
- Easy Installation and Maintenance

The Moog 3-Axis Electrohydraulic Actuator offers a compact, totally integrated, long life wrist assembly for the Robot Industry. Completely enclosed hydraulic and electrical connections eliminate external hydraulic hoses and electrical cables. Life is extended beyond the limitation imposed by dynamic seals by eliminating the high pressure dynamic seals.

The unique electrohydraulic servo package design is sturdy and light weight. Rotary motion for each axis is provided by a single vane laminar actuator\* with an integral servovalve. The structural brackets, designed for strength and light weight, house the rotary position transducers (servopot, resolver or encoder) for closed loop control of each axis.

Maintenance is simplified by the modular nature of the wrist assembly which allows replacement of an actuator unit without disturbing the other two axes.

The assembly is installed by manifold mounting the base of the assembly. Both electrical and hydraulic interfaces are provided at the base manifold with a single electrical connector and o-ring sealed hydraulic supply and return ports.

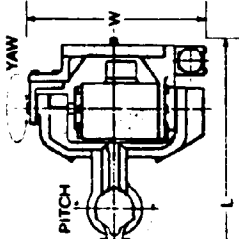
Internal hydraulic porting is the key to the clean and compact design. Each rotary actuator housing in the Moog wrist has two o-ring sealed manifold ports for hydraulic supply and return connections. These ports supply fluid to the integral servovalve and through the actuator shaft and mounting bracket to the actuator of the next outboard axis.\*

The intrinsically safe servovalve coils and rotary transducers used in the design make the wrist safe for operation in hazardous environments of spray painting and adhesive dispensing applications.

Moog 3-Axis Robot Wrist permit operating speeds in excess of 1000 degrees per second. Two types of wrist motion are available. In Type "A" the yaw actuator provides bend motion about an axis parallel to the base. In Type "B" the yaw actuator provides a rotate motion about an axis perpendicular to the base. A bend motion about the pitch axis and a rotate motion about the roll axis are common to both wrist types. The yaw and pitch axes rotate 220 degrees and the roll axis rotates 270 degrees. Moog wrist assemblies with corresponding payloads, weight and size are tabulated below.

\* Patent applied for

## 3-AXIS ELECTROHYDRAULIC ACTUATION



Moog Wrist	Wrist Type	Payload @ 1000 PSI	Payload @ 2000 PSI	Wrist Weight	Wrist Size L, W (inches)
1	A	4 LB	7 LB	17 LB	17.9
2	A	9 LB	18 LB	20 LB	17.9
3	B	9 LB	18 LB	20 LB	21.8
4	A	14 LB	28 LB	36 LB	20.12
5	B	14 LB	28 LB	36 LB	24.12

Wrist 2 and 4 assume yaw motion in the horizontal plane (as depicted)

**Reproduced from  
best available copy**

Pages C112-C116 have been removed.

Due to copyright restrictions, pages C112-C116 have been omitted

**Reproduced from  
best available copy**

Pages 0117-0121 have been removed.

Due to copyright restrictions, pages 0117-0121 have been omitted.

REVIEW OF DOWNHOLE GEOTECHNICAL TOOL

prepared for

SWEET AND AIKEN, INC.  
13810 Champion Forest Drive  
Houston, Texas 77069

by

EQUIPMENT DEVELOPMENTS CO.  
8911 Rocky Lane  
Houston, Texas 77040  
713 937 6873  
July 12, 1985

## REVIEW OF DOWNHOLE GEOTECHNICAL TOOL

### GENERAL

This report is a review of the electronic portion of a downhole geotechnical tool intended for use in making soil measurements during offshore geotechnical drilling. It consists of a mechanical section designed to be run inside the drill string, land and lock in the drill string and extend a tubular member into the soil at the bottom of the borehole. The tubular member is then moved or oscillated in a rotary manner by a hydraulic powered servo mechanism. The response of the tube is then measured electronically by transducers. These electrical signals along with signals from other transducers are transmitted to the surface via electrical conductors.

### OPERATION

The use of the tool is envisioned to be operated from a normal geotechnical drilling vessel and is to be wireline operated. Since the tool is hydraulically powered, it will be connected to a surface control console by an umbilical containing at least a single hydraulic conductor along with the necessary electrical conductors for power, control, and data. During operation, the umbilical should be stored on a powered winch and payed out over an appropriately sized sheave to minimize chances for damage to the umbilical. The winch can be air or electrically powered. It should contain a live hydraulic swivel and an electrical slip ring assembly to allow operation of the tool without having to disconnect the umbilical.

Because of the hostile offshore environment, the operation of the overall system should be kept as simple as possible. Simplicity should be considered through out the design process. As shown in sketch 1, the successful operation of the tool will necessitate the following major components or subsystems:

- Surface hydraulic control console.
- Surface electronics/data acquisition/data recorder console.
- Powered winch and sheave system.
- Umbilical.
- Downhole tool including sensors and downhole electronics package.

### ACTUATOR

The actuator is defined as a hydraulically operated rotary motor coupled to a servo valve using either torque or angular displacement feedback. This system is technically feasible, but will require great care in the design, and ultimately during operation, to insure cleanliness of the hydraulic fluid. Adequate filtration should be designed into the system. There are two ways to handle the hydraulic system: either a return to surface

system using a pressure and a return line in the umbilical, or a waste to sea system that requires only a single pressure line in the umbilical for the actuator. For this tool a waste to sea system is the recommended approach but care must be taken in the design of the vent components to insure that sea water and contaminants do not intrude into the hydraulic fluid. In a waste to sea system, the issue of environmental contamination must be considered. Other considerations for the selection of the hydraulic fluid include specific gravity relative to sea water, viscosity, compatibility with components, and corrosion potential on hydraulic components. One of the water based fluids should be considered.

As an alternative to the hydraulic actuator, an electrical torque motor should be considered for the tool provided that a small size adequately powered motor can be located. A manufacturer such as Globe is a potential supplier for the motor. Although more electrical conductors would be required in the umbilical, the problems associated with maintaining cleanliness of the hydraulic fluid would be eliminated along with the power hydraulic fluid conductor in the umbilical.

Command inputs to the servo motor will be sine wave motion and step inputs. Frequency will be 0.1 sec/cy to 50 sec/cy at amplitudes ranging from approximately plus and minus 0.01 degrees to plus and minus 15 degrees.

#### SENSOR ENVIRONMENT

The sensors or transducers defined for use in the geotechnical tool are to be located inside the tool body and operated in a dry nitrogen environment at just above ambient sea pressure. Since the tool will be operated at water depths up to 1500 feet, the internal pressure will reach approximately 700 psi. This is a technically feasible approach and presents several advantages as far as the transducers are concerned. Intrusion of seawater and contaminants into the tool body will be minimized. The main seal which separates the seawater from the tool body cavity will be pressure balanced thereby minimizing frictional drag that will be seen as an error in some of the measurements. Although seal friction drag can probably be cancelled during calibration, variations in the quantity during operation cannot be accounted for in the calibration.

The approach of using a one atmosphere chamber for the sensors should not be considered; but, using a pressure balanced chamber filled with a dielectric fluid such as Dow Corning fluid number 200 is a good approach and should be considered for this tool. The attached sketch 2 illustrates this concept.

In either case, the selected sensors and transducers must be carefully reviewed with the vendors to insure that they can operate in the elevated ambient pressure environment and that they will maintain their performance characteristics over the

defined pressure and temperature ranges.

#### SENSORS

The following is a list of the sensors defined for use with the geotechnical tool.

A single torque sensor will be required. The Lebow strain gage unit which has been selected is an excellent choice provided that it can perform at the elevated pressure environment and that it will fit into the allocated space envelope.

A single angular displacement transducer will be required. The Trans-Tek unit which has been selected should prove to be an excellent choice if, like the torque sensor, it can operate in the environment and it will fit into the tool.

An angular accelerometer has been defined and will be made by mounting a pair of linear PCB quartz accelerometers on equal length arms 180 degrees apart. This approach should prove satisfactory if calculations show that the accelerometers have the proper range and sensitivity to operate over the frequency and amplitude ranges. Of course operation at the elevated pressure must be checked with PCB engineering.

Three pressure sensors have been defined, two of which will be differential types. The PCB pressure sensors selected are not satisfactory for this application because the PCB quartz sensors are not capable of measuring static pressures. Therefore another selection must be made such as those manufactured by Entran.

#### DOWNHOLE ELECTRONICS PACKAGE

The successful operation of this tool will require the use of a downhole electronics package for transducer signal conditioning, switching and control, amplification, distribution of command signals to the servo drive motor, and multiplexing of data signals to minimize number of conductors in the umbilical. It is a critical component and will be a custom design. There are no known off-the-shelf units to meet the needs of this tool. Unlike the cavity where the transducers and sensors are located, the electronics package should be of the one atmosphere design. Many electronic components will not operate satisfactorily at the elevated pressure of 700 psi. To do so would require special components to be manufactured and qualified over the pressure range. This would be more expensive and time consuming than designing and building the one atmosphere chamber. The design must consider the external pressure and must be carefully sealed to prevent intrusion of either seawater or nitrogen. If possible the seal should be a sealweld and tested for leakage prior to use downhole.

## DATA TRANSMISSION

Based on the known operational requirements and environment for this tool, it is recommended that the data be transmitted from the downhole electronics package via the umbilical to the surface electronics console in analog form. This approach will minimize the electronics component count in the downhole electronics package, thereby improving reliability. It will also give the equipment operator and field engineer maximum flexibility in the use and interpretation of the data. Digitization, other processing and recording can then easily be done in the surface package where space is not at such a premium.

An analysis of the sensors and required data shows that the following number of electrical conductors will be required.

1. Electrical power--probably 12 or 24 volts DC.
2. Power common, signal ground, and shield.
3. Command signal--includes servo command encoded with calibration ON/OFF signal.
4. Angle.
5. Torque.
6. Angular acceleration.
7. Pressure signals, 3 each--multiplexed together using a frequency modulation technique. These are nearly static signals and do not require wide bandwidth. Center frequencies of 100 Hz., 500 Hz., and 2500 Hz. should be satisfactory.
8. Spare.

Data transmission reliability will be improved if very low impedance amplifiers having sufficient current capacity are used to drive the umbilical even in the presence of minor salt water shorts.

## UMBILICAL

The electro-hydraulic umbilical will be a critical component and must perform properly to insure long-term reliable operation in the field. Initially, during field testing of the prototype tool, the umbilical can be made from a multi-conductor hose bundle strapped or taped to a well logging cable. The well logging cable will also have a good tension strength member included in the cable. Ultimately the umbilical should have the hoses and electrical conductors all inside an overall jacket and strength member. During operation, it will be necessary to store the umbilical on a powered winch to insure that it does not become

entangled and kinked.

Do not have any connections or splices in the umbilical. Have a single connection between the tool and the umbilical so that it can be disconnected for repair or storage. As much as possible keep the entire system connected together to minimize the chances for trash and contaminants to enter the hydraulic system. Also it is important to keep the hydraulic umbilical free of entrapped air.

#### OTHER DESIGN CONSIDERATIONS

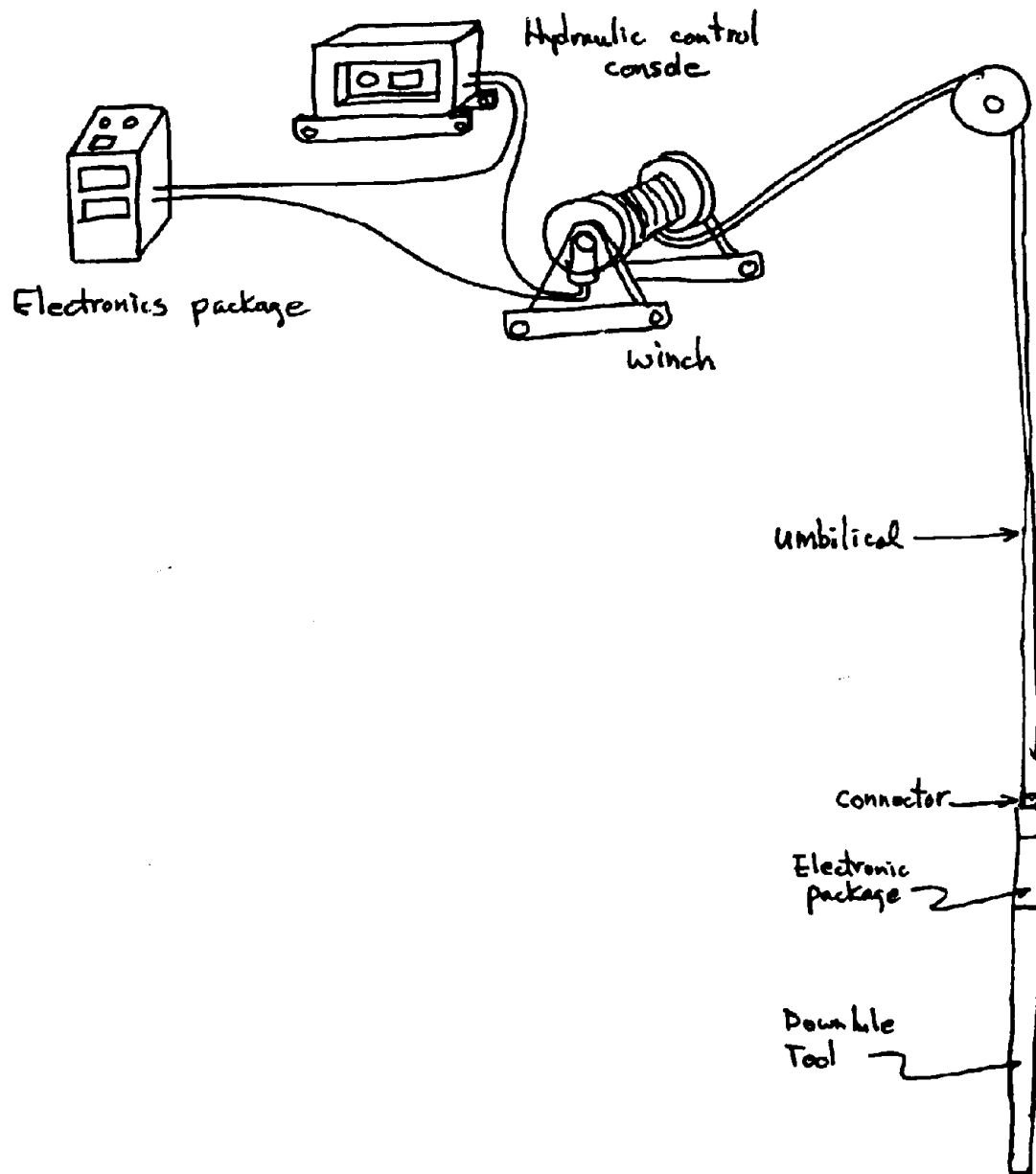
The following are a few tips to consider in the design that will impact the reliability of the data obtained and the successful operation of the tool in the hostile offshore environment.

Minimize the use of dissimilar metals which can cause electrical potentials to be set up in the presence of the salt water electrolyte. A small sacrificial anode might have to be incorporated onto the tool.

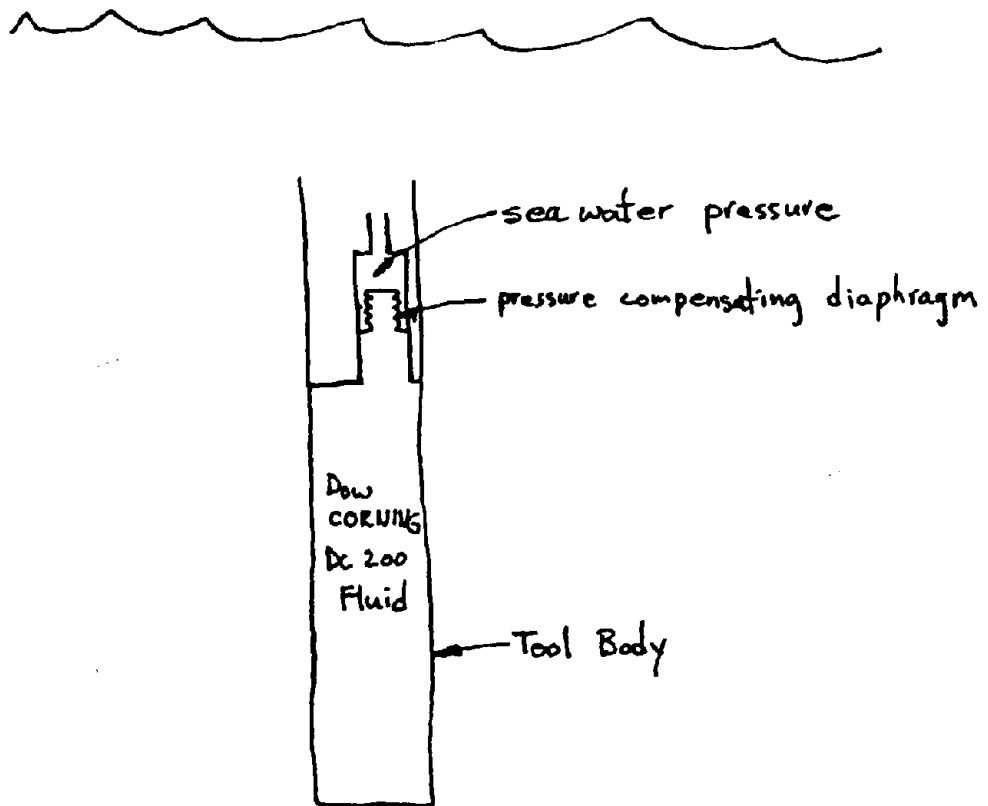
Provide for easy repair and disassembly of the tool to the extent possible. Routing of electrical wires inside the tool body must be done in a careful manner.

Conduct extensive calibration and testing prior to going to the field. Try to work out as many bugs as possible first.

Keep in mind that the various stainless steel alloys that may be used in the tool body are subject to galling, particularly in the threaded areas. Proper tolerancing and lubrication are important.



SKETCH 1: OVERALL SYSTEM SHOWING MAJOR COMPONENTS



SKETCH 2: PRESSURE COMPENSATION TECHNIQUE WITH DIELECTRIC FLUID

INSTRUMENTATION FOR LABORATORY TEST PHASE  
GEOTECHNICAL TOOL

prepared for

SWEET AND AIKEN, INC.  
13810 Champion Forest Drive  
Houston, Texas 77069

by

EQUIPMENT DEVELOPMENTS CO.  
8911 Rocky Lane  
Houston, Texas 77040  
713 937 6873  
July 19, 1985

## INSTRUMENTATION FOR LABORATORY TEST PHASE GEOTECHNICAL TOOL

### INTRODUCTION:

This document discusses the instrumentation needed during a laboratory test phase of a Geotechnical Tool designed to obtain measurements on soils. During this phase the tool will be prototyped and connected to various instruments and computers. This instrumentation set up is not intended to be taken to the field, except for the Field Computer.

This information is furnished in response to your comments and those of Ms. H/enke following the issuance of our report dated July 12, 1985. (23)

Sketch 1 shows a block diagram of the various instruments and thier interconnections.

### FEATURES OF THE SYSTEM:

1. Ease of set-up and operation.
2. Flexibility to meet changing requirements during this phase of testing.
3. Includes analog signal recording on hard copy strip chart record for quick observations.
4. Analog to digital converter and computerized processing of data. Allows development of software on the computer that is suitable for inclusion in the final field system.
5. Majority of components can be either purchased or rented.

### DISCUSSION:

Although this laboratory instrumentation is more bulky and cumbersome than the components that will be eventually used in the field system(except for the Field Computer), it provides a high degree of flexibility that is needed during the laboratory test phase. During this phase it is expected that exact test techniques will evolve along with the software. The use of this system will in no way degrade the eventual performance of the final field unit which will include a downhole electronics package. Likewise the degree of sensitivity and accuracy can be duplicated with the final field unit if proper care is taken during the design of the downhole electronics package, umbilical, and surface electronics package.

At this time it is not expected that the oscilloscope and strip chart recorder will be required in the final surface electronics package.

#### FEASIBILITY OF DOWNHOLE ELECTRONICS PACKAGE:

Based on the known requirements for the Geotechnical Tool, the use of a downhole electronics package is feasible and well within the state of the art for such packages. They are routinely used in well logging tools and, to a certain degree, subsea geotechnical tools such as cone penetrometers. The unit will have to be a custom design to meet the specific requirements of this tool because of size, number of channels, and limited cable conductors, etc. No known off-the-shelf units can meet the specific requirements of this tool.

The package can be designed to fit into the Geotechnical Tool which has an ID of 2.8 inches and operate successfully in the offshore geotechnical environment in water depths up to 1500 feet. Although the exact length of the package cannot be determined at this time, it is expected to be approximately 2 to 4 feet long.

The cost for such a downhole electronics package also cannot be precisely determined at this time, but it is expected that a single unit might range between \$25,000 and \$40,000. It will probably have to be constructed on a cost plus basis for materials plus design and fabrication costs.

#### INSTRUMENTATION LIST:

The appended documents list the required laboratory instrumentation along with sources of supply, and costs both for purchase and rentals. An overall cost estimate is included.

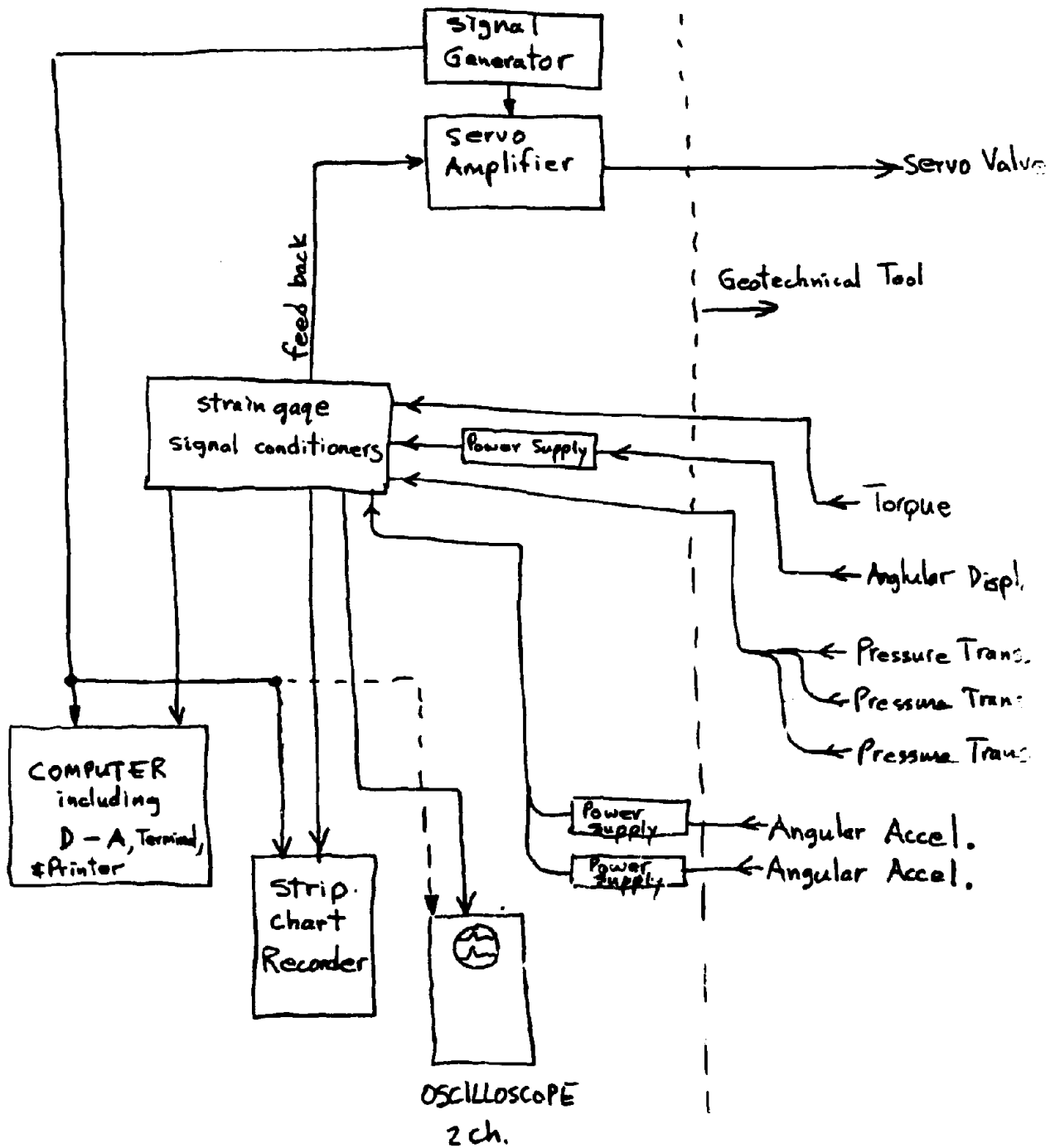
It should be noted that the component called servo amplifier shown on sketch 1 is not listed nor costed in this document. It is peculiar to the hydraulic servo valve and actuator that will be used in the prototype tool.

#### SOFTWARE:

The cost for software development shown on the cost estimate is not intended to be a lump sum amount to cover the cost of all software that might eventually be needed by the laboratory system. It should however be considered reasonable for the development of certain acquisition routines peculiar to this test tool and allow for the training of the test engineer and or technician in further software developments as may be required.

David W. Hughes in Houston is a particularly talented and knowledgeable software development engineer. It is recommended that

he be retained to do this portion of the work. His services can either be arranged through EDC or directly.



Sketch 1  
 (also Sketch A-1)

WV

LABORATORY TEST PHASE      18 July 85  
 INSTRUMENTATION COST ESTIMATE      LJM

1.0 MAJOR INSTRUMENT COMPONENTS:	Purchase	Rent/mo.
Power supply for Angle Trans.	\$150	
Power supplies for angle accel.	\$500	
Strain gage signal conditioners.	\$2700	\$350
Field Computer	\$7200	\$650
Strip Chart Recorder. (used)	\$3100	\$720
Oscilloscope.	\$2665	\$235
Signal Generator	\$4075	\$440
	-----	
	Purchase Total \$20390	
	Rental Total/mo.      \$2395	
	plus purchase      \$650	
	-----	
2.0 LABOR COST FOR SET-UP		
Instrumentation Des.--50.00/hr., est. 40 hrs.		\$2000.
Instrumentation Technician--25.00/hr, est 150hrs=		\$3750.
Software Eng.--50.00/hr.,est 150 hrs=		\$7500.
		-----
		\$13250.
3.0 OTHER EXPENSES		
Shipping and Freight		\$500.
Telephone		\$150.
Travel Expenses(if any) at cost +10%, local 21 cents/mi.		
500 mi.      105		
Lodging,      -----		
Air Travel      -----		
	-----	
	105 + 10%	\$116.
Misc wire, cable, connectors, lab supplies and digital volt meter, etc.		\$600.
Strip Chart paper, floppy discs, printer paper, and other expendable supplies		\$600.
		-----
		\$1966.

INSTRUMENTATION LIST

Item: Power Supply

Nomenclature: D100 Transducer Fixed Voltage Power Supply

Description: Power for use with Trans-Tek Rotary Angular Transducer. Plugs into 117VAC power and provides the correct stable voltage for the transducer.

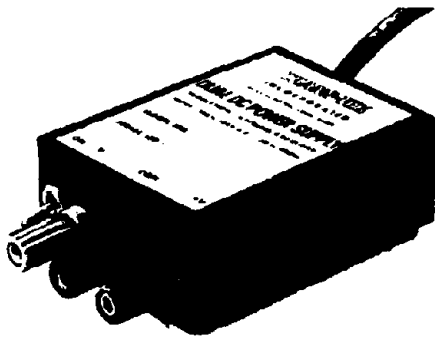
Reason for Selection: Economical. Compatible with the transducer. Manufactured by the same manufacturer as the transducer.

Source of Supply: Technical Products, Inc.  
1710 S. Dairy Ashford  
Houston, Texas 77077  
713 493 6520

Number Required: 1 each

Cost: \$150.00 each, Purchase

**POWER SUPPLIES SERIES D100**



**DUAL VOLTAGE PRESET VOLTAGE POWER SUPPLIES**

- Compatible with Trans-Tek DC Excited Transducers
- Regulation: 0.1% Line, 0.5% Load
- Short circuit protected
- Line cord, 3-wire

**DESIGN HIGHLIGHTS**

Trans-Tek's power supplies are precise, regulated, preset voltage sources, ideally suited for DC excited transducers, discrete and IC function modules. All components are encapsulated to provide reliable continuous operation to rated specifications in laboratory and factory environments.

They are equipped with an on-off switch, line cord, binding post terminals, rubber feet and two #4-40 tapped holes spaced 1.00 inch apart, located on the bottom side for permanent mounting. The holes are connected to earth ground via the power line cord ground terminal.

Dual voltage power supplies allow the user to choose the transducer excitation voltage; for example, Model D12-100 can be used to power a transducer with 12 VDC or 24 VDC. To excite the transducer with 12 VDC, connect the transducer +INPUT and -INPUT to the power supply +V and COM terminals, respectively (or to the power supply COM and -V terminals, respectively). To excite the transducer with 24 VDC, connect the transducer +INPUT and -INPUT to the power supply +V and -V terminals, respectively.

**COMMON SPECIFICATIONS**

Input: 105 to 125 V A.C., 50 to 400 Hz\*  
 Output Voltage tolerance:  $\pm 1\%$  (Fixed)  
 Regulation: Line 0.01% max  
                   Load 0.05% max  
 Temp. Coef: 0.02%/°C Typical  
 Ripple and Noise: 1mv RMS max  
 I/O Isolation: 50 MEGOHMS  
 Overcurrent Protection  
     Current Limiting: Either output to common or other output, indefinitely  
 Operating Temp. Range: -25° to +71°C

Storage Temperature: -40° to +85°C  
 Termination:  
     Line cord, 3-wire, 5 feet long, terminated in line plug with earth ground.  
 Output Terminals: 3-Binding post, 6-way  
     Red - Positive Voltage;  
     Black - Common  
     Violet - Negative Voltage  
 Dimensions: 2.5" Wide x 4.45" Long x 1.25" High (83 x 113 x 32mm)  
 Approx. Weight: 1.25 lbs (575 gm)

\*210 to 250 VAC optionally available by adding K to model number; e.g. D12-100 becomes D12-100K

Output V D C	$\pm 12$	$\pm 12$	$\pm 15$	$\pm 15$
Current, MA	100	200	100	200

All series D100 Trans-Tek products are warranted against defective materials and workmanship for one year, from date of shipment.

Orders should be made out to TRANS-TEK, INC., sent in care of your local Trans-Tek representative, or directly to Box 338, Route 83, Ellington, Conn. 06029. Tel. (203) 872-8351.

TELEX 99207 (TRANS-TEK) U.S.A.

BULLETIN SO12-0013-0500 ALL SPECIFICATIONS SUBJECT TO CHANGE WITHOUT NOTICE

Printed in U.S.A.

DC POWER SUPPLIES

0157

INSTRUMENTATION LIST

Item: Power Supply

Nomenclature: PCB Piezotronics Model 482A Line Power Unit.

Description: Power supply for PCB Accelerometers. Plugs into 117VAC power and provides the correct stable excitation voltage for the accelerometers.

Reason for Selection: Economical. Compatible with the transducers. Manufactured by the same vendor as the accelerometers.

Source of Supply: Technical Products, Inc.  
1710 S. Dairy Ashford  
Houston, Texas 77077  
713 493 6520

Number Required: 2 each

Cost: \$250.00 each, Purchase

Total Cost: \$500.00

*CB*

A. C. MODE, BASIC  
**LINE POWER UNIT**

for voltage-mode transducers

Model 482A



- powers transducers with built-in or attached amplifiers
- supplies power over signal lead
- eliminates bias on output
- monitors normal or faulty system operation
- provides adjustable constant-current excitation

For powering low-impedance piezoelectric transducers with built-in or attached amplifiers and coupling them to versatile readout instruments; and especially for driving long transducer cables.



Model 482A Line Power Unit powers the transducer over the signal lead and couples self-amplifying PCB transducers to oscilloscopes, recorders or other readout instruments. In the coupling process, it eliminates D.C. power bias from the output by means of a coupling capacitor. It also monitors normal operation of the system with a meter that detects such faults as cable and connector open or short circuits and transducer amplifier trouble. With a 24V D.C. regulator, Model 482A provides an output signal range linear to  $\pm 10$  volts. Constant current excitation adjustable from 2 to 20 mA (factory set at 12 mA) is supplied to transducer to improve linearity and cable driving capabilities. Higher magnitude supply currents drive longer cables and provide more available output current. With medium length cables, output current is generally available to within 2 mA of the supply current.

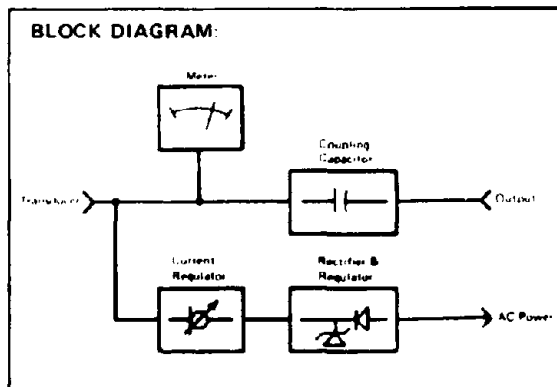
Like the transducer discharge circuit, the capacitive coupling circuit to the readout instrument also eliminates D.C. signal components at an exponential rate. When the readout load impedance is one megohm or more, the coupling time constant exceeds 10 seconds, which is sufficiently long for most applications.

For static calibrating or other purposes, Model 482A can be operated in a D.C. mode by taking the output signal directly off the transducer lead through a "T" connector or by shorting across the internal coupling capacitor. The resulting 11V D.C. bias on the output lead can be eliminated, if necessary, by a series battery or floating D.C. supply.

SPECIFICATIONS: Model No.		482A
Transducer Excitation	VDC	+22
Excitation Current (adjustable) <sup>(1)</sup>	mA	2 to 20
Voltage Gain		1
Coupling Capacitor	$\mu$ F	10
Output Signal, F. S.	$\pm$ volts	10
Output Current	mA	to 10
Noise, Wideband (pk-pk max.)	$\mu$ V	500
Size	in	1.8x4.3x6
Weight	lb	2
Transducer Connector	micro	10-32
Output Connector		BNC
Power Cord (3-wire)	ft	6
Power Required (60 Hz)	V/A	100-125/0.3

OPTIONAL MODELS:	
Four Channel Version	482A04
Fixed Constant - Current Supply (2mA Diode)	482A07
Three Position Gain Switch (X1, 10, 20) (with 4mA Constant-Current Supply)	482A10

NOTE (1) Factory set at 4mA.  
 (2) Output Cable not supplied. Order Model 012A03



INSTRUMENTATION LIST

Item: Strain Gage Signal Conditioner

Nomenclature: Vishay Multi channel Signal Conditioner/Amplifier 2100 System. Configured with power supply and 6 channels of signal conditioning.

Description: Unit accepts strain gage transducers and others, amplifies the signals to appropriate levels for recording and processing. Unit includes calibration capability.

Reason for Selection: Easy to set up and operate. Economical. Provides extra back-up channels for flexibility in laboratory test program. Universal type for use with wide range of other instrumentation and computers needed in the lab test program.

Source of Supply: (Purchase)  
Technical Products, Inc.  
1710 S. Dairy Ashford  
Houston, Texas 77077  
713 493 6520

(Rental)  
General Electric, Quick-Rental Service  
900 South Loop West, Ste 180  
Houston, Texas 77054  
713 741 8137  
1 800 GE RENTS

Number Required: 1 Unit.

Cost: \$2700.00 (estimated), each, Purchase.

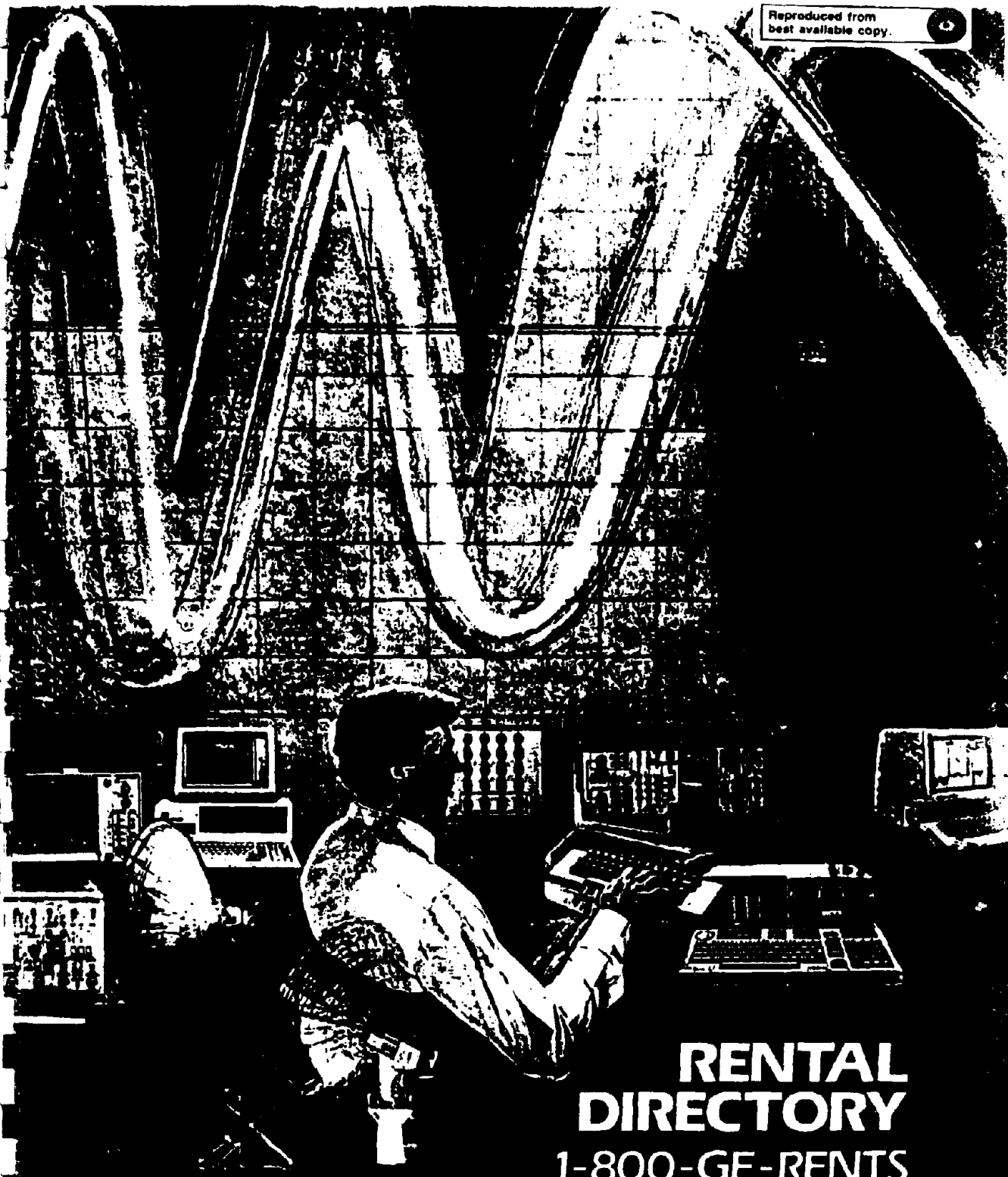
\$350.00/month, Rental.

**Reproduced from  
best available copy**

Pages C141-C146 have been removed.

Due to copyright restrictions, pages C141-C146 have been  
omitted.

Reproduced from  
best available copy.



**RENTAL  
DIRECTORY**  
1-800-GE-RENTS

GENERAL  ELECTRIC

0147

# QUICK-RENTAL<sup>®</sup>

service

## DESCRIPTION RATE/MO.

Signal Conditioners (Continued)

<b>Gould 13-4715-09</b>	<b>\$ 60</b>
Med. gain multi-span dc amp. Measurement range 400 $\mu$ V FS to 100 V FS; in 20 steps; accuracy $\pm 0.1\%$ FS; zero suppression $\pm$ full scale.	
<b>Gould 13-4715-40</b>	<b>\$ 110</b>
Thermocouple amplifier type J. Range $-150^{\circ}$ to $1000^{\circ}$ F or $^{\circ}$ C. Zero suppression.	
<b>Gould 13-4715-41</b>	<b>\$ 110</b>
Thermocouple amplifier type K. Range $-200^{\circ}$ to $1000^{\circ}$ F or $^{\circ}$ C. Zero suppression.	
<b>Gould 13-4715-42</b>	<b>\$ 110</b>
Thermocouple amplifier type T. Range $-200^{\circ}$ to $+400^{\circ}$ F or $^{\circ}$ C. Zero suppression.	
<b>Gould 13-4715-43</b>	<b>\$ 110</b>
Thermocouple amplifier type E. Range $0^{\circ}$ to $+1000^{\circ}$ F or $^{\circ}$ C. Zero suppression.	
<b>Gould 13-4715-44</b>	<b>\$ 125</b>
Thermocouple amplifier type R. Range $+500^{\circ}$ to $+1760^{\circ}$ F or $^{\circ}$ C. Zero suppression.	
<b>Gould 13-4715-45</b>	<b>\$ 125</b>
Thermocouple amplifier type S. Range $+50^{\circ}$ to $+1760^{\circ}$ F or $^{\circ}$ C. Zero suppression.	

**If you have any questions,  
just ask our rental specialists.**

<b>Honeywell Accudata 117-06</b>	<b>\$ 210</b>
Driver amplifier. Gain 0.01-10 in 10 steps. 0.01-25 with vernier, input $\pm 100$ mV to $\pm 300$ V, 6 channels.	
<b>Honeywell Accudata 118-1</b>	<b>\$ 95</b>
Strain gage excitation, control and amplification in a single unit: constant voltage or current gage excitation.	
<b>Honeywell Accudata 120</b>	<b>\$ 70</b>
Differential dc amplifier. Input 2.5 mV to 250 mV; output $\pm 2.5$ V, 85 mA, gain 10-1000 X. 8 steps, can be used with 105-2 above.	
<b>Honeywell Accudata 218-1</b>	<b>\$ 140</b>
Gage control amplifier. Selectable gage excitation voltages, three independent signal outputs, calibrated input suppression.	
<b>Soltec 1280 SM26</b>	<b>\$ 70</b>
High speed input module for use with SU-100 transient storage unit and 1288 recorder. Frequency response 5 kHz. Measurement range 50 mV to 200 V in 12 steps. $\pm 100\%$ zero adjust. Overall accuracy $\pm 0.7\%$ of full scale at $23^{\circ}$ C.	
<b>Soltec 1280 VM88</b>	<b>\$ 50</b>
Multi-span dc plug-in module for use with 1288 recorder. Measurement range 1 mV to 200 V in 17 ranges. $\pm 100\%$ zero adjust. $\pm 400$ zero suppression. Overall accuracy $\pm 0.25\%$ of full scale at $23^{\circ}$ C.	

## DESCRIPTION RATE/MO.

<b>Soltec 3410 4965</b>	<b>\$ 115</b>
Plug-in dc preamplifier for 3400 series recorder. 1 mV/cm to 20 V/cm in 19 ranges. Calibrated zero suppression.	
<b>Soltec SU-100</b>	<b>\$ 600</b>
32 k word (12 bit) 6 channel storage module allows transient/waveform data to be stored and output to 1288 recorder. Sampling frequency from 200 kHz to 200 Hz. Internal or external triggering, pre and post triggering and an AUTO mode that samples data, prints out data and resets system.	
<b>Vishay 2310</b>	<b>\$ 155</b>
Signal conditioning amplifier for strain gages, transducers, potentiometers and dc displacement transducers. All bridge completion built-in including 120 and 350 $\Omega$ dummies. Bridge excitation selectable 0.5-15.0 Vdc. Continuously variable and calibrated amplifier gain: 1.0-11,000. Electronic bridge balance. Three simultaneous buffered outputs: $\pm 10$ V @ 5 mA, tape output $\pm 1.414$ V @ 5 mA and galvanometer output $\pm 10$ V @ 70 mA.	
<b>Vishay 2350</b>	<b>\$ 55</b>
10-channel rack adapter for Vishay 2310 amplifiers.	
<b>Vishay 2360</b>	<b>\$ 55</b>
Portable cabinet for 1 to 4 channels of Vishay 2310 amplifiers.	
<b>Watanabe AH 3101</b>	<b>\$ 55</b>
High gain amplifier. Range 4 mV FS to 500 V FS; vernier gain control.	
<b>Watanabe AL3101</b>	<b>\$ 35</b>
Low gain amplifier. Range 20 mV FS to 400 V FS. Vernier gain control.	
<b>Watanabe AS3101</b>	<b>\$ 75</b>
Differential amplifier with zero suppression. Range 20 mV FS to 80 V FS; calibrated zero suppression; selectable 3 pole input filter; vernier gain control.	

## LIGHT BEAM OSCILLOGRAPHS

<b>Honeywell 1508 B</b>	<b>\$ 650</b>
24-channel, 4 event, visicorder with dc to 25 kHz response, wide range (1200:1) dc servo record drive system, 42 speeds, 0.1-120 ips drive speeds, internal record take-up, accentuated tenth time line; requires galvanometers.	
<b>Honeywell 1858</b>	<b>\$ 900</b>
Up to 18 channels, expandable to 32 channels with Model 1870 amplifier housing. Fiber optic CRT visicorder, dc to 5 kHz response at up to 7.2" trace amplitude, 1 mV to 300 V input sensitivity, 300 V common mode, 42 speeds from 0.1-120 ips, time interval marker, time lines recorder at 5 selectable intervals with 10-line accentuation, better than 0.5% FS accuracy. Requires plug-in signal conditioner next column.	

INSTRUMENTATION LIST

Item: General Purpose Storage Oscilloscope.

Nomenclature: Tektronix 1912 Dual trace, storage oscilloscope,  
or equivalent.

Description: General purpose oscilloscope that can be used for  
general viewing of signals and for set up and calibration of the  
instrumentation system. Allows for the quick and easy look see  
of specific signals.

Reason for Selection: Economical. General purpose oscilloscope.

Number Required: 1 each.

Source of Supply: General Electric Quick Rental Service  
900 South Loop West, Ste. 180  
Houston, Texas 77054  
713 741 8137 Rent  
1 900 GE RENTS

Tektronix, Inc. Purchase  
P. O. Box 4309  
Houston, Tx 77210  
713 933 3000

Cost: \$235.00/month rental.

\$2665.00 Purchase

# QUICK-RENTAL service

DESCRIPTION	RATE/MO.	DESCRIPTION	RATE/MO.
<i>Portable Oscilloscopes (Continued)</i>			
<b>Tektronix 475</b>	\$ 440	<b>Tektronix SC502</b>	\$ 235
DC to 200 MHz, dual trace, 2 mV/div to 5 V/div; time base 0.01 $\mu$ s/div to 0.5 s/div, 10 $\times$ magnifier, calibrated sweep delay, 8 $\times$ 10 cm CRT, trigger view.		DC to 15 MHz; dual trace, 1 mV/div to 20 V/div, time base 0.5 s/div to 0.2 $\mu$ s/div 10 $\times$ magnifier, trigger view, enhanced automatic trigger. Requires TM 500 power module.	
<b>Tektronix 475A</b>	\$ 475	<b>Tektronix SC503</b>	\$ 345
DC to 250 MHz at 5 mV/div, otherwise very similar to model 475.		DC to 10 MHz, dual channel bistable storage scope, 5 mV/div to 20 V/div; time base 2 s/div to 0.5 $\mu$ s/div, 10 $\times$ magnifier. Variable enhancement and integration, auto-erase and X-Y capability. Requires TM500 power module.	
<b>Tektronix 475DM44</b>	\$ 495	<b>Tektronix SC504</b>	\$ 330
Model 475 with 3 $\frac{1}{2}$ -digit multimeter and temperature probe, $\Delta$ delayed sweep with direct numerical readout.		DC to 80 MHz; dual trace; 5 mV/div to 10 V/div; time base 0.2 s/div to 0.2 $\mu$ s/div; 10 $\times$ magnifier; X-Y capability, 8 $\times$ 10 div, 0.25"/div CRT; requires TM500 multicompartiment power module.	
<b>Tektronix 485</b>	\$ 750	<b>Tektronix T912</b>	\$ 235
DC to 350 MHz, dual trace, 5 mV/div to 5 V/div; time base 0.5 s/div to 1 $\mu$ s/div; 8 $\times$ 10 div display, 0.8 cm/div CRT.		DC to 10 MHz, dual trace, bistable storage scope, 2 mV/div to 10 V/div; time base 0.5 s/div to 0.5 $\mu$ s/div, 10 $\times$ magnifier, 8 $\times$ 10 cm CRT, 250 cm/ms stored writing rate.	
<b>Tektronix 2213</b>	\$ 120	<b>Tektronix T922</b>	\$ 150
DC to 60 MHz, dual trace, 2 mV/div sensitivity; time base 0.05 $\mu$ s to 0.5 s/div, delayed sweep. Lightweight and portable.		DC to 15 MHz, dual trace, 2 mV/div to 10 V/div, time base, 0.5 s/div to 0.2 $\mu$ s/div, 10 $\times$ magnifier, 8 $\times$ 10 cm CRT, 110 Vac operation.	
<b>Tektronix 2215</b>	\$ 150	<b>Tektronix T935</b>	\$ 230
Same as Tektronix 2213, except allow simultaneous viewing of delayed and main waveform. Calibrated delayed sweep.		DC to 35 MHz, dual trace, 0.5 s/div to 0.1 $\mu$ s/div, 10 $\times$ magnifier, 2 mV/div to 10 V/div, 8 $\times$ 10 cm CRT, delayed sweep, 110 Vac operation.	
<b>Tektronix 2235</b>	\$ 175	<b>Vu Data PS935/975</b>	\$ 275
Two-channel, dc to 100 MHz bandwidth oscilloscope. Trigger view, dual time base, delayed sweep and X-Y operation.		Miniscope with DMM and counter, dual trace, dc to 50 MHz. Weighs less than 15 lbs. and battery operated.	
<b>Tektronix 2236</b>	\$ 275	<b>Full Size</b>	
Same oscilloscope specifications as the 2235 but with built-in 100 MHz, microprocessor-controlled counter/timer/multimeter. Totalize, dc volts, true rms volts, $\Delta$ time, frequency and period.		<b>H-P 1980B-811</b>	\$1750
<b>Tektronix 2335</b>	\$ 285	Oscilloscope measurement system includes 19800A waveform measurement library, 19860A digital waveform storage module, 1950A 100 MHz, 2-channel expansion module and 19811A plot/sequence ROM. HP-IB programmable, with 10 $\times$ 12 cm CRT display.	
DC to 100 MHz, vertical channel deflections from 5 mV/div to 5 V/div, 10 $\times$ magnifier to increase sweep rate to 5 ns/div, dual trace and delay sweep.		<b>H-P 1950A</b>	\$ 260
<b>Tektronix 2336</b>	\$ 275	Two-channel expansion module. Adds two 100 MHz vertical channels to the 1980. It features continuously calibrated variable deflection factors from 2 mV/div to 10 V/div.	
Same as 2335 with $\Delta$ time.		<b>Nicolet Explorer II 2090-2</b>	\$ 740
<b>Tektronix 2337</b>	\$ 315	DC to 1 MHz, dual channel digital storage scope, complete with 206-2 plug-in amplifier.	
Same as 2335 with $\Delta$ time/DMM.		<b>Nicolet Explorer III 204-2</b>	\$1200
<b>Tektronix 2445</b>	\$ 330	Same as Explorer II above except with pen output, diskette, binary digital I/O. Also includes 204-2, 2-channel plug-in and 2081 IEEE-488 interface.	
150 MHz bandwidth 4-channel oscilloscope, 1 ns/div sweep speed, 2 mV/div vertical sensitivity. CRT readout: scale factors, trigger level, voltage, time, frequency, phase and ratio measurements and mode indicators.			
<b>Tektronix 2485</b>	\$ 480		
Same as 2445 but with 300 MHz bandwidth.			
<b>Tektronix SC501</b>	\$ 115		
DC to 5 MHz, single trace, 10 mV/div to 10 V/div, time base 1 s/div; 5 $\times$ magnifier, 6 $\times$ 10 div, 0.203"/div CRT, requires TM500 power module.			

712

INSTRUMENTATION LIST

Item: Signal Generator

Nomenclature: Hewlett Packard HP3325A Function Generator.

Description: General purpose signal generator to provide command signals to the servo actuator. Can command sinewaves, squarewaves, triangle waves, and ramps.

Reason for Selection: General purpose unit having the capability to meet the expected command functional requirements.

Number Required: 1 each.

Source of Supply: General Electric Quick Rental Service  
900 S. Loop West, Ste. 180  
Houston, Texas 77054  
713 741 8137  
1 800 GE RENTS Rent

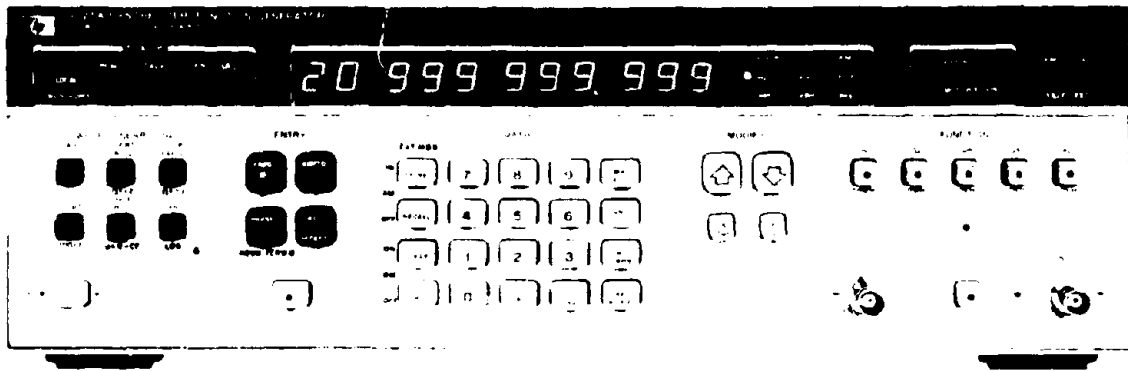
Hewlett Packard Purchase  
10535 Harwin Drive  
Houston, Texas 77042  
713 776 6400

Cost: \$440.00/month Rental

\$4075.00 Purchase

Reproduced from  
best available copy

## Model 3325A



HP 3325A

The HP 3325A Synthesizer/Function Generator is an uncompromising, high performance synthesizer with 11 digit resolution, a function generator with precision waveforms, a wideband sweeper, and a fully programmable systems instrument.

The HP 3325A is first with microhertz resolution below 100 kHz along with frequency coverage from .000001 Hz to 20,999,999,999 MHz. Signal purity, accuracy and stability are as good or better than earlier stand-alone HP synthesizers. Harmonics are 65 dB down below 50 kHz and you can externally modulate with AM and PM.

The HP 3325A is also a high performance function generator providing precision waveforms with synthesizer accuracy and resolution. Squarewaves to 10,999,999,999 MHz have 20 ns rise and fall times. Triangles and ramps with .05% linearity are available up to 10,999,999,999 kHz. All waveforms can be dc and phase offset.

A major contribution is wideband phase continuous sweep, covering up to the full frequency range of each waveform. Sweep log or linear, single or continuous without the phase discontinuities usually associated with synthesizers. Phase lock loop testing is made easier.

Make convenient swept frequency network measurement on filters, amplifiers or any passive or active network. Use the TTL marker to check the frequency of points of interest on a swept frequency display desired. Use the convenient "zoom" functions  $\Delta f \times 2$  and  $\Delta f \div 2$  to quickly change the frequency span for the display desired.

All necessary functions are programmable on the HP-IB, including frequency, amplitude, all functions, phase and dc offset, modulation, all sweep parameters, amplitude cal and self-test, making the HP 3325A a very versatile and powerful addition to automatic test systems. The isolated interface combined with floating outputs and inputs and talk mode make the HP 3325A easy to use in Automatic Test Systems.

The phase of the outputs can be changed  $\pm 109^\circ$  with 0.1% resolution. The phase is advanced (or retarded) with respect to the output

phase. Two HP 3325A units can be phase locked together for dual phase output applications.

DC offset is capable of  $\pm 4.5$  Vdc on the standard instrument. The high voltage option (Opt 002) allows ac voltages up to 40 Vpp and ac + dc up to  $\pm 18$  V total (ac peak + dc).

Ten storage registers can be programmed with ten different combinations of function/parameter settings from the front panel, stored and then recalled.

The HP 3325A can display 11 digits of frequency and 4 digits of volts or millivolts from 1 mV to 10 volts peak to peak. Conversion to RMS or dBm is simple with the touch of a button.

The HP 3325A provides unprecedented performance per dollar thanks to several major contributions from advances in HP technology. A single loop Fractional-N synthesis technique allows synthesizer accuracy with 11 digits of resolution and, as an added bonus, phase continuous frequency sweep. Fewer parts and integrated circuit technology make the difference. A unique method of triangle and ramp waveform generation provides excellent linearity. Add microprocessor control and Hewlett-Packard Interface Bus (HP-IB) operation and the result is more performance, flexibility and versatility on the bench or in automatic test systems than previously available, and at a lower cost.

## Specifications

Refer to the HP 3325A data sheet for complete specifications.

Sine, Square, Triangle, negative and positive Ramps.

### Range

**Sine:** 1  $\mu$ Hz to 20,999,999,999 MHz

**Square:** 1  $\mu$ Hz to 10,999,999,999 MHz

**Triangle/ramps:** 1  $\mu$ Hz to 10,999,999,999 kHz

**Resolution:** 1  $\mu$ Hz  $\div$  100 kHz  
1 mHz  $\div$  100 kHz

**Aqmg rate:**  $\times 10^3$  var, 30 to 300

**Warm-up time:** 30 minutes, to within specified accuracy

1759

**Impedance:** 50  $\Omega$

**Connector:** BNC (switchable to front or rear panel, nonswitchable with option 002, except by internal cable change)

**Range:** 1 mV to 10 V p-p in 8 amplitude ranges, 1-3-10 sequence (10 dB steps), into 50  $\Omega$  load.

Function	Sine		Square		Triangle/Ramp	
	min	max	min	max	min	max
peak-peak	1.000 mV	10.00 V	1.000 mV	10.00 V	1.000 mV	10.00 V
rms	0.354 mV	3.536 V	0.500 mV	5.000 V	0.289 mV	2.887 V
dbm (50 $\Omega$ )	-54.02	-23.96	-53.01	-26.96	-57.78	-22.22

**Resolution:** 0.03% of full range or 0.01 dB (4 digits)

(without dc offset, relative to programmed amplitude and accuracy)

**Sinewave Amplitude Accuracy**

1 MHz to 100 kHz:  $\pm 0.1$  dB,  $\pm 3$  Vpp,  $\pm 0.2$  dB,  $\pm 3$  Vpp  
100 kHz to 20 MHz:  $\pm 0.4$  dB,  $\pm 3$  Vpp,  $\pm 0.6$  dB, 0.1 to 3 Vpp

**Squarewave Amplitude Accuracy**

1 MHz to 100 kHz: 1%,  $\pm 3$  Vpp, 2.2%,  $\pm 3$  Vpp  
100 kHz to 10 MHz: 1.1%,  $\pm 3$  Vpp, 1.6%,  $\pm 3$  Vpp

**Triangle Amplitude Accuracy**

1 MHz to 2 kHz: 1.5%,  $\pm 3$  Vpp, 2.7%,  $\pm 3$  Vpp  
2 kHz to 10 kHz: 5%,  $\pm 3$  Vpp, 6.2%,  $\pm 3$  Vpp

**Phase noise:**  $-60$  dB for a 30 kHz band centered on a 20 MHz carrier (excluding  $\pm 1$  Hz about the carrier) with high-stability option 001 installed.

**Spurious:** all non-harmonically related output signals will be more than 70 dB below the carrier (60 dB with dc offset), or less than  $-90$  dBm, whichever is greater.

**Sinewave harmonic distortion:** harmonically related signals will be less than the following levels (relative to the fundamental) at full output for each range:

Frequency Range	Harmonic Level
0.1 Hz to 50 kHz	$-65$ dB
50 kHz to 200 kHz	$-60$ dB
200 kHz to 2 MHz	$-40$ dB
2 MHz to 15 MHz	$-30$ dB
15 MHz to 20 MHz	$-25$ dB

**Rise/fall time:**  $\leq 20$  ns, 10% to 90% at full output

**Overshoot:**  $\leq 5\%$  of peak to peak amplitude, at full output

**Settling time:**  $\leq 1$   $\mu$ s to settle to within 0.5% of final value

**Range:**  $\pm 719.9^\circ$  with respect to arbitrary starting phase or assigned zero phase

**Resolution:** 0.1 $^\circ$

**Accuracy:**  $\pm 0.2^\circ$

**Range:** dc only (no ac signal): 0 to  $\pm 5.0$  V/50  $\Omega$

dc + ac: Maximum dc offset  $\pm 4.5$  V on highest range, decreasing to  $\pm 4.5$  mV on lowest range

**Resolution:** 4 digits

**Modulation depth at full output for each range:** 0-100%

**Modulation frequency range:** dc to 400 kHz (0-21 MHz carrier frequency)

**Sensitivity:**  $\pm 5$  V peak for 100% modulation

**Sinewave Phase Modulation**

**Range:**  $\pm 850^\circ$ ,  $\pm 5$  V input

**Modulation frequency range:** dc-5 kHz

**Sweep Time**

**Linear:** 0.01 s to 99.99 s

**Logarithmic:** 2 s to 99.99 s single, 0.1 s to 99.99 s continuous

**Maximum sweep width:** full frequency range of the main signal output for the waveform in use, except minimum log start frequency  $\leq 1$  Hz

**Phase continuity:** sweep is phase continuous over the full frequency range of the main output

**Reference input:** for phase-locking HP 3325A to an external frequency reference signal from 0 dBm to  $+20$  dBm into 50  $\Omega$ . Reference signal must be a subharmonic of 10 MHz from 1 MHz to 10 MHz.

**Auxiliary frequency output:** 21 MHz to 60 999 999 999 MHz, under range coverage to 19 000 000 001 MHz, frequency selection from front panel; 0 dBm; output impedance 50  $\Omega$ .

**Sync output:** square wave with V (high)  $> 1.2$  V, V (low)  $\leq 0.2$  V into 50  $\Omega$ .

**X-Axis drive:** 0 to  $\pm 10$  V dc linear ramp proportional to sweep frequency, linearity, 10-90%,  $\pm 0.1\%$  of final value.

**Sweep marker output:** high to low TTL compatible voltage transition at selected marker frequency.

**Z-Axis blank output:** TTL compatible voltage levels capable of sinking 200 mA from a positive source

**1 MHz reference output:** 0 dBm output for phase-locking additional instruments to the HP 3325A.

**10 MHz oven output:** 0 dBm internal high stability frequency reference output for phase-locking HP 3325A (Opt. 001 only)

**HP-IB Interface Functions:** SH1, AH1, T6, L3, SR1, RL1, PP0, DC1, DT0, C0, E1.

**Recommended Accessory:** HP 7090A Measurement Plotting System

**Aging rate:**  $\pm 5 \times 10^{-4}$ /week (72-h warm up);  $\pm 1 \times 10^{-7}$ /month (after 15 days continuous operation).

**Ambient stability:**  $\pm 5 \times 10^{-4}$  ( $0^\circ$  to  $+55^\circ$ C).

**Warm-up time:** reference will be within  $\pm 1 \times 10^{-7}$  of final value 15 minutes after turn-on for an off time of less than 24 hours.

**Frequency range:** 1  $\mu$ Hz to 1 MHz

**Range:** 4.00 mVpp to 40.00 Vpp (500  $\Omega$ ,  $< 500$  pF load).

**Accuracy and Flatness at Full Output**

**Sine, square, and triangle waves:**  $\pm 2\%$  at 2 kHz

**Ramps:**  $\pm 2\%$  at 500 Hz

**Flatness:**  $\pm 10\%$  relative to programmed amplitude

**Sinewave distortion:** harmonically related signals will be the same as the standard instrument to 1 MHz

**Maximum output current:** 80 mApp.

**Output impedance:**  $\leq 2 \Omega$  at dc,  $< 10 \Omega$  at 1 MHz

**DC offset range:** 4 times the specified range of the standard instrument.

**Operating environment**

**Temperature:**  $0^\circ$ C to  $55^\circ$ C.

**Relative humidity:** 95%,  $0^\circ$ C to  $40^\circ$ C.

**Altitude:**  $\leq 15,000$  ft.

**Storage temperature:**  $-40^\circ$ C to  $+75^\circ$ C.

**Storage altitude:**  $< 50,000$  ft.

**Power:** 100/120/220/240 V,  $\pm 5\%$ ,  $-10\%$ , 48 to 66 Hz; 90 VA, 120 VA with all options; 10 VA standby.

**Weight:** 9 kg (20 lb) net; 14.5 kg (32 lb) shipping.

**Size:** 132.6 H x 425.5 W x 497.8 mm D (5.25" x 16.75" x 19.63")

HP 3325A Frequency Synthesizer

Opt. 001 High Stability Frequency Reference

Opt. 002 High Voltage Output

Opt. 007 Front Handle Kit (standalone orders P/N

HP 5061-0089)

Opt. 008 Rack Flange Kit (standalone orders

P/N HP 5061-0077)

Opt. 009 Rack Flange and Handle Combination Kit

(standalone orders P/N HP 5061-0083)

\*HP-IB cable not supplied. See page 675.

3155